Order Number 9101908

The tree-ring record of false spring in the southcentral USA

Stahle, David William, Ph.D.

Arizona State University, 1990

U·M·I
300 N. Zeeb Rd.
Ann Arbor, MI 48106

THE TREE-RING RECORD OF FALSE SPRING IN THE SOUTHCENTRAL USA

by

David W. Stahle

A Dissertation Presented in Partial Fulfillment
of the Requirements for the Degree
Doctor of Philosophy

ARIZONA STATE UNIVERSITY

August 1990

THE TREE-RING RECORD OF FALSE SPRING

IN THE SOUTHCENTRAL USA

by

David W. Stahle

has been approved

May 1990

APPROVED:

_____, Chairperson

_____

_____

_____

_____

Supervisory Committee

ACCEPTED:

_____
Department Chairperson

_____
Dean, Graduate College

ABSTRACT

Frost injuries are common in the annual rings of deciduous oaks of the southcentral United States, and can be identified microscopically by unique anatomical criteria. A chronology of 70 frost ring years between 1650 and 1980 has been developed from 42 collection sites in the Southern Plains. False spring conditions cause frost rings in oaks, and include both an abnormally warm winter and the subsequent severe freeze in spring (temperatures must fall to $\leq 23^{\circ}F$ or $-5^{\circ}C$). Major circulation changes over North American often occur from the warm to cold phase of false spring. An upper level trough over Southern California and surface high over the Southeast favor warm air advection into the Southern Plains during the warm phase. This pattern is usually replaced by a deep upper level trough over the central USA and a strong surface ridge often extending from Canada to Mexico during the cold phase. The resulting cold air advection often causes heavy damage to crops and native vegetation which were prematurely advanced by the preceding mild weather. These false spring episodes include both climatological and meteorological signals, and the consistent registration of specific weather conditions by frost rings establishes the feasibility of "dendrometeorology".

Frost rings in oaks often form during La Nina events, and may reflect a tropical influence on both above and below

average winter temperatures in the Southern Plains and Canada, respectively. Warm winters in the Southern Plains favor premature growth, and cold Canadian winters may help explain the severity of the late cold wave which terminates false spring. False spring occurrence has been nonrandom over the past 331 years, and the many one- and three-year intervals between events may partially reflect La Nina forcing. In contrast, an El Nino influence on the formation of bristlecone pine frost rings and light rings in Canadian black spruce has been detected in previously published chronologies. The co-occurrence of oak frost in spring followed by light rings in summer often reflects an enhanced La Nina-El Nino cycle. An amplified El Nino-Southern Oscillation (ENSO) may be suggested by the four such co-occurrences from 1814 to 1819, which could help explain many ambiguities in the worldwide temperature response to the cataclysmic eruption of Tambora in 1815.

ACKNOWLEDGEMENTS

I would like to thank my supervisory committee for their efforts in the successful completion of this research. I especially thank R.S. Cerveny for his assistance and lengthy discussions, and J.S. Dean for his extra efforts to attend functions in Tempe.

Many people have assisted this research and analysis. Above all others I thank my friend and colleague M.K. Cleaveland for programming and statistical help, ideas, and important criticisms. I also received statistical advice from E. King and J.E. Dunn (who has not been entirely successful in helping me avoid "jumping every time the data twitched"). For assistance in the collection and processing of tree-ring samples I fondly thank Graham Hawks and Jackson Adair, especially for many memorable days and nights on the Southern Plains. I also thank T. Harlan, J. Baldwin, D. Jurney, J. Hehr, P. Chaney, G. Imrie, and K. Thomson for their considerable assistance.

Many of the tree-ring collections used in this analysis were compiled in "Tree-Ring Chronologies for the Southcentral United States" (Stahle et al. 1985a), and that report identified the numerous individual, state, federal, and corporate landowners who allowed fieldwork on their property. I again thank the landowners for permission to collect tree-ring samples from their property.

Most of the tree-ring collections included in this report and a great deal of the analysis has been supported by the Climate Dynamics Program, National Science Foundation, under grant number ATM8006964, ATM8120615, ATM8412912, ATM8612343, and ATM8914561. I gratefully acknowledge the support of the NSF. I also thank the Arkansas Archeological Survey and the University of Arkansas Department of Geography for material assistance at various stages in the course of this work.

Most importantly, I acknowledge the support of my family: Donna, Laurie, and Danny. I apologize for the time spent with this instead of with you.

TABLE OF CONTENTS

LIST OF TABLES

LIST OF FIGURES

I. INTRODUCTION

Frost damaged rings in trees are rare and usually confined to subarctic and subalpine conifers subject to occasional subfreezing temperature stress during the growing season. The anatomical and physiological aspects of frost rings in coniferous and deciduous trees have been reported in some detail (e.g., Harris 1934; Glerum and Farrar 1966), but the only previously reported long chronology of frost rings was developed from bristlecone pine (Pinus longaeva) of the western United States (LaMarche and Hirschboeck 1984). Frost rings in bristlecone pine have been related to shortened growing seasons and large-magnitude volcanic eruptions worldwide (LaMarche and Hirschboeck 1984), but the past meteorological and climatological implications of frost ring chronologies have not been fully exploited. A unique and unusually detailed record of frost damaged rings has recently been discovered in deciduous oaks of the southcentral United States (Stahle et al. 1985b). This study documents the chronology and spatial distribution of 70 frost ring events in the Southern Plains region from A.D. 1650 to 1980. The atmospheric conditions responsible for the observed frost injuries will also be examined, and will be shown to include meteorological and climatological anomalies operating at both the regional and planetary scale, respectively.

Frost rings in post oak (Quercus stellata) and white oak (Q. alba) from this region are found exclusively in the

earlywood or spring growth zone of the annual ring, and result from unusual meteorological events in the late winter and early spring. Paradoxically, both anomalous and prolonged late-winter warmth and a subsequent outbreak of severely cold polar or arctic air appear to be necessary to produce most of the frost-injured rings observed in oaks during the period of instrumental meteorological observation. This unusual sequence of a mild winter followed by a cold spring can be highly destructive to agricultural crops and native vegetation (e.g., Kibler and Martin 1955), and has been referred to variously as "backward spring" or " false spring" (Ludlum 1982). Mild late-winter temperatures allow many plants to break dormancy early in the season, and thus render the new tissues vulnerable to any subsequent outbreaks of subfreezing air. Many costly spring cold waves in the United States have followed mild winters (e.g., Winston 1955).

Post oak and white oak trees may live for more than 300 years and produce well defined annual growth rings that can be dated to their exact year of formation (Duvick and Blasing 1981; Stahle and Hehr 1984). More than 50 post oak and white oak tree-ring chronologies have been developed for the Southern Plains region over the past decade (e.g., Stahle 1978; Stahle et al. 1985a). Many of the trees included in these ring-width chronologies exhibit unmistakable anatomical evidence for the past occurrence of severe subfreezing temperatures during the spring growing season. These unique

intra-annual tree-ring injuries present an interesting opportunity to develop a detailed frost ring chronology for the Southern Plains, and to document the past timing and spatial distribution of the unusual atmospheric conditions responsible for the observed frost damage.

This research has been specifically designed to develop a well-replicated frost-ring chronology for the Southern Plains region, and to identify the weather, climate, and large-scale circulation features involved in the false spring anomalies responsible for these frost injuries. For convenience, the study area is referred to synonomously as the Southern Plains or southcentral United States throughout this discussion. Standard tree-ring crossdating procedures (Stokes and Smiley 1968) were used to determine the exact annual dating of all frost rings. Analyses of the daily maximum and minimum temperatures, and composite mapping of North American weather conditions were used to describe the warm and cold temperature anomalies associated with false spring episodes during the twentieth century. A selected mid-tropospheric circulation index was used to examine large-scale circulation patterns during false spring episodes after 1947. The possible influence of selected internal and external factors of short-period climate change such as the El Nino-Southern Oscillation (ENSO) and explosive volcanic eruptions on false spring anomalies over the Southern Plains was also investigated.

Development of the frost ring chronology for deciduous oaks of the southcentral United States will provide a useful geochronological control for the accurate development of annual tree-ring chronologies and paleoclimatic reconstructions (e.g., Stahle et al. 1985a), and for the absolute dating of oak timbers in historic buildings and sites (e.g., Stahle 1979; Jurney 1987). The frost ring chronology should also be useful as a proxy record of the unusual meteorological conditions responsible for frost injury in centuries prior to meteorological observation.

Annual ring width and ring density data have been widely applied as proxy estimates of past climate conditions (Fritts 1976). Tree-ring width data for deciduous oaks from selected sites are often highly correlated with monthly and seasonalized climate variables, and have been used to reconstruct precipitation and drought indices for 300 years (e.g., Duvick and Blasing 1981; Stahle and Cleaveland 1988). However, because tree growth tends to integrate the physiological effects of instantaneous weather conditions over the entire growing season, it is normally not possible to recover specific short-term meteorological information from tree-ring width or density data (Fritts 1976). Frost-injured rings appear to represent an important exception to this generalization, and may help to establish the feasibility of "dendrometeorology." The persistent late-winter warm spell and subsequent hard freeze typical of severe false spring

episodes constitute atmospheric variability at the timescales of both climate and weather, respectively. If sufficiently severe, these unseasonable atmospheric conditions will result in intraannual frost injury to deciduous oak trees. Consequently, it may be possible to use the long frost ring chronology from deciduous oaks to infer the occurrence of these unseasonable weather and climate conditions for the past three centuries.

The temperature anomalies associated with the warm and cold phases of false spring are both intense and widespread, and may frequently reflect anomalies in the large-scale circulation of the atmosphere. If a consistent link between false spring and atmospheric circulation can be demonstrated, then the frost ring chronology may provide some insight into the past frequency or intensity of these atmospheric conditions during the late winter and early spring.

This study will first review tree-ring dating, the development of frost rings in trees, the study region, and the methods of analysis (Chapters 2, 3, and 4). The evidence for frost injury to deciduous oaks of the Southern Plains region will then be discussed, and the temperature thresholds required to produce this injury will be approximated (Chapter 5). The chronology and spatial distribution of frost injury will also be documented in Chapter 5, along with a brief historical review of all frost ring false spring events registered from 1650 to 1980. The synoptic meteorology and

climatology of false spring episodes, and the possible influence of large-scale circulation, El Nino-Southern Oscillation, and explosive volcanism will be investigated in Chapter 6. Finally, the long frost ring chronology will be used to explore the secular variability of severe false spring weather and climate anomalies over the past 331 years (Chapter 6).

II. BACKGROUND DISCUSSION AND LITERATURE REVIEW

Dendrochronology and Dendroclimatology

Annual growth rings in trees from selected climate sensitive sites vary in width and density due to local and large-scale environmental factors. The patterns of wide and narrow rings through time can often be matched or synchronized among many different forest sites because trees in a given region respond in part to the same governing macroclimatic variations. By sampling living trees and crossdating patterns of wide and narrow rings back in time from the known calendar date of the outermost ring, all annual rings in selected climate-sensitive trees can often be assigned to their exact years of formation. The crossdating of ring width patterns is the fundamental technique of dendrochronology, or tree-ring dating, and is possible when tree growth is at least partially controlled by regional climate variations.

Tree-ring dating is accurate to the year and season of ring formation, and there is no sampling error associated with the derived date. As a result, dendrochronology is the most accurate and precise geochronological dating method available (Smiley 1955), and is routinely used to exactly date past climatic variations (Fritts 1976), prehistoric cultural activities (Douglass 1935; Dean 1969), geomorphic and tectonic processes (LaMarche 1961; Jacoby et al. 1988), and other environmental events over the past few hundred to few thousand years (e.g., Fritts and Swetnam 1989). Varved lake sediments

(Dean et al. 1984), glacial ice layers (Thompson et al. 1985), and banded hermatypic corals (Druffel 1982) may all produce annual laminations that under favorable circumstances, can be exactly dated, but these methods are not as versatile as tree-ring dating and have yet to be widely exploited.

Tree-ring chronologies represent time series of precisely dated annual averages of ring width or density measurements, which usually have been detrended and indexed to remove non-climatic, age-related growth trend and differences in absolute growth rates among individual trees (Fritts 1976; Cook 1985). The interannual variations in tree-ring chronologies are often highly correlated with climate or climate-related variables, and chronologies from old-growth trees have been widely used for the quantitative reconstruction of past precipitation (Duvick and Blasing 1981), temperature (Hughes et al. 1984; Jacoby and D'Arrigo 1989), and streamflow (Stockton 1975; Cook and Jacoby 1983; Cleaveland and Stahle 1989). Because tree-ring chronologies often exceed the total length meteorological records by more than an order of magnitude, they may provide useful proxy estimates of climate variability in the centuries prior to direct weather observation. For example, Jacoby and D'Arrigo (1989) reconstructed Northern Hemisphere temperatures back to A.D. 1671 using subarctic tree-ring data and concluded that their reconstruction supports the hypothesis that the twentieth century warming trend has exceeded the natural variability in temperature over the past several hundred

years. Stockton (1975) reconstructed annual runoff in the Colorado River and found that the gaged runoff data in the early twentieth century was biased by the occurrence of the wettest 40-year period estimated since A.D. 1564. Stahle et al. (1988) reconstructed the June Palmer drought severity index for North Carolina and found significant changes in the mean and variance of growing season moisture conditions on 30- and 10-year timescales, respectively.

Tree-Ring Dating of Extreme Environmental Events

In some circumstances, extreme environmental conditions may radically alter growth rates for many years following an event, or can produce traumatic effects at the cellular level within the annual rings of injured trees. A wide range of environmental events can persistently alter growth rates in trees, including volcanic eruptions (e.g., Yamaguchi 1983), pollution (Nash et al. 1975; Thompson 1981), and insect defoliation (e.g., Swetnam et al. 1985). Fritts (1976), Schweingruber (1988), and Shroder (1980) have discussed further examples of tree-ring width or density response to environmental perturbations. Fewer severe events are actually recorded by traumatic anatomical evidence within growth rings, but when such evidence is present, it may be possible to use dendrochronology to determine the exact year in which the injury occurred. Past fires, floods, landslides, snowslides, ice flows, insect infestations, and severe frosts may all

potentially result in anatomical evidence within the growth rings of surviving trees.

Long histories of wildfires have been developed on the basis of tree-ring dated fire scars within trees. These fire histories have then been used to document presettlement fire rotation times for specific forest regions, and in some cases have been incorporated into forest management practices (e.g., Stokes and Dieterich 1980). Tree-ring dated fire histories in the southwestern United States have also been linked to moisture anomalies associated with the El Nino-Southern Oscillation phenomenon (Swetnam 1988).

Major floods can severely damage floodplain trees, and past floods have been identified and dated through tree-ring analyses of contorted trees and abrasion scars within growth rings (Sigafoos 1964). Large floods which innundate the canopy of certain floodplain species may also result in "flood rings", recognized by abnormally formed or spaced xylem cells and unusually large water-conducting cells (Yanosky 1983). Smaller discharge events that only flood the root systems may also stimulate abnormal anatomical responses in ash trees (Yanosky 1984). These abnormal rings, referred to as "white rings", consist of large thin-walled fiber cells with abrupt radial boundaries, and are found exclusively in the latewood portion of the annual ring (Yanosky 1984). White rings reflect growth surges apparently due to high streamflow or intense precipitation events usually in mid- to late summer,

which greatly increase water availability to these trees (Yanosky 1984). These specific anatomical changes may provide a means to identify and accurately date specific meteorological events such as intense rainstorms in tree-ring data, which normally reflect only the cumulative weather or climate of the entire growing season. However, flood rings and white rings have thus far been identified only in relatively young floodplain species, and will have to be found in species known to attain significant age (> 100 years) before their practical value as streamflow or rainfall proxies will be realized.

Unusual ring anatomy and reduced radial growth have both been identified in oak trees defoliated by insect pests (e.g., Christensen 1987). The anatomical evidence associated with defoliation includes radially flattened parenchyma cells which form an abrupt false growth ring boundary after earlywood formation, and darker than normal latewood (Christensen 1987). Traumatic rings in oak due to defoliation cannot easily be confused with the unique anatomy of frost injury, which occurs exclusively in the earlywood zone of oaks from the southcentral United States.

A variety of geomorphic or surficial processes such as landslides, ice drives, and glacial movement may abrade or fracture living trees, and leave anatomical evidence in the growth rings of surviving trees (e.g., Shroder 1980). Tree-ring data are also used to determine maximum tree ages and

the date of initial forest establishment on new geomorphic surfaces (e.g., Lawrence 1950).

Frost Rings in Trees

Severe subfreezing temperatures during the growing season can damage the new shoot, bud, and cambial tissues of woody plants, and can seriously retard growth or may even result in the death of the organism (Kramer and Kozlowski 1979; Fritts 1976). Freeze injury to tree rings takes place in the vascular cambium where the differentiation of xylem (wood) and phloem (bark) cells occurs in tree stems (Levitt 1980). Freezing of the active cambial layer will result in anatomical damage of varying intensity to existing and subsequently formed xylem cells (Rhoads 1923; Bailey 1925; Harris 1934; Glerum and Farrar 1966). This type of pathology is referred to as a frost ring, and can be recognized by microscopic examination of the unusual and highly characteristic cellular structure.

A reasonably large body of empirical and experimental studies has identified the characteristics of frost damage to trees, including the anatomical effects at the cellular level within the annual ring (e.g., Bailey 1925; Harris 1934; Glerum and Farrar 1966). The unique features of frost rings have been identified primarily in conifers and include underlignified and deformed tracheid cells, irregular layers of collapsed amorphous cells, traumatic parenchyma cells with

thin cell walls and discolored cell contents, and disrupted medullary rays (Glerum and Farrar 1966). These highly diagnostic anatomical features have been identified in rings formed during known frost years, and in rings grown under laboratory conditions and subjected to artificial freezing (Glerum and Farrar 1966). The principal mechanisms of frost injury to tree rings include dehydration of, and external pressure on immature cambial cells and tracheids due to the formation of ice in the intercellular spaces of the cambium (Levitt 1980).

Less work has been conducted on the nature of frost rings in deciduous species including the oaks, but the gross anatomical features resemble frost injury in conifers (Harris 1934). As will be further discussed below, these anatomical features of post oak and white oak include collapsed vessels, disrupted rays, and abnormal parenchyma. These damage features can be unequivocally attributed to severe subfreezing temperatures occurring during the spring growing season from early March to mid-April. Few other causes of cellular damage can account for the histological evidence in these annual rings, and all of these potential alternative mechanisms can be ruled out by the synchronized timing and widespread geographic occurrence of these anatomical abnormalities.

Deciduous trees in certain temperate regions may be more susceptible to frost damage than conifers due to an earlier initiation of spring growth (Boyce 1938), but long frost ring

chronologies have not been previously developed for deciduous species. This may reflect the rarity of frost injury in regions where deciduous chronologies have been developed (e.g., the midwest and eastern United States). In the thousands of tree-ring specimens personally inspected from the southcentral and southeastern United States, including several species of oak, pine, eastern red cedar, and baldcypress, unequivocal frost injury has been noted only in deciduous oaks growing in or near the southern Great Plains. Frost rings are reported to be rare in tree-ring specimens extracted at breast height from Iowa white oak (D.N. Duvick, personal communication), and from white oak and chestnut oak (Q. prinus) in the northeastern United States (E.R. Cook, personal communication). However, the frequency of frost rings in deciduous oaks from the Southern Plains region is extremely high, and trees in this region may prove to be among the most susceptible to late-season frost injury on earth.

Previous applications of frost ring chronologies have been based primarily on cool-site conifers from subarctic and subalpine forests. The most common application of frost rings in dendrochronology has been as an independent control over the absolute dating of tree-ring specimens (LaMarche and Harlan 1973). The time series of wide and narrow ring width patterns in drought stressed trees reflect the succession of wet and dry years, respectively. These unique ring width sequences are shared by most trees in a given climatic region,

and provide the basis for absolute dating in dendrochronology (Stokes and Smiley 1968). However, ring width tends to reflect the cumulative climate of the growing season, while frost rings reflect a specific, intraseasonal weather event which may be independent of the average seasonal climate controlling ring width. Frost injury provides a second large-scale atmospheric signal useful for synchronizing tree-ring data. When frost rings are present, confidence in the dating based on ring width patterns can be greatly increased by the chronological agreement with the regional frost ring chronology. The exact annual dating of the long bristlecone pine chronology from Methuselah Grove in the White Mountains of California, which has been used to correct the systematic error in radiocarbon dating due to long-period fluctuations in atmospheric carbon-14, was confirmed back to 3435 B.C. by ring width and frost ring crossdating with an independently developed bristlecone pine chronology from Campito Mountain (LaMarche and Harlan 1973).

Frost rings in subalpine bristlecone pine of the western United States have been related to worldwide volcanic activity (LaMarche and Hirschboeck 1984). Frost damaged rings in the latewood or summer growth of this high altitude conifer are invariably related to early season (fall) frosts, and a significant proportion of these frost rings occur only a year or two after major volcanic eruptions (LaMarche and Hirschboeck 1984). Very large scale volcanic eruptions may

eject huge quantities of dust and ash into the upper atmosphere. These aerosols may have a significant one- to three-year cooling effect that may be most pronounced at high altitude and high latitude sites [the so-called "Krakatoa effect" of major climate-effective volcanic eruptions (LaMarche and Hirschboeck 1984)]. Many major historic and prehistoric eruptions presently known appear to be registered by frost injury in bristlecone pine, including Agung (1965), Krakatoa (1883), Tambora (1815), and Santorini (1626 B.C.). The occurrence of frost injury in California, in many cases half a world away from the eruption site, may provide evidence for the sensitivity of the global climate to major volcanic eruptions (e.g., Bryson and Goodman 1980).

Meteorological Significance of Frost Rings in Oak Trees

In contrast to bristlecone pine, frost rings in post oak and white oak of the Southern Plains region are found exclusively in the earlywood portion of the annual ring, and result from severe false spring weather conditions in the late winter and early spring. Identification of the weather, climate, and circulation patterns associated with severe false spring events and frost injury in the southcentral United States are among the primary objectives of this research.

The meteorological and statistical properties of spring frosts have been examined in some detail. Davis (1972) identified the important circulation and boundary conditions

associated with frost in Great Britain, and incorporated these antecedent conditions into predictive tables for the onset of spring. Decker (1951) described the meteorological conditions associated with spring frosts in Missouri, and calculated the probabilities for a severe spring freeze after specified calendar dates. Koss et al. (1988) report similar statistical analyses for spring and fall frosts, and for growing season length using 3106 United States weather stations in all 50 states. These and many other similar studies focus on freezing and subfreezing temperature thresholds. However, the phenomenon of false spring includes both unseasonably warm and cold phases, and has not been extensively studied.

Several analyses have focused on the variability of growing season length, and on the date of the last spring freeze. Moran and Morgan (1977), Brinkmann (1979), Pielke et al. (1979), and Skaggs and Baker (1985) all found significant changes in the length of the growing season, but these changes were not necessarily closely tied to larger-scale temperature trends. Suckling (1986) found that the mean date of the last spring freeze in the southeastern United States became significantly later from the period 1916-1950 to 1951-1985. These studies all suggest that the date of the last spring freeze and the length of the growing season have exhibited secular variability on a 20- to 30-year timescale. Thomas Jefferson noted similar decade-long changes in the last date and severity of spring frosts in Virginia during the

eighteenth and early nineteenth centuries (cited in Ludlum 1966).

In contrast, Thom and Shaw (1958) and Rosenberg and Myers (1962) found that the interannual occurrence of the last spring freeze date in Iowa and Nebraska is randomly distributed. However, these two analyses are based on meteorological data available prior to 1960, and many of the changes in spring freeze dates noted by others occur in more recent years (e.g., Suckling 1986). Both the twentieth century instrumental record and the long tree-ring chronology of false spring appear to exhibit significant non random variability through time, but false spring includes both unseasonably warm and cold phases, and constitutes a distinctly different atmospheric phenomenon than simply the date of the last spring freeze. The hypothesized non random occurrence of severe false spring events has important agricultural and climatological implications and will be specifically tested below.

Namias has suggested a number of atmospheric models to explain notable climate anomalies in the twentieth century, including droughts, severe winters, and unusually cold spring conditions (e.g., Namias 1947). The discussion of the abnormal winter of 1946-1947 is particularly relevant because that very warm winter was abruptly terminated in late season by a surge of polar air (Namias 1947), and some of the atmospheric mechanisms believed to have been responsible for

the unusual weather of 1946-1947 may also be involved in the severity of false spring events (e.g., confluence, radiative cooling of isolated Canadian air masses). Dickson and Namias (1976) also describe the circulation features associated with winter temperature anomalies over the southeastern United States, and many of the conditions noted during warm winters were prevalent prior to the freeze event of many false spring episodes.

Daily maximum and minimum temperature analyses and composite mapping of mesoscale weather features will be used to document the warm and cold anomalies associated with severe false spring episodes during the twentieth century. Composite mapping is a retrospective technique which attempts to summarize the synoptic meteorological conditions associated with a given type of weather (e.g., Beebe 1956; Maddox et al. 1979). Several examples of a specific weather event are used to compile a composite map, which ideally includes the crucial meteorological conditions universally associated with the weather event of interest. This ideal is rarely, if ever, achieved. Composite maps have nevertheless been effectively used to identify the regional configuration of weather elements typically associated with severe thunderstorms (e.g., Beebe (1956) and flash flood events (Maddox et al. 1979). Composite maps are an important analog forecasting tool because they summarize the conditions typically involved in the development of specific weather systems.

Objective analyses of mid-tropospheric constant pressure surfaces in the Northern Hemisphere have identified recurrent modes of upper air large-scale circulation on weekly, monthly, and seasonal timescales (e.g., Wallace and Gutzler 1981; Blackmon et al. 1984; Esbenson 1984; Barnston and Livezey 1987). These circulation patterns have a strong influence on surface weather and short-term climate fluctuations (Klein 1983; Barnston and Livezey 1987), and are believed responsible for the remote correlations or teleconnections observed for many meteorological variables. Prominent circulation patterns previously identified include the Southern Oscillation (Horel and Wallace 1981), the North Atlantic Oscillation (Rogers 1984; Barnston and Livezey 1987), and the Pacific/North American pattern (Wallace and Gutzler 1981; Barnston and Livezey 1987). These three patterns may be particularly relevant to an understanding of false spring events over the Southern Plains region because they have all been associated with winter temperature departures over the eastern and southeastern United States. This study examines the possible influence of extremes in the Southern Oscillation and in the Pacific/North American pattern on the development of false spring episodes over the Southern Plains.

III. STUDY AREA

Late season frosts are prevalent in the southern Great Plains (e.g., Koss et al. 1988) due in part to the deep southerly penetration of polar or arctic air under the prevailing ridge and trough longwave circulation pattern over North America during late winter (e.g., Lockwood 1987), and to the absence of major topographic barriers. Frost damaged growth rings are also unusually prevalent in deciduous oak trees of the Southern Plains region. This high incidence of frost rings appears to reflect the sensitivity of early season tree growth to the presence and frequent exchange of tropical and polar air masses over the Southern Plains region. Frost damaged rings do not appear to be common in the deciduous oak or coniferous species used to develop long tree-ring chronologies elsewhere in the eastern United States.

Principal forest types of the study area are oak-hickory forests of the Ozark Plateau, oak-pine forests of the Ouachita Mountains and Gulf Coastal Plain, and post oak-blackjack oak forests that dominate upland forests near the western frontier of the eastern deciduous forest and extend well into the Southern Plains on favorable soils (Bruner 1931; Dyksterhuis 1948; Braun 1950). This region spans a steep gradient in mean annual precipitation (Court 1974), which is reflected by a westward decline in forest diversity, stature (Bruner 1931), and by an increase in tree growth sensitivity to climate (Stahle and Hehr 1984).

Undisturbed old-growth post oak and white oak dominated forests are still widely distributed in the southcentral United States, primarily on less productive, non-commercial sites where most trees were too small or poorly formed to justify logging (Stahle and Hehr 1984). Typically these sites include steep, rocky, south or western exposures on the Ozark Plateau, and rocky or sandy soils in the Cross Timbers and post oak belts of Texas and Oklahoma. Oak trees grown under these adverse conditions near the western margin of their range often grow slowly, attain advanced age, and are sensitive to growing season climate conditions (e.g. Fig. 1). The network of long tree-ring chronologies for the southcentral United States has been based principally on these remnant old-growth oak forests (Stahle et el. 1985a), and verifiable reconstructions of past moisture conditions have been developed using these chronologies (Stockton and Meko 1983; Blasing et al. 1988; Stahle and Cleaveland 1988; Cleaveland and Stahle 1989).

The growing season for post oak and white oak may begin as early as February in southern Texas, and may end as late as September in Missouri due to the seasonal march of temperature across the central United States. Radial growth at breast height usually occurs one to three weeks after the initial flush of growth in the stem apices (Kramer and Kozlowski 1979), and most radial growth at breast height actually occurs between March and July in Texas, and between

Figure 1. Old-growth post oak tree at Wedington Mountain, Arkansas. The radial growth of these trees is correlated with precipitation and temperature, and subfreezing temperature in late winter or early spring frequently cause anatomical damage to active xylem cells (frost rings). The oaks at Wedington Mountain are among the most frost-sensitive trees in the southcentral United States.

March and August in Missouri (e.g., Stahle and Hehr 1984; Stahle and Cleaveland 1988). As will be seen, however, the initiation of radial growth in post oak and white oak of this region can be advanced significantly by warm weather during winter and early spring.

The boundaries between three climatic provinces are located over the southern Great Plains region (Rumney 1987). Consequently, this region is characterized by substantial daily, intraseasonal, and interannual variability in weather and climate, and this variable weather is most pronounced during the cool and transitional seasons (e.g., Bomar 1983; Griffiths and Strauss 1985). The Southern Plains experience the highest interdiurnal range in maximum daily temperature during January, and one of the most variable annual precipitation regimes in the United States (Court 1974). A daily temperature change of 40° to 50°F is not unusual during winter (Mogil 1985). This variability largely reflects rapidly changing air flow and associated air masses from the Gulf of Mexico, Pacific, and Canada. Most damaging late-season frosts in the Southern Plains are the result of large-scale advection associated with changes in upper air flow, and are not due simply to radiative cooling.

The freeze-free period is typically between 180 and 210 days in central Oklahoma and Missouri, but the variance in growing season length for Oklahoma is among the highest for any region in the eastern United States (Decker 1951; Koss et

al. 1988). Spring frosts capable of widespread crop and orchard damage (with temperatures below 28°F) have a ten percent probability of occurrence after April 1 in southcentral and northeast Texas, and the same probability after April 15 across most of westcentral Texas, Oklahoma, and portions of western Arkansas, southern Missouri, and southeast Kansas (Koss et al. 1988). Because of the rapid early growth of vegetation, severe spring frosts that follow unusual late-winter warmth result in greater agricultural losses than late frosts following cool winter and early-spring conditions, but these false spring freeze events occur much less frequently than all late frosts below 28°F.

IV. DATA AND METHODS

Tree-ring chronologies have recently been developed at more than 70 sites in the southcentral and southeastern United States (e.g., Stahle 1979; Stahle et al. 1985a). These chronologies have been based primarily on post oak and baldcypress, but chronologies of shortleaf pine (Pinus echinata), eastern red cedar (Juniperus virginiana), white oak, and overcup oak (Q. lyrata) have been included. The analysis of frost rings in post oak and white oak has been based on approximately 1650 dated tree-ring specimens (cores and cross-sections) included in 42 chronologies derived from living trees and old timbers found in early historic buildings (referred to as modern and historic chronologies, respectively, Fig. 2, Table 1).

Undisturbed old-growth post oak and white oak forests were deliberately selected for collection to minimize or eliminate anthropogenic disturbances such as logging, grazing, or deliberate burning. Anthropogenic disturbances are not likely to seriously affect the frost ring chronology of forest trees, but they may obscure the macroclimatic signal in ring width data, which was the primary motivation for collecting these tree-ring data.

Early historic buildings are a valuable source of old timbers for tree-ring chronology development (Fig. 3). Many historic timbers were cut from virgin forests over 150 years ago, and may help extend modern chronologies based on living

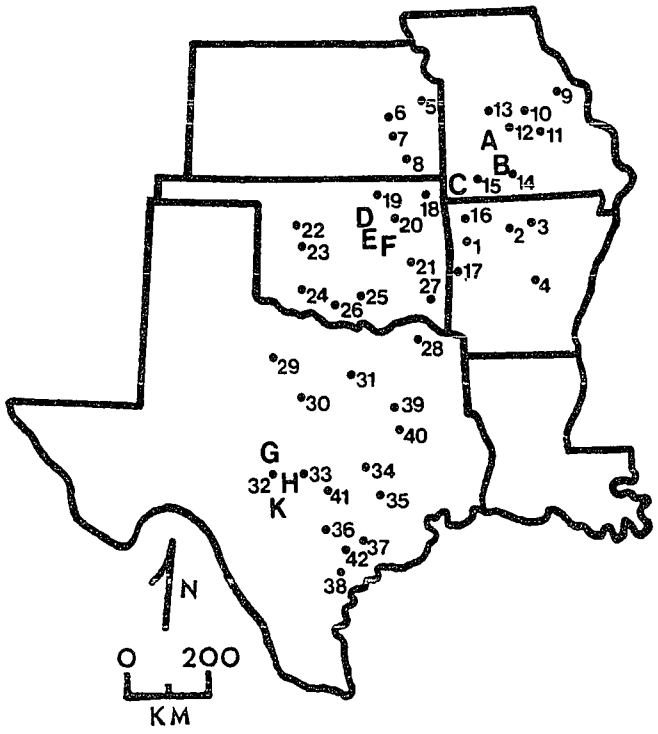

Figure 2. Site locations of the 42 tree-ring collection sites (numbered circles) and the nine weather stations used to develop the regionally averaged maximum and minimum temperature series for southwest Missouri, northcentral Oklahoma, and central Texas (letters). The tree-ring site number refer to the sites identified in Table 1 and Figure 7. The weather stations are Lebanon (A), Mountain Grove (B), and Neosho (C) in Missouri; Stillwater (D), Chandler (E), and Okemah (F) in Oklahoma; and Brady (G), Llano (H), and Fredricksburg (K) in Texas.

Table 1. A list of the historic and modern tree-ring collections used to compile the 42 frost ring chronologies for the southcentral United States. The site number refer to the locations (and site abbreviations) illustrated in Figure 2. The inner and outermost dated ring in each collection is also listed, along with the total number of annual tree rings and frost rings in each collection. The frost ring frequency is the ratio of frost rings to all available rings in each collection (expressed as a percentage of the total rings), and represents the critical background frequency used to assess the significance of frost injury in any given year.

Site No.	Site Name	Dating	Total Rings	Frost Rings	Frost Frequency (%)
	Historic Chronologies				
1	Dutch Mills, AR	1624-1842	4690	240	5.12
2	Magness Barns, AR	1698-1858	5071	218	4.30
3	Jackson Cabin, AR	1654-1849	2861	122	4.26
4	Hinderlighter House, AR	1680-1833	1108	29	2.61
	Modern Chronologies				
5	McClosky Ranch, KS	1714-1982	6746	38	0.56
6	Toronto Lake, KS	1728-1982	8176	79	0.97
7	Fall River, KS	1738-1982	6356	51	0.80
8	Elk River, KS	1720-1982	6282	74	1.18
9	Wegener Woods, MO	1662-1982	9022	43	0.48
10	Maries River, MO	1689-1982	12496	178	1.42
11	Democrat Ridge, MO	1620-1982	7753	118	1.52
12	Hahatonka, MO	1660-1982	6896	165	2.39
13	Pomme de Terre River, MO	1732-1982	8474	125	1.48
14	Clayton Ridge, MO	1696-1982	6467	153	2.37
15	Roaring River, MO	1689-1982	9742	296	3.04
16	Wedington Mountain, AR	1725-1982	11977	401	3.35
17	Blackfork Mtn., AR/OK	1650-1980	11074	197	1.78
18	Neosho River, OK	1675-1982	7691	182	2.37
19	Bluestem Lake, OK	1737-1982	7809	104	1.33
20	Keystone Lake, OK	1611-1982	11536	250	2.17
21	Lake Eufaula, OK	1745-1980	11751	225	1.91
22	Oakwood, OK	1772-1980	5959	113	1.90
23	Canadian River, OK	1680-1982	10265	193	1.88
24	Quanah Mountain, OK	1686-1980	11721	167	1.42
25	Lake Arbuckle, OK	1698-1980	14293	241	1.69
26	Mud Creek, OK	1691-1982	9160	216	2.36
27	McCurtain Wilderness, OK	1627-1982	7570	129	1.69

Site No.	Site Name	Dating	Total Rings	Frost Rings	Frost Frequency (%)
28	Pecan Bayou, TX	1694-1982	8191	156	1.90
29	Nichols Ranch, TX	1681-1980	10111	167	1.65
30	Leon River, TX	1730-1982	8409	176	2.09
31	Ft. Worth, TX	1737-1980	9425	66	0.70
32	Mason Mountain, TX	1677-1982	8001	222	2.77
33	Red Rock Creek, TX	1735-1982	9671	167	1.73
35	Yegua Creek, TX	1671-1981	8220	103	1.25
36	Capote Knob, TX	1712-1982	5694	23	0.40
37	Lavaca River, TX	1668-1982	8450	10	0.12
38	Coleto Creek, TX	1682-1982	9074	12	0.13
Historic Chronologies					
39	Satajaj Cabin, TX	1668-1879	3546	127	3.58
40	Westbrook Barn, TX	1655-1870	1091	49	4.49
41	West-Adkisson Cabin, TX	1647-1854	1723	33	1.92
42	Yoakum Cabin, TX	1668-1847	4078	43	1.05

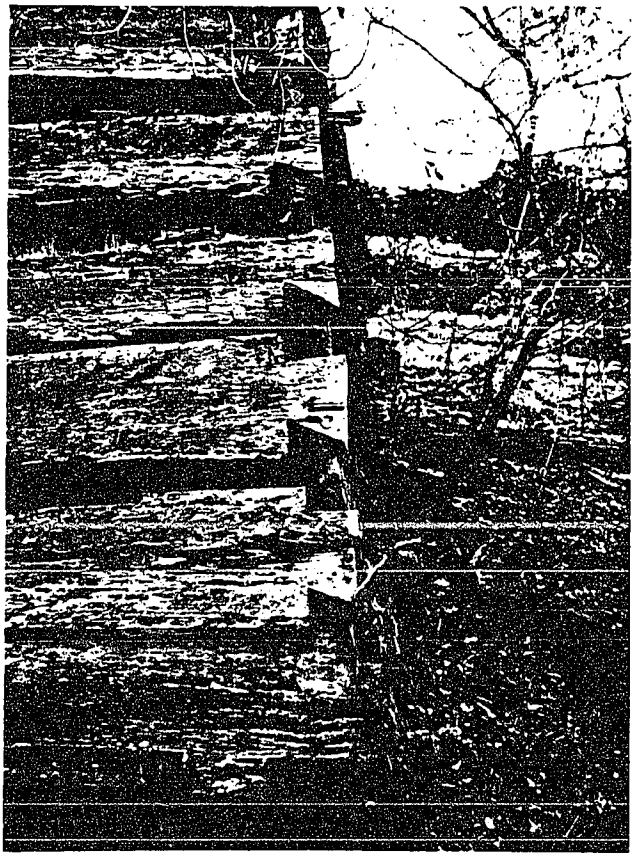

Figure 3. Mature and old growth post oak logs used in the 1879 construction of the Satajaj Cabin, Freestone County, Texas. These timbers contain a detailed record of past frost from 1671 to 1878.

trees 100 or more years further into prehistory than would otherwise be possible (Stahle 1979). Historic oak chronologies from four buildings in Arkansas and four in Texas have been used to supplement the frost ring data available for the seventeenth and eighteenth centuries. These historic timbers all belong to the white oak group and represent either post oak or white oak species (based on the native range of each species), but a more exact species determination for these old timbers cannot be made solely on the basis of wood anatomy (Panshin and DeZeeuw 1970).

Tree-ring cores 4.3 to 5.0 mm in diameter were obtained non-destructively by coring living trees at breast height with Swedish increment borers (Stokes and Smiley 1968). Historic timbers were sampled by extracting 12 mm diameter cores with a coring tube and electric drill. In some cases, cross-sections were cut with a chain saw from old stumps, fallen logs, and ruined buildings. All cross-sections and mounted cores were sanded with progressively finer textures of sandpaper (e.g., 80 to 600 grit). Proper surfacing is an absolute prerequisite in order to accurately observe the minute anatomy of frost-injured xylem cells under magnification ranging from 10x to 70x (usually at or above 40x).

The skeleton plot method of crossdating was used to synchronize the patterns of wide and narrow rings, and to assign absolute annual dates to each growth ring on every

specimen from all 42 sites included in this study (Douglass 1941; Stokes and Smiley 1968). Post oak and white oak have a clear dormant season (Fowells 1965), and produce unequivocally annual growth layers every growing season. Locally absent rings in these species are extremely rare, and missing rings never occurred in the 1650 post and white oak specimens examined for this study. The radial growth of post and white oak in this region is highly and directly correlated with monthly total precipitation, and is inversely correlated with monthly average temperature during and, in some cases, preceeding the growing season (e.g., Harper 1960; Johnson and Risser 1973; Stockton and Meko 1983; Stahle and Hehr 1984; Blasing et al. 1988; Stahle and Cleaveland 1988). Consequently, warm and dry conditions tend to result in poor growth and narrow annual rings, while cool and moist conditions tend to result in good growth and wide annual rings. Because these prevailing climate conditions are often widespread and may affect most sites in a given region, the sequence of wide and narrow rings are similar across broad areas. This climatic influence on growth rings provides the basis for absolute dating and the development of tree-ring chronologies.

Absolute dating is initiated by coring living trees. The outermost ring on living trees is known to be the current year, and crossdating procedures are used to match or synchronize the ring width patterns back in time among all

specimens at a site and among many sites in a region (Douglass 1941). The occasional presence of frost damaged rings provides an added, independent control on dating accuracy (LaMarche and Harlan 1973). The meteorological conditions associated with a spring freeze severe enough to injure the cambial tissues of oak trees also tend to be widespread and contemporaneous to the exact day. However, the conditions responsible for a spring freeze are not necessarily related to the climate conditions governing radial growth. Consequently, frost rings provide an added time-synchronous marker which helps to achieve the exact annual dating of growth rings in trees. Due to strong crossdating based on both ring widths and frost rings, tree-ring series of deciduous oaks from the Southern Plains region can usually be readily dated with great confidence. This dating accuracy has been confirmed through independent crossdating analysis of selected sites by T.P. Harlan (University of Arizona Laboratory of Tree-Ring Research), and using the computer program COFECHA (Holmes 1983) which performs correlation analyses between a master chronology and all possible overlapping 25-year segments available for each dated and measured tree-ring series included in the chronology for each site (e.g., Stahle et al. 1985a).

A standard set of morphological criteria was used to identify dated tree-rings with evidence for frost injury. Most of these criteria have previously been demonstrated on

the basis of empirical and experimental studies to arise specifically from the occurrence of subfreezing temperatures during the active differentiation of cambial cells (e.g., Harris 1934; Glerum and Farrar 1965). The criteria used to identify frost rings in post and white oak included crushed xylem cells (particularly "lunate" vessels), disrupted rays, and abnormal parenchyma cells. The specific anatomical abnormalities of frost rings in oaks, and the various lines of evidence which demonstrate conclusively that these abnormalities are the unique result of subfreezing temperatures during the growing season will be discussed below (see Chapter 5).

Every dated core or cross-section from the 42 oak sites was carefully examined for evidence of frost injury. When two or more anatomical abnormalities typically associated with frost injury were identified in the earlywood of a ring, the date of that ring was recorded as a probable frost ring along with the identification number of the specimen. Other information recorded for each specimen included the cardinal direction from which the core was extracted (when available), the aspect of the microsite, the condition of the core or section, and the dates of rings with other types of abnormalities such as fire scars. In contrast to frost rings, fire scars and other types of growth injuries were exceedingly rare in these oak specimens, and never crossdated between more than just a few trees at a single forest site. However, this

data set consists largely of increment cores extracted at breast height, which is not the ideal sampling strategy for detecting fire scars and investigating past fire history.

Three procedures were followed to help assure the reproducibility of the frost ring chronology presented below. First, at least two anatomical features typical of frost injury were required to identify probable frost rings. Once a list of probable frost rings was compiled for a given site, a statistical test was used to identify those years with evidence for frost injury exceeding the theoretical background frequency of frost ring occurrence in the entire population of dated rings from each site, assuming that the damaged rings occur randomly with respect to year. Finally, only those statistically significant frost years duplicated at two or more well-separated forest sites were included in the final frost ring chronology.

The theoretical or random background frequency of frost rings was calculated for each site simply as the ratio of the number of frost rings to the total number of dated rings at each site (Table 1). This ratio is small, ranging from .0012 to .0335 for modern chronologies (and was only slightly higher for historic timbers, most of which are cross-sections with greater surface area to search for frost injury). Frost rings can be expected to occur in any given year at this approximate frequency (i.e., in .12 to 3.35 percent of all dated rings) if their interannual occurrence is entirely random. The null

hypothesis of random interannual occurrence implies that frost rings are not synchronized phenomena related to some common macroenvironmental signal. Confidence intervals were attached to the number of observed frost rings in a given year at each site. Confidence intervals were calculated using the binomial distribution (Ott 1984), where the width of the intervals are a function of the significance level (in this case $P \leq 0.05$) and $\pm$ 1.0 standard deviation based on the total number of dated rings available during each suspected frost year. The evidence for frost injury was determined to be statistically significant, and the null hypothesis of random interannual occurrence was rejected when the lower confidence interval attached to the proportion of frost rings observed in a given year exceeded the background frequency ratio calculated for each site. This approach permits a consistent and objective evaluation of the significance of a given frequency of frost injured rings in a given year, irrespective of sample size and the differing frost susceptibility of collection sites. Sample size considerations are particularly important for the earliest years in many oak chronologies when the number of dated specimens may be low.

To actually test the reproducibility of the frost ring chronology using the anatomical and statistical criteria listed above, a second observer (J.R. Baldwin) was trained in the basics of ring anatomy and the characteristics of frost rings. This observer was then given a collection of 75 dated

cores from 37 post oak trees collected at Roaring River State Park, Missouri, and asked to identify the exact date of all frost rings on each core. With only limited experience in tree-ring analysis this individual was able to identify 90 percent of the frost rings separately identified by D.W. Stahle, who has had considerable experience in tree-ring dating. This replication test was limited to only one site, but suggests that the basic frost ring chronology reported below wherein individual frost years are found repeatedly in the same years from at least 2 to more than 20 sites, can certainly be duplicated by a trained dendrochronologist adhering to the methods outlined above.

The tree-ring data included in this study were derived by preferentially coring mature and old-growth oak trees located in virgin or only lightly disturbed forests. In some species, however, frost rings are more prevalent in juvenile growth rings, presumably because these young trees have thinner bark and may initiate (or terminate) growth earlier (or later) in the growing season (e.g., LaMarche and Harlan 1973). This tendency does appear to be present in post and white oak, although severe freeze events have demonstrably injured the rings of the oldest, slowest-growing oaks sampled. Nevertheless, some old oaks do appear to be less vulnerable to late season freeze events. Any significant change in frost susceptibility with increasing age would compromise attempts to examine the secular variability of false spring.

Consequently, to help alleviate this age bias in the derived frost chronology, more than 1650 dated cores were included from 42 sites. Young vigorous trees were also deliberately cored at several sites, including four sites that were found to be particularly sensitive to frost injury (i.e., Roaring River, MO; Wedington Mountain, AR; Keystone Lake, OK; Mason, TX). These measures have helped to insure that the derived frost ring chronology based on all available sites is not seriously biased by age-related changes in frost susceptibility over the past 331 years. However, additional representative sampling of all age classes will be required to eliminate age bias in the derived frost ring chronologies of some individual collection sites.

Once the frost injured rings were identified at each site, the frost ring chronologies were compiled for all sites spanning the period 1650 to 1980. A summary frost ring chronology was also developed and tested for changes in the frequency of frost injury through time. The geographic distribution of frost injury during each frost year was mapped, along with the locations of all available collection sites dating to that year. Synoptic weather maps of the warm and cold phases of false spring were also prepared for all events beginning in 1899.

This study focuses on the chronology and spatial distribution of frost injury to trees, rather than the quantitative reconstruction of past climate from standardized

chronologies of tree-ring width data. However, selected values derived from the indexed chronologies for these 42 sites were used to help evaluate the frost ring record. These chronologies are based on measurements of dated tree-ring widths with a precision of 0.01 mm. The ring measurement series available for each core or cross-section were detrended and indexed by fitting a linear regression line, negative exponential, or cubic smoothing spline to the measurements, and then calculating ring width indices as ratios of observed ring width to the fitted curve value. The ring width indices available for each core were then averaged on an annual basis using robust estimation to produce the mean index chronology for each site (Cook 1985; Cook and Holmes 1984). All analyses discussed below involve only the standard chronology, which does not include autoregressive modelling procedures (Cook and Holmes 1984). Further details of the tree-ring data collection and chronology development procedures are discussed by Stahle et al. (1985a).

Several sources of meteorological data were used to define the critical temperature thresholds implied by frost injury to oak trees, and to document the synoptic features associated with false spring. Seven tree-ring sites in three areas where frost injury is especially prevalent were selected for case study. Frost rings are most prevalent in an arc extending from southwest Missouri into central Texas. Long records of daily maximum and minimum temperature for several

stations within this zone of highest susceptibility were used to develop three regional average daily max-min temperature series (for southwestern Missouri, northcentral Oklahoma, and central Texas; Fig. 2). These regional average daily temperature series were then paired with the frost ring data available for two or more tree-ring sites in each area. The southwest Missouri temperature average runs from 1918 to 1980, and includes data from weather stations at Lebanon, Mountain Grove, and Neosho. The frost ring data for the region came from Roaring River State Park, MO, and Wedington Mountain, AR. The northcentral Oklahoma temperature average runs from 1901 to 1980, and includes data from Stillwater, Chandler, and Okemah. Frost ring data for this region came from Bluestem Lake, Lake Keystone, and Lake Eufaula, OK. The central Texas daily temperature average runs from 1896 to 1980, and includes data from Fredricksburg, Llano, and Brady, TX. Frost ring data for the area came from tree-ring sites at Mason and Red Rock, TX (Fig. 2).

In order to achieve a robust definition of false spring, the warmest <u>minimum</u> temperature associated with frost injury during the twentieth century period of meteorological observation was used to define the critical low temperature threshold required to result in frost injury to oak trees. All three regions were included in this assessment, and the warmest minimum observed during a frost ring year in any area was used to define this critical cold temperature threshold.

In addition, the warm spell required to promote early spring tree growth usually associated with frost injury was defined by the fewest number of days preceeding a severe spring frost when daily minimum temperatures exceed certain critical thresholds. These critical warm and cold temperature thresholds were determined empirically for all three case study sites, but the warmest cold threshold and the coolest/shortest warm threshold found in association with frost injury in any region were then adopted as the critical values for the entire southcentral United States. These warm and cold thresholds are consistent with the approximate temperature requirements for plant growth (SCS 1975), and with the subfreezing temperatures necessary to produce "heavy damage to most plants" (Koss et al. 1988) and frost rings in trees (Glerum and Farrar 1965).

Several other meteorological and tree growth variables were evaluated in an effort to define the false spring weather signal registered by frost rings as specifically as possible. Narrow specification of this weather signal is important to the meteorological inferences based on the frost ring data, and is also necessary to help minimize the number of defined false spring events in the meteorological record that for various reasons were not registered by frost rings in trees. Frost rings probably underestimate the true number of severe false spring episodes that actually occurred, due to microclimatic differences between the weather stations and

tree-ring sites, and due to many other environmental and physiological factors that can inhibit radial growth in oak trees even during an unseasonably mild late winter and early spring. Nevertheless, the underestimation of the most severe false spring events is hopefully small, and if the temporal distribution of the misses (i.e., false spring events not registered by frost rings) can be shown to be random, then the frost ring chronology can be analyzed in terms of the secular variability of severe false spring episodes over the past 331 years. The statistical significance of the temperature anomalies associated with the tree-ring record of false spring was evaluated using the three regional temperature averages.

Composite mapping techniques (e.g., Beebe 1956; Maddox et al. 1979) were used to illustrate the salient synoptic features found in the vast majority of false spring anomalies over the southcentral United States. Composite maps are especially useful because they can be used to summarize the typical weather conditions prevailing during the warm and cold phases of modern false spring episodes. The general synoptic features that occur with great consistency during modern false spring episodes can then be inferred to have prevailed during earlier years with widespread frost injury. As will be demonstrated with selected examples, these pre-instrumental false spring weather inferences based on frost rings can often be verified in part by historical weather data and documentary evidence.

Two composite maps were developed to describe the contrasting weather conditions prevalent during the warm and cold phases of false spring. Daily weather maps for the United States are available on microfilm from 1899 to the present through the National Climatic Data Center (NCDC), Asheville, NC. These maps were originally published by the Department of Agriculture, Weather Bureau (referred to as "Daily Weather Map"), and are presently issued by the Department of Commerce, National Weather Service (NWS, and referred to as "Daily Weather Maps, Weekly Series" (Jenne and McKee 1985:1245-1247)). Analyses of the daily surface maps for the United States were supplemented with a review of the daily weather maps available for the Northern Hemisphere in the "Daily Synoptic Series, Historical Weather Maps, Northern Hemisphere Sea Level" published by the Weather Bureau. Since approximately 1947, daily maps of upper air weather conditions analyzed at various constant pressure surfaces in the atmosphere over North America have been issued on facimilie charts by the NWS (Jenne and McKee 1985). The surface and upper air maps used to develop the composite maps of false spring were either available through the University of Arkansas Department of Geography, or were obtained on microfilm from the NCDC.

Surface weather conditions during all frost ring years since 1899 were carefully studied along with upper level conditions for all frost ring years after 1947. The synoptic

features common to most, the majority of frost ring years were then identified. These weather elements were separated into the warm and cold phases of false spring and were the incorporated into the composite maps for each phase. As will be discussed below, several features such as a cyclonic disturbance and cold front were present in all frost years. Several other features were also extremely common to each phase, and have been included on the appropriate composite map.

In the following discussion of false spring, the composite maps are supplemented with references concerning the condition of weather, crops, and native vegetation available for the past century in Monthly Weather Review, Weekly Weather and Crop Bulletin, and regional newspapers.

To investigate the hypothesized link between false spring weather anomalies over the southcentral United States and the general circulation of the atmosphere, daily 700 mb heights from 1947 to 1980 were used to calculate a zonality index for frost ring years and all remaining "non-frost" years. Twice daily 700 mb data issued by the National Meteorological Center (NMC) on a 5 X 5 degree latitude-longitude grid were obtained from the National Center for Atmospheric Research (NCAR), Boulder, CO. 700 mb data for three specific regions or "centers of action" associated with the Pacific/North American pattern of atmospheric circulation (e.g., Wallace and Gutzler 1981; Yarnal and Diaz 1986; Barnston and Livezey 1987) were

selected to measure the nature of mid-tropospheric flow over the North Pacific and North American sectors. These three regions are over the Aleutian Islands (50oN 170°W), the Pacific Northwest (50°N 120°W), and the southeastern United States (35°N 85°W).

In an attempt to verify the pre-instrumental record of false spring in oak trees and to help delineate the regional extent of these events, primary and secondary sources of historical weather references were consulted. These references include early meteorological records, surveys of early weather data (e.g., Ludlum 1966, 1968), and early newspaper accounts (e.g., Arkansas Gazette, April, 1828).

Possible relationships between the weather anomalies associated with frost rings in the Southern Plains, worldwide volcanic activity, and the El Nino/Southern Oscillation (ENSO) were also evaluated. Volcanic eruption data were obtained from Lamb (1970), Simkin et al. (1981), and Newhall and Self (1981). ENSO data were obtained from Quinn et al. (1978), Kiladis and Diaz (1989), and Jones (cf 1988, and personal communication).

Finally, comparisons were also made between the frost ring chronologies based on oak and high-altitude bristlecone pine from the western United States (LaMarche and Hirschboeck 1984) and light rings in black spruce (Picea mariana) from eastern Canada (Filion et al. 1986).

V. RESULTS

There is overwhelming circumstantial evidence indicating that the unique anatomical features of suspected frost rings in post oak and white oak are the invariable specific result of severe subfreezing temperatures early in the growing season. Frost injury to oaks occurs either well into spring, or during years of abnormal late winter-early spring warmth. Mild late-winter conditions promote the early initiation of cambial activity, and render the trees vulnerable to the subsequent outbreak of subfreezing air. The evidence for freeze damage will be reviewed in this chapter, and the critical temperature thresholds required to produce traumatic anatomical response will be approximated. The frost ring chronologies for all 42 sites in the southcentral United States will then be presented, followed by a brief description of each frost year from A.D. 1650 to 1980.

Evidence for Frost Damaged Rings in Deciduous Oaks of the Southcentral United States

The anatomical characteristics of frost rings have been previously identified in many conifers and selected hardwood species (e.g., Rhoads 1923; Bailey 1925; Harris 1924; Glerum and Farrar 1966). The abnormal anatomy of frost rings in post oak and white oak is entirely consistent with these earlier studies, and frost rings can be readily distinguished from normal growth rings given adequate specimen preparation and

proper magnification. Figures 4 and 5 illustrate the key anatomical features of normal and frost injured rings in post and white oak. A normal growth ring for 1720 is illustrated in Figure 4, and the major structural details of ring porous species in the white oak group are apparent (also see Panshin and de Zeeuw 1970; Fahn 1974; Kramer and Kozlowski 1979). Note specifically the earlywood and latewood zones; the terminal parenchyma (a fine dark line which outlines the boundary between annual rings on well preserved and properly surfaced specimens); the large circular vessels which dominate the earlywood zone, function as conductive tissues and form an abrupt boundary with the terminal parenchyma of the previous ring; the prominent transverse medullary rays which eminate radially from the pith and transect the annual rings at approximately right angles; the smaller latewood pores arranged in broad "flame-shaped tracts" (Panshin and de Zeeuw 1970) in the latewood zone tangential to the ring boundary; and the narrow banded rows of trachied and parenchyma cells parallel to the ring boundary (Fig. 4). Irregular, filamentous tyloses also occlude the interior of the large earlywood vessels, and are normal, diagnostic features of the heartwood anatomy of species in the white oak group [Leucobalanus (Panshin and de Zeeuw 1970)].

The severely frost damaged ring of 1719 illustrates the obvious anatomical abnormalities which clearly distinguish frost rings from normal rings (Fig. 4). The abnormalities used

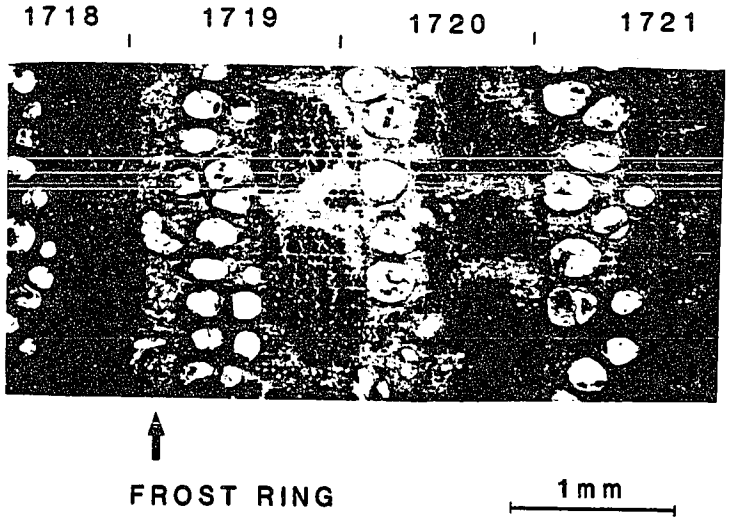

Figure 4. The anatomical features of normal and frost damaged annual growth rings in deciduous oaks are illustrated in this transverse or cross-sectional view of the rings from 1718 to 1721 for a post oak specimen from the Brazos River site, Texas (BRA10B). The structural details of normal growth rings are illustrated by the 1720 ring, where the large circular vessels which constitute the earlywood zone on the left margin of the ring immediately abut the terminal parenchyma of the previous ring (i.e., the fine dark line which terminates the right margin of 1719). The ring for 1719 exhibits unmistakable evidence for intense frost injury and can be readily distinguished from the earlywood anatomy of normal rings. Two crushed or lunate vessels are present at the beginning of the 1719 ring (left margin). Lunate vessels are highly diagnostic of frost injury and have never been observed in rings other than frost rings, given adequate replication. Other diagnostic features of frost rings include the broad lesion between the terminal parenchyma of the previous ring (1718) and the normal circular vessels formed after the frost event of 1719. This lesion is usually discolored and contains abnormal parenchyma cells indicative of traumatic injury. The medullary rays are also frequently distorted as they transect frost rings (not shown). The earlywood and latewood structures formed after the injury in 1719 are normal, but the zone of abnormal tissues at the beginning of 1719 clearly distinguishes this type of ring from normal growth rings, and the structural details of this lesion are consistent with the previously identified anatomical features of frost rings (e.g., Bailey 1925; Boyce 1929; Harris 1934; Glock 1951; Glerum and Farrar 1966; Panshin and de Zeeuw 1970).

to identify frost rings in deciduous oaks were: (1) crushed xylem cells, particularly collapsed or "lunate" vessels; (2) disrupted medullary rays; (3) abnormal parenchyma cells in the earlywood zone (with overly abundant and discolored cell contents); (4) discoloration at beginning of earlywood formation (dominated by traumatic parenchyma cells); (5) the boundary between the terminal parenchyma of the previous ring and the normal vessels of frost rings formed after the injury is not abrupt, instead the normal vessels begin very late in the growth ring.

The single most obvious and diagnostic feature of frost rings are the large lunate or crescent-shaped vessels in the earlywood zone (Figures 4 and 5A) which strongly suggests pore-wall collapse due to external expansion associated with the freezing of extracellular tissues and moisture. Crushed or lunate vessels in post and white oak of the southcentral United States have never been observed in any rings other than frost rings, which synchronize (crossdate) to the same exact year among many trees growing at several sites across a broad geographic area.

The second most consistent feature of frost rings is the broad zone of abnormal cells located at the beginning of the earlywood. This abnormal zone appears discolored and callused, is usually free of vessels other than lunate vessels, contains traumatic parenchyma cells with overly lignified cell walls, and medullary rays become seriously disrupted or disappear

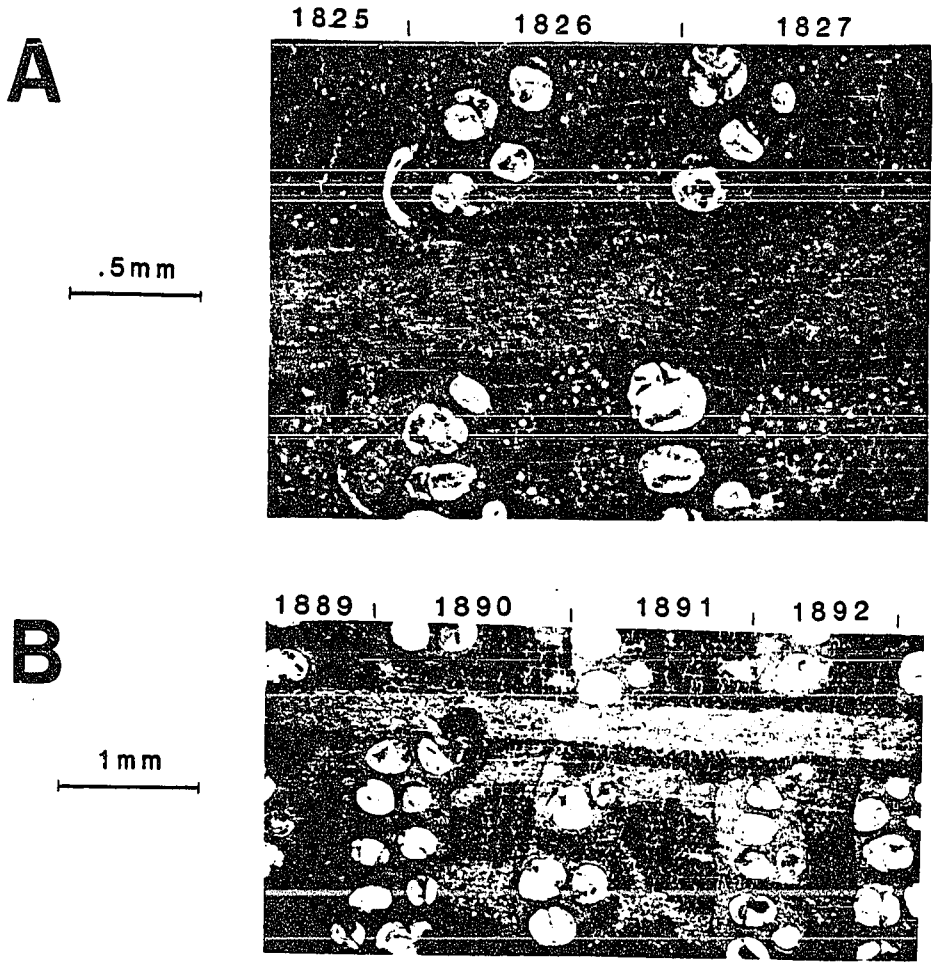

Figure 5. (A) The growth ring for 1826 on specimen BLU14A from Bluestem Lake, Oklahoma, further illustrates the abnormal earlywood anatomy of severely frost damaged rings. Note particularly the lunate vessel at the lower left margin of the ring, and the broad zone of anomalous tissues which separate the terminal parenchyma of the previous ring (1825) from the normal vessels formed after the hard freeze of 1826. Frost injury was more intense and widespread during 1826, than for any other year from 1650 to 1980. (B) The growth rings for 1890 and 1892 on specimen MAS26B from Mason Mountain, Texas, both illustrate frost injury, but the degree of injury is much less pronounced than illustrated in Figures 4 and 5A. No lunate vessels are apparent in either ring, but both contain the unusual lesion which interrupts the normally abrupt boundary between the terminal parenchyma of the previous ring and the earlywood vessels of the subsequent ring (compare with the normal boundary between 1890 and 1891). The lesions at the beginning of 1890 and 1892 both are discolored and contain abnormal parenchyma growth, and both rings were identified as probable frost rings based on these anatomical characteristics.

entirely in this area.

Frequently, the extent of anatomical injury due to frost is not as severe as illustrated in Fig. 4, but there is no doubt that even these less prominent characteristics are the specific result of frost injury. Fig. 5B illustrates two frost rings which exhibits only moderate injury. The anatomy of these mildly injured rings is clearly abnormal (compare 1890 and 1892 with 1891 in Fig. 5B) and these more moderate injuries also often occur elsewhere along the circumference of specific annual rings exhibiting severe frost injury. To help assure the replicability of the frost ring chronology, only those rings with evidence for at least two of the abnormalities listed above were recorded as frost rings.

Several other abnormalities were sometimes noted in frost rings, including smaller than normal earlywood vessels, a double tangental row of normal vessels, fewer vessels than normal or vessels were sometimes entirely absent from the 4.3 to 5.0 mm wide core sample. However, these other possible frost effects were not widespread and were not included in the criteria used to identify frost rings in this study. It should also be emphasized that frost rings do not resemble false rings in deciduous oaks. Frost rings are restricted to the earlywood, while false rings in these species are common only in the latewood zone where they usually appear as darkened tangential bands of parenchyma cells with thickened cell walls.

Several lines of evidence demonstrate conclusively that deciduous oak rings with the earlywood abnormalities listed above are the invariable result of a hard freeze during the growing season.

(1) Frost Ring Anatomy. Previous studies have associated most of these specific anatomical abnormalities with frost injury. Similar traumatic effects have been shown to have occurred following previous spring frosts (e.g. Harris 1934; Glock 1951), and plants subjected to artificial subfreezing temperatures suffered similar injuries (Glerum and Farrar 1966).

(2) Frost Rings Crossdate. Frost injury is present in the earlywood of annual rings formed in exactly the same year in many trees growing at many different forest sites across a wide geographic area. Conversely, it is extremely rare to find the typical anatomical features of frost rings in non-frost years, or when the injury evidence is not widely replicated. These observations rule out local environmental factors such as most wildfires, insect pests, wind damage, or other biotic factors, and strongly imply a time-synchronous region-wide environmental event such as low temperatures.

The results of the statistical tests used to identify significant evidence for frost injury at each collection site substantiate the synchronous, regional nature of the signal. If the anatomical abnormalities are not due to frost or any other common large-scale environmental factor, they should

occur in all years with the same approximate frequency (which would be approximately 1 to 3 percent, or the ratio of all "frost" rings to all dated rings at each of the 42 sites). This is definitely not the case. When the binomial distribution is used to attach 95% confidence intervals to the observed frequency of frost-injured rings in a given year, the lower confidence band is usually well above the expected background frequency, which is based on the assumption of random interannual occurrence of damaged rings. These statistical results were duplicated for the same year at most tree-ring sites in a given region, and indicate that these damaged rings are related to a synchronized macroenvironmental phenomenon.

(3) Subfreezing Temperature. All suspected frost rings contemporaneous with meteorological data occurred during years with severe subfreezing temperatures early in the growing season (March or April). This includes all 17 twentieth and most nineteenth century events for which meteorological data are available. Most frost rings also followed abnormal late winter warmth, and those that did not occurred very late and well into the spring growing season. No other unusual surface weather conditions are consistently associated with these years of suspected frost injury. For this reason, glaze ice storms, severe spring drought, torrential rainstorms, or other extreme meteorological conditions that might induce stress in trees can be ruled out as possible factors in the formation

of suspected frost rings. Subfreezing temperatures during the growing season is the only surface weather condition universally associated with the suspected frost damaged rings.

The regional patterns of suspected frost-injured rings during specific years with meteorological data are entirely consistent with the frost explanation for this injury, and with phenological considerations (i.e., north-south differences in the initiation of tree growth due to the march of seasons). In some years, frost rings are restricted to trees in Texas (e.g. 1943, 1962, 1965), and reflect early March cold waves which penetrated to the Gulf of Mexico. These early March frosts certainly occurred in Missouri and Oklahoma as well, but trees in this region were still dormant and were not injured. In other years, such as 1955, frost injury was restricted to trees in Oklahoma, Arkansas, Missouri and Kansas. The late March cold front responsible for this injury definitely penetrated through southern Texas (Kibler and Martin 1955), and Texas post oak were certainly not dormant at this time, but the critical subfreezing isotherm necessary to produce traumatic injury in oak trees did not penetrate far south of the Red River (see Fig. 33B below).

Three other important, though less compelling, lines of evidence further support the frost explanation for the injured oak rings.

(4) Regional Distribution of Frost Injury. The regional pattern of "frost" ring frequency at each site is consistent

with the frost explanation for this injury (Fig. 6). The highest frequency of frost rings occurs in a zone extending from southwestern Missouri through central Oklahoma into central Texas (Fig. 6). Frost injury was noted in over 2 percent of all dated annual rings available sites from this region (Fig. 6). The frequency of frost rings drops off sharply to the south and north of this arc, as might be expected in the case of frost injury to oak trees. The frequency of spring frosts is substantially lower in southern Texas than in central Texas and Oklahoma, and the isolines of spring frost occurrence (Koss et al. 1988) in fact conform to the northeast-southwest trend in frost ring frequency illustrated in Fig. 6. The decline in frost ring frequency northward into central Kansas and Missouri might reflect differences in frost hardiness, photoperiod, and growing season length.

(5) Cardinal Direction of Frost Damage. Suspected frost injury appaers to be more prevalent and intense on the north and west sides of oak trees, where subfreezing temperatures at breast height would persist the longest on clear calm days in the study area.

(6) Intra Annual Pattern of Frost Ring Injury. Another observation consistent with the frost explanation for injured rings concerns the specific intra-ring location of traumatic effects. During some widespread and presumably intense freeze events (e.g., 1826, 1779), the zone of injury is found

Figure 6. The frequency of frost rings in oaks of the southcentral United States is illustrated here by the percentage of frost rings in the total sample of dated rings at each collection site. The observed frequency ranges from 0.12 to 3.35% (Table 1), and the contour interval is 0.50%. All historic chronologies and the modern chronology for the Ft. Worth Nature Center were excluded from this map. The Ft. Worth collection has a very low frequency of frost injury which may reflect microsite factors or a strong age bias associated with the sample of exclusively old-growth trees (Table 1). The historic chronologies exhibit a uniformly higher frequency of frost damage than the modern chronologies (Table 1). This probably reflects several non-climatic factors, including a higher proportion of young trees. Also, the modern chronologies are based largely on increment cores, while the historic collections consist largely of cross-sections of historic timbers, which provide a greater surface area to search for evidence of frost injury.

abruptly at the beginning of the earlywood in Missouri, but well into the earlywood growth zone farther south in Oklahoma or northern Texas. This probably reflects north-south differences in phenology. Radial growth normally begins earlier in the season in southern Oklahoma than in Missouri, and when an intense spring freeze occurs the actively differentiating xylem cells are most susceptible to injury (Levitt 1980). If some radial growth has already occurred in southern Oklahoma, the damaged cells will be located within the earlywood, while damage from the same frost event will be found only at the beginning of the earlywood in Missouri trees just initiating radial growth at breast height. (Therefore, frost lesions in oaks could in some cases be used as time synchronous markers useful for physiological or phenological studies of radial growth.)

The weight of the foregoing evidence indicates emphatically and unambiguously that the morphological criteria used to identify suspected frost rings can be attributed to subfreezing temperatures during the growing season. Because the suspected frost ring chronology reported below has been based on the presence of two or more anatomical abnormalities for each identified frost ring, on statistically significant proportions of frost injured specimens at each site, and on the agreement between at least two separate tree-ring sites, it can be confidently concluded that this chronology does indeed represent a history of severe growing season frosts

over the southcentral United States.

Other traumatic injuries can sometimes cause anatomical abnormalities which vaguely resemble frost injury. These injuries may result from wildfire, lightning, or other wounds resulting from physical impact (e.g., falling trees) or branch loss due to high wind or glaze ice storms. However, none of these possible alternative mechanisms can easily account for the widespread geographic extent of cell damage occurring in exactly the same year and season of radial growth at breast height. Wind and ice storms tend to damage tree canopies, and the shearing of branches usually damage several rings adjacent to the wound. The physiological response to such injury usually involves obvious reaction wood forming a collar around the wound over several years.

Similar responses attend lightning and fire scars (e.g. Stokes and Dieterich 1975). Wildfires often increase in frequency during dry years, but it is highly unlikely that wildfires would cover the wide area and diversity of microhabitats represented during most years of frost-injured rings (e.g., 1716, 1779, 1826, 1955, see below). Fire scars are occasionally present in post oak of the Southern Plains, and they are easily distinguished from frost rings by extensive multiyear reaction wood and the frequent presence of carbonized wood. Fire scars in deciduous oaks of the study area are far less numerous than frost rings, and they rarely crossdate beyond a single forest site. The frost rings

identified in this study never included charred or reaction wood typical of fire scars.

Deciduous oaks in the southcentral United States are host to a variety of diseases and insect pests (Fowells 1965), but the possible impact of pests on the anatomy of annual rings has not been investigated. The anatomical effects of defoliating insects in European oak have been described by Christensen (1987), and these features are restricted to the latewood and bear no resemblance to frost rings.

Improperly surfaced tree-ring specimens include rings which appear to be injured, but this simply reflects mechanical damage by the coring or sanding device and disappears when properly surfaced. Medullary rays occasionally terminate within an annual ring and may cause local distortion, but this too can be easily distinguished from frost rings.

Meteorological Definition of False Spring

All frost injured rings contemporaneous with daily temperature data available during the nineteenth and twentieth centuries are associated with late season frosts. However, the specific temperature thresholds associated with frost rings must be determined for an explicit definition of the false spring anomaly necessary to produce frost injury in oaks of the southcentral United States. An explicit definition of false spring will allow the identification of all such events

in the meteorological record, and permit an evaluation of the possible underestimation bias inherent in the frost-ring record of false spring.

Frost ring and daily temperature data in three regions were used to establish the critical warm and cold temperature thresholds of false spring events associated with frost injury to trees. Based on these data in southwest Missouri, northcentral Oklahoma, and central Texas, the false spring weather anomaly registered by frost rings in post and white oak of the southcentral United States can be defined as:

Frost event: Any daily low temperature $\leq$ 23°F (-5.0°C) on or after March 1 in Texas, and March 21 in Oklahoma and Missouri, following a warm spell as defined as;

Warm spell: A 10-day warm spell starting 13 days before the frost event with a mean daily minimum temperature of $\geq$ 40°F (4.4°C), and with no daily temperature falling below 27°F (-2.8°C) during this 10-day period.

These thresholds approximate the minimum temperature excursions required to produce traumatic anatomical effects at the cellular level in deciduous oaks of the southcentral United States. The actual warm and cold temperature extremes measured during false spring events associated with frost rings of the past century are usually much more pronounced.

The hard freeze associated with false spring events

during the twentieth century all resulted from large-scale advection of polar or arctic air masses and did not arise simply from radiative frosts (see Chapter 6). All warm spells associated with frost rings had mean daily maximum temperatures above 62°F (16.7°C), but for simplicity only the minimum temperature threshold was used to define false spring.

The definition of false spring has been based on the regionally-averaged daily temperature data available in each area during all local frost ring years. There are 16 total frost rings during the twentieth century, but only 13 occurred in the vicinity of the three regional temperature series (1913 and 1932 occurred in southern Oklahoma, while 1914 occurred prior to the 1918 starting date of the southwest Missouri temperature series). The exact calendar date and minimum temperature of the late freeze events associated with these 13 frost rings were recorded (Table 2). The warmest subfreezing temperature associated with any of the frost ring events in Table 2 was 22.7°F in 1926, and this figure was rounded to 23°F (-5.0°C) and adopted as the mildest cold temperature associated with frost ring injury anywhere in the study area. The earliest calendar date of a late freeze below 23°F (-5.0°C) associated with frost injury was then determined for Texas (March 1, 1962, Table 2), and for Oklahoma and Missouri combined (March 21, 1974, Table 2). These two dates were adopted as the earliest spring freeze events associated with frost rings in Texas and Oklahoma-Missouri, and were used

to define the earliest possible date for the cold wave of false spring in each region. In some cases the cold wave with severe subfreezing temperatures persisted for several days (e.g, 1955, 1974). When this happened, the first date with a temperature below 23°F was identified as the frost event.

The temperature characteristics of the warm spell associated with each frost ring year were also examined for each area. The warm spell preceding the severe spring freeze varied considerably from 10 days to well over 30 days in length. The warm spell also ended one to five days prior to the coldest day of the frost event. Consequently, the warm spell threshold was defined simply as the mean minimum daily temperature $\geq$ 40°F (4.4°C) for a 10 day period beginning 13 days prior to the frost event (Table 2). This lag in the calculation of the warm spell temperature excluded the falling temperatures often associated with the development of intense cold waves in the southcentral United States. Finally, the lowest minimum daily temperature observed during the ten day warm spell associated with each frost ring event was also tabulated. This value never fell below 27°F (-2.8°C). This minimum threshold was also incorporated into the definition of the warm spell to eliminate four years not recorded by frost injury that had late season temperatures below 23°F and a 10-day mean temperature above 40°F, but which were characterized by large inter-diurnal changes and several cold daily temperatures below 24°F during the "warm" period (i.e.,

Table 2. The calendar dates and minimum temperature averages are listed for each hard freeze event responsible for the 13 frost ring years which occurred near one of the three regional temperature averages during the twentieth century. The average and coldest daily temperatures for the 10 day warm spells preceding each cold wave are also listed (all in °F).

Year	Month	Day	State	Hard Freeze Minimum Temp. Average	Warm Spell Average Temp.	Warm Spell Coldest Daily Temp.
1920	4	5	MO	19.7	44.3	31.0
1921	3	29	MO	20.7	44.6	35.7
1923	3	20	TX	19.0	44.5	27.0
1926	3	27	OK	22.7	42.4	27.0
1931	3	28	OK	17.0	39.6	27.3
1936	4	3	MO	16.7	41.4	27.7
1940	4	12	MO	21.7	46.8	35.7
1943	3	3	TX	14.0	43.4	32.7
1955	3	22	MO	11.7	43.7	33.7
1957	4	13	MO	15.7	41.3	29.0
1962	3	1	TX	18.3	43.6	36.0
1965	3	20	TX	20.3	44.6	30.3
1974	3	21	MO	18.3	42.8	28.0

1922, 1928, 1950, and 1968).

Based on this definition of false spring, the daily temperature data in the three areas indicate a total of 17 false spring episodes since 1901 in northcentral Oklahoma, since 1903 in central Texas, and since 1918 in southwestern Missouri. Frost rings were recorded in the vicinity of these temperature series during 13 of these false spring episodes, for an accuracy of approximately 76 percent (the frost ring years of 1913, 1914, 1932, were excluded because they were not located near, or were not contemporaneous with one of the three regional temperature averages). The four false spring years not recorded by frost rings were 1917, 1948, 1951, and

1966, and the temperature thresholds for these years are tabulated in Table 3. Possible explanations for these discrepancies are considered below.

The temperature criteria used to define false spring represent the minimum thresholds observed in association with frost rings, and most false spring temperature anomalies were more extreme (Table 2). Only four frost ring years were associated with daily minimum temperatures above 20°F (-6.7°C) during the freeze event, while only three other frost ring years had mean minimum temperatures below 42°F (5.6°C) during the warm spell. In some of these cases, the spatial distribution of subfreezing temperatures suggests that temperatures at the tree-ring sites may have been colder than indicated by the regional average minimum temperatures used to establish the critical thresholds for this study (e.g., 1926, 1940, and 1965). At the same time, minimum temperatures in the vicinity of all tree-ring sites in Texas on March 13, 1951 (a suggested false spring event not recorded by frost rings, Table 3) were generally above 24°F (-4.4°C), and only Brady recorded a temperature of 18°F. These observations suggest that a more accurate estimate of the critical low temperature required to produce frost injury to oak trees might be only 21°F (-6.1°C) based on the data for 1921 (Table 2). If correct, 1951 would not qualify as a false spring event, lowering the total number of such events to 16 and also lowering the underestimation bias of the frost ring record of

false spring perhaps to 19 percent (i.e., 13 of 16 events were registered by frost rings).

Many warm spell anomalies lasted much longer than 10 days (although in some cases not continuously), and many also greatly exceeded the 10-day mean minimum temperature threshold of 40°F (4.4°C) used to define false spring. Of the four false spring events not recorded by frost rings (Table 3), two occurred quite early in the season (March 5, 1917 in Texas; and March 24, 1966 in Missouri), and the warm spell which exceeded 40°F for the 10-day period was intense but very brief for two other events. These years meet the false spring

Table 3. Same as Table 2 for the four false spring events apparent in the three regional temperature averages between 1901 and 1980 that were not registered by frost rings in oak trees of the Southern Plains.

Year	Month	Day	State	Hard Freeze Minimum Temp. Average	Warm Spell Average Temp.	Warm Spell Coldest Daily Temp.
1917	3	5	TX	16.0	45.0	37.0
1948	3	11	TX	13.7	40.7	29.3
1951	3	13	TX	21.7	51.6	38.0
1966	3	24	MO	17.7	44.7	38.3

criteria listed above, but no significant frost ring damage was observed, suggesting that conditions prior to the 10-day warm spell may often be crucial to the susceptibility of these trees to the subsequent hard freeze (factors such as the

consistency of daily temperature levels, photoperiod, or moisture availability). It should be possible to define more specifically the temperature requirements for frost injury to deciduous oaks in the Southern Plains region, but ideally this would entail detailed micrometeorological observations at selected tree-ring sites distributed across the study area, or at the very least more detailed analyses of daily temperatures and extremes for an expanded network of weather stations.

As presently stated, the false spring definition given above is quite exclusive and less than 10 events not registered by frost rings even came close to the stated temperature thresholds. Only the four events in Table 3 which failed to induce frost injury actually fulfilled the criteria, and 1951 does so only marginally. Therefore, it seems safe to conclude from the available evidence that the frost ring record of false spring underestimates the true number of false spring events by approximately 24 percent, and this underestimation error might be narrowed by a more precise definition of the meteorological variables actually responsible for frost injury to oak trees. In fact, the frost ring chronology may not underestimate at all the true suite of meteorological variables actually responsible for this injury, although these variables have yet to be fully defined.

A more precise definition of the false spring signal is certainly desirable, but the apparent underestimation error

of approximately 24 percent associated with the simple definition used in this study does not preclude interesting observations concerning the past occurrence, intensity, and distribution of false spring events over the southcentral United States. This may be demonstrated by analyses comparing the chronology of all 17 observed false spring events with the 13 events registered by frost rings during the twentieth century. Using the 1918 to 1980 common period for Texas, Oklahoma and Missouri, the frequency of false spring occurrence is about 2.7 events per decade for events recorded in the meteorological data and about 2.1 per decade for events recorded by frost rings. Contingency table tests comparing the number of false spring events per decade (1918-1977) in the meteorological and frost ring data with their respective expected frequencies are essentially the same, no decade has a higher or lower number of false spring events than expected in either the meteorological or frost ring data.

Frost Ring Chronology: 1650 to 1980

The frost ring chronologies for all 42 sites in the Southern Plains region are illustrated in Figure 7 from 1650 to 1980. Figure 7 includes data from both living trees and historic timbers, so the ending and particularly the beginning dates of the chronologies vary substantially. Data prior to 1650 have not been included in this analyses because the number of available sites and specimens declines sharply.

However, these limited data suggest that another frost injury event occurred in Arkansas during 1637.

The frost ring data in Figure 7 are arranged by site in a roughly north-south scheme (top to bottom), and several patterns emerge. Frost injury is usually found at several sites within a given region, and with a few exceptions the Red River region marks an important north-south difference in the frost ring chronology (located approximately between sites 27 and 28 in Figure 7). The Texas frost ring chronology frequently does not correspond with the chronology observed north of the Red River, and these differences can be attributed to both the earlier onset of the growth in Texas, and to the occurrence of many false spring freeze events which failed to penetrate into central Texas. In several exceptional years, however, frost injury occurred at the vast majority of sites either north or south the Red River (e.g., 1716, 1779, 1826, 1828, 1870, 1920, 1921, 1955; Fig. 6).

Examining the frost ring data for just the modern chronologies in Figure 7, it is apparent that the incidence of frost injured rings tapers off to the north and to the south. As previously discussed, this probably reflects a decreased frequency of false spring episodes in southern Texas and in central Kansas and central Missouri, as well as a substantially later onset of growth in the north.

The frost ring data for the historic sites in Arkansas and Texas are listed at the top and bottom of Figure 7,

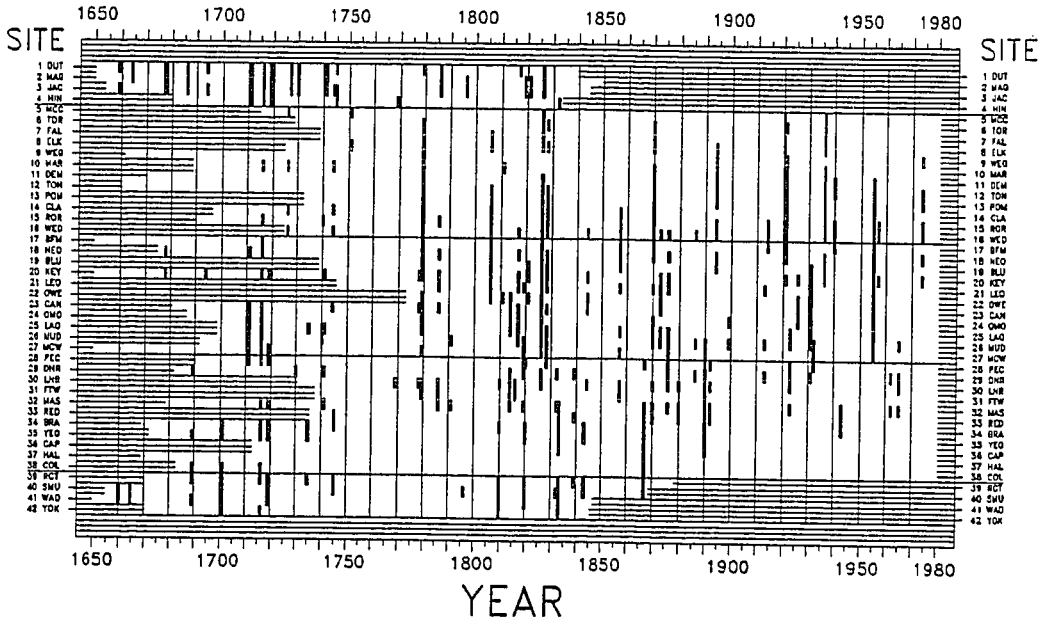

Figure 7. The frost ring chronologies based on post oak and white oak samples from all 42 collection sites in the Southern Plains region are illustrated from 1650 to 1980. Years with evidence for frost injury are identified for each collection site by a heavy vertical bar, which frequently join into long vertical bars during years of widespread frost injury at many sites in the Southern Plains region (e.g., 1779, 1826, 1920, 1955). The four frost ring chronologies based on historic timbers from Arkansas are listed at the top of the chart, and the four historic chronologies from Texas are listed at the bottom (sites 1-4 and 39-42, respectively). These historic collections begin during the mid-seventeenth century and end in the mid-nineteenth century, as indicated by the light horizontal lines. The "modern" frost ring chronologies based on living trees are arranged in a roughly north-south fashion beginning with site 5 in Kansas and ending with site 38 in southern Texas (refer to Table 1 and Figure 2 for additional site information and locations). All modern chronologies end in 1980 (or later), but begin as early as 1650 (e.g., sites 17, 20, and 27) or as late as 1772 (site 22), as indicated by the light horizontal lines. The horizontal line between site numbers 16 and 17 separate sites in Kansas, Missouri and Arkansas from Oklahoma sites, while the horizontal line between site numbers 27 and 28 approximates the Red River region and separates Oklahoma and Texas sites. While some exceptional freeze events resulted in anatomical damage across the entire Southern Plains (e.g., 1716, 1870), the frost ring chronology often differs north or south of the Red River region.

respectively. There are 24 frost events in the 200-year period covered by the historic chronologies for Arkansas, and most of these sites are actually located in or near the zone of highest frost ring frequency illustrated in Figure 6 on the basis of modern chronologies. There are only 13 frost rings during this same approximate interval in the historic chronologies from Texas, and this also probably reflects the decreased frequency of false spring episodes in Texas.

The approximate intensity of a given false spring episode is implied by the number of sites with significant frost injury (Fig. 7). However, due to microclimate differences not all tree-ring collection sites are equally sensitive to frost injury. Microclimatic differences between tree-ring sites, and between tree sites and weather stations may moderate the local effects of either the warm or cold phases of false spring, and may account for many of the spatial discontinuities in the frost ring data (Fig. 7 and Figures 8 to 43 below). For example, the tree-ring data for Red Rock, Texas, were obtained from two adjacent microsites in rolling terrain of only slight relief. Half of the trees were collected from an open upland position, while the other half were collected along a very broad and shallow valley bottom. Frost rings are prevalent on the upland site, but are virtually absent from the valley bottom site. These differences presumably reflect frequent cold air drainage through the valley site delaying the onset of spring growth

even during the warm spells of false spring, while warmer conditions prevailing at the higher site may favor early growth initiation and frost susceptibility.

In addition to the spatial changes in frost frequency, Figure 7 suggests that the occurrence of false spring events in the southcentral United States has not been randomly distributed through time. Some time periods with a notably low or high incidence of false spring seem to have occurred over the past 331 years. The period from 1746 to 1777 in particular stands out as a time of evidently few false spring anomalies, while during the time period from 1810 to 1828 false spring events appear to have been especially prevalent (Fig. 7).

Some of the apparent changes of frost ring frequency through time could simply reflect bias due to changes in the susceptibility of trees to frost injury with increasing age (e.g., LaMarche 1970), or to the declining number of sites available during the seventeenth and early eighteenth centuries (Fig. 7). Old-growth oak trees were preferentially sampled to develop the longest tree-ring chronologies possible for paleoclimatic reconstruction (Stahle et al. 1985a). Old trees typically exhibit a lower growth rate, reduced vigor, and probably experience a shorter growing season than would be typical of juvenile or mature trees (e.g., Fritts 1969; LaMarche 1970; Kramer and Kozlowski 1979). If old post and white oak trees tend to initiate growth later in the season

than younger trees, they will be vulnerable to fewer late season frosts. The frost ring chronology of some oak trees and sites definitely exhibit a decline in the frequency of frost rings with advanced age. For example, no frost rings were recorded in the last 90 years of the Fort Worth Nature Center post oak collection (Fig. 7). However, age bias is not as obvious in most frost ring chronologies in Figure 7. When considering the summary frost ring chronology for all available collection sites in the southcentral United States (Fig. 51 below), age bias has been ameliorated to a great extent by the large number of tree-ring sites (42), many of which include specimens from young, vigorous trees in all time periods.

A specific attempt was also made to evaluate and rectify possible age bias in the susceptibility to spring frost by sampling all age classes (young, mature and old trees) at four of the most frost sensitive tree-ring sites in the study area (i.e., Roaring River, MO; Wedington Mountain, AR; Keystone Lake, OK; and Mason Mountain, TX). Adding the frost ring data from the young trees to the data based on mature and old trees changed the frost ring chronology at only one of these sites. Two additional years with statistically significant evidence for frost injury were added to the chronology for Keystone Lake, Oklahoma. However, a small, non significant percentage of frost rings had previously been identified at Keystone for both years, and these years were also registered by other

tree-ring sites in the vicinity (Fig. 7).

Examination of the frost ring data for most individual collections in Figure 7 and summarized in for all collection sites in Figure 51 (below) indicates that the chronology of frost rings for the southcentral United States as a whole does not appear to be seriously biased by the decreasing susceptibility of old oak trees to spring frost injury. This conclusion is subtantiated by contingency table analyses of the frequency of frost injury through time. When the summary frost ring chronology from 1650 to 1980 (Figure 51) is subdivided into 20, 25, and 50 year intervals, the observed numbers of frost rings in the various intervals are not significantly higher or lower than the number expected by chance (data not shown). In all three tests, however, the observed number of frost years during the twentieth century equal or exceed the number of expected frosts.

Although the frost ring chronology for the southcentral United States as a whole does not appear to be seriously biased by an age-related change in frost susceptibility, the data in Figures 7 and 51 definitely suggest that the past occurrence of frost rings in this region has been nonrandom. This possible nonrandom secular variability will be evaluated in Chapter 6, after the meteorological implications of the frost ring chronology have been described.

A Brief Historical Summary of False Spring: 1650 to 1980

All 70 false spring years from 1650 to 1980 are summarized in chronological order below. Each summary includes a map locating all tree-ring sites available during a given year, and those sites with statistically significant evidence for frost injury (Figures 8 to 21, 24, 29, 34 and 39). Beginning in 1899, daily synoptic weather maps are presented describing selected meteorological conditions during the warm and cold phases of false spring (Figures 22, 25-28, 30-33, 35-38, and 40-43). The discussions of each false spring event include estimates of the intensity of frost damage (based only on the number of tree-ring sites affected and/or the severity of the available frost ring lesions), a review of any corroborative documentary evidence for specific false spring events, and after 1899 a discussion of the available meteorological evidence for false spring.

The number of sites with frost injury in a given year provides a rough intensity measure of the false spring event, and this tree-ring based estimate can sometimes be substantiated with documentary evidence concerning crop damage or meteorological data on weather conditions. The intensity of false spring episodes should normally be evaluated by considering sites located either north or south of the Red River, due to frequent latitudinal differences in phenological development and/or the southern penetration of critical subfreezing temperatures required to produce frost rings. In

many cases, the distribution of frost-injured sites define the approximate southern boundary of the critical 23°F isotherm associated with frost rings in oak trees (e.g., Fig. 38B). However, some cases of discontinuous frost injury may only reflect inadequate replication for a given year at a particular tree-ring site, or microclimatic differences between sites which can moderate or amplify the local temperature effects of false spring (e.g., Fig. 26B below).

Daily weather maps available for the Northern Hemisphere since 1895 and for the United States since 1899 were examined during years of frost injury in order to identify the essential meteorological features of false spring. Two composite weather maps are presented for each frost year from 1899 to 1974. These composite maps depict selected weather variables observed during the height of the warm and cold phases of each false spring year. The specific weather variables included were selected for the purpose of depicting the temperature and circulation patterns of false spring. These weather variables include the position of warm and cold fronts, surface winds, the critical 23°F isotherm, the 60°F maximum temperature isotherm during the warm phase, low and high pressure centers at the surface and 500 mb level, upper level winds and confluent zones, and air mass types. All weather variables and symbols used in the following synoptic maps are identified in the legend on Fig. 23.

The surface weather variables were mapped for all 17

false spring episodes since 1899, but upper level data were available only for the five most recent frost events (after 1947). Upper air flow is a particularly important feature of false spring, and it changes dramatically from the warm to cold phase of many false spring events. The general upper air flow is represented by the 500 mb wind maxima for events after 1947, and the tracks of low and high pressure centers are used as a surrogate for the upper air flow for events prior to 1947. These pressure center tracks conform reasonably well to the upper level flow pattern (e.g., Harman 1971; Anderson and Gyakum 1989), as can be seen in the maps for 1955, 1957, 1962, 1965, and 1974 when both pressure center tracks and 500 mb wind maxima are mapped (Figures 38 and 40-43). The daily 700 mb isotherms were obtained for only the 1962, 1965, and 1974 false spring episodes, and are used as a surrogate for 500-1000 mb thickness data in order to make inferences concerning large-scale temperature advection during the warm and cold phases of false spring (these data are not illustrated on the synoptic maps).

Two qualifications should be made concerning the synoptic weather maps of false spring events after 1899. First, the time of surface weather observations changed from 1899 to 1974, and the surface and upper level observation times are not precisely matched in all cases after 1947. All surface and upper level observation times are noted in the caption for each synoptic map. Second, some subjectivity was involved in

the selection of specific days to be mapped for each false spring event. The date of the hard freeze was easily identified in most cases by the lowest subfreezing temperature. When severely cold temperatures persisted for several days, such as during 1955, the first day below the subfreezing threshold was mapped. More subjectivity was usually involved in selecting a particular day during the warm spell for composite mapping. In all cases, however, the warm day selected for mapping occurred within the 13 day period prior to the hard freeze used to specifically define false spring (see above). The warm day mapped was usually also at or very near the peak warmth, and was often fairly typical of other days during the warm spell.

Based on the timing of frost events in the twentieth century, the cold wave associated with false spring in Texas usually occurs during the first three weeks of March, and between March 20 and April 15 in Oklahoma and Missouri. The preceding warm spell in both regions typically persists from two to four weeks, althouth mild temperatures may prevail all winter.

1659 Frost injury occurred only in Arkansas at 2 out of 7 sites north of the Red River (or 9 total sites, Fig. 8A).

1660 Frost injury was restricted to Texas, and occurred at both available sites south of the Red River (9 total sites,

Fig. 8B).

1664 Frost injury was found from central Texas to northern Arkansas at 4 of 11 total sites in the study area (Fig. 9A).

1667 Frost injury occurred in northern Arkansas at 3 of 10 sites north of the Red River (17 total, Fig. 9B).

1678 Frost injury occurred in northern Oklahoma and Arkansas at 5 of 10 sites (17 total, Fig. 9C).

1686 Frost injury occurred in northern Arkansas at 3 of 12 sites (22 total, Fig. 9D).

1689 Frost injury occurred in Texas at 5 of 10 sites south of the Red River (23 total, Fig. 10A).

1694 Scattered frost injury occurred in northern Oklahoma and Arkansas at 3 of 16 sites north of the Red River (27 total, Fig. 10B).

1701 Widespread and intense frost injury was found at 7 of 11 sites in Texas (29 total, Fig. 10C).

1711 Widespread and intense frost injury was found at 11 of 19 sites in Oklahoma and Arkansas (29 total, Fig. 10D).

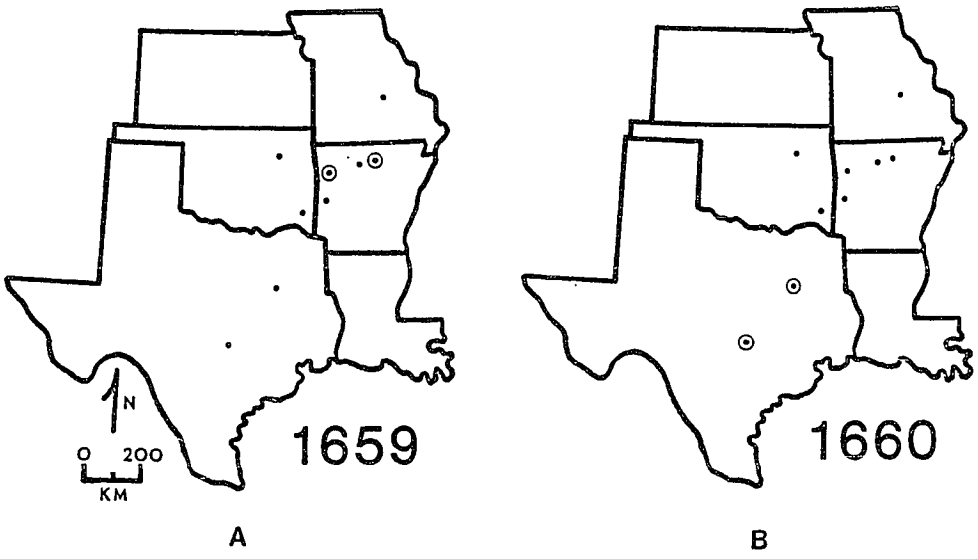

Figure 8. Frost injury in 1659 and 1660. The distribution of all available tree-ring collection sites that date to 1659 and 1660 are indicated by solid dots, and the location of sites which exhibit a statistically significant incidence of frost damaged rings in 1659 and 1660 are located by the circled dots (A = 1659, B = 1660).

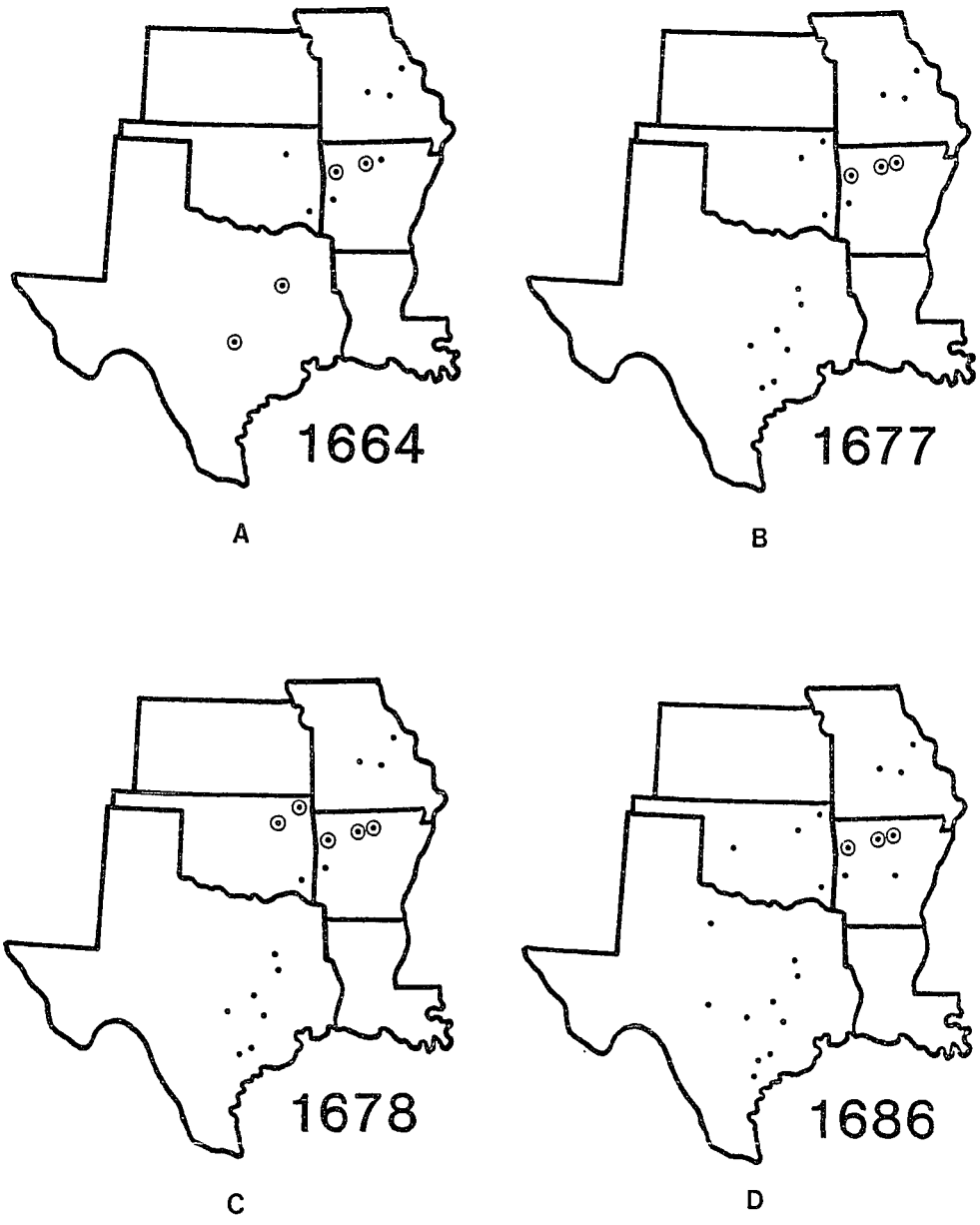

Figure 9. Same as Figure 8 for 1664(A), 1677(B), 1678(C), and 1686.

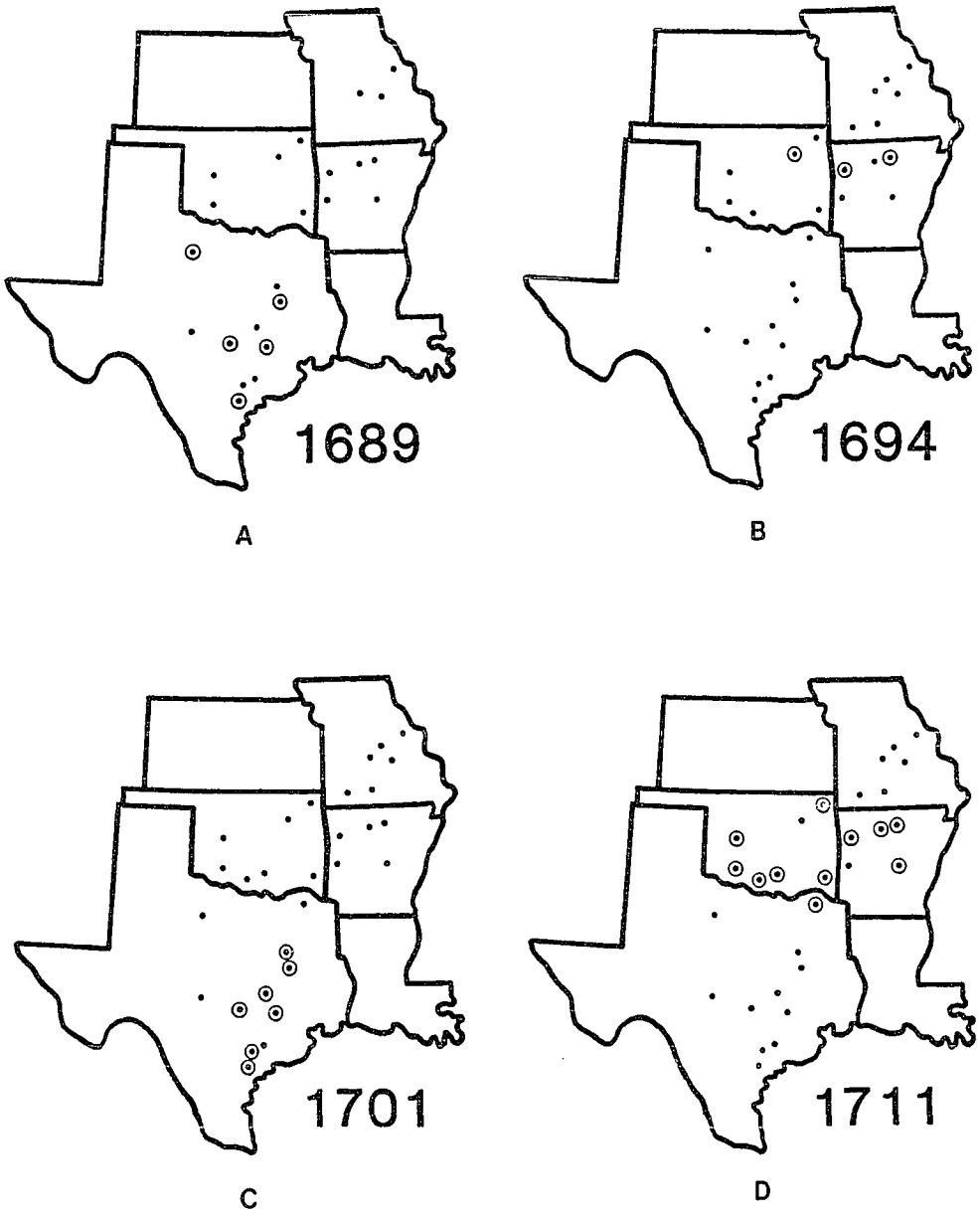

Figure 10. Same as Figure 8 for 1689(A), 1694(B), 1701(C), and 1711(D).

1716 Intense frost injury was very prevalent at 21 sites extending from central Missouri all the way to southern Texas (out of a total of 31 sites dating to 1716, Fig. 11A). The frost injury of 1716 occurred across a larger portion of the southcentral United States than in any other year from 1650 to 1980. The intensity of frost injury in 1716, reflected by the number of sites affected, was exceeded only in 1779 and 1826. However, two separate false spring events might have occurred in 1716, one in early to mid-March in Texas and a second event in late-March or April in the Missouri-northern Oklahoma region. Alternatively, an intense freeze event in mid-to late March following a very pronounced region-wide warm spell might have produced the observed injury.

1719 Another intense and widespread frost ring event occurred at 13 out of a region-wide total of 31 sites from southern Texas into northern Arkansas in 1719 (Fig. 11B). The frost rings of 1701, 1711, 1716, and 1719 are the most prominent recorded in the first 129 years of the frost ring chronology (until 1779), and are very useful for crossdating purposes.

1726 Scattered frost injury occurred in Kansas, Missouri and northern Arkansas at 4 of 21 sites north of the Red River (33 total, Fig. 11C).

1727 Frost injury occurred in northern Arkansas at a cluster

of 3 out of 21 sites north of the Red River (33 total, Fig. 11D).

1730 Scattered frost injury in northern Arkansas and northcentral Texas occurred at only 4 of 34 total sites (Fig. 12A).

1735 Scattered frost injury occurred in southern Oklahoma and Texas at 4 of 13 nearby sites (or 34 total sites available regionwide, Fig. 12B).

1740 Scattered frost injury occurred in southern Oklahoma and north Arkansas-southwest Missouri at 6 of 25 sites north of the Red River (40 total, Fig. 12C).

1741 Frost injury occurred on a scattered basis from central Texas to northern Arkansas at 7 sites, out of a total of 40 dating to this period in the whole study area (Fig. 12D). A hard winter occurred in 1740-1741 on the Atlantic seaboard, and included severe cold in November and February, and thaws in early December and late January (Ludlum 1984, 20). Rivers in the northeast area remained frozen until mid-April (Ludlum 1984, 20).

1744 Scattered frost injury occurred from western Oklahoma into central Missouri at 5 of 25 sites north of the Red River

(40 total, Fig. 13A). The winter of 1740-1741 was one of the two most severe of the eighteenth century in the northeast, and the three months from December to February were the coldest in the early temperature record for Charleston, South Carolina (1738 to 1761; Ludlum 1966, 140).

1745 Scattered frost injury occurred in central Texas and northern Arkansas at 7 out of 40 sites in the entire study area (Fig. 13B). The occurrence of anomalous weather during 1745 is also suggested by the "sudden change" in temperature recorded at Charleston, South Carolina, where temperatures fell from 70°F on January 10 to 26°F the following morning (Ludlum 1966, 141).

1751 Frost injury occurred on a limited basis at only 2 sites in eastern Kansas (out of 26 north of the Red River, and 41 sites overall, Fig. 13C).

1769 Limited frost injury occurred in central Texas and central Arkansas at only 2 sites out of 41 total in the study area (Fig. 13D). The 17-year period from 1752 to 1768 is the longest period without frost injury in the entire chronology. Considerable confidence can be placed on this frost-ring-free period because hundreds of dated tree-ring specimens are available during this interval at 41 of the 42 different collection sites.

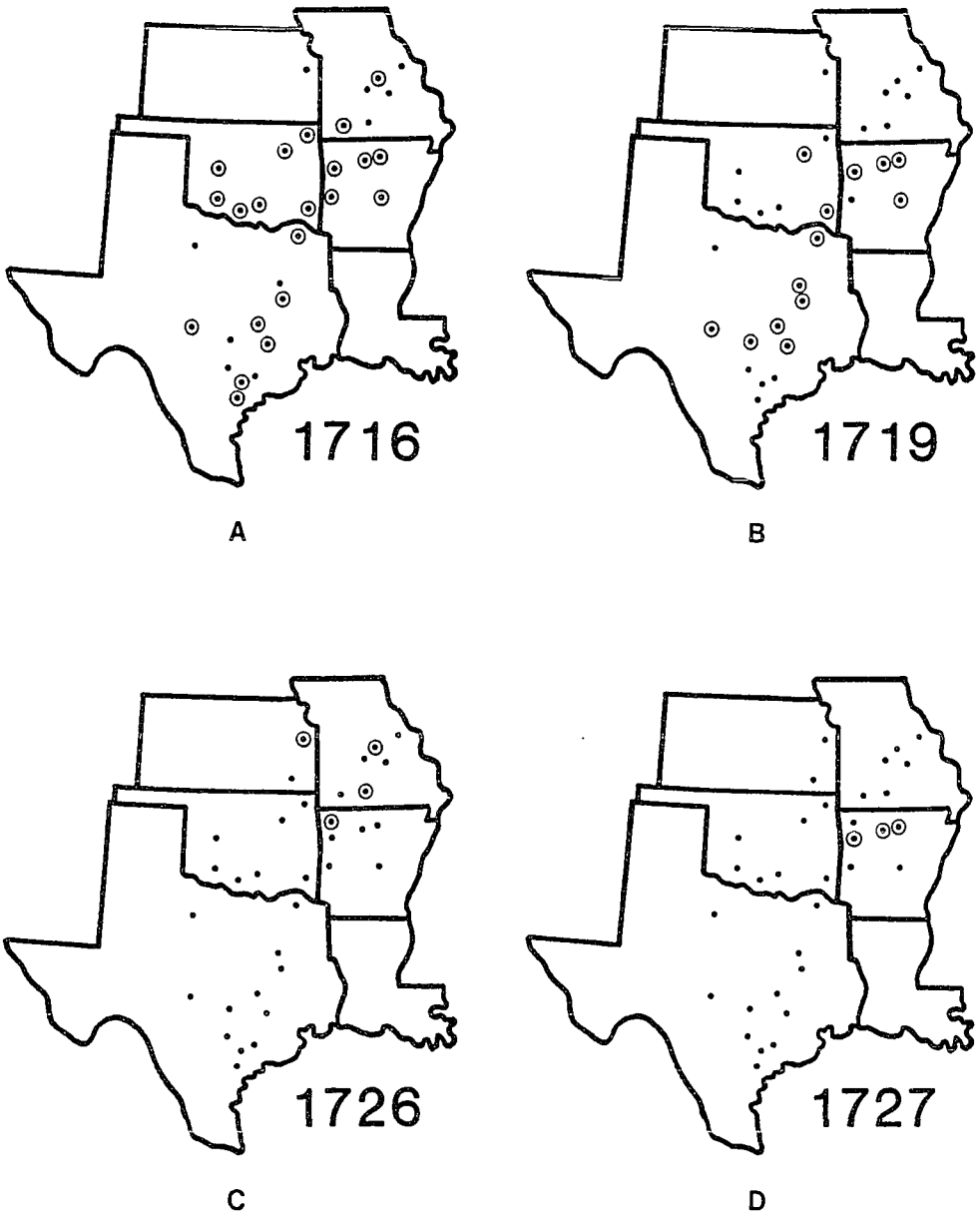

Figure 11. Same as Figure 8 for 1716(A), 1719(B), 1726(C), and 1727(D).

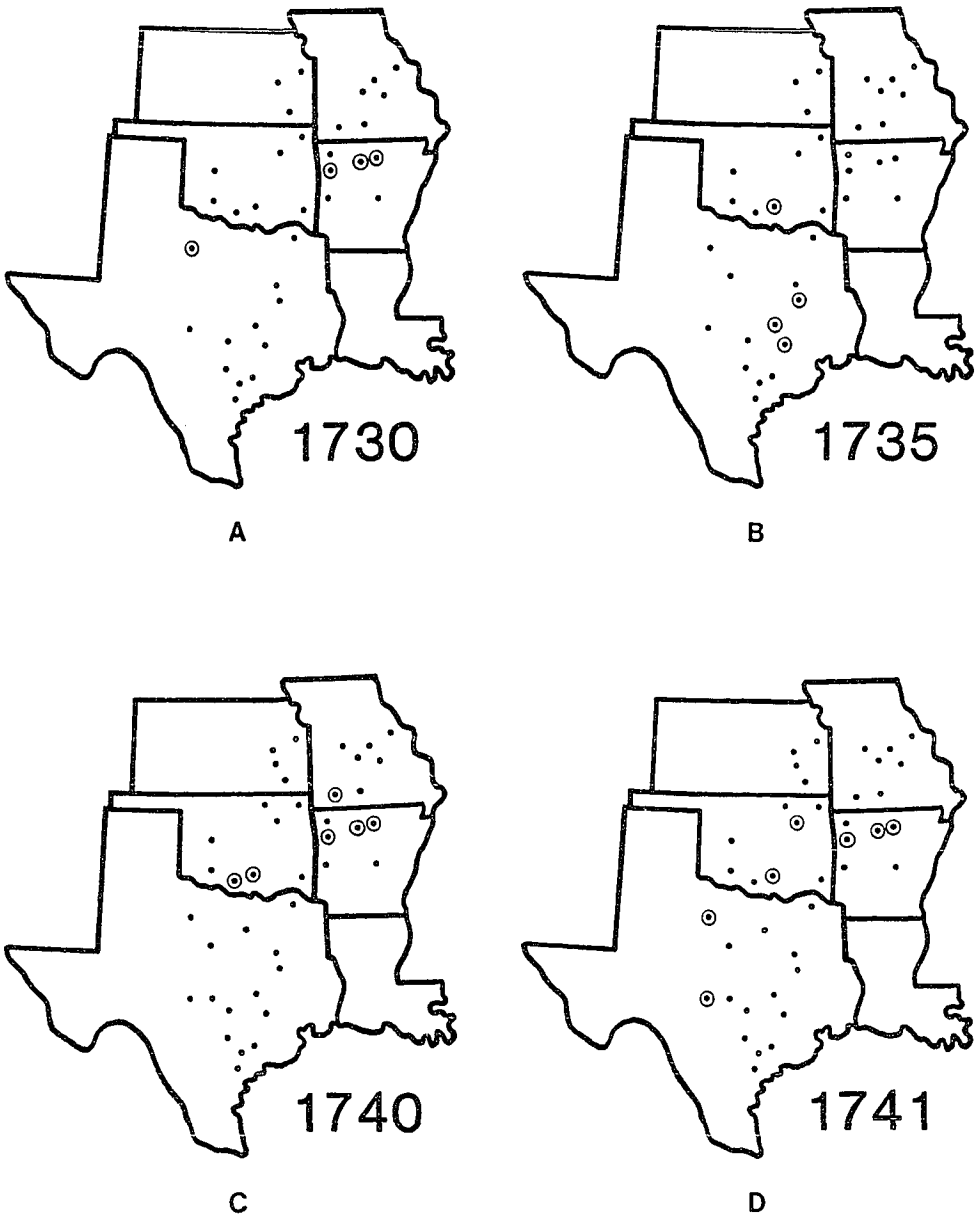

Figure 12. Same as Figure 8 for 1730(A), 1735(B), 1740(C), and 1741(D).

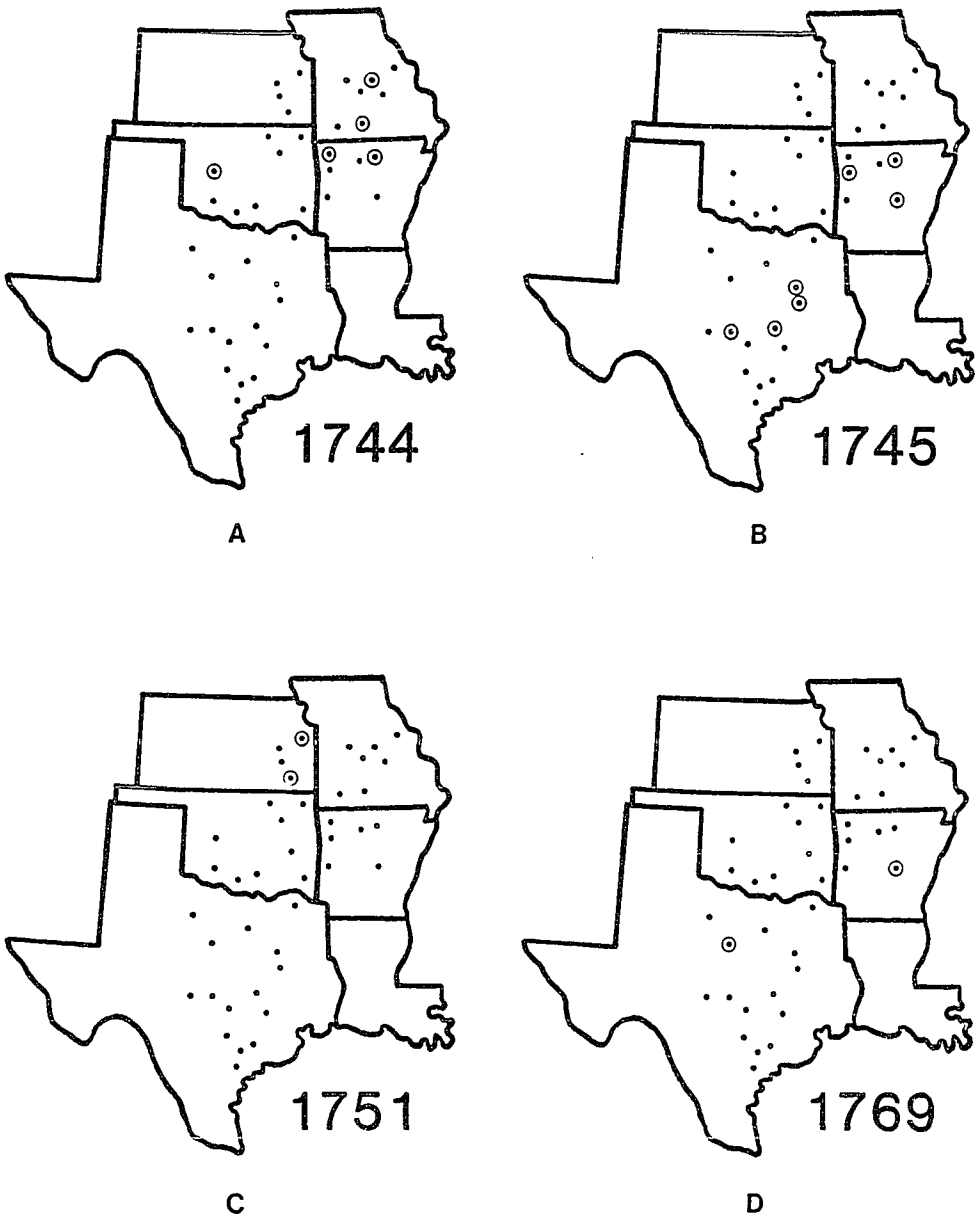

Figure 13. Same as Figure 8 for 1744(A), 1745(B), 1751(C), and 1769(D).

1778 Scattered frost injury occurred in Oklahoma and central Texas at only 3 of 42 total sites (Fig. 14A).

1779 Intense frost injury occurred at most tree-ring sites from northern Texas into central Missouri (23 out of 42 total sites, Fig. 14B). In terms of the number of sites affected, the intensity of the false spring event in 1779 was exceeded only once in 1826, when 26 sites recorded frost injury. While no direct connection can be claimed, it may be more than coincidence that the following winter of 1779-1780 was the "coldest ever known" in Louisiana (Ludlum 1966, 151), and may have been the most severe in American history (Ludlum 1984, 25).

1786 Frost injury occurred from central Texas into northern Oklahoma, Arkansas, and southernmost Missouri at 11 of 42 total sites (Fig. 14C). A "backward spring" occurred in New Hampshire during 1786 (Ludlum 1966, 86).

1791 Frost injury occurred at only 2 sites in Texas and Oklahoma (out of 42 total sites, Fig. 14D).

1796 Frost injury occurred at only 3 sites in Texas and Arkansas (out of 42 total sites, Fig. 15A).

1806 Frost injury occurred in Oklahoma, Kansas and Missouri

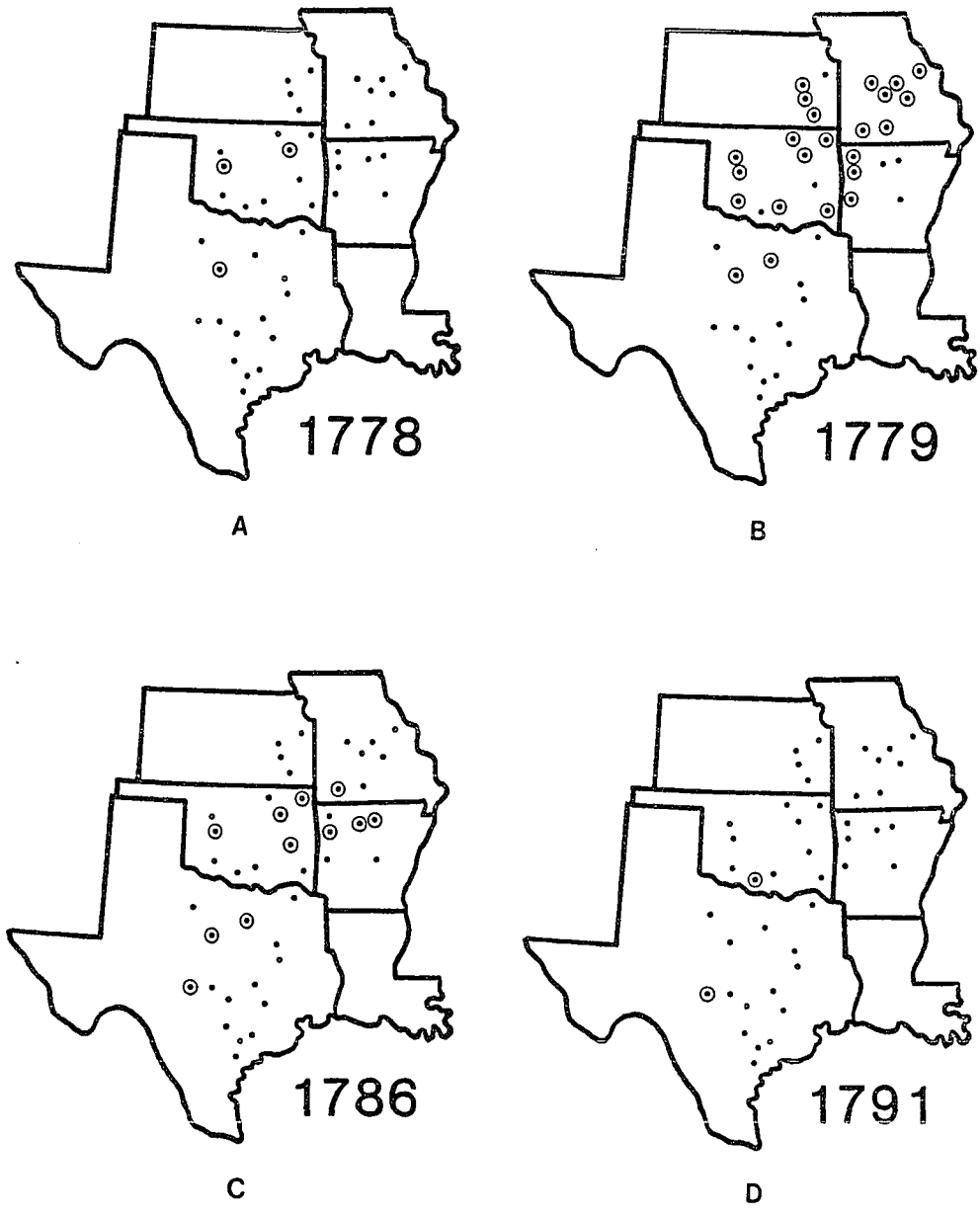

Figure 14. Same as Figure 8 for 1778(A), 1779(B), 1786(C), and 1791(D).

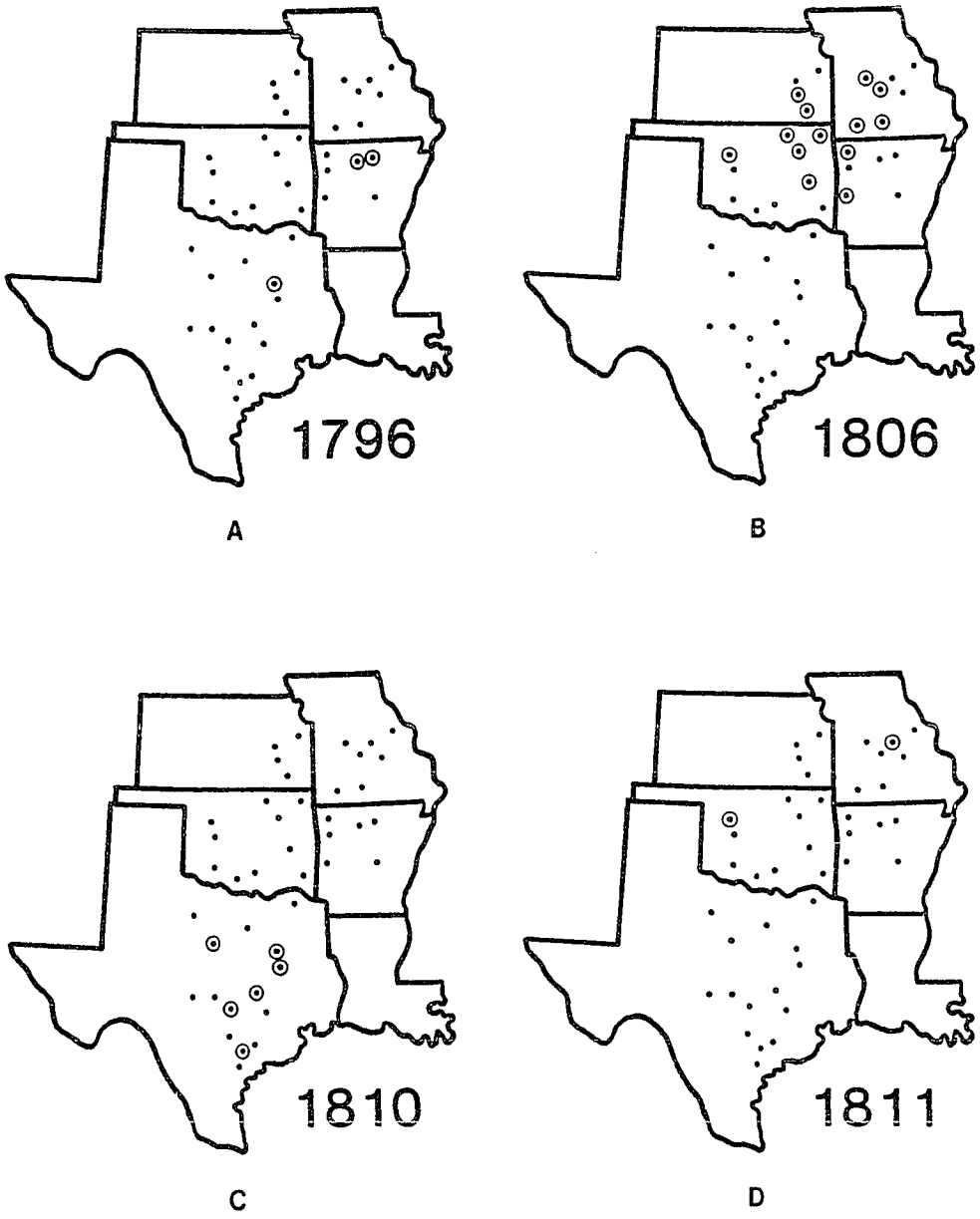

Figure 15. Same as Figure 8 for 1796(A), 1806(B), 1810(C), and 1811(D).

at 13 of 27 sites north of the Red River (42 total, Fig. 15B).

1810 Frost injury occurred in Texas at 6 of 15 sites south of the Red River (42 total, Fig. 15C). Based on the early weather observations of William Dunbar near Natchez, Mississippi, this frost event probably occurred on March 13, 1810 (Ludlum 1966, 204). Dunbar reported a hail storm with one inch diameter hailstones associated with the passage of the cold front. He recorded a temperature of 62°F at 9 P.M. on March 12th, and 35°F at 6 A.M. on the 13th. It seems likely that temperatures may have fallen well below freezing on the 13th or 14th in the central Texas area of frost injury (Fig. 15C).

1811 Frost injury occurred at only two widely separated sites in Oklahoma and Missouri, out of 27 sites available north of the Red River, and 42 overall (Fig. 15D).

1814 Frost injury occurred in Oklahoma and Texas at 8 of 42 total sites (Fig. 16A). A warm winter was recorded in eastern Ohio during 1813-1814 (Ludlum 1966, 236). Warm temperatures reached 65°F on February 13, 1814, but a cold wave in early March resulted in the coldest temperatures of the winter (-2°F, March 1). This outbreak of cold air in early March may have penetrated into Oklahoma and Texas to produce the observed frost injury.

1816 Frost injury occurred at only two adjacent sites in northcentral Texas (out of 15 sites south of the Red River, and 42 total, Fig. 16B). 1816 was the "year without a summer" in the northeastern United States, and included a "backward spring" with record late snows in June (Ludlum 1966, 190).

1817 Frost injury occurred in Oklahoma and Arkansas at 9 of 27 sites north of the Red River (42 total, Fig. 16C). In North Carolina, it froze very hard at night during the week of March 21, 1817, followed by warm weather and a temperature of 83°F on March 25th, and then a March 28 to 30 snow storm which was not melted away until April 3 (Ludlum 1966, 208). These weather conditions in North Carolina may have been part of the same storm systems that caused frost injury in Oklahoma and Arkansas.

1819 Frost injury occurred on a scattered basis from central Texas into northern Arkansas at 8 of 42 total sites (Fig. 16D).

1820 Frost injury recurred at 6 of 15 sites in Texas (Fig. 17A). In North Carolina, weather was unusually warm during mid-February, and "a hard storm from the northwest" brought "piercingly cold" temperatures as low as -10°F on March 3 (Ludlum 1966, 209). Hickman (1920) also cites evidence for an early March snow storm at Little Rock, Arkansas, and this

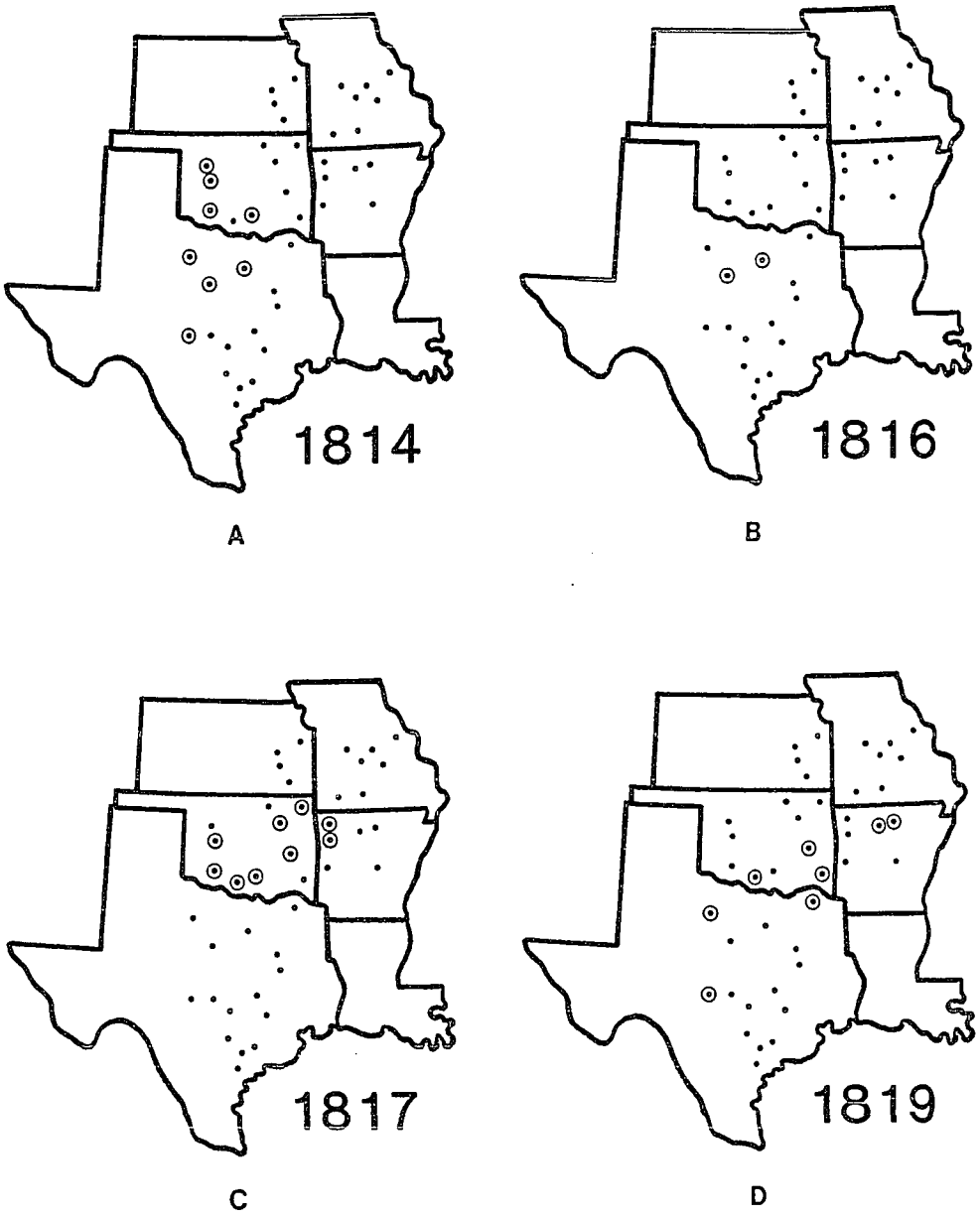

Figure 16. Same as Figure 8 for 1814(A), 1816(B), 1817(C), and 1819(D).

same storm system may have caused the frost injury observed in Texas.

1821 Frost injury occurred in northern Oklahoma and Arkansas at 5 of 27 sites north of the Red River (42 total, Fig. 17B). Hickman's (1920) sources indicate that the winter of 1820-1821 in Arkansas was the most severe in 40 years. Temperatures during the winter of 1820-1821 also averaged below normal in the Midwest (e.g., Ohio, Illinois, Wisconsin, Minnesota), but February temperatures were well above normal and actually exceeded the average for March (Ludlum 1968, 139).

1826 Intense frost injury occurred at most tree-ring sites in Missouri, Kansas, Arkansas, Oklahoma, and northern Texas (Fig. 17C). Significant frost injury was noted at 26 of 30 sites north of northern Texas, and a vast majority of trees available at many sites exhibit frost damage. Frost injury occurred at more sites during 1826 than in any other year from 1650 to 1980, and 1826 is easily the most dramatic example of frost injury and false spring in the entire data set. However, there is very little direct meteorological or documentary evidence concerning what must have been a severe freeze event in late March or early April, 1826. Henry Tooley's temperature record for Natchez, Mississippi, from 1825 to 1850 is summarized on a monthly basis by Ludlum (1968, 117). March, 1826 had the second warmest average temperature for the 26-

Natchez during March, 1826, was only 46°F (Ludlum 1968, 117). These observations suggest that the cold wave came in April 1826, which would be consistent with the distribution of frost damaged rings in the northern portion of the study area (Figure 17C). Temperature data for Ft. Snelling, Minnesota, indicates a late spring, with a temperature of 4°F on April 10, 1826 (Ludlum 1968, 184). Hickman (1920) states that the spring of 1826 was late in Arkansas, and the Arkansas Gazette (1826) reported on March 7, 1826 that spring was opening after warm, wet weather for some time. Peach trees had been in bloom for weeks near Little Rock (Arkansas Gazette 1826). On March 28, the Arkansas Gazette (1826) noted that the "severity of cold has been greater to the north during the present winter than for several seasons", without identifying the specific region being referred to. Because little specific reference was made to a severe spring freeze in 1826, the damaging effects of this intense false spring episode may have been largely confined to the Southern Plains region.

1828 Frost injury in 1828 occurred over the same general area affected by the intense event of 1826, but fewer sites exhibit significant frost damage (i.e., 16 sites out of 27 north of the Red River, and 42 sites overall, Fig. 17D). Unlike 1826, there are many varied and vivid accounts of the damaging false spring event of 1828. Ludlum's (1968, 97) description of the

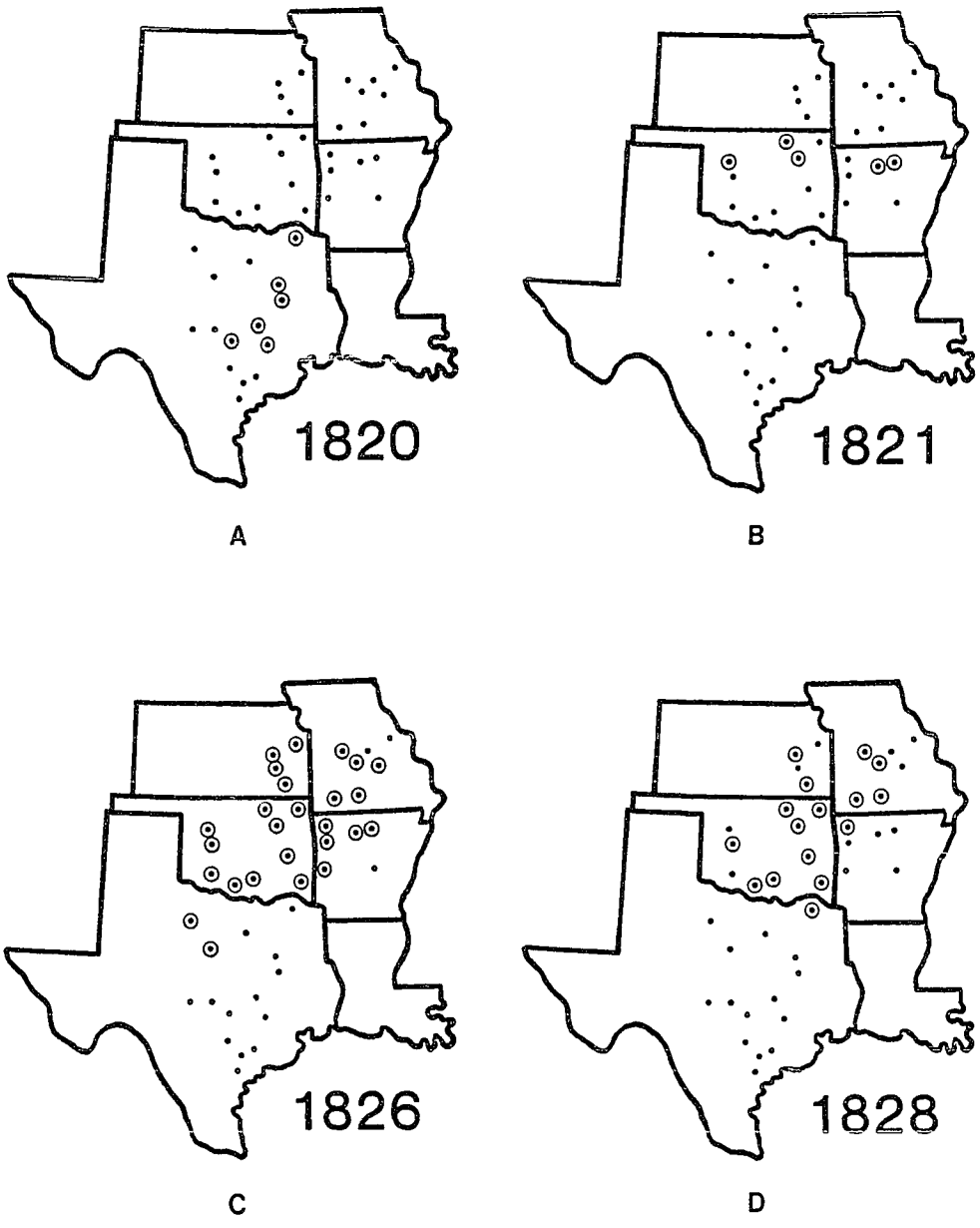

Figure 17. Same as Figure 8 for 1820(A), 1821(B), 1826(C), and 1828(D).

of the warm winter conditions is particularly graphic: "The winter season of 1827-1828, or more truly the lack of it, constituted an outstanding event in the meteorological history of the eastern half of the United States. No other winter in our period was so warm. The wide geographical extent and the unbroken duration of the warmth appeared to be unique in the American experience. The consistent above normal zone extended from the Gulf of Mexico to Canada and westward encompassed all settled sections of the United States."

The warm winter of 1826 was certainly an exceptional event, but the frost ring data strongly suggest that the warmth of 1828 was not unprecedented. If better meteorological records were available, conditions during 1826, 1806, 1779, 1719, 1716, and 1711 might well prove to have been comparable or even more unusual.

Nevertheless, the weather and crop conditions of 1828 were remarkable, and have been reasonably well documented. Peach trees near Little Rock, Arkansas, blossomed at Christmas (Hickman 1920) and were blooming by February 6 (Arkansas Gazette 1828a). Frogs began their seasonal croaking on March 24th in Ohio (Ludlum 1968, 141). False spring was terminated in early April when a subfreezing air mass moved southward and penetrated to the Gulf of Mexico and central Florida (Ludlum 1968, 97). This cold wave destroyed fruit trees and crops across the South, and as a result of the "remarkably cold" weather the "young leaves of oaks and many other forest trees

have changed their color to a dark hue" in the forests around Little Rock, Arkansas (Arkansas Gazette 1828b).

1832 Scattered frost injury occurred from central Texas into central Arkansas at 4 of 42 total sites (Fig. 18A). This freeze damage probably occurred in early March because the mean monthly temperature of 60°F recorded by Henry Tooley at Natchez tied for the second warmest in 26 years (1832-1850, Ludlum 1968, 117), and the White River at Batesville, Arkansas, froze over on February 29, 1832 (Hickman 1920). Overall, the winter of 1831-1832 appears to have been colder than average in the southcentral United States (e.g., Hickman 1920), and the lowest December mean temperature from 1825 to 1850 was recorded for 1831 (Ludlum 1968, 117).

1833 Intense frost injury occurred only in central Texas at 9 of 15 sites south of the Red River (Fig. 18B). Along with 1701, 1867, and 1890, 1833 is among the most prominent years of frost injury in Texas since 1650. The available secondary sources all indicate that the winter of 1832-1833 was very mild, but that an intense cold wave may have penetrated into Texas early in March. Henry Tooley's data for Natchez, Mississippi, indicates that December of 1832 was the warmest December, and February 1833 was the third warmest February from 1825 to 1850 (Ludlum 1968, 117). The evidence also indicates that the winter was mild in Arkansas (Hickman 1920),

Ohio, and Minnesota (Ludlum 1968, 141). However, a minimum daily temperature of 25°F was recorded at Natchez sometime during March (Ludlum 1968, 117), probably during or after March 1st or 2nd when the coldest days of the entire winter, with low temperatures of -14°F and -20°F, were recorded at Ft. Snelling, Minnesota (near Minneapolis, Ludlum 1968, 187). The frost ring data indicate that subfreezing air penetrated to the Gulf of Mexico in 1833, probably during the first week of March.

1839 Scattered frost injury occurred at only 3 of 15 sites in Texas (or 41 total sites, Fig. 18C). January and February temperatures were above normal and two cold spells occurred during the first two weeks of March at Ft. Snelling, Minnesota (Ludlum 1968, 186). The third lowest 5 A.M. March temperature from 1825 to 1850 was recorded at Natchez in 1839 (27°F, Ludlum 1968, 117).

1843 Frost injury occurred in east-central Texas at 4 of 15 Texas sites (or 40 total sites, Fig. 18D). The winter of 1842-1843 was one of the longest and most severe in the history of the eastern United States, although "a spectacular circulation reversal of about a months duration" made January relatively warm in the Northeast, Midwest and South (Ludlum 1968, 42, 104, 153). Dr. Nathan Smith recorded the lowest average temperature of any month from 1840 to 1860 at Washington,

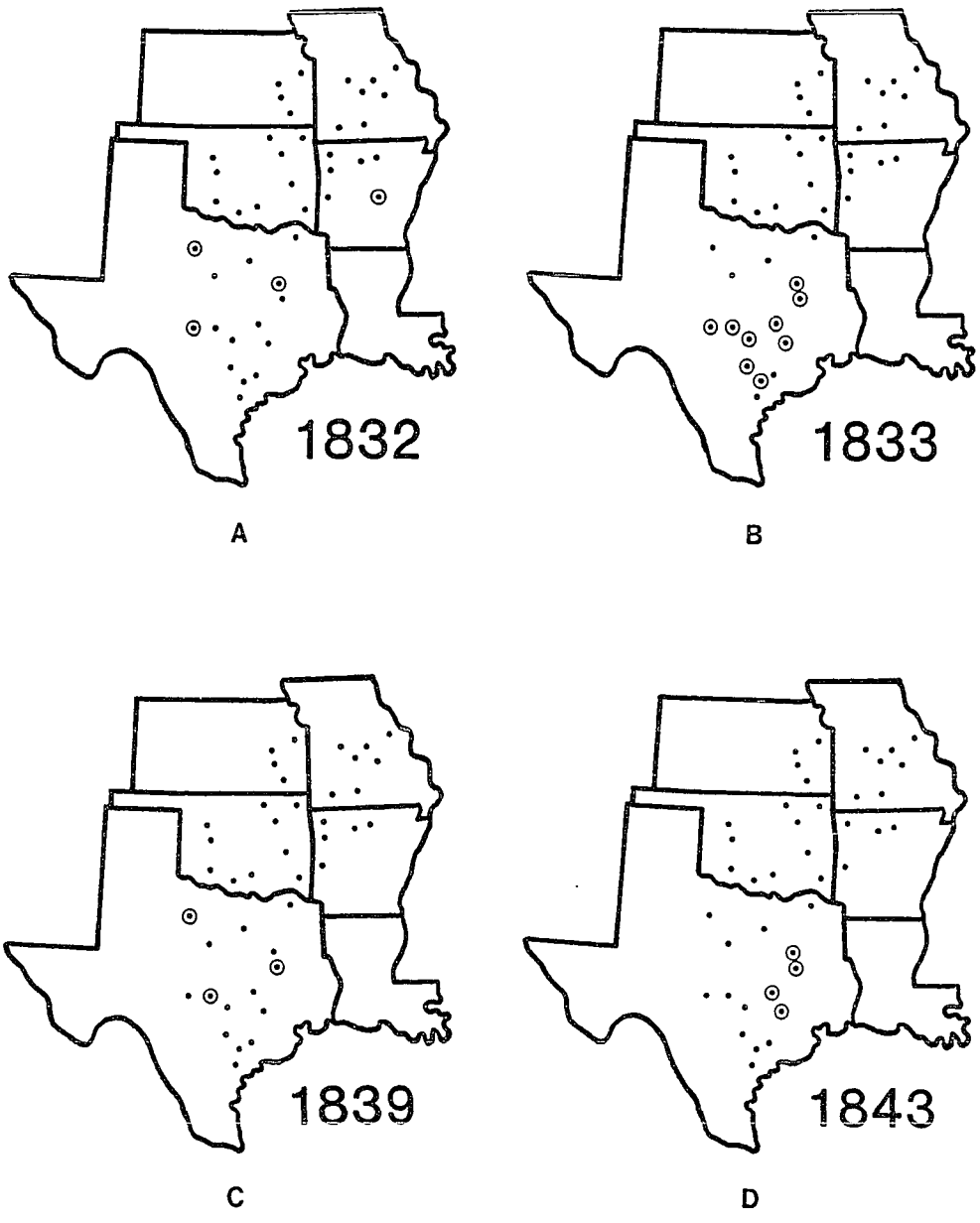

Figure 18. Same as Figure 8 for 1832(A), 1833(B), 1839(C), and 1843(D).

Arkansas, in March of 1843 (Ludlum 1968, 119). The lowest average March temperature from 1825 to 1850 was also recorded by Henry Tooley at Natchez in 1843, including a 5 A.M. temperature of 23°F sometime during March of 1843 (Ludlum 1968, 117). The hard freeze responsible for the frost injury in Texas may have occurred on March 16, 1843 when a minimum of 6°F was recorded by Dr. Smith at Washington, Arkansas (Ludlum 1968, 105).

1844 Scattered frost injury occurred in north Texas, northern Oklahoma and northwest Arkansas at 5 of 40 total sites (Fig. 19A). No meteorological or documentary evidence has been found to verify the occurrence of a false spring episode in the Southern Plains during 1844.

1857 Intense frost injury occurred from northern Texas into southern Missouri at 11 of 36 total sites in the study area (Fig. 19B). The winter of 1857 was characterized by a series of widely divergent temperature anomalies over the central United States, including a backward spring (Ludlum 1968). The average temperature for January set record or near record lows in Minnesota, Ohio, and Arkansas, while February of 1857 was the warmest February from 1840 to 1859 at Washington, Arkansas, and was also record or near record warm in Ohio (Ludlum 1968, 119, 139). March and April were cold months again in the central United States (Ludlum 1968), and the

frost damage probably occurred on or after April 7 when snow fell in every state and the temperature fell to 21°F (-6°C) at Houston, Texas (Ludlum 1982, 71). The temperature at Little Rock, Arkansas fell to 31°F on April 10 (Arkansas Gazette 1857), and Hickman (1920) states that cold weather in April of 1857 damaged fruit, vegetables and corn.

1867 Intense frost injury occurred in Texas at 10 of 13 sites south of the Red River (or 36 total, Fig. 19C). February appears to have been warm and March cold over the southcentral United States. At St. Louis, Missouri, the average monthly temperature was the fourth warmest for any February from 1836 to 1870, while the average March temperature was the second coldest for March over the same period (Ludlum 1968, 211). It was the coldest March in Minnesota since 1843 (Ludlum 1968, 207). The Texas frost damage may have occurred around March 5th, when snow fell at Little Rock, Arkansas, or perhaps after March 13th when the temperature fell to -20°F in Minnesota (Ludlum 1968, 207).

1870 One of the most intense and widespread frost ring events occurred in 1870 at 19 of 35 total sites located from central Texas into eastern Kansas (Fig. 19D). False spring weather anomalies are reasonably well documented for 1870, and these data along with the wide distribution of frost damage suggest that there might have been two separate freeze events, the

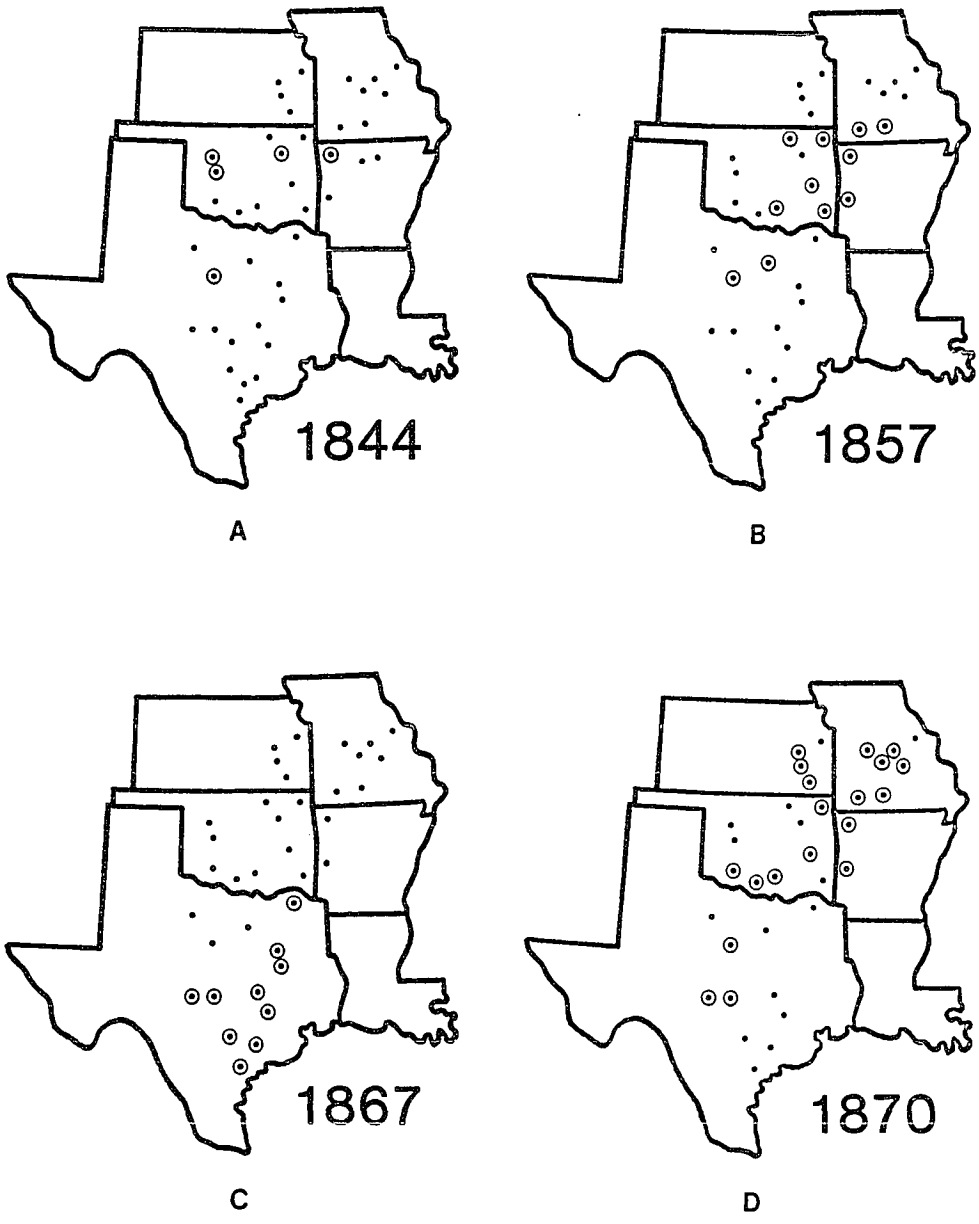

Figure 19. Same as Figure 8 for 1844(A), 1857(B), 1867(C), and 1870(D).

first causing damage in Texas, and a second cold wave causing damage further north. December through late February were unusually warm in Iowa (Ludlum 1968, 175) and Arkansas (Hickman 1920). Peach blossom began to bloom by February 17 near Little Rock, Arkansas (Arkansas Gazette 1870a). March turned cold and "The Great March Blizzard" struck Iowa on March 14, 1870, with temperatures falling as low as 0°F during the next two to four days. This cold wave may have been responsible for all of the frost rings observed in 1870, although spring was reported to have been late in Little Rock (Hickman 1920), with snow on April 17 and subfreezing weather on April 19 (Arkansas Gazette 1870b). It is possible that the March 14 cold wave damaged trees only in the southern portion of the study area, and the later cold wave of April may have damaged trees further north. The Arkansas Gazette (1870b) noted that the April 19 freeze may have destroyed the fruit crop.

1873 Frost injury occurred over most of Oklahoma and into western Arkansas at 7 our of 23 sites north of the Red River (or 35 total, Fig. 20A). Frost damage may have occurred during the three day "Easter Blizzard" that struck Kansas, Nebraska, and South Dakota on April 14th (Ludlum 1982, 73). This is supported by weather summaries published by the War Department which do not mention any particularly severe cold waves during March, but do refer to prevailing southerly winds

during the first week of April followed by a "severe norther" on April 15th in Texas (War Department 1873). The storm center associated with this Easter cold wave passed over Missouri and moved to the northeast "as a very severe storm along the New England coast" (War Department 1873), and was probably a nor'easter.

1876 Frost injury occurred from central Texas into northwest Arkansas at 11 of 35 total sites (Fig. 20B). On March 24th, the Arkansas Gazette (1876) reported that a damaging frost had just swept across Arkansas, and cited the following descriptions: "There will not be a peach produced in Garland County [west-central Arkansas] this summer, judging from the present appearances" and "peach leaves...have been deadened by the recent cold weather."

1880 Frost injury occurred in central Texas at 3 of 11 sites south of the Red River (or 34 total sites, Fig. 20C). January was extremely warm in Texas, March was cold, and several Texas weather stations had lower mean temperatures for March than for January (Griffiths and Ainsworth 1981). The storm responsible for the frost injury in central Texas probably occurred from March 12-15 when a low pressure center moved from the southwest into the Eastern Gulf States, bringing rain and snow to the Texas coast" from the 13th to 15th (War Department 1880).

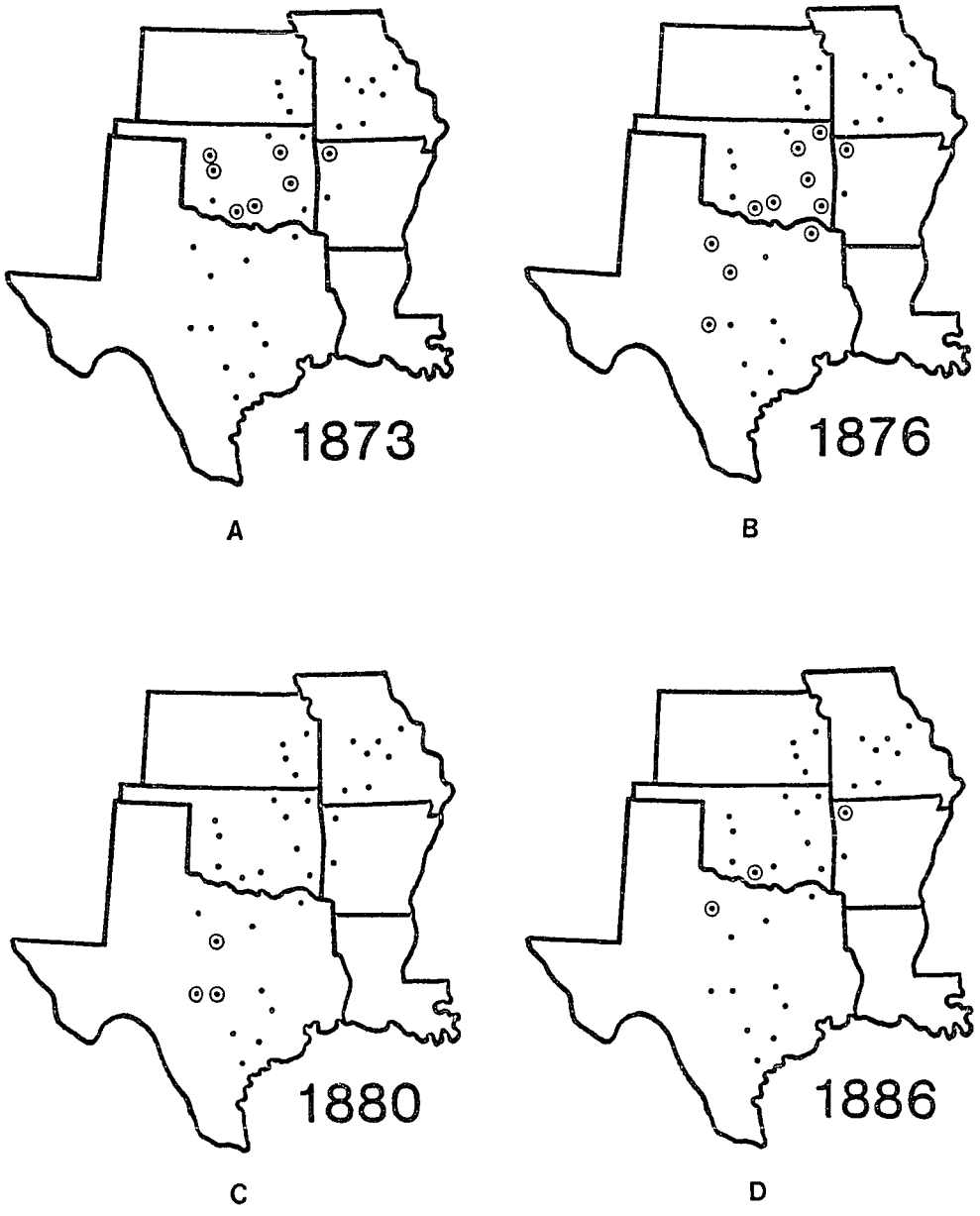

Figure 20. Same as Figure 8 for 1873(A), 1876(B), 1880(C), and 1886(D).

1886 Widely scattered frost injury in Texas, Oklahoma, and Arkansas occurred at only 3 of 34 total sites in the study area (Fig. 20D). Both January and March were cold during 1886 (Griffiths and Ainsworth 1981).

1890 Intense frost injury occurred uniformly across southern Oklahoma and Texas at 11 of 34 total sites (Fig. 21A). This injury appears to have been the result of "unusually warm" temperatures during January and February (Greely 1890), and record low temperatures early in March (Griffiths and Ainsworth 1981). Freezing temperatures were reported at Brownsville and 28°F was recorded at Corpus Christi during this cold wave (Griffiths and Ainsworth 1981). This early March cold wave also affected the Midwest and penetrated into North Carolina and Georgia, injuring fruit, vegetables, and the corn and wheat crops (Greely 1890).

1892 Frost injury was restricted to 4 out of 11 sites in Texas during 1892 (Fig. 21B). February was warmer than average (Griffiths and Ainsworth 1981), and a severe cold wave crossed Texas in mid-March and caused serious damage to fruit, garden, field crops, and livestock in Texas and southern Arkansas (Cline 1892; Clarke 1892). This was the "severest cold wave which has ever passed over the state of Texas later than the first of March" (Cline 1892), and this same system caused record heavy snowfall in Tennessee (Ludlum 1982, 56).

1894 Frost injury occurred in northern Oklahoma, Arkansas, Missouri, and Kansas at 10 out of 23 sites north of the Red River (Fig. 21C). Temperatures fell below freezing in Little Rock, Arkansas, from March 26 to 29 and caused considerable damage to crops and trees (Arkansas Gazette 1894). Frost injury was reported to have been most severe in northwest Arkansas (Arkansas Gazette 1894), and temperatures probably fell well below freezing in the region of frost injured tree rings (Fig. 21C). Stillwater, Oklahoma, is located in the region of frost injury, and daily high temperatures recorded at Stillwater exceeded 70°F for 14 of the first 21 days of March, reached 84°F on two days, and did not fall below freezing during this entire warm period [U.S. Weather Bureau (A)1894]. However, the temperature at Stillwater fell to 20°F on March 26th and again on March 29th [U.S. Weather Bureau (A)1894.

1899 Frost injury occurred at only two sites in southern Oklahoma (out of 34 total sites or 23 north of the Red River, Fig. 21D). Frost damage may have been limited in 1899 by record cold temperatures across the eastern United States during February, which probably prevented widespread early-season tree growth. The frost event probably occurred on March 28th when a frost killed the corn, fruit, and injured the vegetable crop in Texas (Cline 1899). A strong Bermuda high during mid-March forced storm centers to track

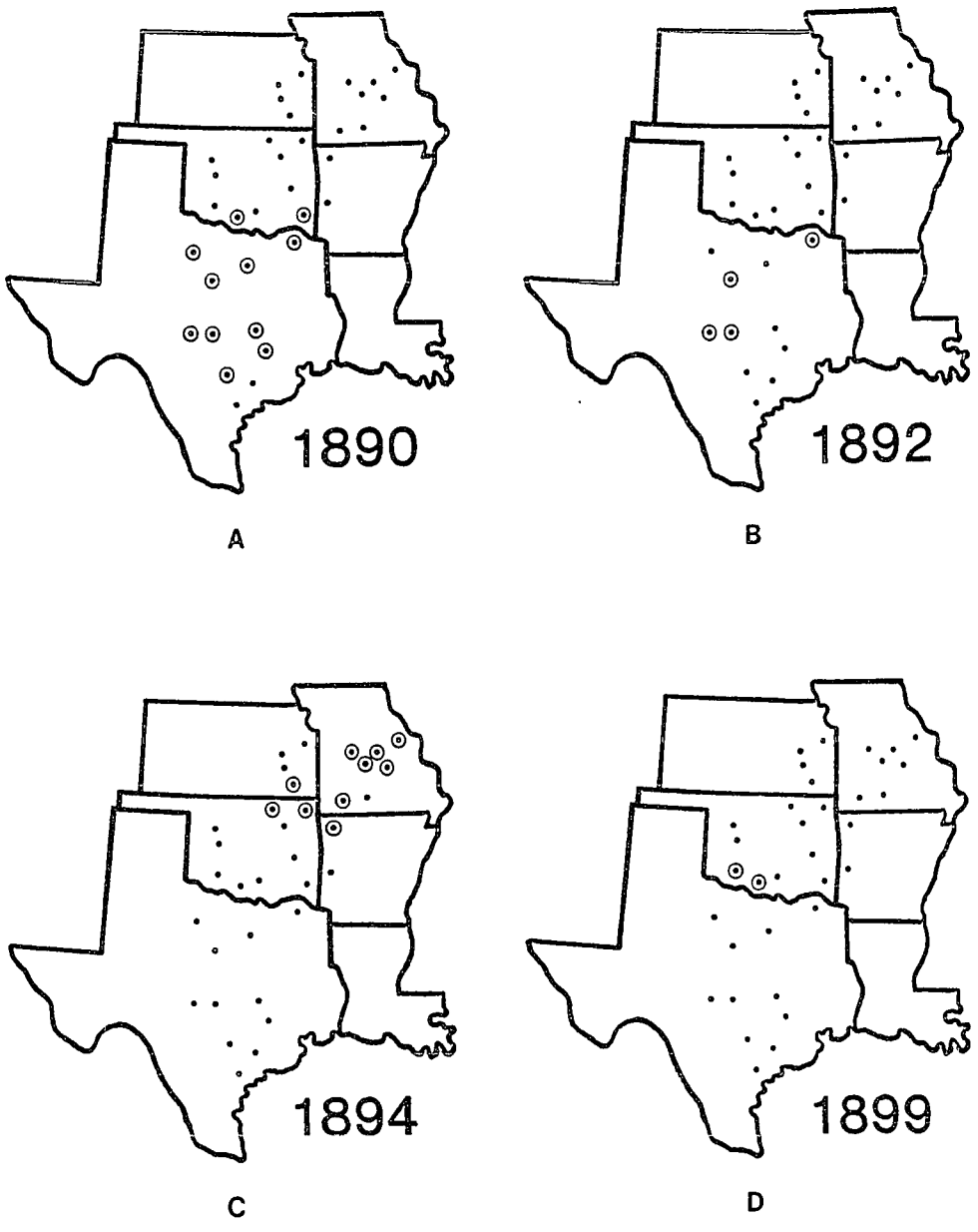

Figure 21. Same as Figure 8 for 1890(A), 1892(B), 1894(C), and 1899(D).

northeastward across Missouri and the Ohio Valley (U.S. Weather Bureau (B)1899, Figures 22A and 23), but by March 25th this anticyclone had weakened and a cold front swept southeastward across the Southern Plains on March 27th and 28th (Fig. 22B). A pronounced high pressure ridge developed behind the cold front, stretching from the arctic to southern Texas (Fig. 22B). The 23°F isotherm was located as far south as northern Texas on March 28th, when a minimum temperature of 16°F was recorded at Stillwater, Oklahoma [U.S. Weather Bureau (A)1899]. Abnormally cold weather continued until April 10th, with light to heavy frosts extending from Texas into the Gulf and southern Atlantic states (Henry 1899).

1913 Frost injury occurred in northern Texas and southern Oklahoma at only 3 out of 34 total sites (Fig. 24A). This freeze event probably occurred on March 15th and 16th when temperatures fell to 22°F and 21°F at Frederick in southwest Oklahoma [U.S. Weather Bureu (A)1913]. Minimum temperatures during the preceding 13 days were generally well above freezing at Frederick [U.S. Weather Bureau (A)1913]. Two additional cold fronts crossed Oklahoma on March 21st and 27th [U.S. Weather Bureau (B)1913], and might have been responsible for the observed frost rings. Griffiths and Ainsworth (1981) state that a late freeze in March caused widespread crop damage in Texas, and presumably this same freeze caused frost rings as well. A strong anticyclone was present off the

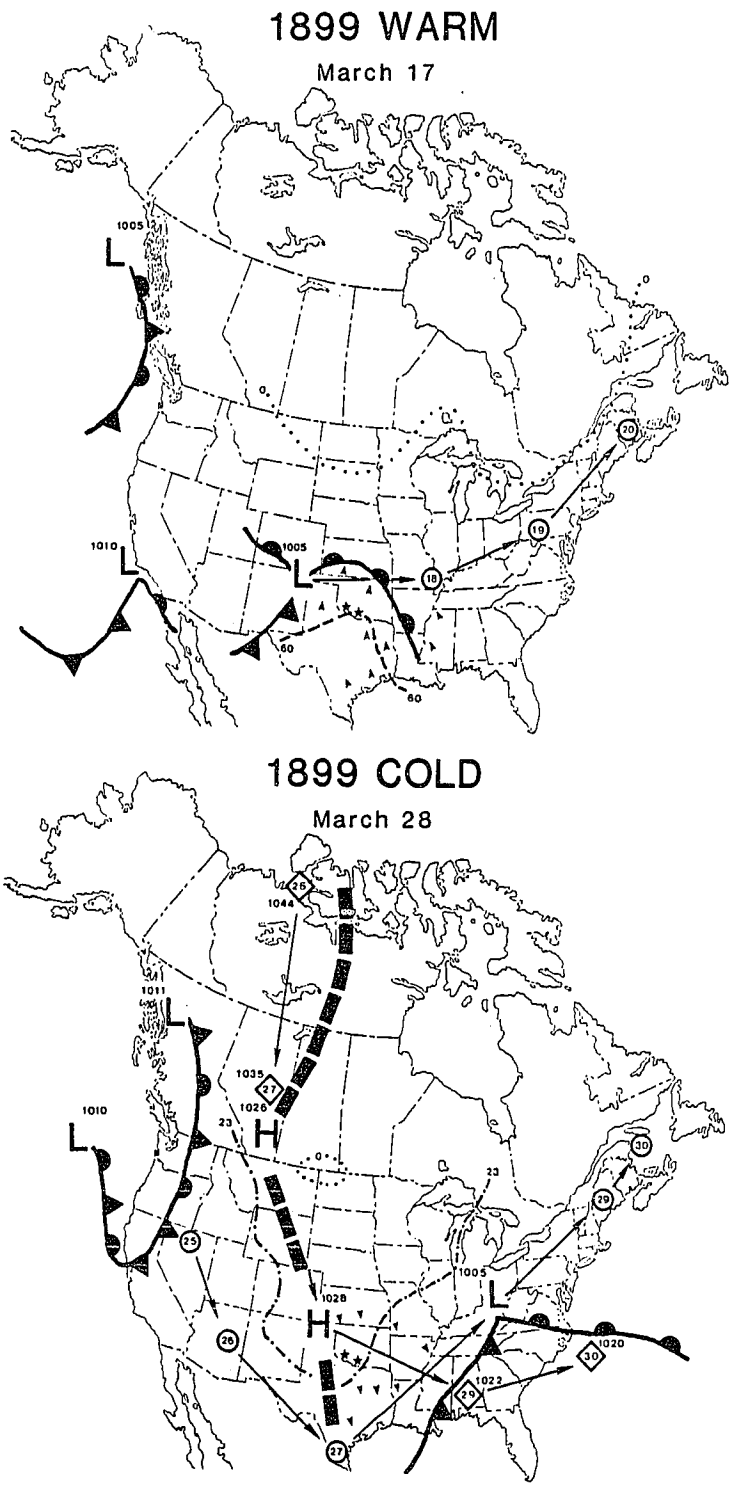

Figure 22. Daily synoptic weather maps for 1899 illustrating selected weather variables for the warm and cold phases of false spring. The legend for this map is presented in Figure 23. Weather conditions at 13:00 GMT are summarized for March 17 (A:warm) and 28 (B:cold).

SYNOPTIC MAP SYMBOLS

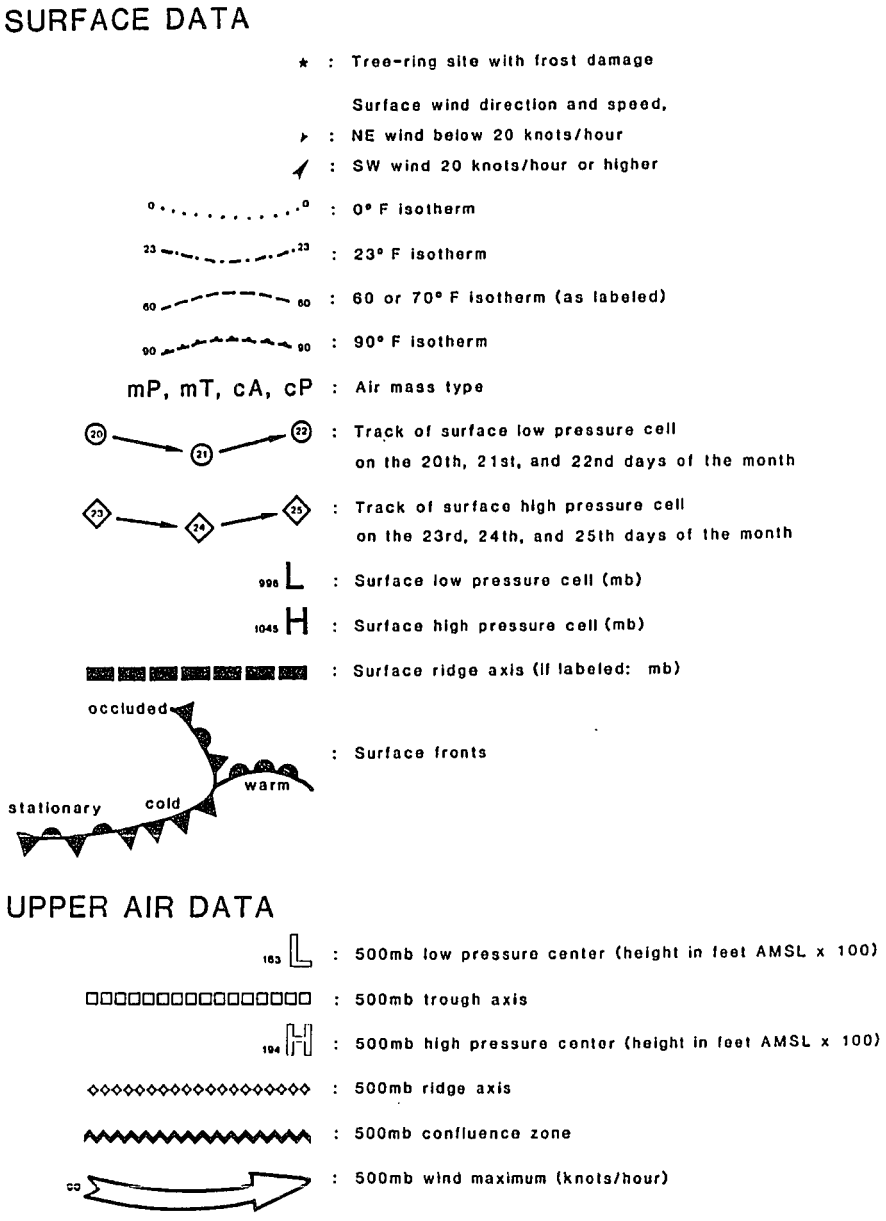

Figure 23. Map legend for the synoptic symbols used to depict selected weather conditions during the warm and cold phases of false spring episodes from 1899 to 1974 (various figures). The surface variables are used on all maps, but the upper air variables appear only after 1947. These data were obtained from the Daily Weather Maps of the United States, and of the Northern Hemisphere, analyzed by the United States Weather Bureau (and subsequently by the National Weather Service, NOAA).

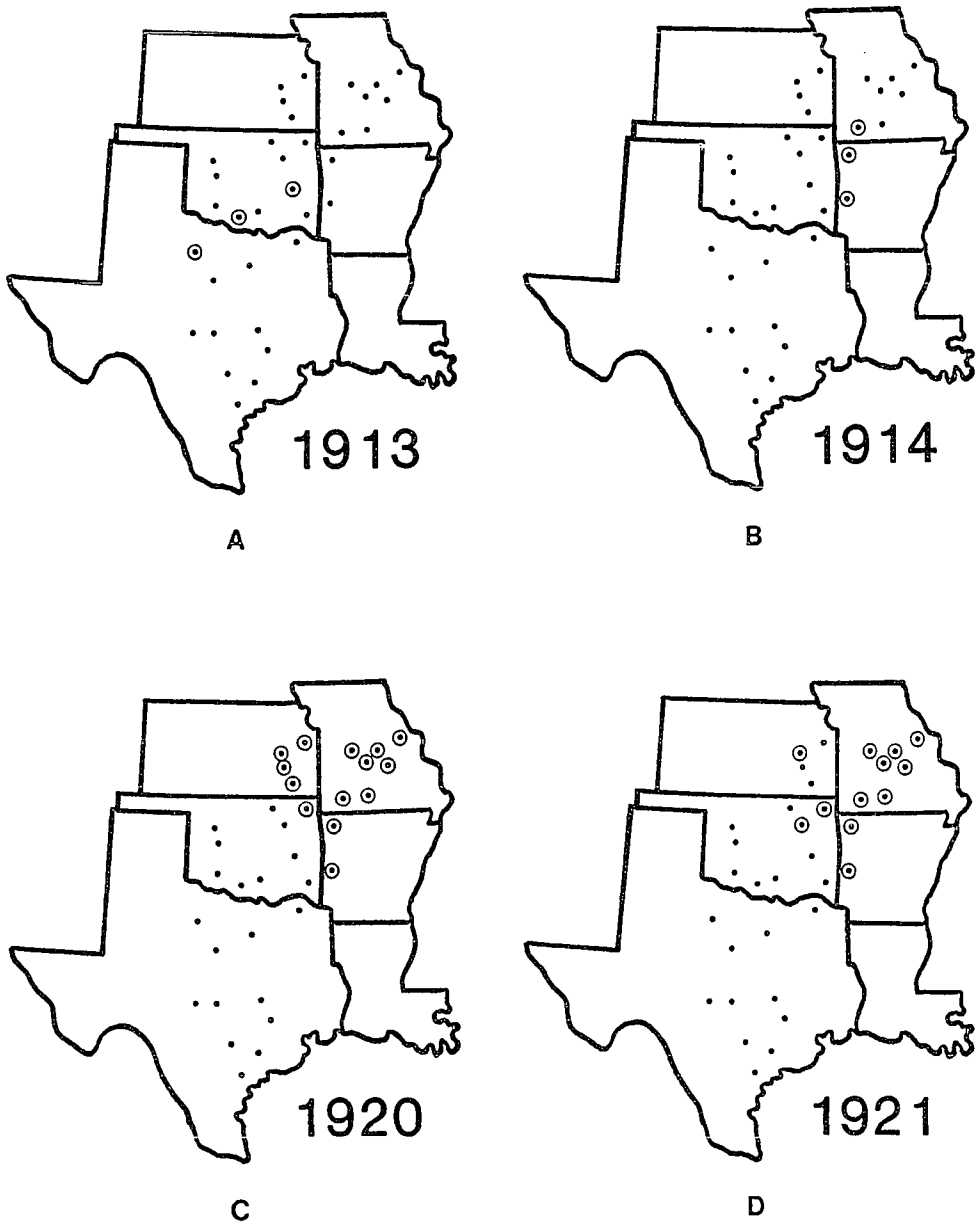

Figure 24. Same as Figure 8 for 1913(A), 1914(B), 1920(C), and 1921(D).

Southeast coast for several days early in March, when storm centers tended to track across the Great Lakes region and southerly flow predominated over the Southern Plains (Fig. 25A). By March 15th the Atlantic high moved off to the northeast and a high pressure cell migrated from Alaska to the south and east across central Texas (Fig. 25B). Strong northwest winds and the 23°F isotherm were located over the Red River region on March 15th (Fig. 25B).

1914 Frost injury occurred in western Arkansas and southwestern Missouri at only 3 of 23 sites north of the Red River (Figures 24B and 26A). Although the 23°F isotherm was located well to the north on April 9th [U.S. Weather Bureau (B)1914; Fig. 26B), frost injury probably occurred in this region on the 9th because a minimum temperature of 21°F was recorded at Eureka Springs, Arkansas, and a pocket of temperatures below 23 degrees was also reported in central Oklahoma (Fig. 26B). Two of the sites with frost injury are located near Eureka Springs, and the third site is located at 2200' on top of Blackfork Mountain in extreme west-central Arkansas (Fig. 24B). The cold wave on April 9th was preceded by 16 days with maximum daily temperatures above 60°F, and minimum temperatures above 35°F at Eureka Springs [U.S. Weather Bureau (A)1914]. A large anticyclone was present in the North Atlantic for several days during this warm spell, and appears to have favored southerly winds over the Southeast

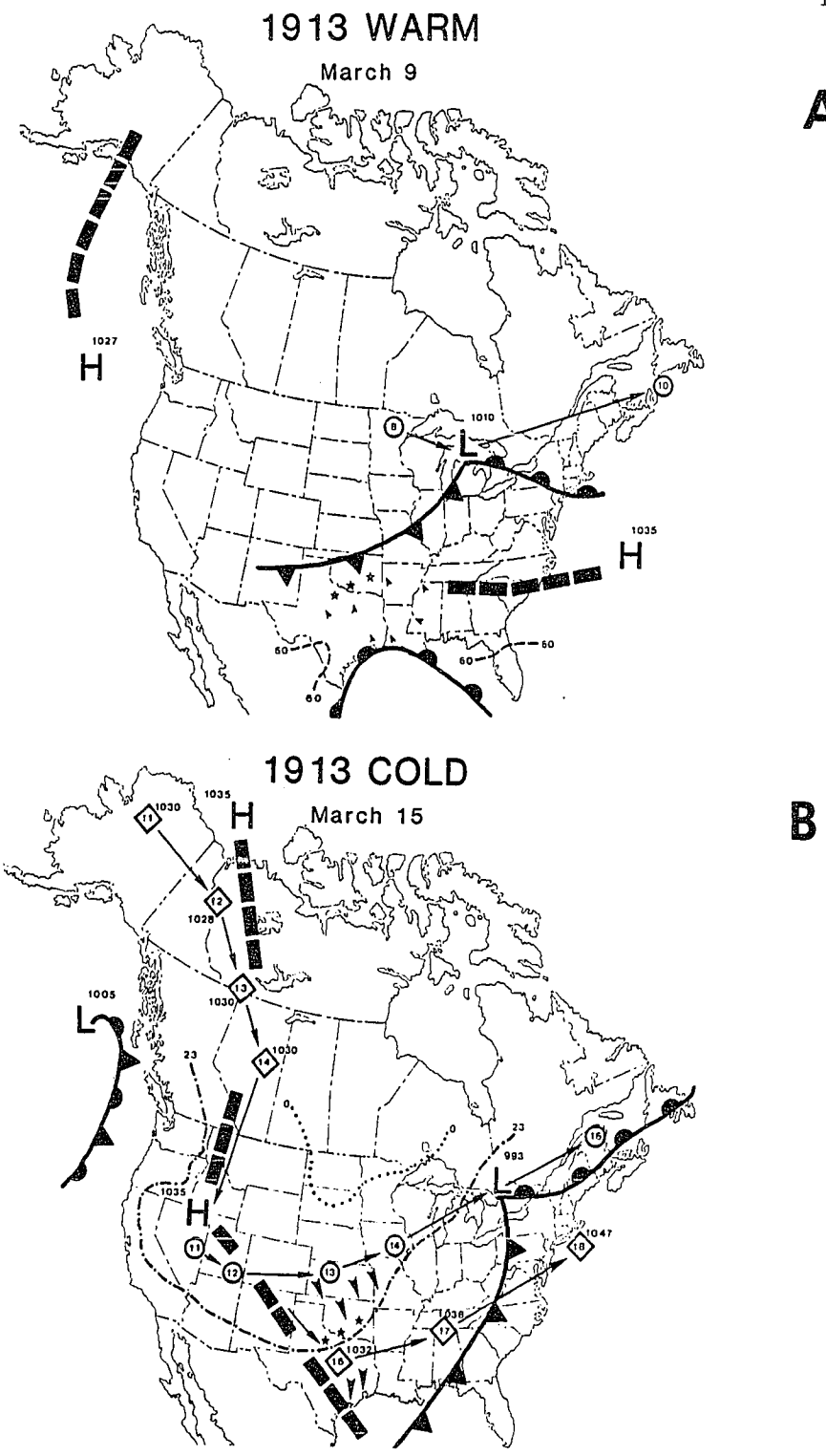

Figure 25. Same as Figure 22 for the 1913 warm and cold phases of false spring (A:March 9; B:March 15). See Figure 23 for the map legend.

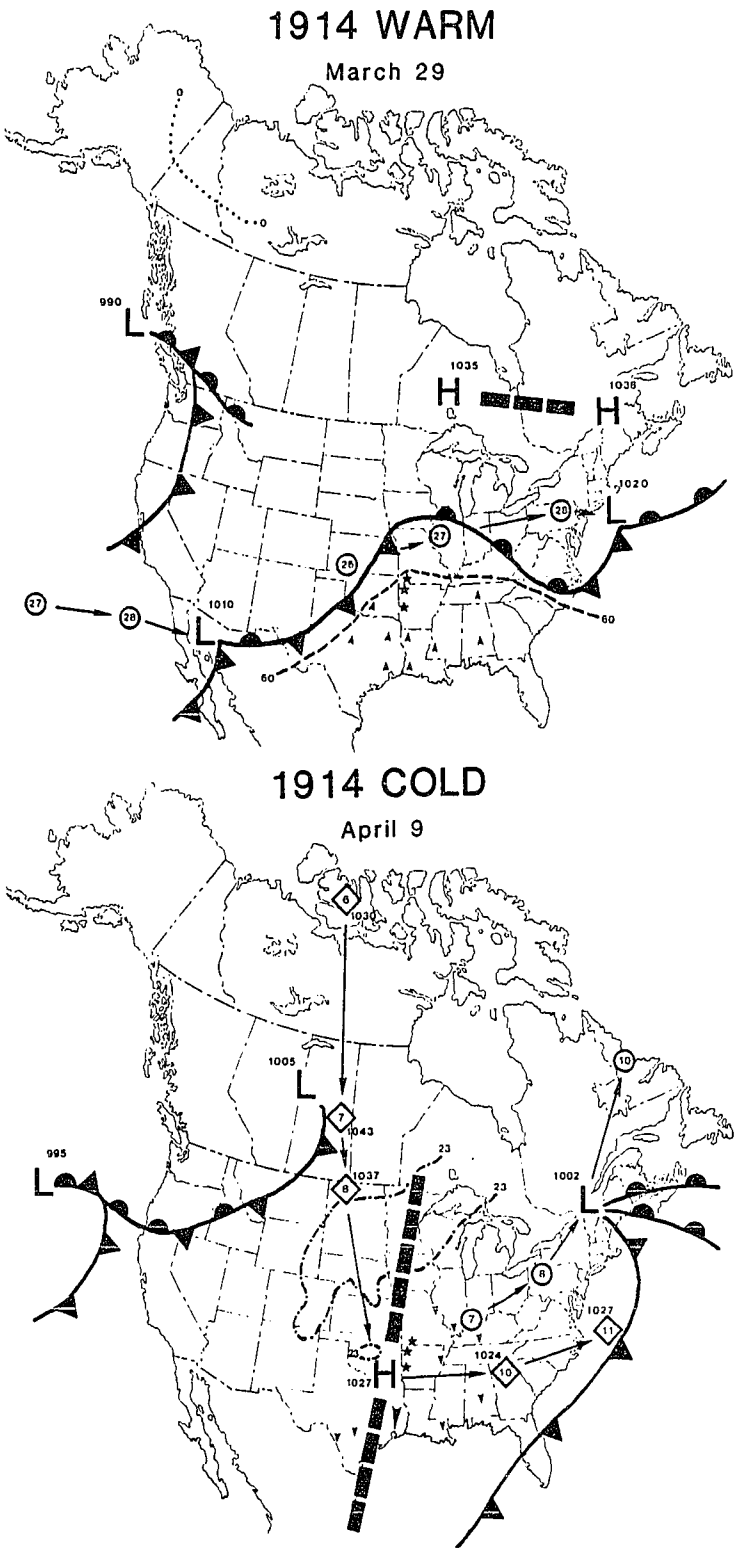

Figure 26. Same as Figure 22 for the 1914 warm and cold phases of false spring (A:March 29; B:April 9). See Figure 23 for the map legend.

and a storm track located to the north over the Ohio Valley (Fig. 26A). This flow pattern changed dramatically by April 9th when a high pressure cell from northern Canada moved south over east Texas behind a storm system which developed into a nor'easter along the coast of New England (Fig. 26B). Freezing temperatures on April 9th extended to the interior Gulf states, and the first half of April was unseasonably cold over the Great Plains and eastern United States (Day 1914).

1920 Intense frost injury occurred primarily in Kansas, Missouri, and western Arkansas at 14 of 23 sites north of the Red River (Fig. 24C). This freeze event occurred on April 5th following the passage of a severe storm which brought freezing temperatures south to central Texas and the central Gulf states (Day 1920). Record low temperatures for April were set April 5th at many stations throughout the Great Plains from Canada to the Gulf of Mexico (Day 1920). The severe freeze killed fruit and truck crops, and damaged field crops throughout the central United States, particularly in Oklahoma, Arkansas, and Missouri (Smith 1920; Arkansas Gazette 1920). The record freeze was preceded by generally above average temperatures for 27 days in southwest Missouri (Table 2). A strong anticyclone was present in the North Atlantic with a ridge extending into the mid-Atlantic states during the last 10 days of March, favoring warm southerly flow into the Southern Plains (Fig. 27A). When this anticyclone weakened

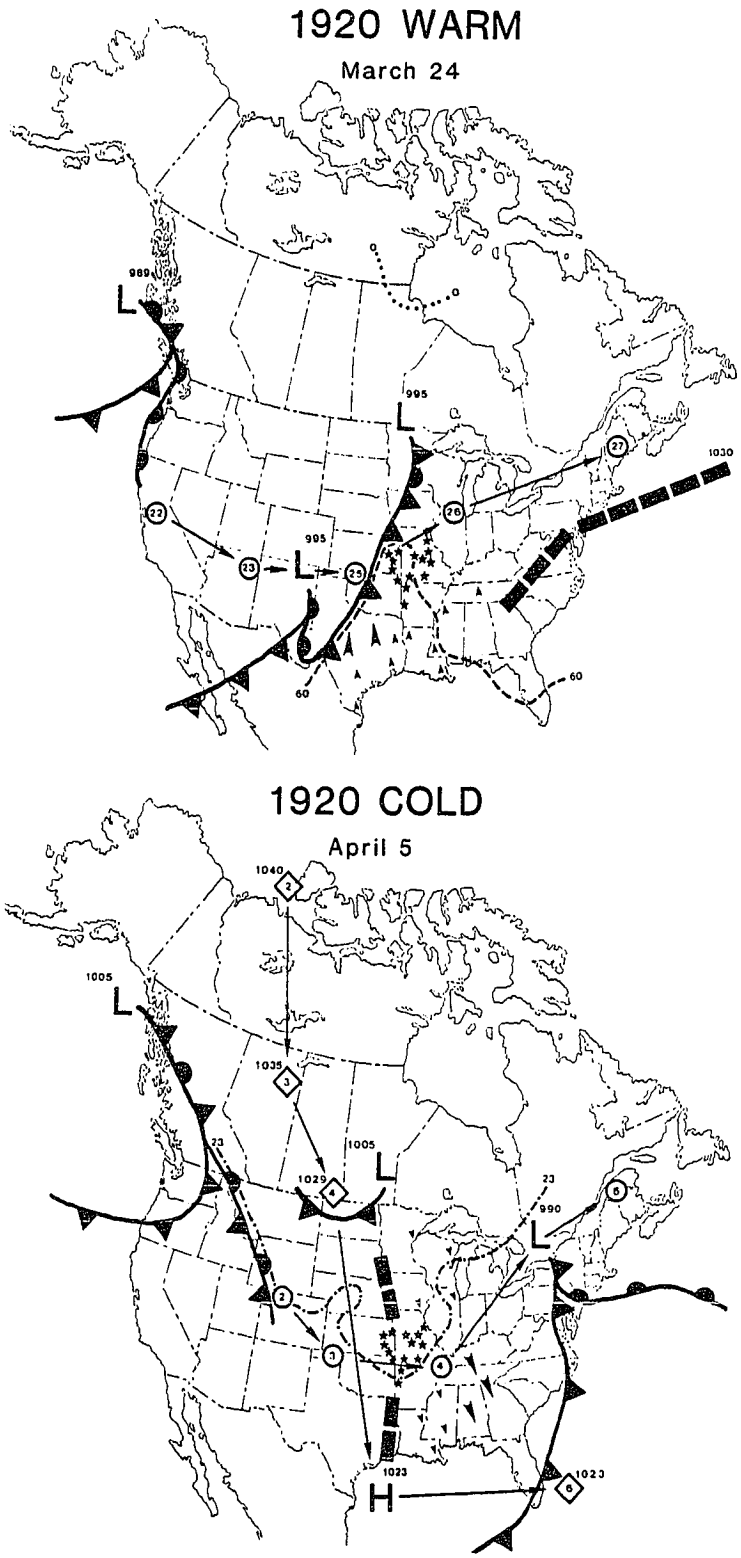

Figure 27. Same as Figure 22 for the 1920 warm and cold phases of false spring (A:March 24; B:April 5). See Figure 23 for the map legend.

and moved northeast early in April, the strong cyclonic storm and associated cold front swept across the Southern Plains, followed by a ridge of high pressure and cold air from the Canadian arctic [U.S. Weather Bureau (C)1920; Fig. 27B]. The only tree-ring site with frost injury located south of the 23°F isotherm was Blackfork Mountain, but at an elevation of 2200' this site probably experienced temperatures below 23°F.

1921 Frost injury in 1921 occurred at 12 of 23 sites north of the Red River in the same area affected by frost damage in 1920 (centered on southwest Missouri, Fig. 24D). The hard freeze occurred on March 29th when a "disastrous cold wave" covered most of the United States and brought freezing temperatures into Texas and the Southeast (Smith 1921a). This freeze followed unusually warm conditions all winter (MWR, Jan.-Mar. 1921), which led to prematurely developed fruit, truck, and field crops in the central and southern United States (Smith 1921a). As a whole, 1921 may have been "the warmest year ever across Texas," in spite of the late March freeze and cool weather in April. The temperature change associated with the March 29th cold front was extremely rapid, with temperatures falling 20°F in 15 minutes in Arkansas (Arkansas Gazette, March 28, 1921), and falling from 85°F (29°C) to 26°F (-3°C) on the 29th in Washington, D.C. (Ludlum 1982, 57). Fruit and crop damage was severe in the central United States, with total destruction in several states. In

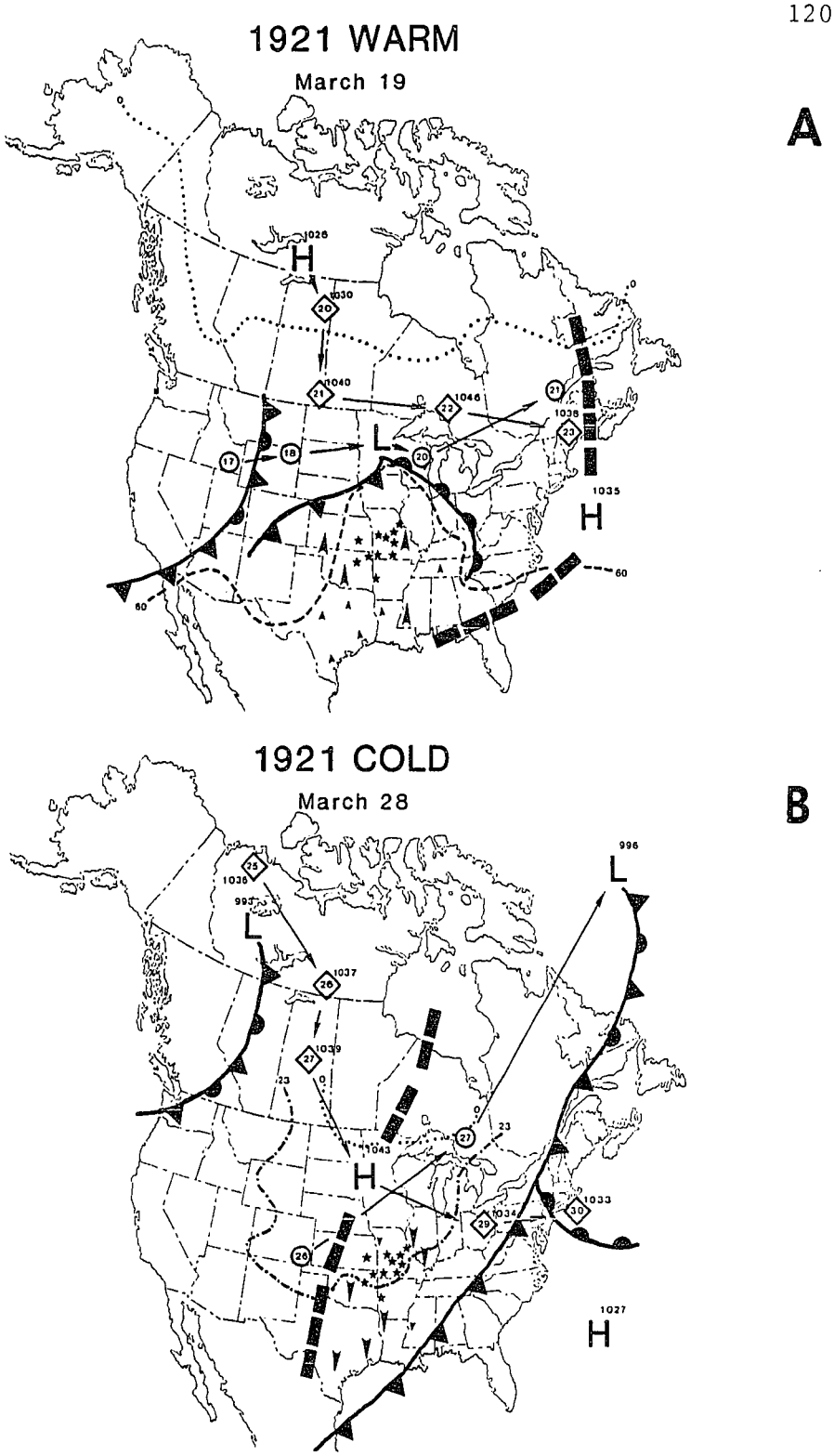

Figure 28. Same as for Figure 22 for the 1921 warm and cold phases of false spring (A:March 19; B:March 28). See Figure 23 for the map legend.

Oklahoma all vegetation was "frozen stiff" (Smith 1921b). Synoptically, the warm spell during the third week of March was dominated by a strong high pressure center and ridge off the East coast, which favored a storm track near the Canadian border and allowed warm southerly flow into the South and Midwest (Fig. 28A). By March 28th this high pressure cell had weakened and shifted south (Fig. 28B). This permitted the southerly penetration of cold air associated with a strong cold front and the migration of an intensifying Canadian high pressure cell. The high elevation Blackfork Mountain site was again the only tree-ring location south of the 23°F isotherm to experience frost injury.

1923 Frost injury occurred in southern Oklahoma and Texas at 6 of 34 total sites (Fig. 29A). On March 20th a severe cold wave swept across the entire country east of the Rocky Mountains and dropped temperatures to 10°F in central Oklahoma (Kincer 1923), and to 19°F or lower in central Texas (e.g., Table 2). This freeze caused severe damage to fruit and oats in Oklahoma and to cotton in southern Georgia (Kincer 1923). This costly freeze extended to south of Corpus Christi, Texas (Griffiths and Ainsworth 1981), and was particularly damaging because of mild temperatures early in March and in January. January of 1923 was the warmest January on record in Texas (Griffiths and Ainsworth 1981), and was among the warmest for large portions of the Great Plains (Day 1923). Synoptically,

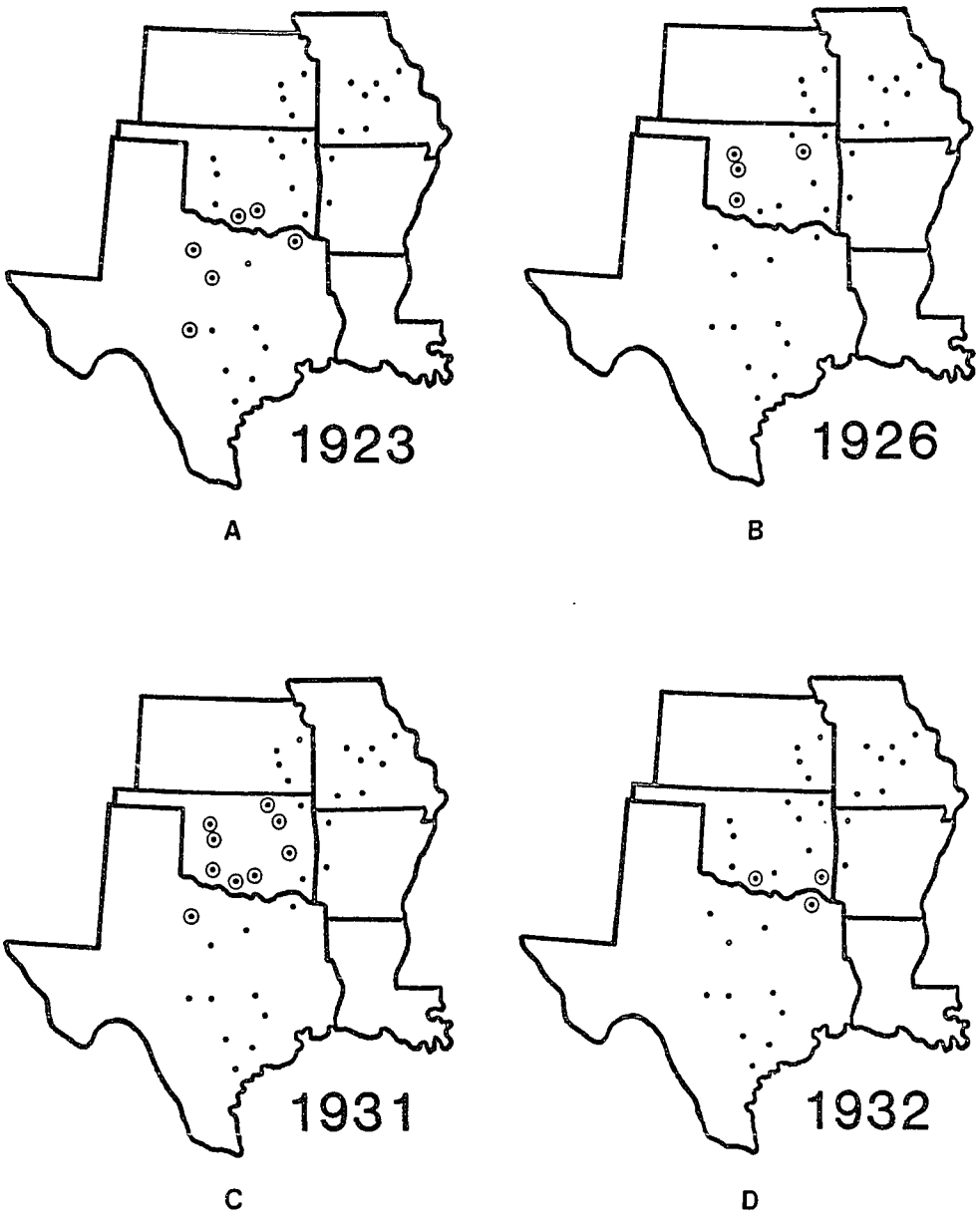

Figure 29. Same as Figure 8 for 1923(A), 1926(B), 1931(C), and 1932(D).

the United States appears to have been dominated in March by a quasi-stationary Bermuda high off the east coast and a prominent ridge extending from the eastern Pacific into the Central Plains (Fig. 30A). The principal storm track was near the Canadian border until the third week of March when the Bermuda high weakened and moved well off to the northcentral Atlantic [U.S. Weather Bureau (C)1923]. The storm track then became more meridional and intensely cold Canadian air penetrated into the central United States behind a strong cyclonic storm, which deepened dramatically and finally occluded over the Davis Straits [U.S. Weather Bureau (C)1923; Fig. 30B].

1926 Frost injury occurred primarily in western Oklahoma at 4 out of 23 sites north of the Red River (Fig. 29B). This freeze occurred on March 27th (Table 2), following an abnormally warm winter which set many new record high temperature averages for February (Day 1926; Griffiths and Ainsworth 1981). Widespread frost damage to fruit and vegetables occurred in the Southeast during a mid-March cold wave, and the frost of March 27th did additional crop damage in the southcentral states and southern Rocky Mountains (Kincer 1926). Southerly flow dominated the Southern Plains during most of March, and the storm track was located at times in Canada (e.g., Fig. 31A). On March 26th a strong high pressure cell near Great Slave Lake was associated with a

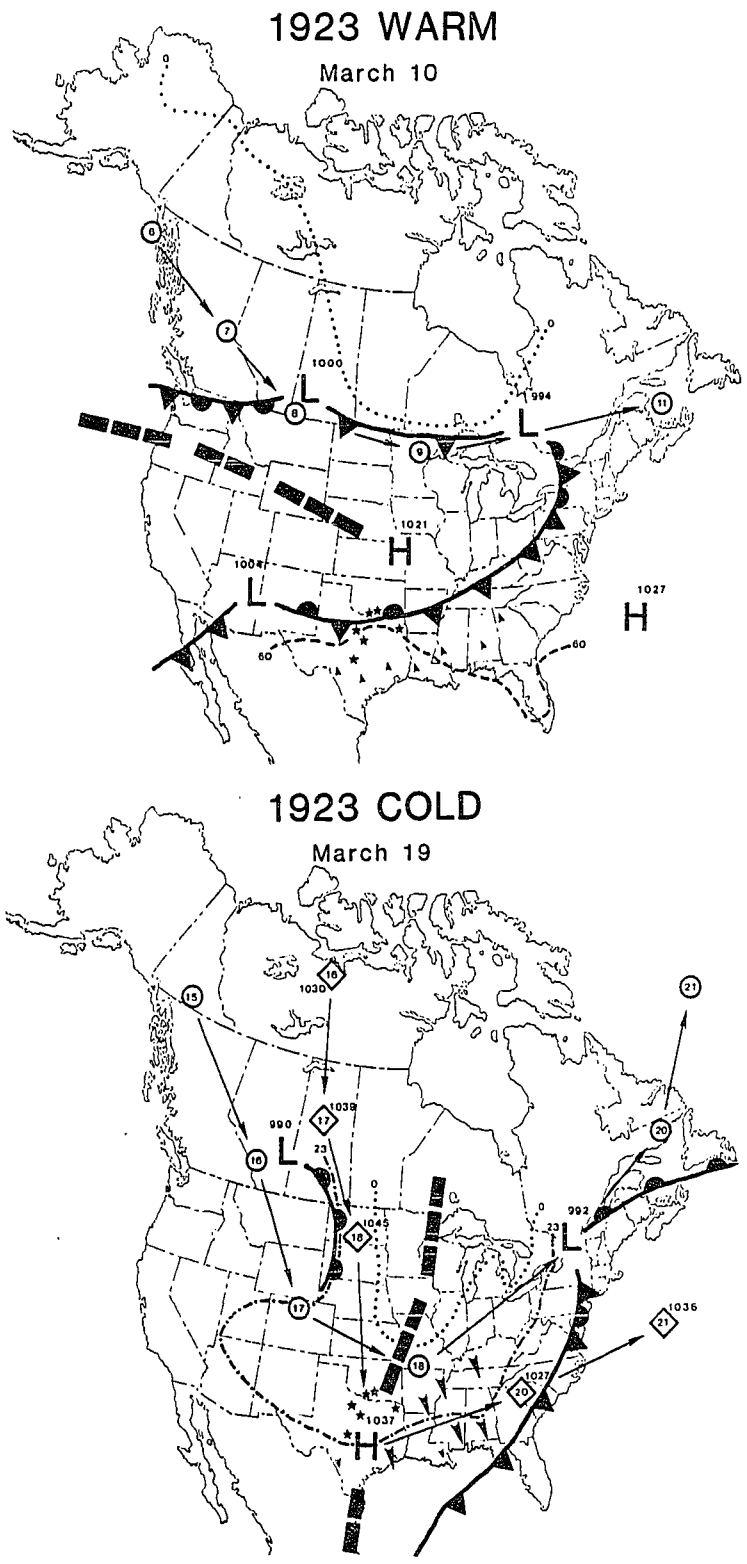

Figure 30. Same as Figure 22 for the 1923 warm and cold phases of false spring (A:March 10; B:March 19). See Figure 23 for the map legend.

ridge extending south to the Texas Gulf coast, and the 23°F isotherm penetrated into central Oklahoma (Fig. 31B).

1931 Intense frost injury occurred in Oklahoma and northern Texas at 9 out of 34 total sites, including all Oklahoma tree-ring sites except two along the eastern border (Fig. 29C). An "exceptionally severe blizzard" crossed Oklahoma on March 28th (WWCB 1931) and dropped the average temperature for northcentral Oklahoma to 17°F (Table 2). January and February averaged much warmer than normal over virtually the entire country (Bennett 1931a, 1931b), but temperatures fell in March and resulted in one of the coldest March averages ever recorded in Florida (Bennett 1931c) and Texas (Griffiths and Ainsworth 1981). Severe fruit and crop losses occurred in Kansas, Oklahoma, Arkansas, Texas, and Louisiana, with the "the ground and all vegetation frozen" in Oklahoma (WWCB 1931). The early advance of vegetation probably began during the warm February, but one brief period of warming during mid-March is illustrated in Figure 32A when a weak anticyclone off Florida and a developing cyclone over Colorado resulted in southerly flow into Oklahoma, and may have further stimulated early season tree growth. By March 28th, a Canadian high pressure cell which had been intensifying for the previous three days finally spilled south behind a cold front, and brought subfreezing temperatures into northern Texas (Fig. 32B).

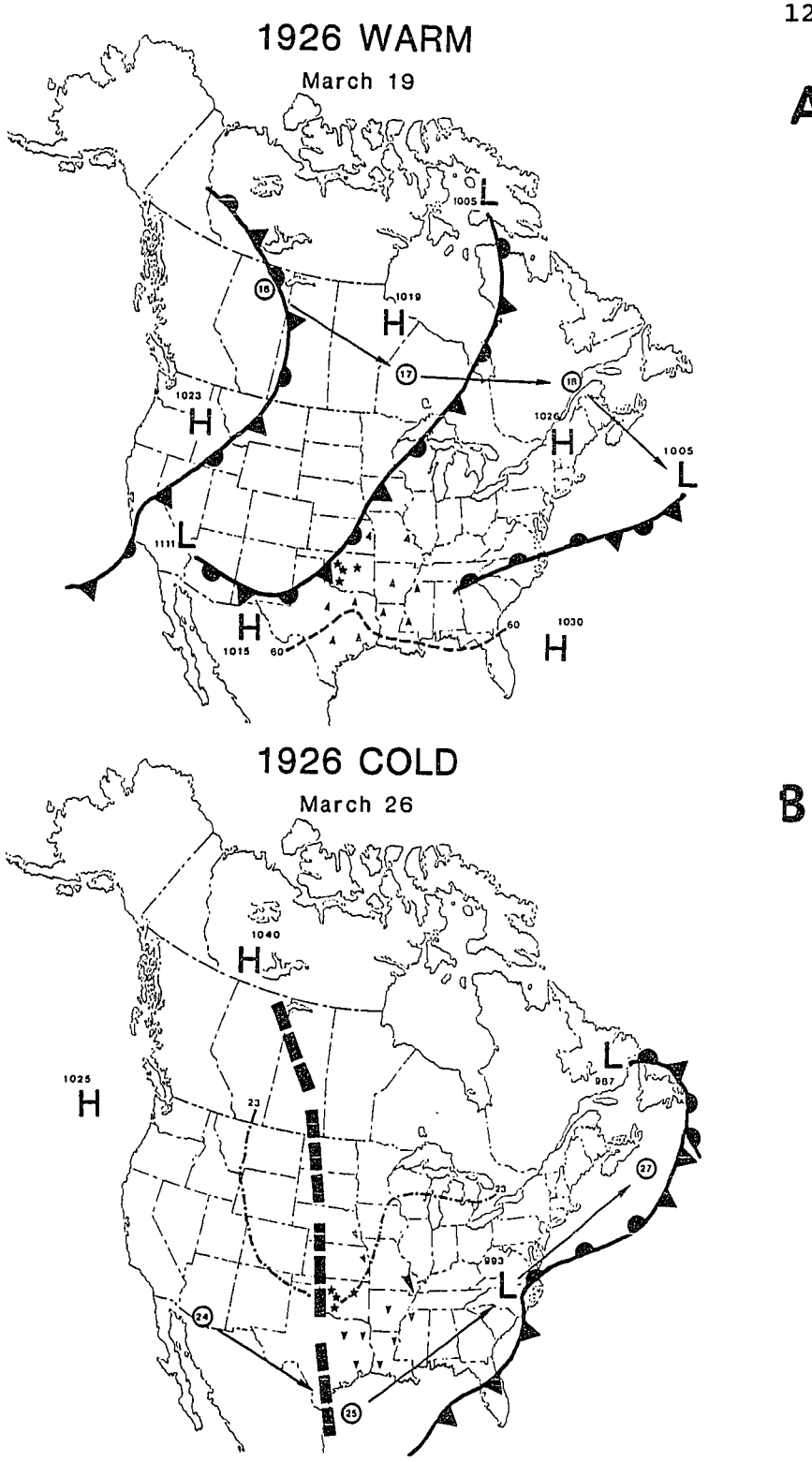

Figure 31. Same as for Figure 22 for the 1926 warm and cold phases of false spring (A:March 19; B:March 26). See Figure 23 for the map legend.

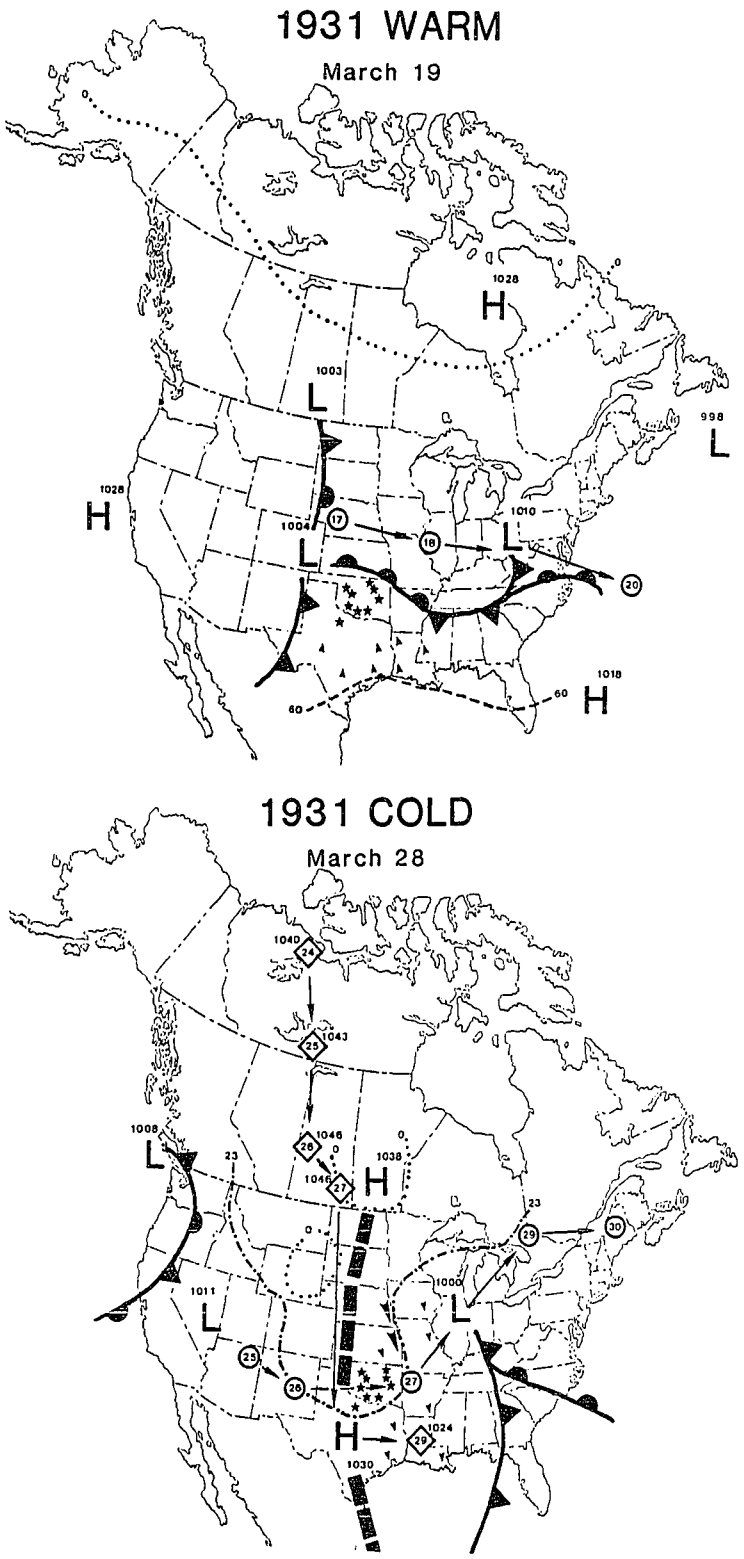

Figure 32. Same as Figure 22 for the 1931 warm and cold phases of false spring (A:March 19; B:March 28). See Figure 23 for the map legend.

1932 Frost injury occurred only along the Red River in Oklahoma and northeast Texas at just 3 of 34 total sites (Fig. 29D). The false spring event of 1932 culminated in a hard freeze between the 5th and 15th of March, but was not included in the statistical analysis (Chapter 6) because local temperature data were not compiled. The damaging freeze event appears to have occurred during the second week of March when many stations east of the Rockies reported record low March temperatures, and/or the coldest week ever for March (WWCB 1932). The preceding six months had been abnormally warm east of the Rockies, and February was the warmest or near warmest ever recorded in most of the southcentral United States (Bennett 1932). Fruit and crops from the Midwest south to the Rio Grande Valley and the interior of southern Florida were prematurely advanced during this warm spell, and were then killed or severely damaged by the hard freeze (WWCB 1932). During the last 10 days of February the principal storm track was located in Canada and mild maritime tropical or Pacific air masses dominated the southcentral United States (Fig. 33A). This circulation pattern completely reversed by March 9th when a strong ridge developed from the Yukon to south Texas behind an intense cyclonic storm which moved up the east coast as a classic nor'easter (Fig. 33B). Continental polar air penetrated into the southern United States and most of the country was within the 23°F isotherm (Fig. 33B).

1936 Intense frost injury occurred continuously across eastern Kansas, southern Missouri, and northern Oklahoma and Arkansas at 14 out of 23 sites north of the Red River (Fig. 34A). February was the coldest since 1905 in Missouri [U.S. Weather Bureau (A)1932], but March was an abnormally warm month across the central and eastern United States (WWCB 1936). The storm track was generally oriented from the southern Rockies to the Northeast during mid to late March, and a surface high off Florida favored warm southerly flow into the southcentral United States (Fig. 35A). Two energetic storm systems crossed the United States in early April, bringing severe weather and record breaking cold temperatures to the central and southeastern United States. The average temperature for southwest Missouri fell to 16.7°F on April 3rd (Table 2), following the southward movement of a Canadian high pressure cell from the Yukon (Fig. 35b). This cold wave killed or damaged fruit, corn, oats, and other field and garden crops from the Southern Plains to the southern Appalachian Mountains [WWCB 1936; Arkansas Gazette, April 4, 1936; U.S. Weather Bureau (A)1936). The storm of April 3rd, and the next storm on the 5th and 6th spawned several tornadoes that killed hundreds of people and caused over $16 million in damage in Cordele and Gainesville, Georgia, and Tupelo, Mississippi (WWCB 1936; Ludlum 1982). These storms also raised disastrous dust storms in Texas and Oklahoma, devastating the winter wheat crop (WWCB 1936).

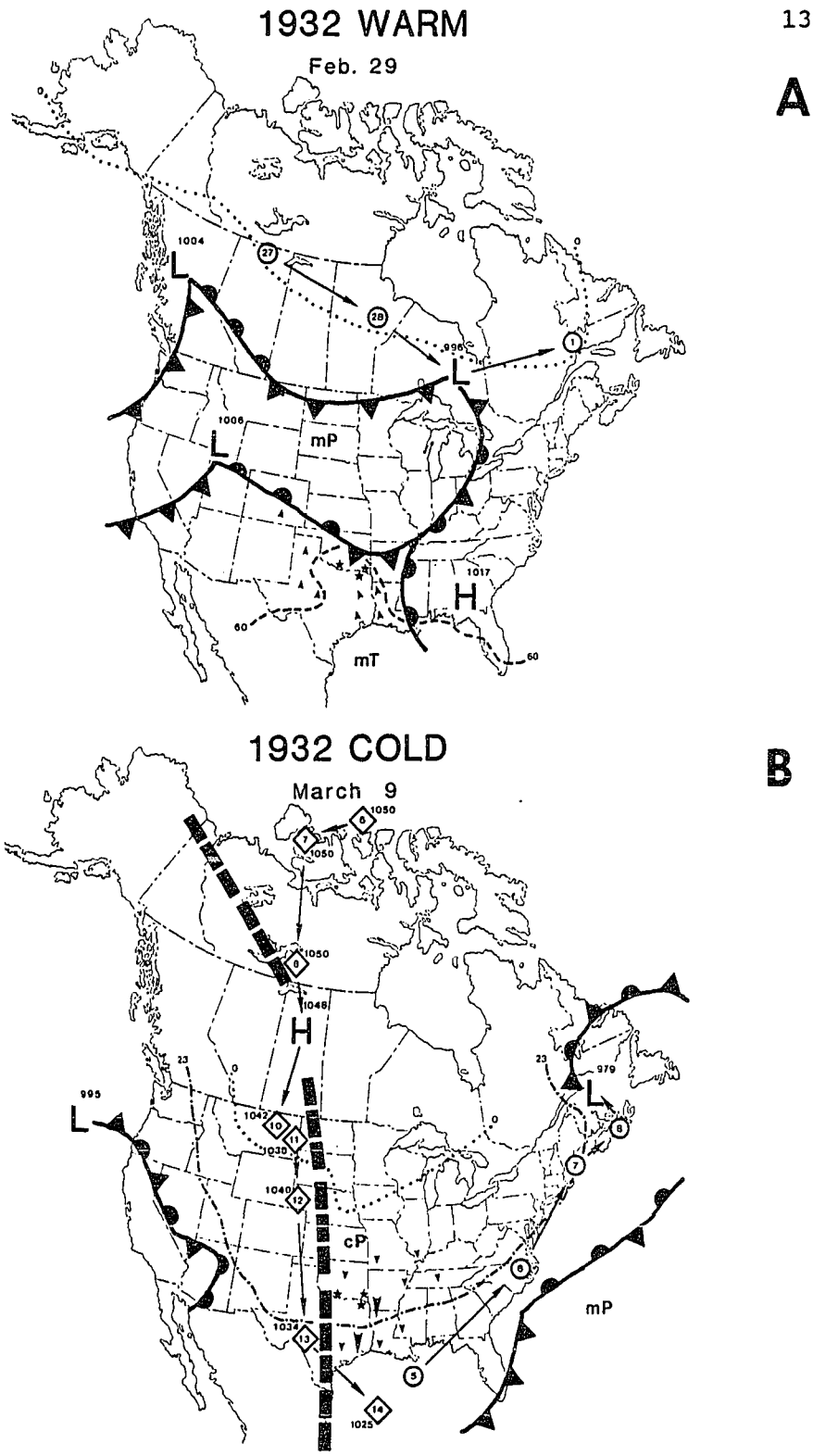

Figure 33. Same as Figure 22 for the 1932 warm and cold phases of false spring (A:February 29; B:March 9). See Figure 23 for the map legend.

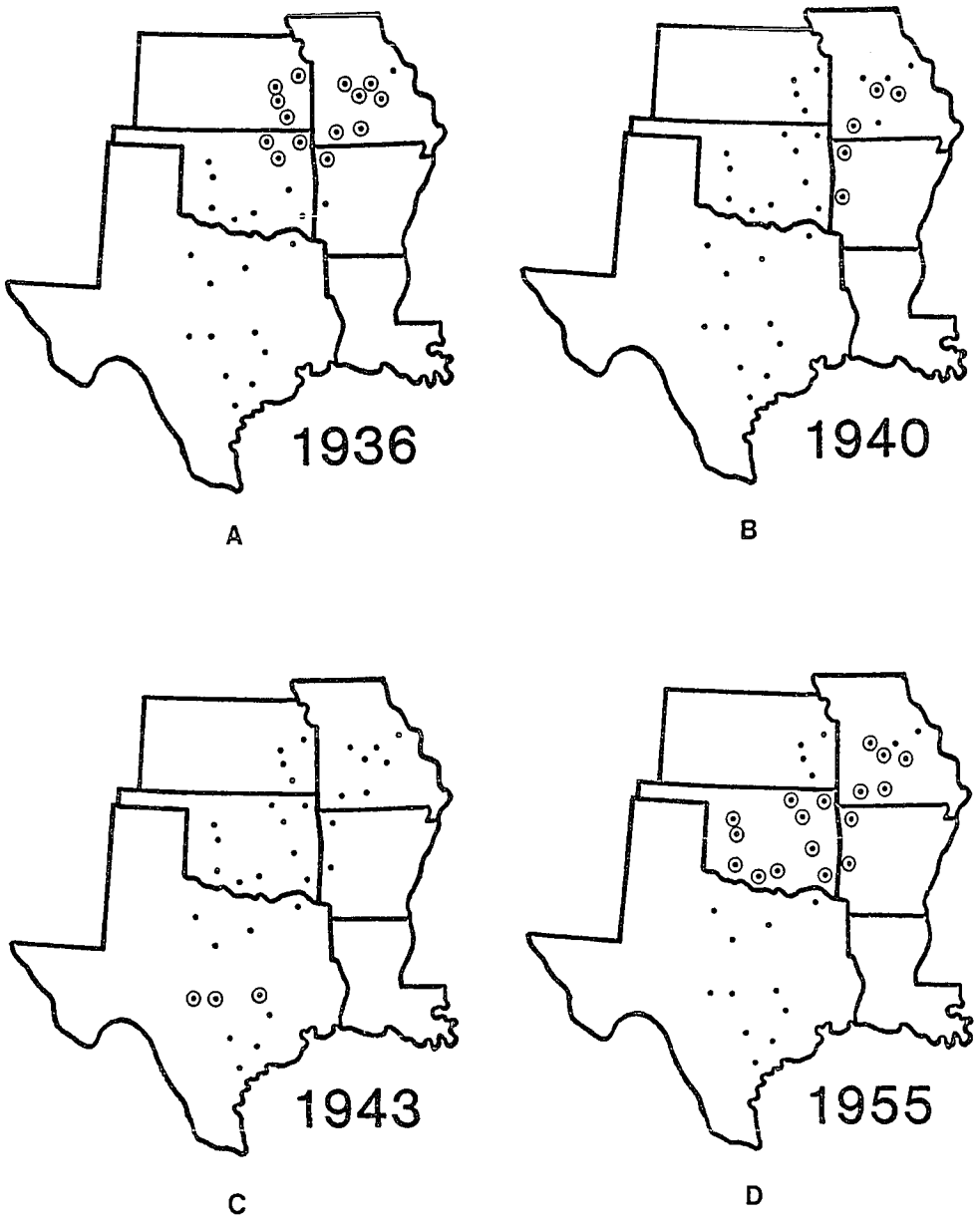

Figure 34. Same as Figure 8 for 1936(A), 1940(B), 1943(C), and 1955(D).

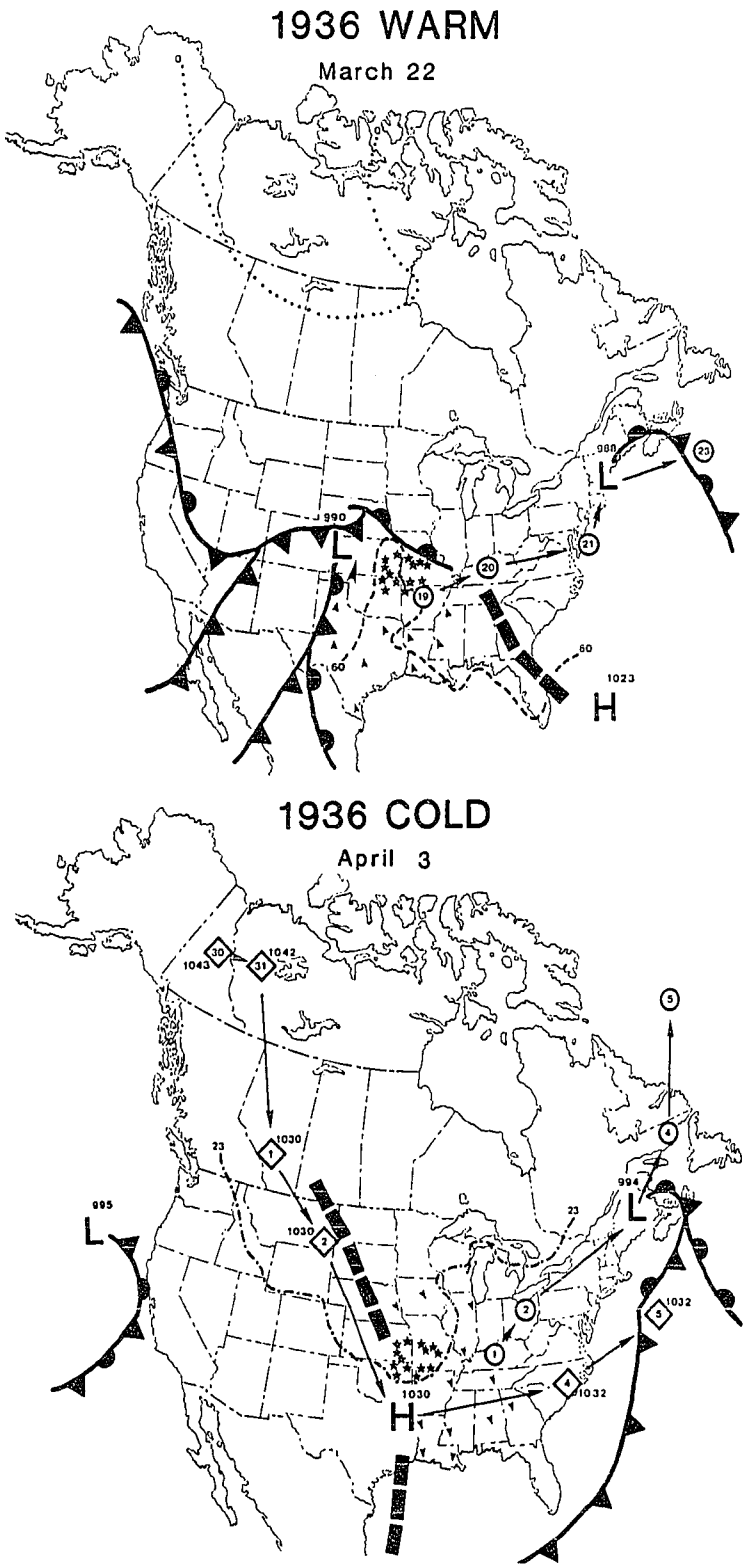

Figure 35. Same as Figure 22 for the 1936 warm and cold phases of false spring (A:March 22; B:April 3). See Figure 23 for the map legend.

1940 Frost injury occurred from western Arkansas into central Missouri at 5 out of 23 sites north of the Red River (Fig. 34B). A cold wave crossed Missouri on April 12th and lowered the southwest Missouri minimum temperature average to 21.7°F (Table 2). This cold wave brought freezing temperatures close to the eastern Gulf coast and killed or severely damaged fruit, crops, and gardens from New Mexico and Colorado eastward to the Atlantic coast (WWCB 1940). "Serious damage to all vegetation" was reported in Alabama (WWCB 1940). Extremely warm air quickly returned to the Southern Plains after the April 12th cold wave. Temperatures as low as 10°F were reported in northwest Oklahoma on the 12th, and temperatures of 90°F or higher were reported on the 14th and 15th (WWCB 1940). Warm conditions over the Southeast in late March and early April were related in part to a strong high pressure cell in the Atlantic and a weaker high off Florida, which together favored southerly flow into the South and a more northerly storm track across the northcentral United States [U.S. Weather Bureau (C)1940; Fig. 36A]. The cold wave in April followed the development of a strong high pressure system over Great Bear Lake beginning around April 4th. This high intensified dramatically and migrated south, registering a central high pressure of 1042.7 mb over western Oklahoma on April 12th (Fig. 36B). The location of the 23°F isotherm on April 12th at 1:30 pm EST (Fig. 36B) does not precisely portray the lowest temperatures because a minimum temperature

of 22°F was recorded at Eureka Springs, Arkansas, near two frost injured tree-ring sites located south of the 23°F isotherm. The third frost injured site south of the critical 23°F isotherm in Figure 31B is again Blackfork Mountain, where elevation appears to introduce a surface temperature gradient.

1943 Frost injury occurred at three sites in central Texas, out of 11 total sites south of the Red River (Fig. 34C). Extreme variations in temperature occurred across the eastern United States in February (WWCB 1943a), but averaged markedly above normal from the Mississippi River to the Rockies (WWCB 1943b). A strong high pressure cell was located over the Southeast from February 17 to 25, resulting in a southerly flow of mild maritime tropical air into Texas (Fig. 37A). During this period the storm track was located well to the north in southern Canada [U.S. Weather Bureau (C)1943]. The Southeastern high weakened and an unprecedented cold wave swept across the eastern United States during the first week of March. This system "was easily the coldest for the season of year since countrywide climatological records have been collected by the Weather Bureau" (WWCB 1943c). The 23°F isotherm penetrated into central Texas (Fig. 37B), and freezing temperatures extended into south Florida near Arcadia and Vero Beach (WWCB 1943c). The central Texas average minimum temperature fell to 14°F on March 3rd (Table 2), and extensive damage to fruit, oats, corn and garden crops was

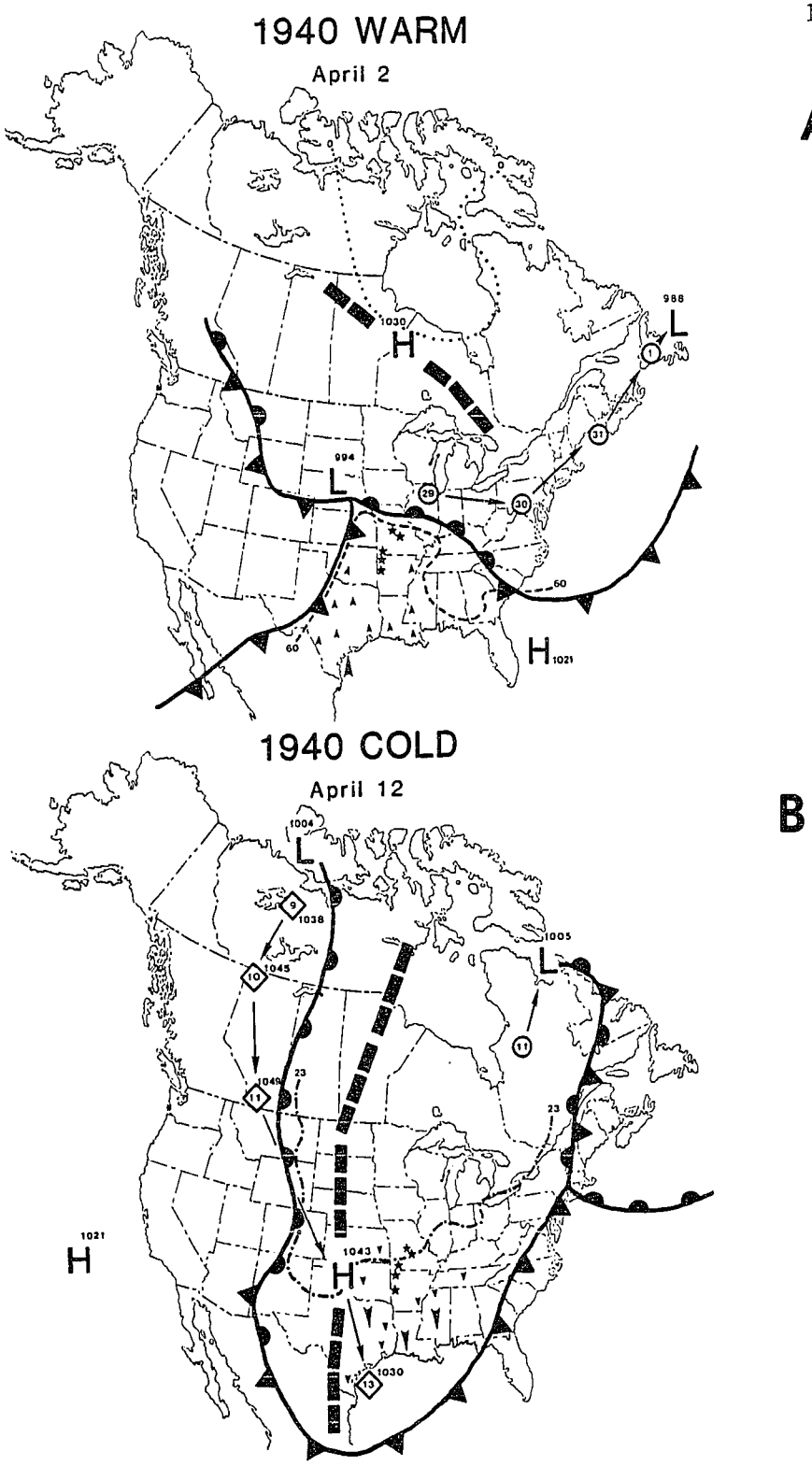

Figure 36. Same as Figure 22 for the 1940 warm and cold phases of false spring at 12:30 GMT (A:April 2; B:April 12). See Figure 23 for the map legend.

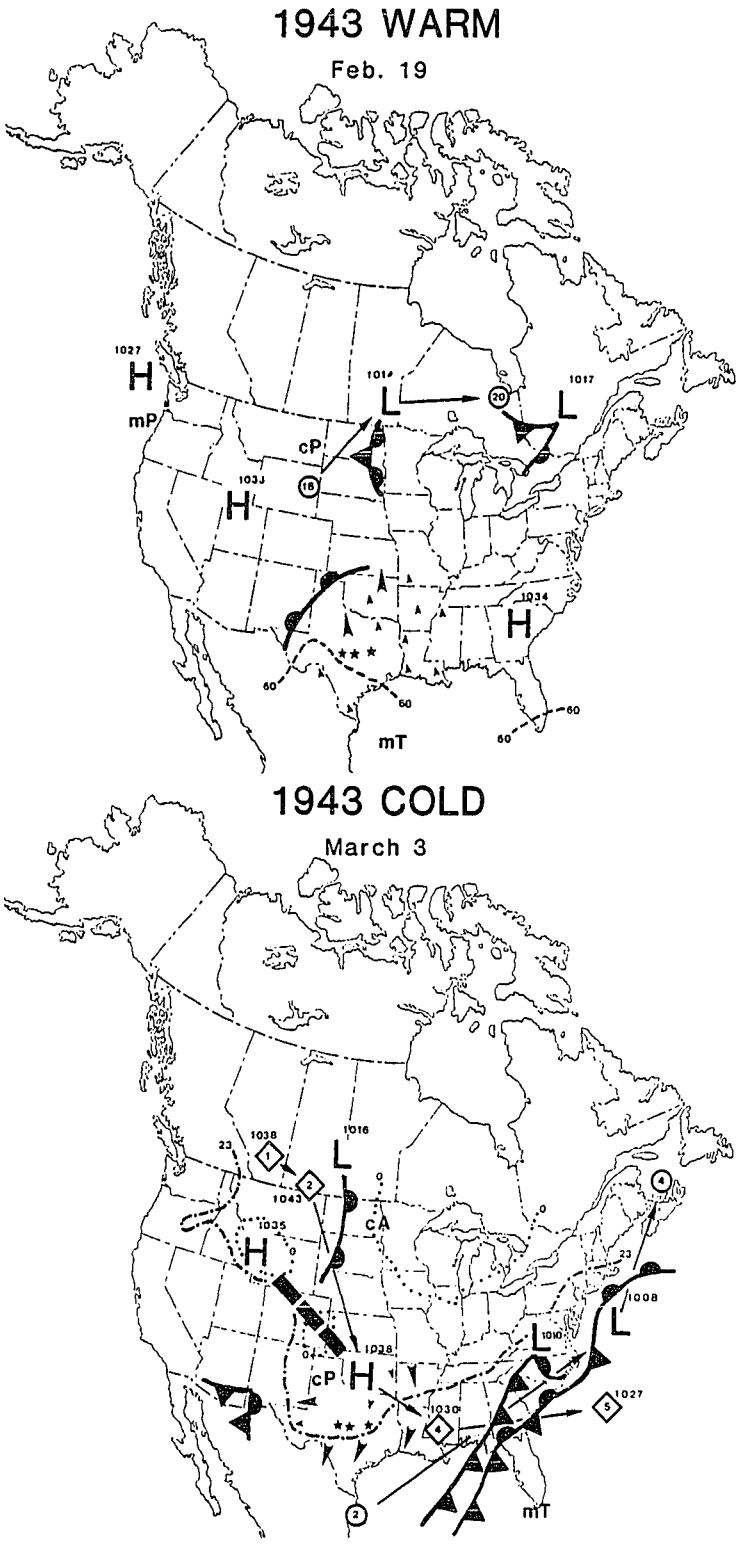

Figure 37. Same as Figure 22 for the 1943 warm and cold phases of false spring at 1:30 a.m. EWT (A:February 19; B:March 3). See Figure 23 for the map legend.

reported throughout the Southeast (WWCB 1943c). These temperature extremes reflected a pronounced southward migration of the main storm track, and presumably a similar shift in the prevailing upper air flow from late February to early March (e.g., Fig. 37A,B).

1955 Intense frost injury occurred continuously across all of Oklahoma and into central Missouri at 17 out of 23 sites north of the Red River (Fig. 34D). Record early season warmth occurred in the central and eastern United States during the second and third weeks of March when confluence aloft confined cold air masses to Canada (Winston 1955). Fast zonal flow from a 500 mb low off the California coast and circulation around a subtropical anticyclone at the surface in the Southeast led to the advection of warm air into the central and eastern United States (Winston 1955). The storm track was generally located near the Canadian border during this warm episode, and daily maximum temperatures rose to 90°F over much of Texas (Fig. 38A). A blocking anticyclone became established near Greenland around mid-March, and helped promote the southward depression of cyclonic activity and the westerlies into the eastern United States (Winston 1955). At the same time, a 500 mb ridge developed in the eastern Pacific and Gulf of Alaska, replacing the 500 mb trough present off California during the warm spell (Fig. 38B). A deep trough at 500 mb covered most of the continental United States

between the ridges off the east and west coasts of North America (Fig. 38B). A surface ridge extending from an arctic high swept south into southern Texas from March 18th to 22nd, behind a very intense cyclonic disturbance [U.S. Weather Bureau (C)1955]. The surge of arctic air on March 22nd and 23rd resulted in record breaking low temperatures for this late in the season at most weather stations in the Midwest and South (WWCB 1955). The southwest Missouri minimum temperature average fell to 11.7°F on March 22nd, the lowest recorded for any false spring event during the period of meteorological observation (Table 2). This storm system brought blizzard conditions to eastern Oklahoma and elsewhere, and spawned tornadoes, dust storms, gale-force winds, floods, and ice-jammed rivers throughout the eastern United States (WWCB 1955). The fruit crop was in full bloom and was wiped out across the South, and all crops were killed or severely damaged from Texas to the Carolinas (WWCB 1955). Severe temperatures as far south as central Texas, northern portions of the Gulf states, and western North Carolina (WWCB 1957). There were many aberrant features of the weather and circulation during the first four months of 1957, but frost drought conditions moderated the freeze damage because it was too dry to plant in many areas. Damage estimates nevertheless exceeded $50 million (Winston 1955; WWCB 1955). The late spring freeze of 1955 was evidently one of the most severe false spring episodes since 1650, and meteorologically is

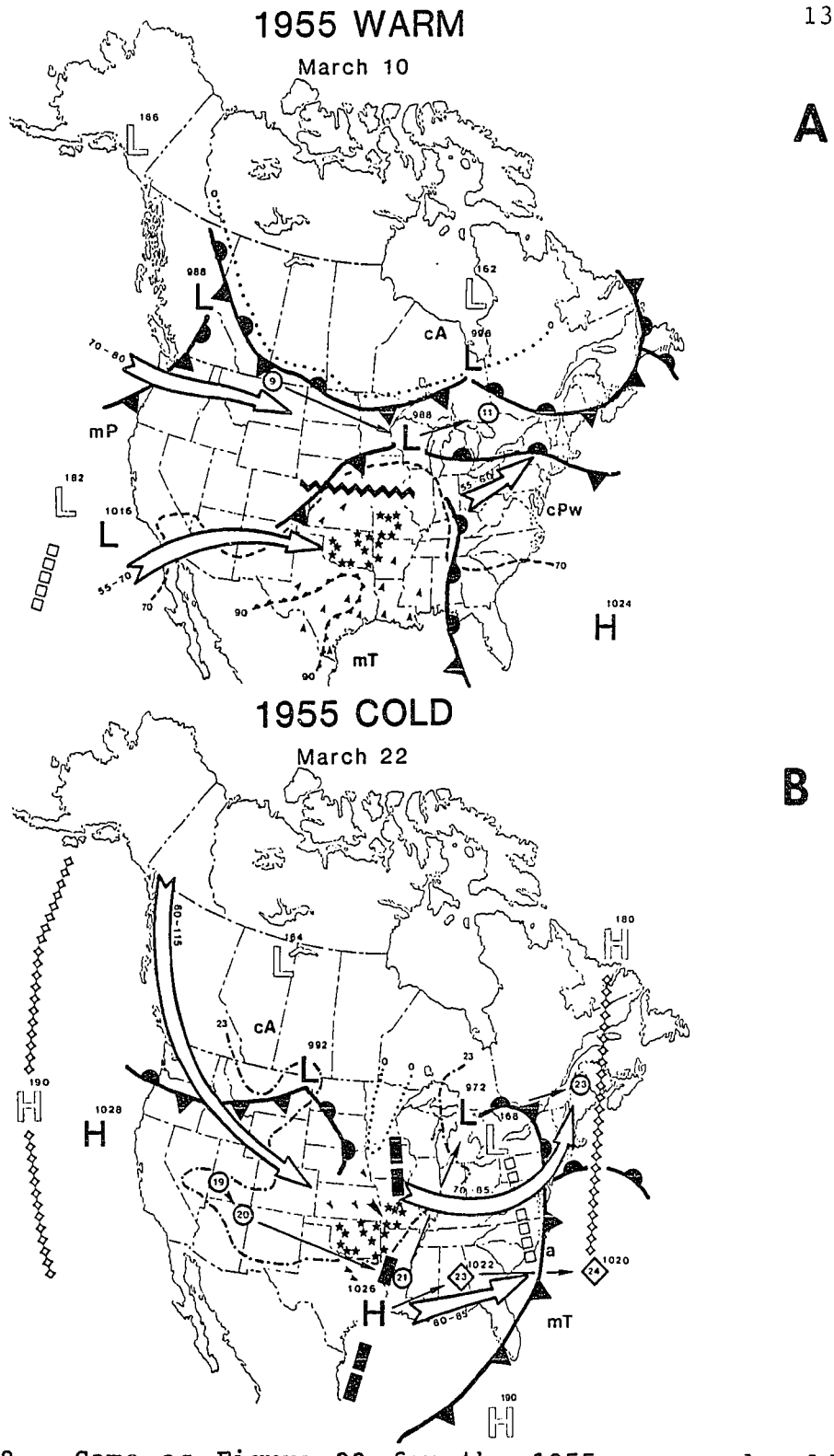

Figure 38. Same as Figure 22 for the 1955 warm and cold phases of false spring at 1:30 EST (A:March 10; B:March 22). See Figure 23 for the map legend.

certainly the best documented event (e.g., Winston 1955; Kibler and Martin 1955). The southern margin of the region of frost damaged trees in 1955 closely conforms to the critical 23°F isotherm (Fig. 38B), the approximate temperature threshold required to produce traumatic anatomical injury to the growth rings of oak trees.

The meteorological conditions prevailing during the 1955 false spring episode may provide a reasonable analog for several other severe false spring events registered by tree-ring data since 1650, particularly the events of 1711, 1716, 1779, 1806, 1826, 1828, and 1870 based on their similar intensity and distribution.

1957 Frost injury occurred in the tri-state region of Arkansas, Oklahoma, and Missouri at only 3 of 23 sites north of the Red River (Fig. 39A). The hard freeze responsible for this damage occurred on April 13th when the average minimum temperature for southwest Missouri fell to 15.7°F (Table 2). Many new record minimum temperatures were set from April 11th through the 13th when a polar air mass penetrated the eastern United States and brought freezing temperatures as far south as central Texas, northern portions of the Gulf states, and western North Carolina (WWCB 1957). There were many aberrant features of the weather and circulation during the first four months of 1957, but frost damage to trees and crops from the cold surge during the second week of April was not extensive

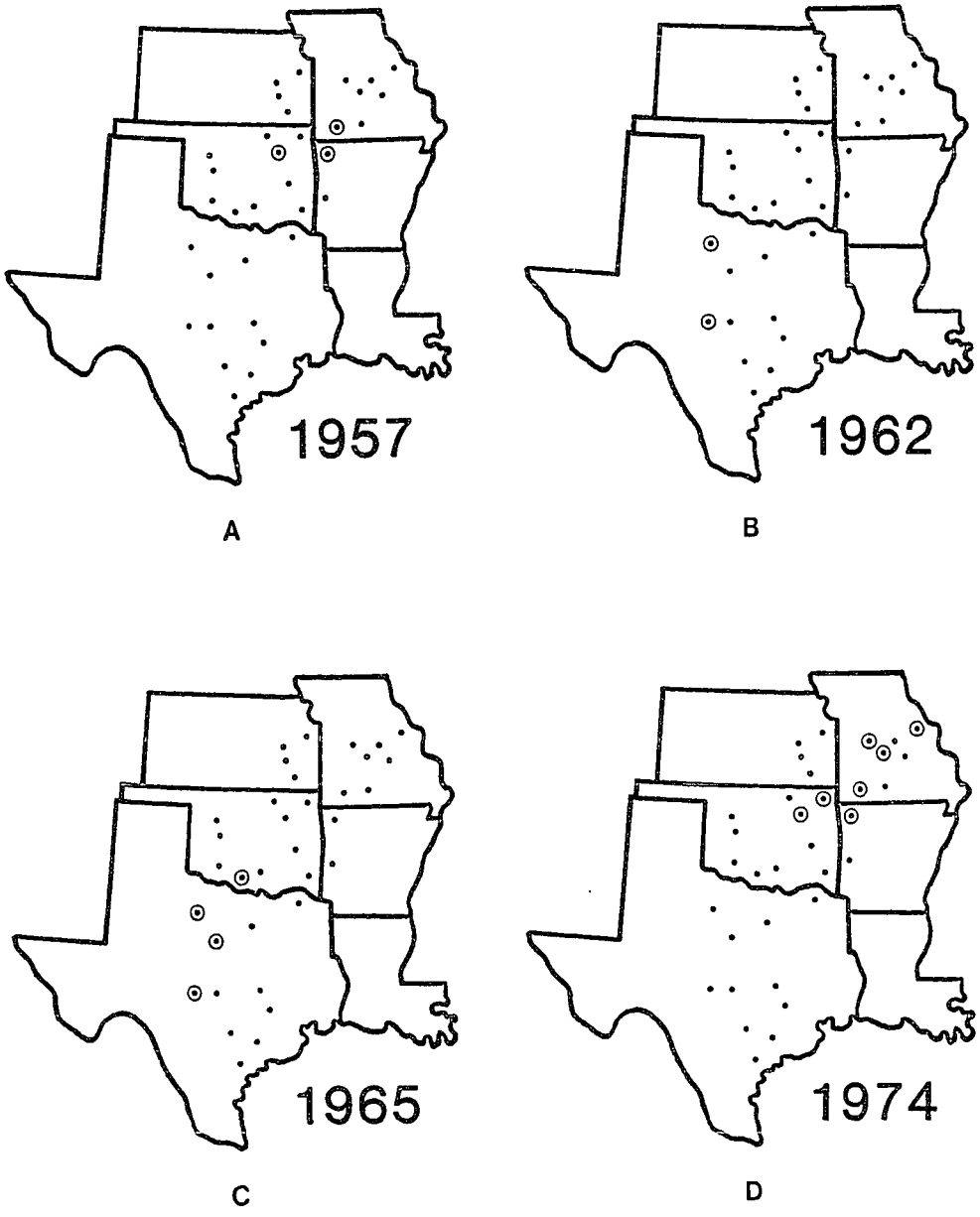

Figure 39. Same as Figure 8 for 1957(A), 1962(B), 1965(C), and 1974(D).

because the circulation and surface temperature anomalies were not synchronized with phenology in the southcentral United States. An unusual blocking anticyclone over the Gulf of Alaska was responsible for northwesterly flow of continental polar air and below normal temperatures in the central United States during January (Stark 1957). This anticyclone largely weakened and moved west during February, and a southwesterly flow of maritime tropical air resulted in a temperature reversal and an unusually warm February for most of the continental United States (Woffinden 1957). Confluence and a strong westerly jet also developed along the Canadian border to help contain cold polar air (Woffinden 1957). The region of polar blocking shifted to the Davis Straits in March, and a deep trough in the mid-tropospheric circulation developed over the central United States. The circumpolar vortex expanded well south into the United States, resulting in increased middle latitude cyclonic activity, cooler temperatures, and heavy precipitation (Frazier 1957). Record March rainfall in portions of Texas helped break the prolonged drought of the 1950's, but the cooler March temperatures also delayed the growing season and thereby moderated the vegetation damage from the subsequent April freeze. A brief period of warming occurred over the southcentral United States early in April, when confluence aloft became reestablished over the Great Lakes and a 500 mb trough over the Southwest favored warm air advection into the central United States

(Fig. 40A). By April 13th an anomalous 500 mb ridge redeveloped over the Gulf of Alaska, and a surface ridge and cold Canadian air moved south into Kansas and Oklahoma (Fig. 40B).

The false spring episode of 1957 was not a classic event due to the absence of warmer than normal temperatures during the weeks prior to the hard freeze, but the April 13th freeze was late enough in the season that some trees and crops had initiated growth and were injured. In fact, the 1957 freeze was the latest associated with any false spring event during the twentieth century (Table 2). Crop damage was largely confined to the southcentral United States where the coldest temperatures were observed from the 11th to 13th (WWCB 1957).

1962 Frost injury was recorded at only 2 out of 11 sites in Texas during 1962 (Fig. 39B). February temperature was summerlike in Texas with highs well into the 80's (e.g., Fig. 41A). The warmest February since 1878 was recorded at Brownsville (Andrews 1962). Severely cold air moved into the United States on March 1st and established many new minimum temperature records (Posey 1962). The average minimum temperature in central Texas fell to 18.3°F (Table 2), and subzero temperatures extended south into southern Kansas and Missouri (Fig. 41B). Rio Grande City, Texas, recorded 29°F on March 1st (WWCB 1962). Peach trees and other fruits were in full bloom when the cold front passed, and a complete fruit

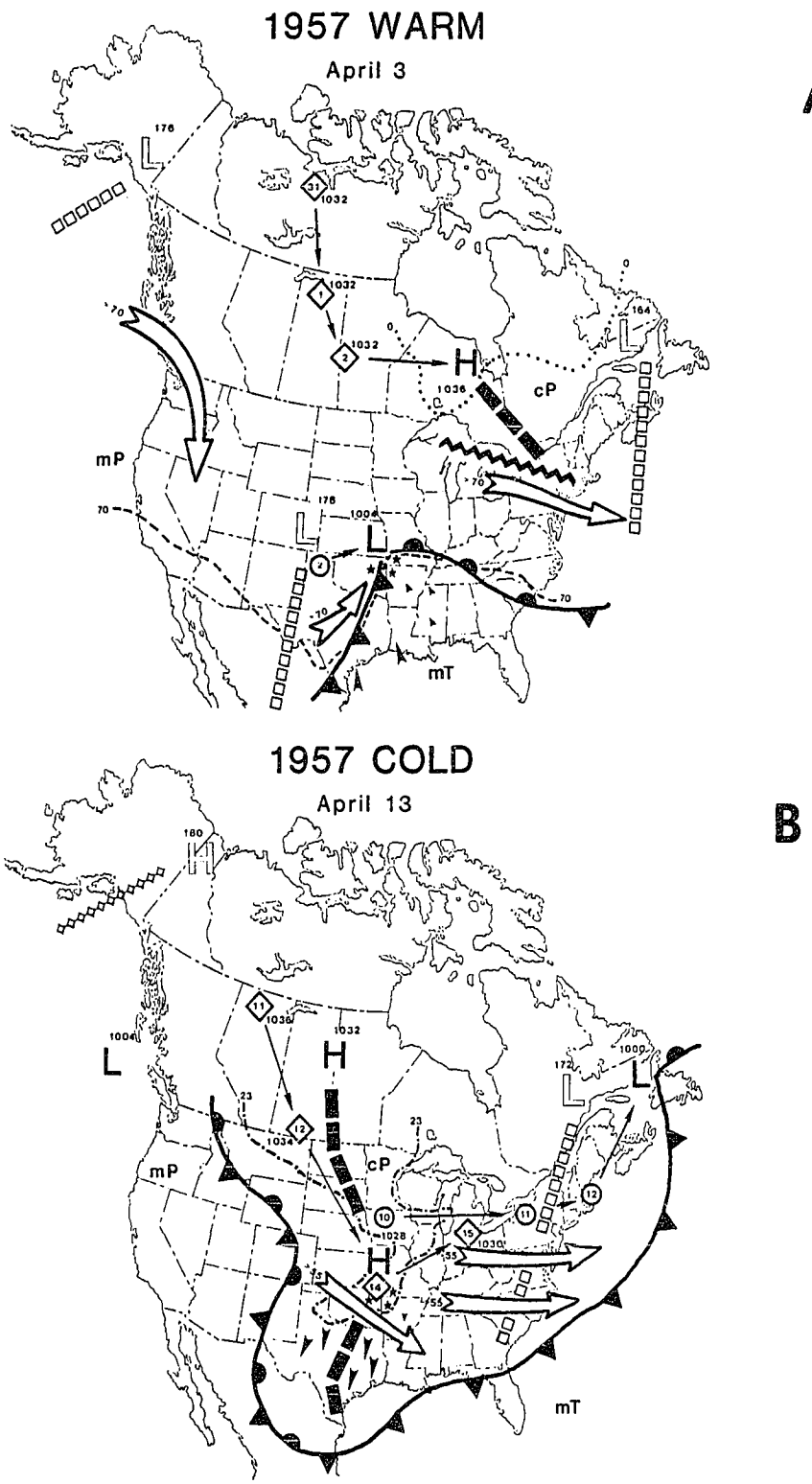

Figure 40. Same as Figure 22 for the 1957 warm and cold phases of false spring at 1:30 EST (A:April 3; B:April 13). See Figure 23 for the map legend.

kill was reported in many areas of Texas and Louisiana (WWCB 1962). A sharp change in the circulation over North America during February was largely responsible for the shift from above to below normal surface temperatures over the Southern Plains late in the month (Fig. 41A,B). A near normal 700 mb ridge over the western United States and trough over the Atlantic seaboard were associated with a confluent zone in the mid-troposphere over the Midwest, which tended to confine polar anticyclones and cold air to the Northern Plains and eastern Canada (Andrews 1962). Warmer air prevailed south of this confluence. During the height of the warm spell on February 14th, a 500 mb trough was located over New England, and a ridge extended from the Gulf of Mexico into the Southeast (Fig. 41A). This circulation pattern resulted in warm air advection into Texas, reflected in part by a prominent ridge in the 700 mb isotherms extending from Texas up the front range of the Rocky Mountains (NWS 1962, not illustrated).

In the latter half of February the western North American ridge at 700 mb retrograded and an anomalous blocking ridge developed at 700 and 500 mb over the Gulf of Alaska (e.g., Fig. 41B). A deep upper level trough replaced the ridge over the western and central United States late in February, and another blocking ridge developed downstream over the North Atlantic (Andrews 1962; Fig. 41B). This pronounced circulation change persisted into early March (Posey 1962),

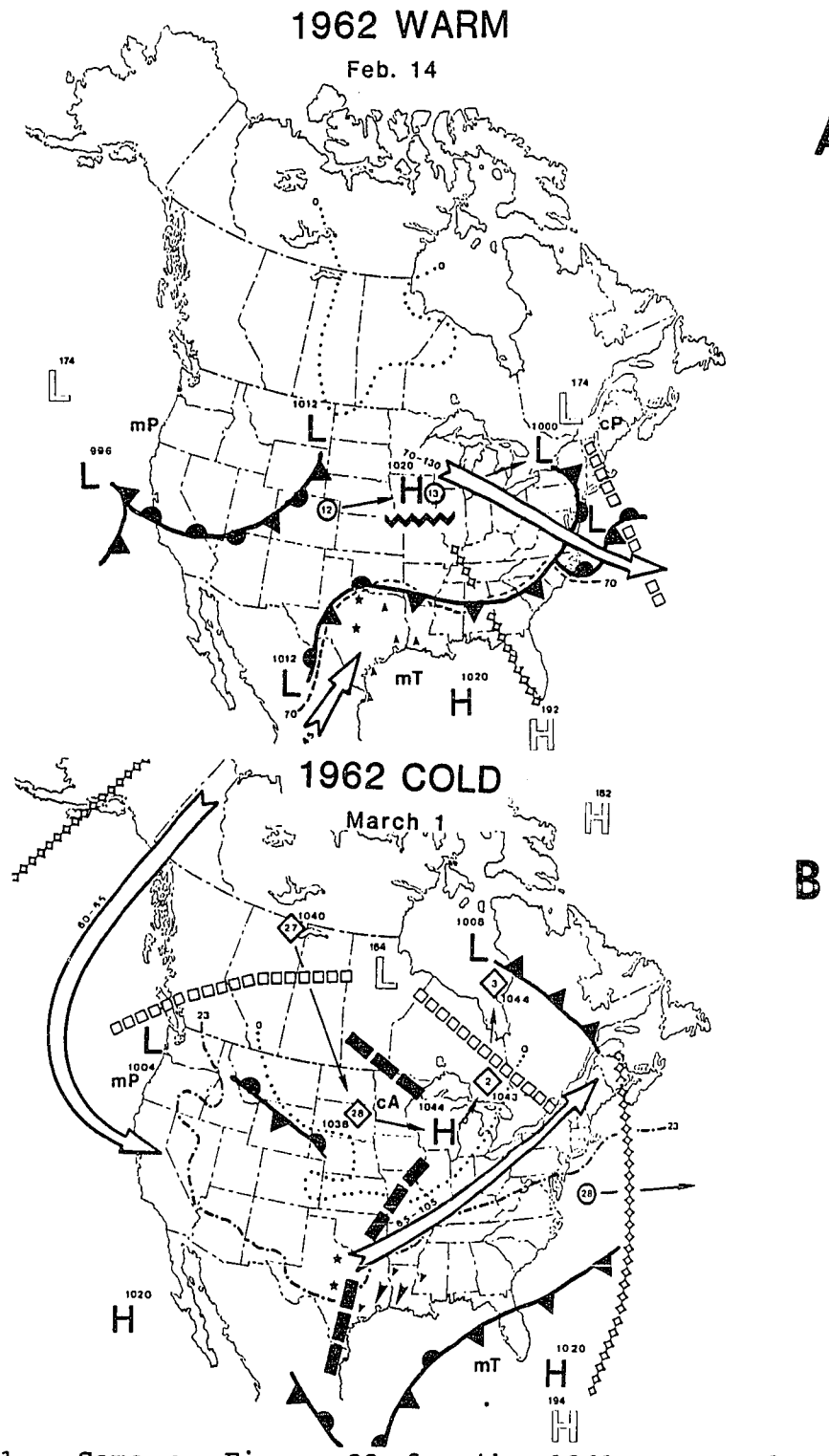

Figure 41. Same as Figure 22 for the 1962 warm and cold phases of false spring at 1:00pm EST (A:February 14; B:March 1). The surface winds were analyzed at 7:00am EST for Figure 41B. The 500 mb data were analyzed at 7:00pm EST on February 28 for Figure 41B. See Figure 23 for the map legend.

and led to southward displacement of the westerlies and abrupt temperature changes over the western and central United States, including the Texas cold wave of March 1st.

Circulation reversals appear to be quite typical of false spring events (e.g., 1955, 1974), but the frost injury associated with the 1962 event was not extensive because the freeze occurred very early in the growing season. The hard freeze of March 1st, 1962, was the earliest freeze associated with any twentieth century false spring event (Table 2).

1965 Frost injury occurred in Texas and southern Oklahoma at 4 out of 34 total sites (Fig. 39C). The hard freeze occurred on March 20th, when the average minimum temperature for central Texas fell to 20.3°F (Table 2). The frost damage associated with this cold wave was minimal (WWCB 1965) because temperatures over most of Texas had averaged below normal since the last week in January (Stark 1965). Frost injury was recorded at the four tree-ring sites probably due in part to above normal January temperatures (Griffiths and Ainsworth 1981), and because spring growth is normally in full progress from central Texas to South Carolina by the third week of March (WWCB 1965). Also, a brief warming trend occurred in Texas during the second week of March when a 500 mb trough developed off the Southern California coast (Fig. 42A). Strong zonal flow across the Southern Plains, confluence aloft over southern Colorado (Fig. 42A), and a surface anticyclone

off the Southeast coast (not shown) all favored modest warm air advection into Texas during mid-March. This advection is reflected by surface winds, the 70°F isotherm (Fig. 42A), and by a modest ridge in the 700 mb isotherms over Texas on March 14th (NWS 1965, not illustrated).

An anomalous 500 mb ridge over the Gulf of Alaska and a deep trough over the central United States became re-established by March 20 (Fig. 42B). A ridge of surface high pressure from the Yukon and severe subzero air surged rapidly south into the southcentral United States from the 16th to 20th (Fig. 42B). This cold air advection is reflected by a huge 700 mb thermal trough covering the entire continental United States and centered over Texas on March 20th (NWS 1965, not illustrated). New record low temperatures for so late in the season were set from Texas to Minnesota and West Virginia (Green 1965).

1974 Frost injury occurred in Missouri and northern Oklahoma at 7 out of 23 sites north of the Red River in 1974 (Fig. 39D). The hard freeze occurred on March 21st, when the average minimum temperature for southwest Missouri fell to 18.3°F (Table 2). February and early March temperatures had averaged well above normal across most of the United States (Dickson 1974), but a complete circulation reversal in mid-March resulted in a damaging cold wave that reached southern Texas (Fig. 43). Record warm temperatures for so early in the

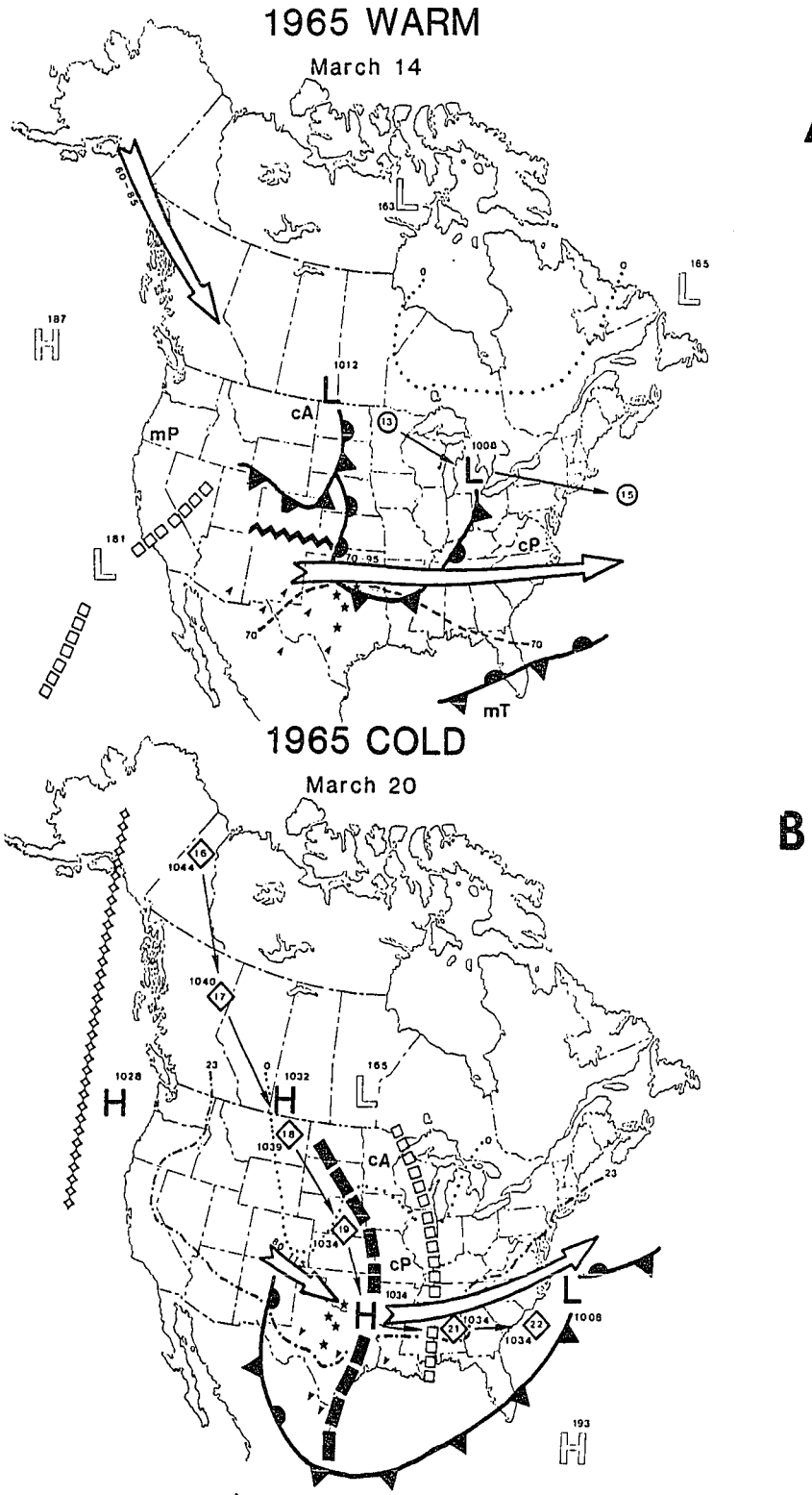

Figure 42. Same as Figure 22 for the 1965 warm and cold phases of false spring (A:March 14; March 20). The surface winds were analyzed at 1:00 a.m. EST on March 20(B). See Figure 23 for the map legend.

season prevailed at many stations in the central and eastern United States early in March when an east coast ridge and a west coast trough extending from the surface up to at least the 500 mb level resulted in westerly and southwesterly flow (e.g., Taubensee 1974; Fig. 43A). This circulation pattern resulted in warm air advection into the Midwest, reflected by a huge thermal ridge at the 700 mb level (NWS 1974, not illustrated), while confluence aloft over Quebec tended to confine polar high pressure systems in Canada (Fig. 43A).

The atmospheric circulation pattern over North America completely reversed during the third week of March, and was replaced by a sharp and anomalous ridge in the Gulf of Alaska and a broad deep trough over the central United States (Taubensee 1974; NOAA 1974a; Fig. 43B). This upper level flow favored the southerly penetration of a surface high pressure ridge and associated cold air mass from Canada to Texas (Fig. 43B). This cold air advection is reflected by a deep thermal trough at the 700 mb level extending from Hudson Bay to Texas on March 21st (NWS 1974, not illustrated). Clear skies and bitter cold air moved into Oklahoma and Missouri on the 21st, when record low temperatures were set for so late in the season at stations from Minnesota to Texas (WWCB 1974). Heavy freeze damage to fruit crops occurred in Arkansas, Oklahoma, and Missouri (WWCB 1974). An estimated $5 million to the peach and apple crops was reported for western and northern Oklahoma alone (NOAA 1974b).

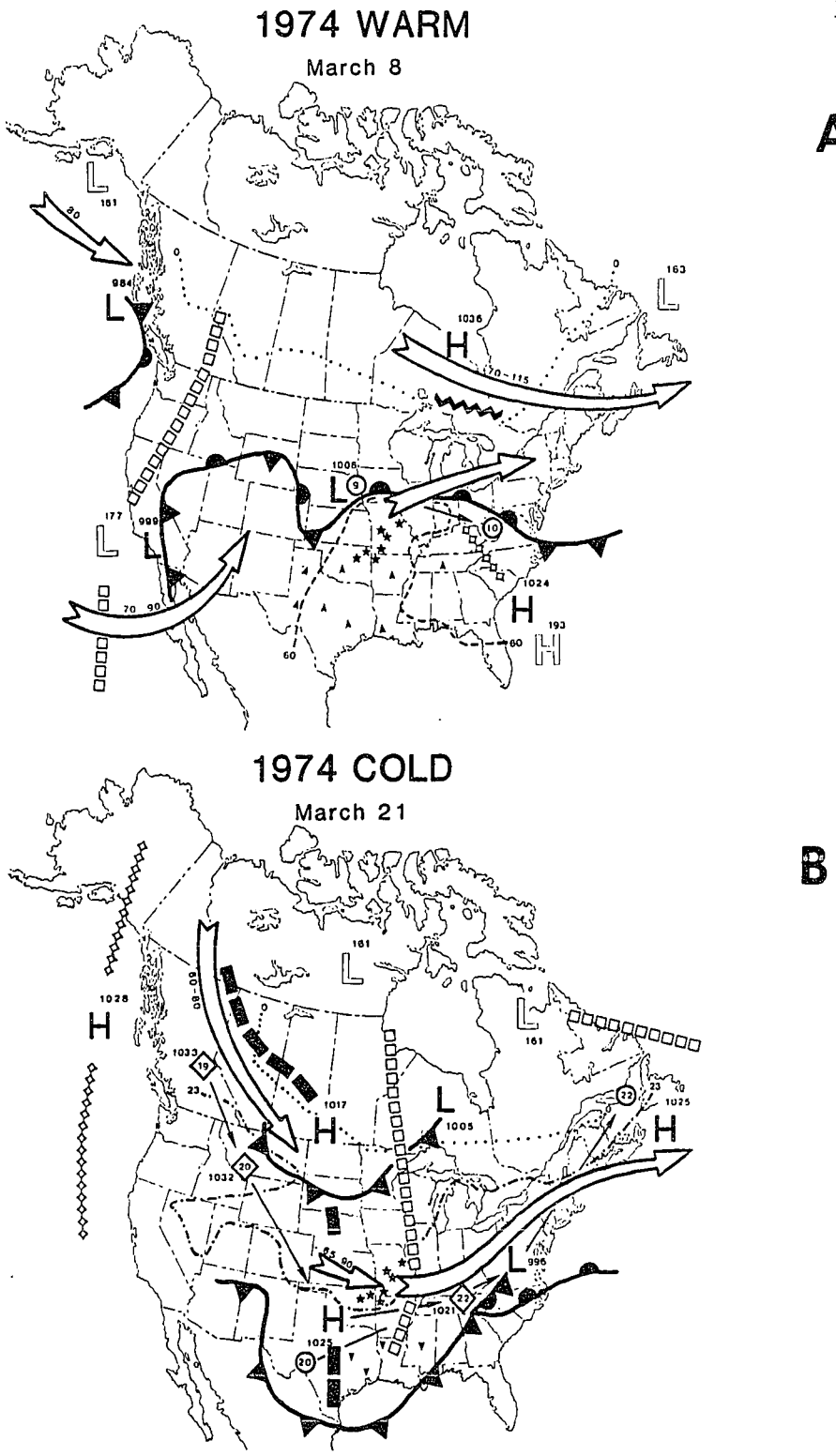

Figure 43. Same as Figure 22 for the 1974 warm (A:March 8, 6:00am EST) and cold phases of false spring (B:March 21, 7:00am EST). See Figure 23 for the map legend.

VI. ANALYSIS

Examination of the synoptic maps illustrated in Chapter 5 indicates that the weather anomalies of false spring tend to be widespread over the eastern United States, and the sudden change from warm to cold conditions frequently coincides with a major reversal in the general circulation over North America. In this chapter the temperature anomalies during twentieth century false spring events are evaluated, and composite weather maps are used to summarize the typical meteorological conditions over North America during the warm and cold phases of false spring. Mid-tropospheric circulation data are available for the five most recent false spring events, and a selected circulation index is used to examine the possible role of circulation changes in false spring.

False spring events over the Southern Plains also appear to be linked to certain extreme configurations of the El Nino-Southern Oscillation, and to the chronology of large magnitude explosive volcanic eruptions. These phenomena are believed to be capable of causing short-period climate changes in the extratropics (e.g., Horel and Wallace 1981; Kelley and Sear 1984), presumably through an effect on the general circulation. Consequently, these potential internal and external factors of short-period climate change might also be related to false spring anomalies over the Southern Plains region, and these possibilities are examined in this section. Finally, a summary chronology of frost ring occurrence is

compiled for all available oak sites in the Southern Plains region, and is used to investigate the secular variability of false spring weather anomalies for the past 331 years.

Daily Temperature Analysis

The meteorological definition of false spring and the descriptions of past episodes (Chapter 5) clearly imply that the warm and cold phases of false spring represent significant departures from the normal seasonal march of temperature over the Southern Plains region. The regionally averaged daily temperature series compiled for southwest Missouri, northcentral Oklahoma, and central Texas were used to test the statistical significance of these apparent temperature anomalies. The daily maximum and minimum temperature data for the 13 "frost" years which occurred in the vicinity of each regional temperature average from 1918 to 1980 were separated for comparison with all remaining "non-frost" years. These 13 frost years are 1920, 1921, 1936, 1940, 1955, 1957 and 1974 in the southwest Missouri region, 1926 and 1931 in northcentral Oklahoma, and 1923, 1943, 1962 and 1965 in central Texas. Because the exact timing of these frost events differs from year to year, and tends to be later in the season in central Missouri than in central Texas, the date of the hard freeze (K) was used as the reference date to sort or "event-center" the daily temperature data for all frost years. This sorting procedure allows the use of temperature data for

all 13 events regardless of exactly where or when they occurred. For comparative purposes, the remaining non-frost years in each region were also sorted by the appropriate freeze dates (K) in each region. Because this resulted in unequal sample sizes and sometimes in unequal variances between the two groups, the appropriate corrections were used in computing the test statistic (SAS Institute 1985).

Two approaches were then used to test hypotheses stating that daily maximum and minimum temperatures were both above normal during the warm phase, and below normal during the cold phase of false spring. The first approach used two-tailed t-tests for differences between means of daily temperature during frost and non-frost years. The second approach used time series plots of mean daily temperatures and associated confidence intervals for all frost and non-frost years, after the daily data for each group were event centered.

Tests were performed for two time periods before, and one time period after the frost event (Table 4). The periods tested were the three week interval beginning 28 days prior, and ending 7 days prior to the freeze event (i.e., K-28 to K-7); the ten day period beginning 13 days prior, and ending 4 days prior to the freeze date (K-13 to K-4); and the ten day period beginning 1 day before, and ending 8 days after the freeze (K-1 to K+8). The three day period just prior to the freeze event was excluded from the warm period tests because the weather tends to be transitional between the warm and cold

Table 4. Tests comparing mean daily maximum (MAX) and minimum (MIN) temperatures (°F) of frost and non-frost years for three short time periods before and after the hard freeze event (K) of false spring. The variances were unequal ($p < 0.05$) for all comparisons except for the minimum temperature averages for K-28 to K-7. The degrees of freedom exceed 132 and 8561 for all frost and non-frost averages, respectively.

Time Period [Days Before/ After Hard Freeze (K)]	Frost Years	Non-Frost Years	t-test	p
Warm Spell				
A. K-28 to K-7, MAX	65.18	61.22	-6.28	<0.0001
K-28 to K-7, MIN	39.12	35.92	-4.93	<0.0001
B. K-13 to K-4, MAX	68.07	64.31	-4.52	<0.0001
K-13 to K-4, MIN	43.30	38.59	-6.22	<0.0001
Cold Spell				
C. K-1 to K+8, MAX	58.70	68.44	8.60	<0.0001
K-1 to K+8, MIN	33.21	42.71	9.18	<0.0001

phases.

The t-tests indicate that the daily maximum and minimum temperatures during the three week and ten day intervals before the freeze are both about 4°F above normal for the average false spring data, and these differences are significant at $P < 0.0001$ (Table 4). The cold anomaly of false spring is not usually as prolonged as the warm spell, but the temperature departures are more extreme. The average daily maximum and minimum temperatures for false spring years during the ten day cold phase are both at least 9.5°F below

normal ($p < 0.0001$, Table 4).

These results clearly confirm the extreme nature of the warm and cold temperature phases of false spring, but the t-tests impose rather arbitrary time groupings that conceal considerable detail in the evolution of the daily temperature anomalies of false spring. As an alternative, the time series of daily average temperature for the frost and non-frost year means are plotted simultaneously with their associated confidence intervals. Daily maximum and minimum temperature means for frost and non-frost years are both plotted, after the data in each group were event-centered and sorted for the 40 days before and 19 days following the freeze event (Fig. 44). The confidence intervals for both frost and non-frost time series are based on the two standard errors associated with the daily means. Figure 44 illustrates the highly anomalous nature of the warm and cold temperature excursions of false spring. The average daily maximum temperature during frost years is continuously above the normal daily temperatures of non-frost years for three weeks during the warm phase, but the daily means are not significantly different until the five day period from K-13 to K-9 when the confidence intervals associated with the frost and non-frost samples do not overlap. The average daily minimum temperatures of frost years are also significantly warmer than the non-frost year daily normals during this same five day period (beginning and ending one day later, K-12 to K-8; Fig.

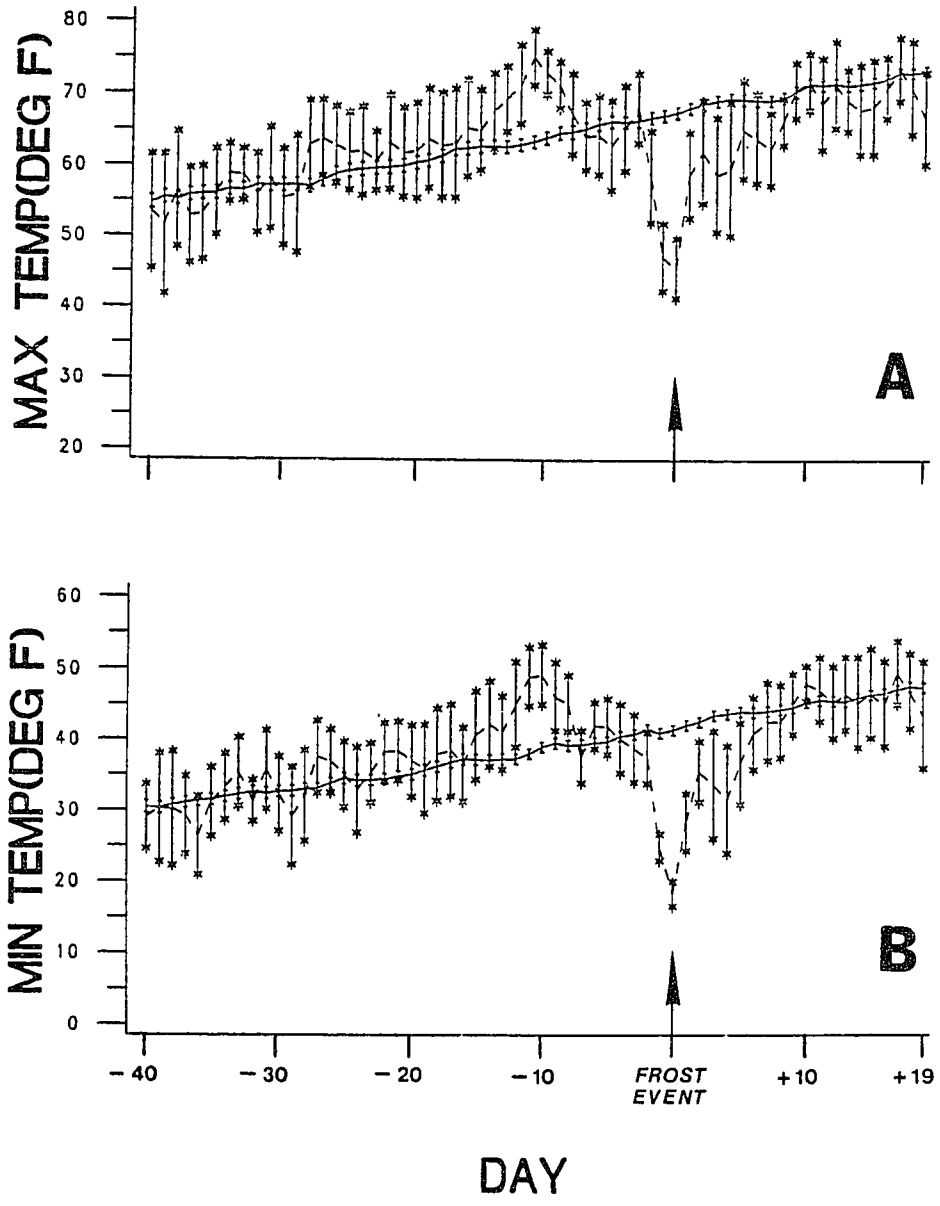

Figure 44. The composite daily average maximum (A) and minimum (B) temperature anomalies of 13 twentieth century false spring episodes are plotted for 40 days before and 19 days after the hard freeze event (K=day 0), along with the average daily temperatures computed from the 50 remaining non-frost years between 1918 and 1980. The confidence intervals represent the two standard errors associated with each daily average. See text for further details on the sorting procedure used to compile these data.

44).

Figure 44 also indicates that the cold phase tends to be more intense, but less prolonged than the warm phase of false spring. Average daily minimum temperatures during frost years are significantly below daily normals for non-frost years for seven days from K-1 to K+5, but return to normal by nine days after the freeze. Average daily maximum temperatures are also significantly below normal during most of this week-long cold phase. These time series confirm the highly anomalous character of false spring, and identify specifically the timing and intensity of the unusual weather conditions typical of twentieth century false spring episodes. The most extreme high temperatures during the long warm spell usually begin two weeks prior to the hard freeze and last for five days, while the most extreme cold weather tends to begin a day or two before the hard freeze and lasts for one week (Fig 44).

The Climatology of False Spring

The sudden and severe freeze is certainly the most extraordinary meteorological feature of false spring, but above normal winter temperature is paradoxically the primary climatological signal of false spring. This can be illustrated with t-tests comparing daily maximum and minimum temperatures between frost and non-frost years for three long time periods before, during, and after the cold wave (Table 5). Average daily maximum and minimum temperatures are

significantly above the non-frost year averages for three winter months preceding the cold wave (K-90 to K-7, Table 5), while they are significantly below the non-frost normal for the 61 day period during and after the cold wave of false spring (K-1 to K+59). However, when the week-long cold wave is excluded from the time interval following false spring (i.e., K+7 to K+59), daily average minimum temperatures are slightly above the non-frost year normals (the difference is not significant). Daily maximum temperatures are below average during this period, but this difference is only marginally significant (Table 5). This comparison emphasizes that the seven or eight day cold wave of false spring years is highly anomalous, but daily temperatures for the remainder of spring tend to be near normal during these years.

The prolonged warm winter of false spring actually represents a significant climatological signal, while the shorter, contrasting, and more extreme cold wave represents a significant meteorological signal of false spring. The recovery of both climatological and meteorological signals from proxy tree-ring data is quite rare, but the frost ring chronology from the Southern Plains provides a detailed record of these two highly contrasting signals over the past 331 years.

The Synoptic Meteorology of False Spring

The meteorological conditions over most of North America

Table 5. Tests comparing mean daily maximum (MAX) and minimum (MIN) temperatures (°F) of frost and non-frost years for three long time periods before and after the hard freeze event (K) of false spring. The variances of both samples compared in A and B are unequal, while the variances of the samples in C are equal. The degrees of freedom exceed 395 in all comparisons.

Time Period [Days Before/ After Hard Freeze (K)]	Frost Years	Non-Frost Years	t-test	P
3 Months Before Freeze				
A. K-90 to K-7, MAX	55.87	55.02	-1.87	0.0610
K-90 to K-7, MIN	30.84	31.81	-2.65	0.0081
2 Months During and After Freeze				
B. K-1 to K+59, MAX	70.12	73.18	5.75	<0.0001
K-1 to K+59, MIN	45.41	47.56	4.02	<0.0001
50 Days After Freeze				
C. K+9 to K+59, MAX	73.86	74.70	1.66	0.0975
K+9 to K+59, MIN	49.56	49.15	-0.88	0.3814

during the height of the warm and cold phases of false spring have been illustrated chronologically from 1899 to 1974 in Chapter 5. Examination of these synoptic weather maps reveals several recurrent, and in some cases universal meteorological features of false spring. Composite weather maps have been used to summarize the synoptic conditions typical of the warm and cold phases of false spring (Fig. 45).

A very common and important meteorological feature of the

warm spell is the presence of a surface anticyclone usually located near the Southeast coast (Fig. 45A). This anticyclone, or a ridge extending into the Southeast from the Atlantic, was clearly present during the warm spell of 13 out of the 17 warm events illustrated in Chapter 5, and favored southerly air flow and warm air advection into the Southern Plains. Warm air advection is further indicated on the composite map of the warm spell by the surface wind arrows, the penetration of the 60°F isotherm and maritime tropical air into the Central Plains, and by the warm front often located across the Ohio Valley (Fig. 45A). Analyses of the 700 mb isotherms available for three warm events (NWS 1962, 1965, and 1974) also illustrate large-scale advection of warm air in the lower troposphere into the Southern Plains (not shown).

Examination of the 500 mb pressure surface during the five most recent false spring events, and the tracks of well-defined low pressure centers for all 17 events since 1899 indicate that a 500 mb trough is frequently located near Southern California during the height of the warm spell (Fig. 45A). Due to the lack of upper air data prior to 1947, this feature is not as well documented as the surface high off the Southeast coast. But when present, this trough in the upper air flow would certainly favor warm air advection into the Southern Plains. Dickson and Namias (1976) examined the 700 mb height departures associated with warm and cold winters over the southeastern United States, and found that above

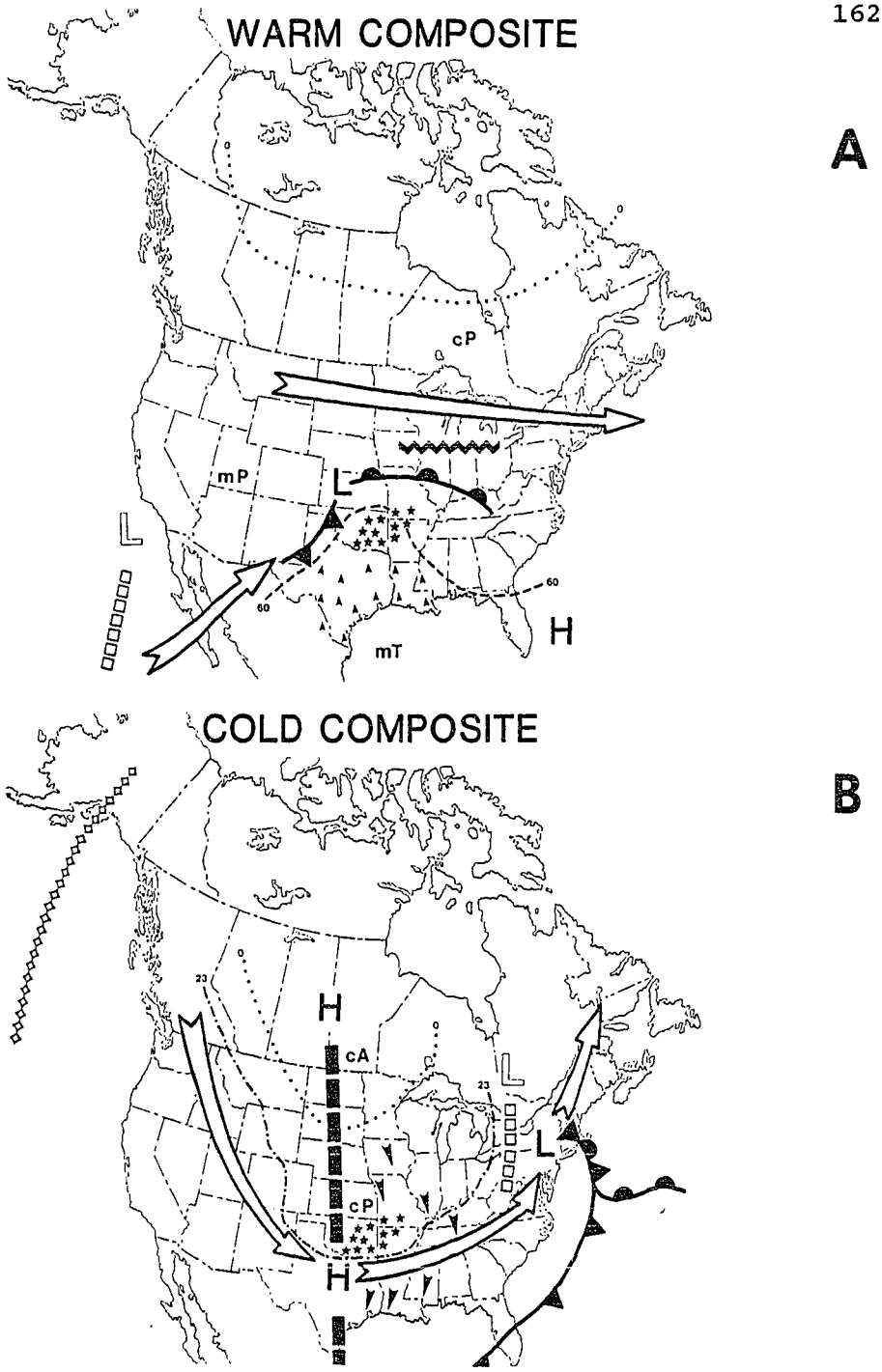

Figure 45. Composite weather maps illustrating the typical North American meteorological features often associated with the warm (A) and cold phases (B) of false spring over the southcentral United States. These "dendrometeorological" maps specifically summarize the synoptic meteorology prevalent during the 17 false spring episodes which occurred from 1899 to 1974 (Chapter V). The map legend is presented in Figure 23.

normal heights over the northeast Pacific and over the southeastern United States, along with below normal heights over western Canada down to Southern California were associated with warm winters in the Southeast. This particular configuration of atmospheric circulation is described as the reverse Pacific/North American pattern (Wallace and Gutzler 1981; Yarnal and Diaz 1986; Barnston and Livezey 1987), and it appears to be consistent with the prevailing circulation during the warm spell of many twentieth century false spring episodes.

A prominent 500 mb trough was located off Southern California during the warm phase of false spring in 1955, 1965, and 1974, and a weaker 500 mb trough was located west of the region of frost injury during the 1957 warm spell (Chapter 5). Fast zonal flow near the Canadian border is also indicated at the 500 mb level during the warm phase of false spring (Fig. 45A). This general circulation pattern tends to favor above normal temperatures in the eastern United States and a mean storm track extending from the Central or Northern Plains across the Great Lakes and into New England. This approximate storm track was actually observed during at least 13 of the 17 warm spells since 1899 (Chapter 5).

Other recurrent features during the warm phase include a surface cyclonic disturbance and associated warm front over the northern U.S., and a region of confluence in the upper level winds typically located near the Great Lakes (Fig. 45A).

This confluence aloft and the fast westerly flow tend to confine cold polar air masses to the north (e.g., Namias 1950), and this may be reflected by the isolation of the 0°F isotherm and continental polar air in Canada (Fig. 45A). Confluence was observed during the warm spell for all five false spring events with upper air data (Chapter 5). Confluence may help to magnify the subsequent cold air surge by isolating cold continental air in the polar and subpolar region, where radiative cooling can further lower air temperature (Namias 1950).

The strong zonal flow pattern at 500 mb across the northern United States, the upper level trough off the Southern California coast, and the surface anticyclone near the Southeast coast were by far the most prevalent circulation features observed during the warm phase of twentieth century false spring episodes. However, this general circulation pattern was not universal, and different circulation regimes were observed during some warm spells. These differing patterns are not illustrated in the selected synoptic maps of Chapter 5, but included a more meridional regime consisting of a broad ridge located over western North America. This ridge was spread longitudinally well eastward of the Southern Plains, tending to prevent the penetration of cold air into Texas and favoring some warm air advection under the ridge [warm advection would be greatly increased under this meridional pattern given the development of a cut-off low over

Southern California, as occurred on March 7, 1965 during a strongly meridional longwave regime over North America (U.S. Weather Bureau (C)1965)].

Meteorological conditions during the cold phase of false spring were much more consistent than during the warm phase, and always involved a deep low pressure disturbance and associated cold front migrating across the Southern Plains (Figure 45B). Based on 500 mb height data for the five most recent events, the tracks of surface pressure centers, and anomalies in the surface temperature field, a deep upper level low over the Midwest or eastern United States and a pronounced trough in the upper level flow over the central United States were also very prevalent during the cold phase of false spring. This upper air pattern usually reflected a dramatic reversal from the circulation regime prevailing during the warm spell, and resulted in large-scale cold air advection into the southcentral and eastern United States (Figure 45B). This circulation pattern conforms to the 700 mb flow pattern typical of cold winters in the Southeast (Dickson and Namias 1976).

The surge of cold air into the Southern Plains is illustrated by the 23°F and 0°F isotherms, the powerful ridge of surface high pressure extending from northern Canada into Mexico (Fig. 45B), and by the deep trough in the 700 mb isotherms over the Southern Plains during the three most recent events (not shown). Northerly winds and continental

polar or arctic air masses over the central United States, and an anomalous 500 mb ridge over the Gulf of Alaska complete the typical synoptic features of the cold phase of false spring. These specific dendrometeorological conditions were highly consistent between most hard freeze events of the twentieth century. Cooler than normal conditions over the Southern Plains typically lasted for seven to ten days, but severely cold temperatures at or below 23°F usually lasted only one or two days (e.g., Fig. 44).

The composite weather maps illustrate a major reversal in atmospheric circulation over the North American sector from the warm to cold phase of false spring (Fig. 45). This reversal of "backward" weather regimes during early spring has a high potential for widespread freeze damage to crops and native vegetation, as documented by the numerous historical and modern descriptions of false spring impact cited in Chapter 5. Certainly, the selection of weather conditions near the peak warm and cold spells for synoptic mapping, and the compositing technique have tended to magnify the circulation reversal. Nevertheless, these contrasting meteorological conditions have been witnessed during most warm and cold phases of twentieth century false spring episodes, and are consistent with the circulation and surface temperature anomalies typical of warm and cold winters over the entire eastern United States (Dickson and Namias 1976).

Atmospheric Circulation and False Spring

The sudden change between widespread temperature extremes suggest that anomalous atmospheric circulation may frequently be responsible for false spring episodes over the southcentral United States. Major changes in circulation over North America definitely occurred from the peak of the warm to cold phase during many twentieth century false spring episodes (Fig. 45). If anomalous circulation is actually an essential ingredient of false spring weather conditions, then the frost ring chronology might provide a partial record of unusual late winter-early spring circulation regimes over the North American sector for the past 331 years.

The possible role of circulation is examined in this section on a daily and monthly basis using a selected index of mid-tropospheric flow available only for the five most recent false spring events. Daily 700 mb heights recorded from 1947 to 1980 were obtained for three regions over the North Pacific and North America which are associated with the Pacific/North American (PNA) pattern of atmospheric circulation. The PNA pattern is a recurring configuration of cool-season circulation over the North Pacific and North American sectors, and has been related to winter temperature regimes over the eastern United States (Wallace and Gutzler 1981). The PNA pattern has been identified in the geopotential height field at the 700 and 500 mb levels (Barnston and Livezey 1987; Wallace and Gutzler 1981), and in

surface pressure data (Wallace and Gutzler 1981). The PNA pattern has been documented in weekly, monthly, and seasonal average data (e.g., Barnston and Livezey 1987), but baroclinic disturbances may obscure its importance in daily data. Nevertheless daily PNA indices were computed for this study to identify any consistencies on the timing, evolution, or magnitude of PNA-related circulation conditions during false spring. These daily PNA indices were also averaged over one- to three-week long intervals to investigate possible changes associated with false spring in longer, equivalently barotropic time averages of this circulation index.

The normal mode of circulation in the PNA pattern includes three principal centers of action, with a longwave ridge located over western North America (centered near 50°N, 110°W), associated with longwave troughs over the northcentral Pacific near the Aleutian Islands and over the southeastern United States (centered near 50°N, 170°W and 30°N, 85°W, respectively). Wallace and Gutzler (1981) identify a fourth center near Hawaii in 500 mb data. Several indices of the PNA pattern have been used primarily with monthly data (e.g., Wallace and Gutzler 1981; Yarnal and Diaz 1986; Barnston and Livezey 1987). The PNA index used in this study was based on daily mean 700 mb data, and was calculated as:

$$PNA = 0.33[-Z^*(50^\circ N, 170^\circ W) + Z^*(50^\circ N, 110^\circ W) - Z^*(30^\circ N, 85^\circ W)]$$

where Z* represents the normalized 700 mb height value for each location (Yarnal and Diaz 1986). Positive PNA indices reflect an increasingly amplified or meridional longwave pattern, anchored by the ridge over western North America and favoring cool surface air temperatures in the deeper than normal trough over the Southeast. Negative PNA indices represent a reversal of the normal pattern, with upper level ridges developing over the North Pacific and over the Southeast, and a trough located over western North America. This configuration is referred to as a "reverse PNA" pattern (Yarnal and Diaz 1986), and corresponds to a more zonal flow pattern across the United States and above normal winter temperatures over the Southeast. Because the long late-winter warm spell is the principal climatological signal during false spring episodes, one-tailed t-tests and composite time series plots were used to test the hypothesis that false spring events occur most frequently under a reverse PNA circulation pattern.

To compute the PNA index, twice daily measurements of the 700 mb geopotential height surface, interpolated to a 5° x 5° latitude/longitude grid by the National Weather Service, were averaged into daily values for the three locations near the centers of the PNA pattern (i.e., 50°N, 170°W; 50°N, 110°W; 30°N, 85°W). These daily 700 mb height series were normalized, and then used to compute a daily PNA index from January 1 to April 30 for each year from 1947 to 1980.

Two composite time series of the average daily PNA indices and the associated confidence intervals observed during the 5 frost and 29 non-frost years between 1947 and 1980 are presented in Fig. 46, with daily averages of both groups calculated for 59 days before and 20 days after the calendar date (K) of each of the five hard freeze events. Figure 46 does not indicate any persistent, statistically significant differences between the daily average PNA indices of frost and non-frost years. However, the average PNA indices for the five frost years were lower than the indices for all remaining non-frost years during the 10-day warm spell prior to the hard freeze (K-13 to K-4), and this difference is marginally significant based on a one-tailed t-test (PNA indices = -0.128 and -0.006 for the frost and non-frost years, respectively; $p = 0.077$). There were no significant differences between the PNA indices of frost and non-frost for other subperiods of false spring (i.e., K-28 to K-7 and K-1 to K+8).

Plots of the daily PNA indices for each individual frost year available after 1947, compared with the daily average indices for all non-frost years do indicate that the daily PNA indices during some frost years were significantly different than the average daily PNA indices of non-frost years (e.g., 1955, 1957, and 1965; Fig. 47). However, the timing and sign of these significant daily circulation departures are not consistent.

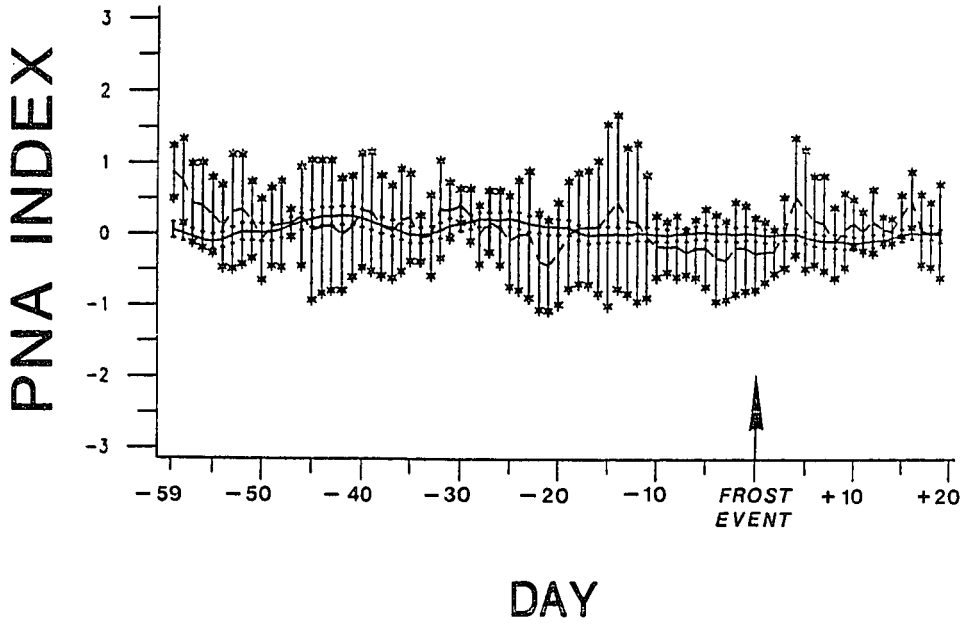

Figure 46. Composite daily average indices of the Pacific-North American pattern (PNA) are plotted for the five most recent false spring episodes (1955, 1957, 1962, 1965, 1974), along with the normal daily PNA indices fore all 29 remaining "non-frost" years from 1947 to 1980. The non-frost year indices were sorted according to the hard freeze date for each false spring year, and these 145 sorted non-frost year PNA series (5 x 29) were averaged into the daily normal indices for 59 days before and 20 days following the freeze event. The average PNA indices for the five false spring years were also sorted and averaged for the 59 days before and 20 days after their respective hard freeze event (K=day 0). The confidence intervals represented two standard errors associated with each daily average series.

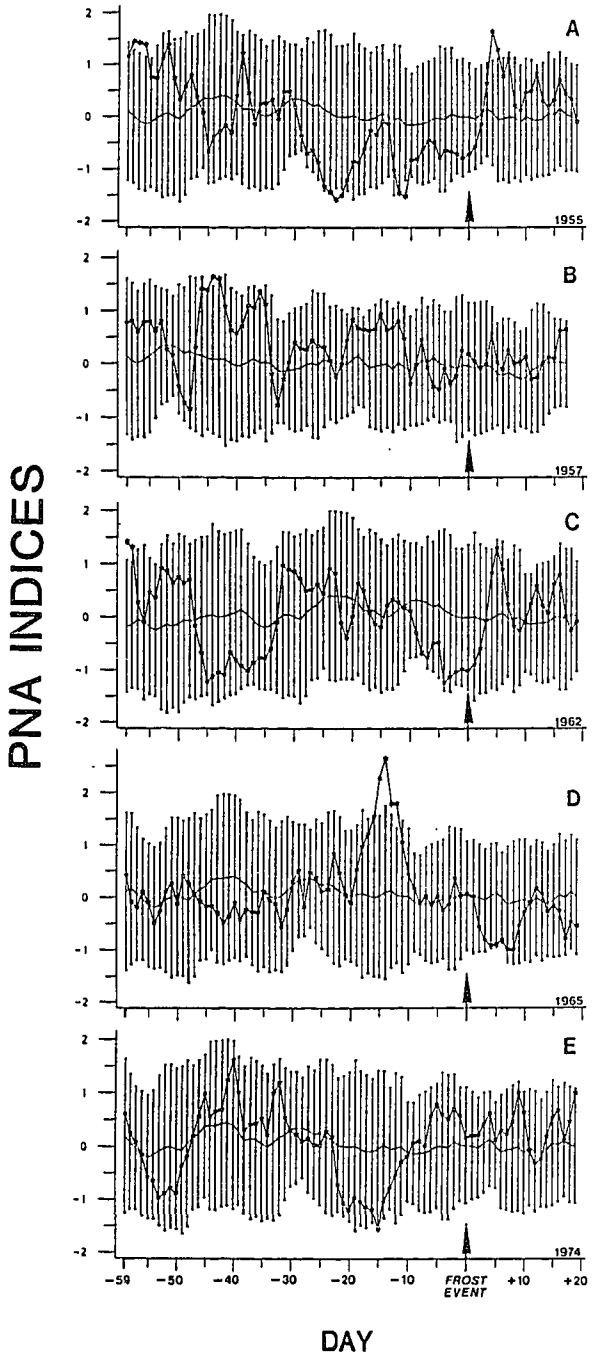

Figure 47. The daily PNA indices observed during the five most recent false spring episodes are plotted with the daily average indices and associated two standard deviation confidence limits for 59 days before and 20 days after the hard freeze event (A:1955; B:1957; C:1962; D:1965; E:19740).

These results do not demonstrate consistent large-magnitude departures from the daily PNA pattern of atmospheric circulation during the three weeks immediately preceding or the one week following the five most recent false spring events (Figures 46 and 47). However, the average PNA indices for the five frost years do appear to have been below average during the 10-day warm spell (i.e., reverse PNA), and may have changed from persistently negative to positive values near the date of the hard freeze (Fig. 46). When the mean daily PNA indices for just the five most recent frost years are compared for the 10 days before and the 10 days following the hard freeze, the persistent change from a reverse PNA to positive PNA pattern may be statistically significant ($p = 0.0138$), although this has been biased by the post hoc selection of periods tested.

Longer time averages of the PNA index also suggest a possible association between the reverse PNA pattern and the warm winter phase of false spring. Yarnal and Diaz (1986) identify reverse PNA conditions during February of 1955, January and February of 1957, February of 1962, December of 1964 (frost damage occurred in March of 1965), and January of 1974. Yarnal and Diaz (1986) do not identify the opposite positive PNA circulation pattern during any winter month (DJF) associated with frost damage after 1947. Using different methods and a hemispheric data set, Barnston and Livezey (1987) identify a reverse PNA pattern during February for four

of the five false spring years after 1950 (i.e., February PNA principal component time series < 0.0), with strong reverse PNA conditions ($\leq$ - 0.76) for three of these months (1955, 1957, and 1965).

A change from a reverse PNA to PNA circulation pattern, such as might be suggested near the freeze event in Fig. 46 would tend to be associated with a change from above to below average surface air temperature over the eastern United States (e.g., Wallace and Gutzler 1981), and suggests a sequence of upper air flow patterns which would favor false spring anomalies over the Southern Plains. An upper-level trough is typically present over western North America extending south into Southern California during a reverse PNA pattern (Wallace and Gutzler 1981; Barnston and Livezey 1987), and may remain stationary in this region for several days. This stagnated circulation pattern would favor warm air advection into the southcentral and eastern United States, and this situation appears to have occurred during the height of the warm spell in several twentieth century false spring episodes (e.g., Fig. 45A). Subsequently, this upper-level trough often migrates eastward into the southeastern United States. Cold air can then be advected behind the migrating trough, resulting in a major change in the temperature regime over the Southern Plains and occasionally a freeze cold enough to cause severe injury to physiologically active vegetation which was prematurely advanced by the preceding warm spell.

At the time of the hard freeze over the Southern Plains, the upper-level ridge normally over western North America is still farther west than normal over the Gulf of Alaska (Fig. 45B). But the migration of the upper-level trough into the southeastern United States, which must partially reflect a weakening or movement of the upper-level ridge over the Southeast and western North Atlantic typical of the reverse PNA pattern (Fig. 45A), helps to re-establish a normal or amplified upper-level ridge and trough system over the western and eastern United States typical of the PNA pattern.

This sequence of circulation patterns definitely occurred during the false spring episode of 1955 (e.g., Klein 1955; Fig. 47A). Based on the number of tree-ring sites with significant frost injury, as well as the vivid descriptions of the impact of this record setting spring cold wave (Kibler and Martin 1955), 1955 was one of the most intense false spring events since 1650 (Fig. 38). A similar sequence of events occurred during the false spring episodes of 1957, 1962, and 1974 (Fig. 47B,C,E), although the timing and magnitude of the circulation changes did not precisely replicate the 1955 event.

Examination of the daily weather maps during false spring episodes clearly reveals, however, that a simple change from a reverse to positive PNA pattern is not sufficient to explain all the circulation features associated with false spring events (Chapter 5). While a shift from a strongly zonal to

meridional circulation regime during the spring growing season has a high potential to result in damaging cold waves, other circulation regimes can also result in false spring weather patterns over the Southern Plains region. A good example occurred in 1965 when a strong, statistically significant positive PNA pattern became established during a portion of the warm spell (approximately March 1-10; Fig. 47D). In spite of this meridional PNA pattern which typically favors below normal temperatures over the eastern United States, a cut-off low at the 500 mb level stagnated over Southern California from at least March 7 to 15 and resulted in warm air advection into Texas [U.S. Weather Bureau (C)1965]. A sharp temperature gradient developed from the Southern to Central Plains during this period, and Texas remained warm until the cut-off low began to migrate northeastward on March 16. On March 18th the cut-off low was reabsorbed into the main upper-level flow over the Northeast, and a strong cold front swept across Texas and the coldest subfreezing temperatures occurred two days later on the morning of March 20th [U.S. Weather Bureau (C)1965].

A similar situation occurred just prior to the hard freeze in 1974 when an upper level disturbance or mesoscale trough migrated on a positive PNA longwave pattern (e.g., Fig. 47E) from the Pacific Northwest across the Southern Plains from March 16 to 19, and helped advect severely cold air into the southcentral United States on March 21st (NOAA 1974A). Earlier in the 1974 warm phase, however, a strong

reverse PNA pattern was associated with above average temperatures over the southcentral United States. A cut-off low also developed at the 500 mb level over Southern California (NOAA 1974A), and the eastward migration of this cut-off in March 10 helped to terminate the reverse PNA pattern.

The role of circulation over North America in the occurrence of false spring anomalies over the Southern Plains region will be difficult to define with only five events. The presence of an upper level cut-off low or mesoscale trough near Southern California can promote warm air advection into the Southern Plains under a longwave regime typical of either a reverse or positive PNA pattern. Nevertheless, the reverse PNA pattern does appear to have been prevalent during some winter months of false spring (e.g., Yarnal and Diaz 1986; Barnston and Livezey 1987), and the abrupt transition from a strong reverse PNA to positive PNA pattern can definitely result in false spring weather anomalies over the southcentral United States (e.g., 1955).

La Nina and False Spring

The relationship between the El Nino-Southern Oscillation and winter temperature over the southeastern United States was first described early in the twentieth century by Walker (Philander 1990), and recent studies have substantiated this ENSO teleconnection and extended it to cool-season temperature

and precipitation in portions of Texas and the Southern Plains (e.g., Douglas and Englehart 1981; Ropelewski and Halpert 1986; Kiladis and Diaz 1989). Because the two ENSO extremes, El Nino and La Nina (Philander 1990), are associated with winter-spring temperature anomalies over the southern Great Plains, these ENSO extremes might also be related to false spring weather or climate anomalies in this region.

A chronology of El Nino and La Nina events (Bradley et al. 1987; Kiladis and Diaz 1989), and the Southern Oscillation Index (SOI) developed at the Climatic Research Unit (CRU) and based on the normalized sea level pressure difference between Tahiti and Darwin were used to test the hypothesized ENSO influence in false spring in the Southern Plains region (see Jones 1988; personal communication). Kiladis and Diaz (1989) compiled a chronology of EL Nino and La Nina episodes from 1877 to the present based on seasonal values of the SOI, and a seasonalized index of concurrent sea surface temperature (SST) anomalies in the eastern equatorial Pacific.

El Nino (warm) events were identified by positive SST and negative SOI indices over at least three seasons, and the SST had to be at least 0.5°C above the mean for one season while the seasonalized SOI indices had to remain below -1.0 for all three seasons (Kiladis and Diaz 1989). La Nina (cold) events were identified using the opposite criteria. Kiladis and Diaz (1989) specify the first year of a warm or cold event when the SOI changes sign and the SST anomaly becomes strongly

positive or negative. Using these criteria, Kiladis and Diaz (1989) identify the starting year of 25 El Nino and 20 La Nina events between 1877 and 1980. The monthly SOI (e.g., Jones 1988) from 1866 to 1980 was used to identify one El Nino and La Nina event each before 1877 (based simply on persistent, large magnitude SOI departures), and to identify multiple year events (i.e., when SOI departures of a given sign persisted into the following early spring, Appendix 1).

The chronology of El Nino and La Nina events from 1877 to 1980 used in this analysis is included in Appendix 1 with the chronology of all significant frost ring years from 1650 to 1980. Because previous studies indicate a teleconnection between the ENSO and winter-spring climate over portions of the southern and southcentral United States during the following year (e.g., Douglas and Englehart 1981; Ropelewski and Halpert 1986; Kiladis and Diaz 1989), frost ring events are compared with ENSO events which developed or persisted through the previous year and continued into the current winter-spring.

Assuming that either phase of the ENSO is capable of sufficiently perturbing the circulation over North America to occasionally cause false spring anomalies, a 2 X 3 contingency table was constructed to test the joint association of El Nino and La Nina events with false spring (Steel and Torrie 1980). The results of this analysis indicate that false spring is significantly contingent upon the two extreme states of the

ENSO ($p < 0.05$, Table 6). Examination of Table 6 reveals that this association is explained primarily by the higher than expected number of false spring events which occur in the year after a La Nina event.

Because the number of frost events observed in the year following El Nino episodes is close to the number expected by chance (Table 6), a 2 X 2 contingency table was used to compare only La Nina and false spring events (Table 7). This analysis indicates that the number of frost ring years (11) which occur during La Nina conditions between 1877 and 1980 (27) is considerably higher than expected by chance ($0.01 < p < 0.025$), and suggests that extratropical circulation anomalies associated with mature La Nina episodes may often be capable of promoting false spring climate anomalies over the southern Great Plains region. These results do not change appreciably if the comparison with frost rings is based on the full 1866 to 1980 period covered by both the frost ring and CRU SOI series, or if the subsequent years of multiple-year La Nina episodes are excluded (Appendix 1).

Another way to analyze the apparent La Nina signal in false spring is to average the monthly SOI values for the 26 frost ring years from 1866 to 1980 for several seasons before and after the false spring event. This composite SOI for 26 false spring events is illustrated in Fig. 48A, and indicates that the SOI is continuously positive for seven months during the winter and spring of frost years and for 10 of the 12

Table 6. Contingency table comparing oak frost ring years with El Nino and La Nina episodes from 1877 to 1980. The first year of El Nino or La Nina events were identified by Kiladis and Diaz (1989), and subsequent years of multi-year events were identified using the CRU SO index (Jones, personal communication; Appendix 1). Events which began in the previous year, or persisted into the winter prior to frost injury were considered as a match.

	Frost Ring (Expected)	No Frost Ring (Expected)	Total
El Nino	7 (6.35)	23 (23.65)	30
La Nina	10 (5.71)	17 (21.29)	27
Neither	5 (9.94)	42 (37.06)	47
Total	22	82	104

X^2observed = 7.27 X^2critical (0.05) = 5.99

Table 7. Contingency table comparing oak frost ring years with La Nina episodes from 1877 to 1980. La Nina events which began in or persisted through the year and winter prior to frost injury were considered as a match. The first year of La Nina events were identified by Kiladis and Diaz (1989), and subsequent years of multi-year events were identified using the CRU SO index (Jones, personal communication; Appendix 1).

	Frost Ring (Expected)	No Frost Ring (Expected)	Total
La Nina	10 (5.71)	17 (21.29)	27
No La Nina	12 (16.29)	65 (60.71)	77
Total	22	82	104

X^2observed = 5.51 X^2critical (0.025) = 5.02

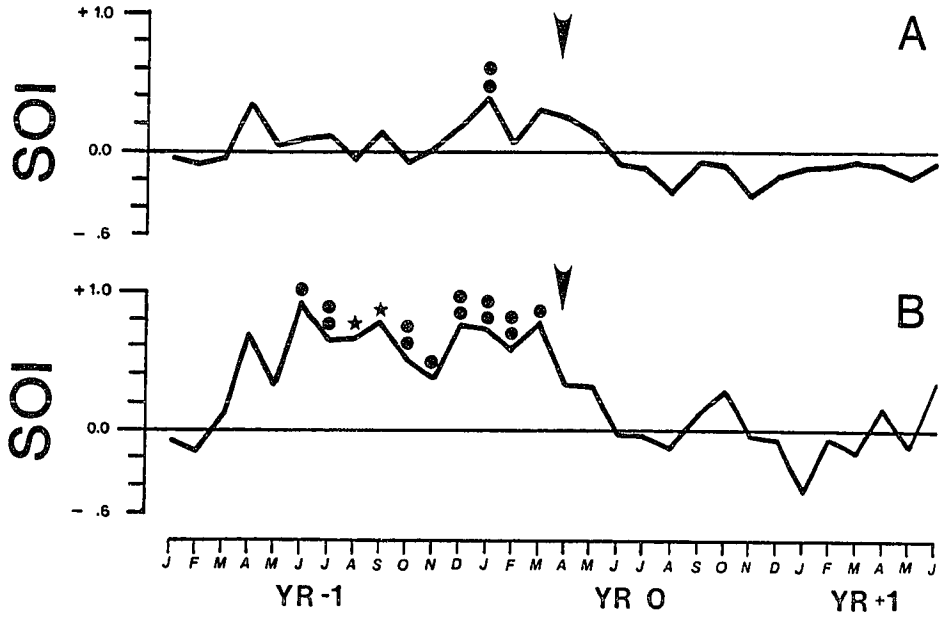

Figure 48(A). The monthly average Southern Oscillation indices (SOI) for all 26 false spring events from 1866 to 1980 are plotted for a 30 month period before, during, and after false spring (arrow indicates approximate timing of false spring). (B) The monthly average SOI indices for just the 11 false spring events which followed La Nina conditions are also plotted (otherwise as in 48A). Significant departures from the monthly "normal" SOI are indicated above or below the appropriate month (these two-tailed t-tests excluded the 26 or 11 years plotted in (A) or (B) from the monthly normal). The significance levels are one circle = $p \leq 0.10$; two circles = [≤ 0.05; and one star = $p \leq 0.01$. Note that the monthly mean SOI for all years (1866-1985) ranges from +0.12 in April to -0.15 in August, and monthly standard deviations range from 0.89 in February to 1.31 in June (based on the data from Jones, personal communication).

months preceding April of frost years. When the monthly SOI averages for 26 frost years are compared with the monthly SOI means for the remaining non-frost years, the January mean for frost years is significantly higher than the non-frost SOI mean ($p = 0.02$), documenting the prevalence of La Nina conditions during the winter of false spring years (Fig. 48A). When a winter-spring SOI average is calculated (Dec.-May), it is positive for 19 of 26 frost years from 1866 to 1985, and is below -0.5 only during two frost years (1913 and 1926). These comparisons further illustrate the nature of the ENSO influence on false spring.

The composite SOI also indicates a slight tendency for a persistent change from positive values prevalent before and during false spring, to negative SOI values beginning in summer and continuing into the next year (Fig. 48A). This change may vaguely reflect the "biennial tendency" of the ENSO phenomenon, where the two extreme, roughly inverse conditions tend to oscillate between adjacent years (e.g., Meehl 1987; Kiladis and Diaz 1989).

The composite SOI data in Fig. 48A illustrates the timing of the La Nina signal apparent in all frost ring events after 1866. The winter peak of this signal is consistent with the seasonality of the previously identified La Nina teleconnection with winter temperature in the southern United States. However, the composite SOI includes three frost years that occurred during El Nino episodes, and others that

occurred when neither ENSO extreme was active. Clearly, atmospheric anomalies unrelated to La Nina episodes are capable of resulting in false spring anomalies over the Southern Plains.

In order to portray the SOI signal associated with false spring over the Southern Plains as clearly as possible, another composite SOI series was compiled using the monthly SOI data for just the 11 frost ring years that occurred during La Nina conditions (Fig. 48B). The La Nina signal during the 12 month period prior these 11 to frost events is, of course, considerably enhanced. The monthly SOI values for this subset of frost years are significantly above the monthly SOI averages of non-frost years continuously from the previous June to the current March of false spring. After March of false spring the SOI falls sharply and remains near zero for the next year, (Fig. 48B) but does not become persistently negative as was the case for the SOI composite based on all 26 frost years (Fig. 48A). In terms of the seasonal development, evolution, and even magnitude, the SOI composite for the 11 frost years following of La Nina conditions closely resemble the cold event (La Nina) SOI composite based on all episodes from 1886 to 1975 (Bradley et al. 1987).

The frequent co-occurrence of La Nina events and false spring over the Southern Plains the following year is consistent with the temperature teleconnection, where above average winter-spring temperatures (and below normal

precipitation) over the southeastern United States tend to follow La Nina events of the previous year (e.g., Ropelewski and Halpert 1986; Kiladis and Diaz 1989). The temperature analysis reported above does, in fact, indicate above average minimum and maximum daily temperatures during the winter prior to false spring. Above average winter temperature would favor an early break in dormancy, and render trees vulnerable to any subsequent hard freeze. Conversely, El Nino events tend to be associated with cooler (and wetter) conditions over the Southeast during the following winter and spring (Ropelewski and Halpert 1986; Kiladis and Diaz 1989), which might help maintain dormancy later into the spring and may explain the lack of significant association between El Nino events and false spring.

Yarnal and Diaz (1986) have linked the reverse PNA pattern during winter to La Nina events, and the circulation typical of the reverse PNA pattern is consistent with the synoptic meteorology frequently, but not always, observed during the warm phase of false spring (e.g., Fig. 45A). Yarnal and Diaz (1986) propose a dynamical model to explain the empirical link between La Nina episodes and the reverse PNA pattern. This model essentially relates enhanced convection over the western equatorial Pacific during La Nina events to an enhanced east Asian jet stream, and the anomalous downstream developments of a mid-Pacific ridge, East Pacific trough near California, and a ridge over the southeastern

United States (all at the upper level). This circulation pattern over the North Pacific and North America is typical of the reverse PNA mode, and has been associated with unusually cool winters over the Pacific Northwest coast (Yarnal and Diaz 1986).

The PNA pattern is also associated with surface air temperature over the Southern Plains and other regions of the United States. In particular, the reverse PNA pattern strongly favors warm air advection into the Southern Plains, given the presence of an upper-level trough near California and a ridge over the Southeast. This can be substantiated by comparing state-averaged monthly temperature data for Texas, Oklahoma, and Missouri (Karl et al. 1983a,b,c) during those winter months classified into the reverse PNA pattern by Yarnal and Diaz (1986, Table 13) with the normal monthly temperature for each of these 29 months between 1947 and 1980. These comparisons are summarized in Table 8A, and indicate that the reverse PNA pattern is associated with significantly above average winter temperatures in all three states of the Southern Plains region. Conversely, these same tests were conducted for winter months classified as positive PNA by Yarnal and Diaz (1986) and the corresponding state average monthly temperatures for Texas, Oklahoma, and Missouri (Karl et al. 1983a,b,c). These results are presented in Table 8B and indicate that positive PNA conditions are associated with significantly colder winter months over the Southern Plains.

Table 8. Winter temperatures for Missouri, Oklahoma, and Texas were averaged for the 29 reverse PNA months and the 29 positive PNA months identified by Yarnal and Diaz (1986; Table 13), and each average was compared to the "normal" winter temperature average for all remaining months (DJF) from January 1947 to February 1979 using one-tailed t-tests. The state average monthly temperature data (DJF) for just the period 1947 to 1979 were taken from Karl et al. (1983a,b,c). All temperatures are in °F.

A. Reverse PNA

State	Reverse PNA Mean Temperature	Normal Temperature	t	df	p
Missouri	34.30	32.11	-1.95	97	0.0271
Oklahoma	41.20	39.35	-1.42	97	0.0786
Texas	49.95	46.79	-3.88	97	0.0001

B. Positive PNA

State	Positive PNA Mean Temperature	Normal Temperature	t	df	p
Missouri	29.67	34.02	4.12	97	0.0001
Oklahoma	37.94	40.54	2.60	97	0.0053
Texas	45.41	48.67	4.02	97	0.0001

Consequently, positive PNA conditions would tend to suppress false spring conditions (unless a mesoscale feature such as a cutoff low over Southern California also develops, as in 1965). Thus, the association of El Nino conditions with the positive PNA circulation pattern (e.g., Yarnal and Diaz 1986), and with cool winters over the Southern Plains, helps explain the lack of a significant association between El Nino events and false spring.

Above average temperatures in Texas, Oklahoma, and

Missouri were also observed during the winter and early spring following the development of La Nina events in the previous year. State-averaged temperatures for January, February, and March available since the late nineteenth century (Karl et al. 1983a,b,c) were seasonally averaged, and the seasonal averages following the La Nina events identified in Kiladis and Diaz (1989) were compared with the average seasonal temperatures for all remaining years in each state (Table 9). These comparisons indicate that the winter-spring temperatures following La Nina episodes are significantly above average in Texas and Oklahoma. The above average winter-spring temperature following La Nina events in Missouri is not statistically significant (Table 9).

These results demonstrate that the La Nina and reverse PNA phenomena are both associated with above average winter temperatures over the Southern Plains region. In fact, warm winter temperature departures appear to be even more pronounced in Oklahoma when both La Nina and reverse PNA conditions occur during the same winter (not shown).

These comparisons between actual temperature data for the Southern Plains, and the La Nina and reverse PNA patterns help explain the statistically significant associations between La Nina episodes and the frost ring record of false spring. Both La Nina and the reverse PNA pattern are individually related to above average winter temperature over the Southern Plains. However, La Nina conditions appear to

Table 9. State averaged winter temperatures (JFM) for Missouri, Oklahoma, and Texas (Karl et al. 1983a,b,c) during La Nina years are compared with the "normal" winter temperature calculated for all remaining years from 1888 (MO,TX) or 1892 (OK) to 1980 using one-tailed t-tests. The temperature data were compiled for La Nina episodes which began in the previous year (identified by Kiladis and Diaz 1989, and by Jones, personal communication for multiple-year events). All temperatures are in °F.

State	La Nina Winter Temperature Average	Normal Winter Temperature Average	t	df	p
Missouri	36.78	35.77	-1.19	93	NS
Oklahoma	44.13	42.83	-1.70	89	<0.05
Texas	53.06	50.83	-3.65	93	<0.0003

NS = not significant

favor development of the reverse PNA circulation pattern (Yarnal and Diaz 1986), and when these two circulation patterns occur together the likelihood of a warm winter in the Southern Plains probably increases. Under these general climatic conditions, abnormal winter warmth would favor the early growth of vegetation, which would then be susceptible to any subsequent hard freeze. A variety of transitory synoptic conditions might lead to a hard freeze following a winter and early spring of unusual warmth (e.g., Konrad and Colucci 1989), including the southward surge of cold air in the wake of an eastward migrating reverse PNA pattern.

Explosive Volcanic Eruptions

Theoretical studies indicate that the stratospheric dust

veils of large-magnitude explosive volcanic eruptions may be capable of altering the global energy balance (Gilliland and Schneider 1984), particularly those veils that are rich in sulphate aerosols (Rampino and Self 1984). A one- to three-year decline in hemispheric surface air temperatures of varying intensity has been detected following some selected, very large eruptions (e.g., Kelly and Sear 1985; Bradley 1988; Mass and Portman 1989). Kelly and Sear (1984) and Bradley (1988) report a rapid surface air temperature response to major eruptions in the Northern Hemisphere beginning as early as one to three months after the eruption. However, Mass and Portman (1989) do not detect a rapid climate response to selected large eruptions, and cast doubt over the likelihood of such a response.

Long-term tree-ring data have been previously related to chronologies of worldwide volcanic activity, and these apparent associations are believed to reflect cold surface air temperatures at the tree-ring sites during the growing season. LaMarche and Hirschboeck (1984) have linked frost injured rings in high elevation bristlecone pine of the western United States to explosive volcanic activity, and suggest that the planetary-scale circulation of the atmosphere may ultimately be involved in this apparent worldwide association. The early season (fall) frosts recorded by latewood trauma in bristlecone pine apparently reflect a shortened growing season due to the early onset of cold

temperatures in fall, and/or to cold temperatures early in summer which might delay the onset of the growing season and prolong it into fall, thereby rendering these trees vulnerable to subfreezing temperatures in September (LaMarche and Hirschboeck 1984). Filion et al. (1986) relate a chronology of "light rings" in black spruce trees sampled near the subarctic treeline in northern Quebec to worldwide volcanic activity, and also attribute these ring anomalies to low temperatures late in the growing season (i.e., August-September). Using tree-ring reconstructed temperature data, Lough and Fritts (1987) detect decreased spring and summer temperatures over the central United States for two years following selected large-scale eruptions from 1602 to 1900.

Because large-magnitude volcanic eruptions may be capable of global-scale climatic effects, including cooler spring-summer temperatures over the central USA, the tree-ring record of false spring weather and climate anomalies over the Southern Plains might also be related to explosive volcanic activity worldwide. Any relationship between explosive volcanism and oak frost rings would presumably involve the late season cold wave actually responsible for frost injury, and not the prolonged warm winter conditions also involved in false spring anomalies.

The possible association between explosive volcanism and frost rings of the Southern Plains can be evaluated on a very preliminary basis by comparing the historical record of

large-magnitude eruptions with the frost ring chronology from 1650 to 1980. Newhall and Self (1982) have developed the Volcanic Explosivity Index (VEI), which provides a general measure of the explosive power and pyroclastic discharge of volcanic eruptions. The VEI ranks eruptions on a magnitude scale from 0 to 8, based on a hierarchy of quantitative and qualitative volcanological information. However, the VEI does not necessarily measure the sulphate content, stratospheric injection, or probable climate effectiveness of volcanic aerosols (Newhall and Self 1982; Mass and Portman 1989). Also, the chronology of volcanic eruptions during the past 331 years is incomplete and subject to error, due inevitably to the nature of the available, often anecdotal historical record. This appears to be particularly true for low intensity and Southern Hemisphere eruptions, while the record of large eruptions may be more complete back to the early nineteenth century (Newhall and Self 1982).

Newhall and Self (1982) list the calendar dates and estimated explosivity of all known large-magnitude eruptions from 1500 to 1980 (with VEI $\geq$ 4). For purposes of comparison with the frost ring chronology, all eruptions with VEI $\geq$ 4, which occurred during a 14-month "year" beginning January 1 and ending no later than February 29 of the next year were lumped into one eruption year. A second comparison was also made using only eruptions north of latitude 10°S, because Southern Hemisphere eruptions may not have an equal impact on

Northern Hemisphere air temperatures (Kelly and Sear 1984; Bradley 1988; Mass and Portman 1989), and the VEI appears to be severely under-reported for the Southern Hemisphere.

The co-occurrence of an explosive eruption and frost injury was determined when a frost event was preceded by one or more eruptions with a VEI $\geq$ 4 recorded during the previous calendar year, or no later than February 29 of the same year, provided that the exact eruption date preceded the earliest probable date of frost injury by at least 30 days. The earliest likely freeze date for false spring in Texas is March 1st, and March 21st in Missouri and Oklahoma (see Table 2). This 14-month eruption window prior to a frost year allows for the possibility that a single eruption in January or February could be associated with two frost rings, one occurring later in the same year and the second during the following year. However, no such cases were observed between 1649 to 1979 (Appendix 1). If two eruptions occurred prior to a frost year, one in the previous year and one early in the same year of frost damage, then the two eruptions were counted as only one eruption year match (Appendix 1). Using these procedures, 80 eruption years were identified in the Newhall and Self (1982) eruption chronology during 331 total years from 1649 to 1979 (Appendix 1).

The comparison with the VEI indicates a statistically significant contingency of false spring events on the available worldwide chronology of large-magnitude explosive

volcanic eruptions ($p < 0.025$, Table 10). Of the 70 frost ring dates between 1650 and 1980, 19 followed a VEI $\geq$ 4 during the previous year, and 6 more followed a VEI $\geq$ 4 early in the same year (Appendix 1). This co-occurrence is slightly more pronounced considering only eruptions north of latitude 10°S, which eliminates only four eruption years between 1649 and 1979 (Newhall and Self 1982), but these particular years were not followed by frost injury. Based on the earliest probable date of frost occurrence in a given area (e.g., Table 2), only two frost events that may have followed an eruption by as few as 30 days were counted in Table 10.

The true significance of the apparent link between false spring and explosive eruptions remains in considerable doubt because the results in Table 10 are definitely biased by the under reporting of eruptions during the seventeenth and eighteenth centuries (e.g., Newhall and Self 1982; Simkin and Siebert 1984). This bias can be illustrated by comparing eruption and false spring events during two long subperiods. The highest co-occurrence between volcanic eruptions and false spring actually occurred during the nineteenth century, when frost injury was registered after 11 of the 25 recorded large eruptions (Appendix 1). However, the co-occurrence of eruptions and frost events is not statistically significant during the twentieth century (1899-1979) when the record of large magnitude eruptions is most complete. Also, the identified co-occurrence of six frost rings with eruptions

earlier in the same year (Appendix 1) assumes a rapid one- to four-month climate response over the Southern Plains to these eruptions, and the physical plausibility of such a rapid climate response has been strenuously questioned (e.g., Mass and Portman 1989).

Table 10. Contingency table comparing oak frost ring years with the Newhall and Self (1982) Volcanic Explosivity Index (VEI) from 1650 to 1980 (see text for selection details).

	Oak Frost Ring (Expected)	No Oak Frost Ring (Expected)	Total
VEI $\geq$ 4	25 (17.55)	58 (65.45)	83
No VEI $\geq$ 4	45 (52.45)	203 (195.55)	248
Total	70	261	331
	X^2observed = 5.35	X^2critical (0.025) = 5.02	

The incomplete record of historic volcanism is a major constraint on the evaluation of explosive eruptions and false spring, and no attempt has been to include the possible climate effectiveness of each eruption listed by Newhall and Self (1982) in this evaluation. However, there is no apparent association between oak frost rings and Lamb's (1970) Dust Veil Index (DVI), which does attempt to incorporate the likely climate impact of explosive eruptions. Oak frost rings between 1650 and 1968 occurred after only 4 of the 13 DVI's compiled by LaMarche and Hirschboeck (1984) in their analysis of volcanic signal in bristlecone pine frost rings. Also, the

comparisons between VEI and false spring have been limited to one year, but the climatic effects of some very large or sulphate rich eruptions might persist over two or three years (e.g., Kelly and Sear 1984; Mass and Portman 1989).

The enormous eruption of Tambora in 1815 (VEI = 7), which was preceded and followed by three additional large eruptions in 1814 and 1818 (VEI > 4, Newhall and Self 1982), might provide an example of a more extended volcanic impact on climate. These four eruptions appear to have formed an unusually dense atmospheric dust veil (e.g., Lamb 1970; LaMarche and Hirschboeck 1984), and it may not be merely coincidental that frost injury occurred in the Southern Plains region during 1814, 1816, 1817, 1819, 1820, and 1821. A frost ring was also recorded in bristlecone pine during 1817 (LaMarche and Hirschboeck 1984), and light rings were registered in Canadian black spruce during 1814, 1816, 1817, 1819, and 1822 (Filion et al. 1986). In addition, the largest radial growth in 400 years occurred in Colorado Plateau douglas fir in 1816 and 1817, and probably reflects cooler and/or wetter conditions during the summer growing season (Cleaveland in press). The evidence for an association between these North American tree ring anomalies and the Tambora eruption is entirely circumstantial, but such an association is certainly plausible given the suspected size of the dust veil and the climate anomalies reported to have occurred in portions of North America during this period

(e.g., Ludlum 1966; Horstmeyer 1989).

Given the reported volcanic signal in bristlecone pine frost rings and black spruce light rings (LaMarche and Hirschboeck 1984, Filion et al. 1986), and the possible volcanic signal in oak frost rings, the question naturally arises as to whether these three chronologies exhibit any significant agreement over the past 330 years which might reflect common volcanic forcing. Filion et al. (1986) report several chronological agreements between light rings in Quebec and frost rings in the western United States which they suggest might reflect the common influence of explosive eruptions on the climate in each region.

The chronology of frost rings in oaks of the Southern Plains is listed in Appendix 1 along with the bristlecone pine frost ring (LaMarche and Hirschboeck 1984) and black spruce light ring chronologies (Filion et al. 1986). Oak frost rings formed in the same year as bristlecone pine frost injuries only 4 times between 1650 and 1969, out of a total of 15 bristlecone pine and 69 oak frost ring events during this period. Oak frost rings formed in the same year as spruce light rings only 15 times between 1650 and 1980, out of a total of 56 light ring and 70 frost ring events during the period. This level of co-occurrence is not higher than would be expected by chance for either comparison. In addition, oak frost rings formed int eh spring immediately following only 4 bristlecone pine frost rings between 1650 and 1969 (Appendix

1), which also does not exceed the chance expectation. However, oak frost injury occurred in the spring following light ring formation in Canada only 6 times between 1650 and 1980, which is significantly lower than the chance expectation ($p < 0.05$).

The chronological comparisons tabulated in Appendix 1 provide no evidence for the synchronous formation of frost rings in oaks during the same year or year after either bristlecone pine frost or spruce light rings, and therefore do not indicate a common response to explosive volcanism or any other climate forcing mechanism. Instead, the very infrequent occurrence of light rings in the late summer before false spring episodes may tend to reflect an out-of-phase response in Canadian spruce and Southern Plains oak to some large scale climate forcing. Because the El Nino-Southern Oscillation (ENSO) is the strongest planetary-scale climate signal presently known and exhibits teleconnections with the late-summer climate of the western United States and Canada, and with the winter-spring climate of the Southern Plains (e.g., Rasmussen and Wallace 1983; Ropelewski and Halpert 1986; Kiladis and Diaz 1989; Schonher and Nicholson 1989), the ENSO phenomenon might be responsible in part for the formation of bristlecone pine frost rings, spruce light rings, and also the infrequent occurrence of light rings in Canada in the late summer before false spring.

El Nino Influence on Frost Rings in Bristlecone Pine and Light Rings in Black Spruce

The only large-scale geophysical signal yet detected in the cold late summer conditions responsible for bristlecone pine frost and spruce light rings has been explosive volcanism (LaMarche and Hirschboeck 1984; Filion et al. 1986). However, as will be discussed below, the El Nino signal detected in modern meteorological data in Quebec can be plausibly related to cold temperatures late in the growing season of black spruce. The El Nino signal detected in California climate data might also be reasonably related to cool conditions at 3000m, or to an extension of the bristlecone pine growing season into September when subfreezing temperatures become more likely. Consequently, the possible influence of El Nino conditions on the formation of frost rings in bristlecone pine and light rings in black spruce should be examined. If an El Nino signal exists in these data, it could help explain the very infrequent co-occurrence between the oak frost ring and spruce light ring chronologies, because frost rings in oaks (i.e., false spring) appear to be often influenced by the opposite ENSO phase frequently referred to as La Nina (Philander 1990).

Contingency tables and composite SOI data were used to test the hypothesized association between El Nino events and frost rings in bristlecone pine and light rings in black spruce. The chronology of El Nino events used in these tests

extends from 1726 to 1982 and is based on the historical data compiled and analyzed from 1726 to 1865 by Quinn et al. (1978) and the El Nino chronology presented in Appendix 1 from 1866 to 1982 based on the SOI and SST data analyzed by Kiladis and Diaz (1989). Multiple year events were identified using the SO index obtained from P.D. Jones (personal communication). Because the El Nino chronology available prior to 1866 is subject to error due to the nature of the often incomplete archival data used to estimate past events (Quinn et al. 1978), chi-square tests were conducted with both the El Nino record available after 1866, as well as with the full chronology from 1726 to 1969 or 1982.

Only five frost rings were registered in the latewood of bristlecone pine from 1866 to 1969, but three occurred during the late summer or early fall of strong El Nino events (Year 0), and the other two frosts occurred during seasons with negative SO indices of lesser magnitude (e.g., Kiladis and Diaz 1989; Jones, personal communication; Appendix 1). The bristlecone pine frost ring of 1902 occurred during earlywood formation (probably on July 4th; LaMarche and Hirschboeck 1984), and was excluded from this analysis because it is not related to the hypothesized climate conditions, possibly influenced by El Nino events, which may at times be responsible for latewood frost rings in bristlecone pine (see below).

For the full period from 1726 to 1969, 6 of 12

bristlecone frost rings (latewood damage) occurred during El Nino years identified in Appendix 1 (1866-1969) and by Quinn et al. (1978) for events from 1726 to 1866 ($p < 0.025$, Table 11). In Table 11, the expected number of frost rings following El Nino events falls below the suggested minimum [i.e., no more than 20% of the expected frequencies should fall below 5 (Cochran 1954)]. Nevertheless, the expected value of 2.52 probably has little effect at the 5% level of significance because Steel and Torrie (1980) cite evidence indicating that the chi square for expectations below five is actually conservative (i.e. rejects the null hypothesis too infrequently).

The monthly SOI values (Jones, personal communication) for the five bristlecone pine frost ring years which occurred after 1865 were also used to illustrate the apparent El Nino influence on the climate conditions responsible for latewood frost injury (Fig. 49A). The composite SOI is significantly below the average of all other monthly SO indices from 1866 to 1985 ($p \leq 0.05$) for six of nine months preceding September of these five bristlecone pine frost years, and for 10 of 14 months ($p \leq 0.01$) from the previous December to January following frost damage (Fig. 49A). The 12-month SOI average for the five bristlecone pine frost years (Jan.-Dec.) is also well below the average of all other SOI years from 1866 to 1985, and reflects the prominent El Nino events of 1912, 1941, and 1965 (the SOI $x = -0.81$, $t = 7.63$ for unequal variances,

Table 11. Contingency table comparing frost rings in bristlecone pine (LaMarche and Hirschboeck 1984) with the chronology of El Nino events (year 0) from 1726 to 1969 (1726-1865=Quinn et al. 1978; 1866-1969=Kiladis and Diaz 1989; Jones, personal communication; Appendix 1). The earlywood frost of 1902 was excluded (LaMarche and Hirschboeck 1984).

	Bristlecone Frost Ring	No Bristlecone Frost Ring	Total
El Nino	6 (2.52)	45 (48.48)	51
No El Nino	6 (9.48)	186 (182.52)	192
Total	12	231	243

X^2observed = 6.37 X^2critical (0.025) = 5.02

Table 12. Contingency table comparing light rings in black spruce of northern Quebec (Filion et al. 1986) with the chronology of El Nino events (Year 0) from 1866 to 1982 (Appendix 1; Kiladis and Diaz 1989; Jones, personal communication).

	Spruce Light Ring	No Spruce Light Ring	Total
El Nino	12 (6.77)	21 (26.23)	33
No El Nino	12 (17.23)	72 (66.77)	84
Total	24	93	117

X^2observed = 7.06 X^2critical (0.01) = 6.63

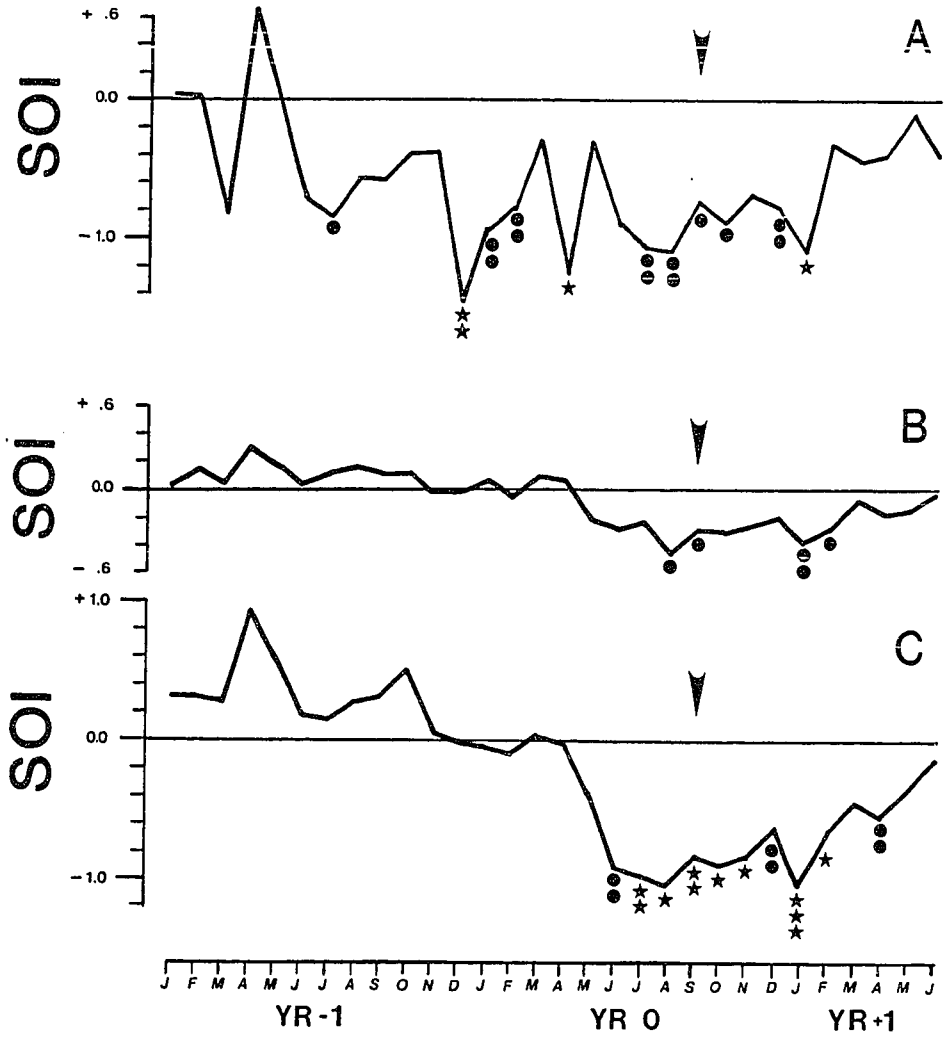

Figure 49. Same as in Figure 48A except for the five bristlecone pine frost ring years from 1866 to 1969 (A); the 24 black spruce light ring years between 1866 and 1982 (B); and the 12 light ring years which followed El Nino events between 1866 and 1982(C). Arrows indicate approximate timing of bristlecone frost injury or spruce light ring formation. In addition to the symbols used to indicate significant monthly SOI departures in Figure 48, two stars = $p \leq 0.001$, and three stars = $p \leq 0.0001$.

df= 68, $p < 0.0001$). The occurrence of significantly negative SO indices during July, August, and September concurrent with frost damage to bristlecone pine would certainly be expected if El Nino conditions are actually involved in the temperature anomalies responsible for the late growing season frost damage at high altitude bristlecone pine sites in the Great Basin.

Examination of the light ring chronology for black spruce trees of northern Quebec (Filion et al. 1986) indicates that 12 of 24 light rings recorded between 1866 and 1982 occurred during the late summer of El Nino events (Year 0; $p < 0.01$, Table 12; Appendix 1). The comparison between light rings and the full El Nino chronology from 1726 to 1982 (based on the Quinn et al. (1978) record before 1866 and the El Nino chronology in Appendix 1 after 1865) also indicates a significant association between the light ring and El Nino chronologies ($p < 0.025$, Table 13). Most of this apparent association reflects the frequent agreement between the two series after 1865. However, the El Nino chronology is also most reliable during this period.

The apparent El Nino influence on the formation of light rings can also be illustrated with composite plots of the average monthly SOI during light ring years. A plot of the average monthly SO indices for the 24 light ring years noted from 1866 to 1982 (Filion et al. 1986) is presented in Fig. 49B. The monthly SOI averages for light ring years are continuously below the average of all other monthly SO indices

Table 13. Contingency table comparing the occurrence of light rings in black spruce of northern Quebec (Filion et al. 1986) with the chronology of El Nino events (Year 0) from 1726 to 1982 (1726-1865=Quinn et al. 1978; 1866-1982=Kiladis and Diaz 1989; Jones, personal communication; Appendix 1).

	Spruce Light Ring	No Spruce Light Ring	Total
El Nino	18 (11.71)	41 (47.29)	59
No El Nino	33 (39.29)	165 (158.71)	198
Total	51	206	257
	X^2observed = 5.44	X^2critical (0.025) = 5.02	

formation through the following May. The light ring SOI means are significantly below average during the current August and September when light ring formation occurs ($p < 0.10$), as well as during the next January ($p < 0.05$) and February ($p < 0.10$, Fig. 49B). The 12-month SOI average for these 24 light ring years (Jan.-Dec.) is also significantly below the average of all other SOI years from 1866 to 1985 (the light ring year SOI mean = -0.18, $t = 2.7$, $df = 1438$, $p < 0.01$).

The timing of the apparent El Nino influence in the climate conditions responsible for light ring formation can be better depicted by compositing the monthly SO indices for just the 12 light ring years associated with El Nino conditions (Appendix 1). The general features of the SOI composite based on all 24 light ring years are replicated and considerably enhanced in this composite (Fig. 49C).

Persistent and at times significantly positive SOI values were observed in the year prior to light ring formation (La Nina conditions), changing over in the late spring of light ring years to persistent and in most cases strongly negative SOI values (Fig. 49C). The monthly SO indices were significantly below the monthly averages of all other remaining years during the August-September period of light ring formation, suggesting an El Nino influence on light ring formation ($p < 0.01$, Fig. 49C). The change from La Nina conditions during the previous year to El Nino conditions during the summer and following winter of light ring formation may reflect the tendency for the ENSO phenomenon to oscillate between opposite extremes on an approximately biennial basis (e.g., Meehl 1987).

The occurrence of light rings in northern Quebec during the late summer or early fall of many El Nino years is consistent with the ENSO temperature teleconnection identified in meteorological data (Kiladis and Diaz 1989), and may reflect the amplification of the Pacific/North American circulation pattern shown to frequently develop during the winter of El Nino years (Horel and Wallace 1981). Kiladis and Diaz (1989) report below normal temperatures over northern Canada (including Quebec) from September through November for years when El Nino conditions develop in the tropical Pacific [usually during the previous Northern Hemisphere spring (Bradley et al. 1987)]. Below normal temperatures may also

be associated with El Nino years during the summer (June-August, Kiladis and Diaz (1989), Fig. 4E). Cold late summer or early fall conditions over northern Quebec during El Nino years could prematurely terminate the black spruce growing season before the formation latewood cells was complete, or could inhibit the lignification of latewood cell walls. Either one or both of these circumstances could lead to the formation of a light ring.

The development of frost rings in bristlecone pine may also frequently reflect El Nino conditions, but the evidence for a possible El Nino influence on the climate conditions responsible for frost ring formation in bristlecone pine is not as compelling as may be the case for light rings in black spruce. Kiladis and Diaz (1989) report an ENSO signal during the fall (September-November) over Southern California and the southern Great Basin region where most bristlecone pine sites are located (LaMarche and Hirschboeck 1984). Fall precipitation is found to be higher in this region during El Nino events when compared with La Nina events (Year 0 in both cases, Kiladis and Diaz 1989). This above average precipitation signal may also exist during the summer of El Nino years (June-August, Year 0), although it does not appear to be as strong or regionally coherent as the signal during fall (Kiladis and Diaz 1989, Fig. 5E). Schonher and Nicholson (1989) also report heavy annual precipitation amounts during many El Nino years over Southern California, which may include

the bristlecone pine localities in the White Mountains.

If El Nino events favor wet conditions over Great Basin bristlecone pine sites during the late summer and early fall (especially August and September), these wet conditions might also at times favor frost ring formation in at least two ways. Wet conditions during August or September might very well equate with cooler conditions or occasional cold waves and snow, which might infrequently cause frost damage at the subalpine bristlecone pine sites, which range in elevation from 2896 to 3536m in the White Mountains (Fritts 1969). Alternatively, wetter conditions during the late summer or early fall of El Nino years might favor frost ring formation in bristlecone pine by providing soil moisture and helping to prolong active tree growth into early fall (M.K. Cleaveland, personal communication). Most bristlecone pine sites in the Great Basin are exceedingly arid, particularly those near the lower forest limit of the species range, and increased soil moisture in August has been shown to result in continued radial growth (Fritts 1969,13-15). Extension of bristlecone pine growth into early fall given favorable soil moisture conditions might render these trees more vulnerable to early season frosts, which in normal years are likely as early as late September at these high elevation forests (LaMarche and Hirschboeck 1984).

If El Nino conditions are often responsible for frost rings in bristlecone pine, then the hundred-year long

intervals without any bristlecone pine frost rings that occur over the past 1400 years (LaMarche and Hirschboeck 1984) raise questions concerning the reliability of the bristlecone pine frost ring chronology, the stability of the hypothesized El Nino influence on frost ring formation, or possibly even long-period changes in the frequency/intensity of the El Nino phenomenon. Given the relatively low number of long bristlecone pine chronologies and the often thin specimen replication available for these exceptional series, it would be unwise to attribute the long frost-free intervals in the bristlecone frost ring chronology to anything other than inadequate sampling (e.g., LaMarche and Hirschboeck 1984). The recent extensive sampling of these remote bristlecone pine sites (Graybill 1987) promises to provide the necessary tree ring samples to develop a fully replicated bristlecone pine frost-ring chronology covering at least the past 1000 years.

The apparent La Nina signal in oak frost rings, the possible El Nino signal in frost and light rings of bristlecone pine and black spruce, as well as differences in the seasonality of these ring abnormalities tend not to favor the co-occurrence of frost ring years in oaks with ring anomalies in the pine or spruce. As previously discussed, the occurrence of oak frost rings in the same year as frost rings in bristlecone pine or light rings in black spruce is not higher than would be expected by chance. However, only 6 spruce light rings occurred during the year (i.e., late

summer) immediately prior to the formation of oak frost rings from 1650 to 1980, and this number is well below the number expected by chance ($p < 0.05$, Table 14).

The low incidence of light ring occurrence in the year prior to oak frost injury is consistent with the frequent development of La Nina conditions during the year prior to false spring (e.g., Fig. 48), and the development of El Nino conditions during the summer and fall of light ring formation (e.g., Fig. 49B,C). These contrasting El Nino and La Nina signals would tend to inhibit the formation of spruce light rings during the year prior to oak frost rings, as documented in Table 14. Likewise, the prevalence of El Nino conditions during the summer, fall, and winter of light ring years in Quebec does not favor warm winter temperatures and false sping conditions over the Southern Plains during the next spring.

The apparent phase relationship between the oak and spruce chronologies may be further illustrated with a composite plot of monthly SOI averages for the six years between 1866 and 1980 when light rings were recorded in the late summer following frost damage to oaks during spring (i.e., 1894, 1923, 1936, 1955, 1957, 1965, Appendix 1). Positive SO indices were observed for 17 months before and during oak frost injury, including 4 months significantly above the annual SOI average for all other years (Fig. 50). The composite SO indices then change in May after false spring to persistent negative indices during the summer and fall of

Table 14. Contingency table comparing the formation of light rings in black spruce trees of northern Quebec (Filion et al. 1986) in the year immediately preceding the formation of frost rings in oaks of the Southern Plains (1650-1980; Appendix 1).

	Oak Frost Rings (Yr t)	No Oak Frost Rings (Yr t)	Total
Spruce Light Rings (Yr t-1)	6 (11.84)	50 (44.16)	56
No Spruce Light Rings (Yr t-1)	64 (58.16)	211 (216.84)	275
Total	70	261	331
	X^2observed = 4.39	X^2critical (0.05) = 3.84	

light ring formation, and the November SOI average for these particular six years is significantly below the annual SOI average based on all remaining years ($p < 0.05$, Fig. 50).

When these six years are used to calculate seasonal SOI averages, the winter-spring period (Nov.-April) before and during false spring is significantly higher than the annual SOI mean ($t = 1.67$, $p < 0.05$), and the summer-fall period (June-Nov.) is significantly below the annual SOI mean ($t = -11.82$, $p < 0.001$). These results further document the tendency for La Nina conditions to precede oak frosts, for El Nino conditions to precede light rings, and help explain why light rings in Quebec do not normally form during the year prior to frost injury to oaks of the Southern Plains (Table 14), and why oak frost rings do not usually form during the

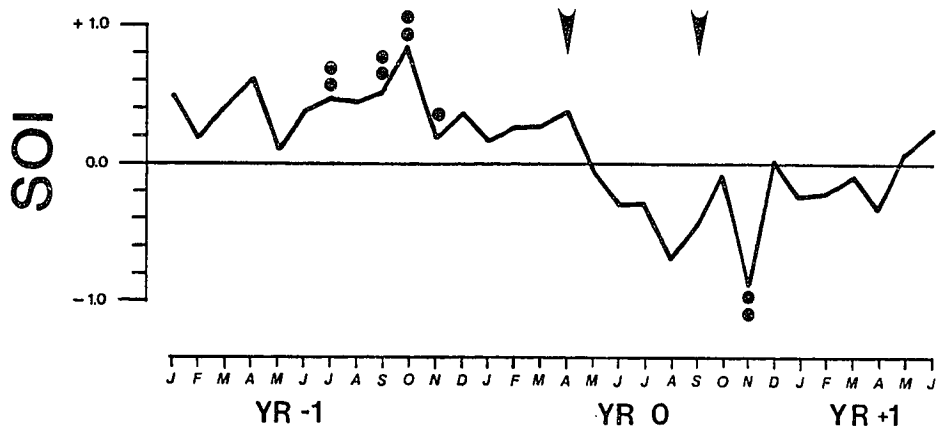

Figure 50. Same as Figure 48A except for the six years when light rings were registered in Canadian black spruce in the late summer following false spring occurrence over the Southern Plains. Significant monthly SOI departures are indicated as in Figure 48. The approximate timing of oak frost injury and spruce light ring formation are indicated by the left and right arrows, respectively.

year after light ring formation in Quebec. The change from generally positive to negative SO indices may again reflect the "biennial tendency" of the ENSO phenomenon, where the coupled ocean and atmosphere in the tropical Pacific tend to oscillate between opposite ENSO extremes (Meehl 1987; Kiladis and Diaz 1989).

The apparently contrasting ENSO signals in oak and spruce (Fig. 50) suggests that periods characterized by a high frequency of light rings and a low frequency of oak frost rings might reflect more frequent El Nino conditions. Conversely, periods with many frost rings in oaks, but few light rings could imply more frequent La Nina conditions (e.g., Appendix 1). However, a Spearman's rank correlation test (Conover 1980) between decade totals of spruce light rings and oak frost rings from 1710 to 1979 (when both series chronologies are not correlated on the decodal scale.

Secular Variability of False Spring: 1650 to 1980

The chronologies of frost rings for the Southern Plains indicates several decade-long periods with a high or low incidence of frost injury (Fig. 7), suggesting that the occurrence of false spring episodes from 1650 to 1980 may have been nonrandom. To test the possible secular variability of false spring, a summary chronology of frost injury at all available sites in the Southern Plains region was compiled. This summary chronology illustrates the number of tree-ring

sites with significant frost injury for each year from 1650 to 1980 (Fig. 51). Because the tree-ring data appear to register at least 75% of all false spring events actually recorded in the meteorological data during the twentieth century, the summary chronology should represent a conservative record of false spring episodes in the Southern Plains for the past 331 years. The percentage of the total available sites with frost damage in any given year may also provide a rough approximation of the intensity of past false spring events, although the decreased frost susceptibility of old-growth oak trees may bias intensity estimates at some collection sites during the past century (Figures 7 and 51).

The possible secular variability of false spring occurrence was evaluated using Lilliefor's test (Conover 1980). Lilliefor's test assumes that the frequency distribution of intervals (in years) between false spring events will approximate an exponential, with many short intervals and fewer intervals of increasing length, if the interannual occurrence of these events is random. This null hypothesis is rejected when an exponential curve cannot be fit to the observed distribution of intervals.

The frequency distribution of annual intervals between frost rings during this 331-year period illustrated in Figure 52. Lilliefor's test on these data indicates a significant departure from an exponential distribution ($p < 0.001$). The null hypothesis of random frost ring occurrence through time

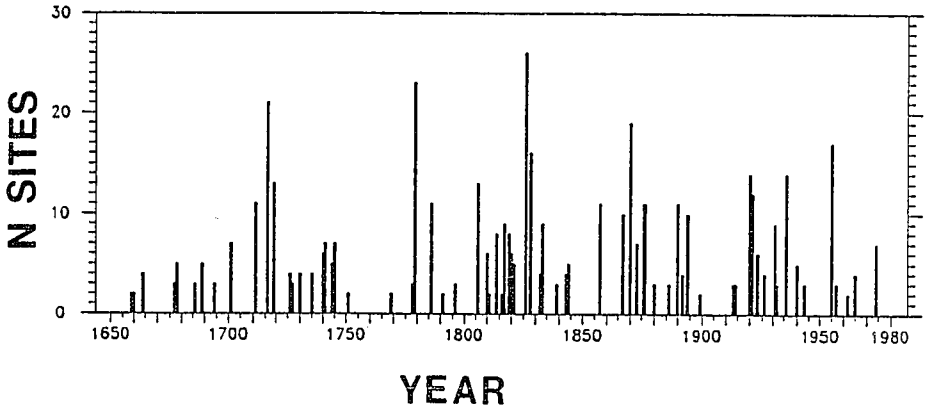

Figure 51. A summary chronology of frost injury at all available collection sites in the Southern Plains region. The total number of sites with significant evidence for frost injury is plotted for all 70 false spring events between 1650 and 1980. The decline in the number of sites with frost damage before ca. 1700 simply reflects a decline in the number of available collections.

is rejected largely because there are more one and three-year intervals between frost rings than expected given a random (exponential) distribution. Several periods with a particularly high incidence of frost rings stand out: 1740 to 1745, 1810 to 1828, and 1920 to 1936 (Fig. 51). There were also several ten year or longer intervals between frost rings, including one 18 year long period between 1751 and 1769 when no frost injury was registered (Figures 51 and 52).

These results indicate that the frequency of intense false spring episodes over the Southern Plains has increased and decreased substantially over the past 331 years. This conclusion assumes, however, that the underestimation error inherent in the tree-ring record of false spring is random, or at least has not significantly biased the available chronology. One way to assess the possible bias that might be introduced into this analysis by the occurrence of intense false spring events <u>not</u> registered by frost injury to trees, is to test the actual chronology of false spring episodes observed in the twentieth century meteorological record. Using the three regional temperature averages for southwest Missouri, northcentral Oklahoma, and central Texas, and the specific definition of false spring discussed above, 4 false spring events (1917, 1948, 1951, 1966) can be added to the 15 already recorded in these three regions from 1913 to 1980 with the frost ring data. This meteorological chronology has a mean interval of 3.39 years between intense false spring

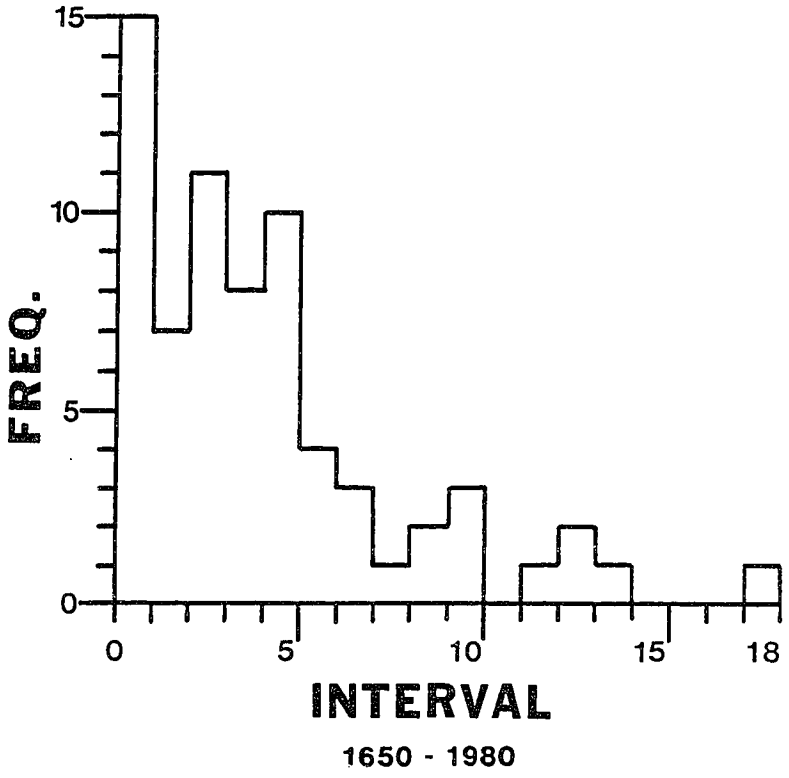

Figure 52. The frequency of intervals (in years) between the frost ring years illustrated in Figure 51. The shortest interval observed is only one year, and the longest was 18 years. The relatively high incidence of one and three-year intervals between these frost ring or false spring episodes is greater than expected given a random distribution of intervals between events ($p \leq 0.001$).

episodes, and a standard deviation of 1.79 years. Lilliefor's test indicates that the frequency distribution of intervals cannot be approximated by an exponential function ($p < 0.01$). In the case of the meteorological data, there are more one year ($p < 0.05$), two year ($p < 0.05$) and three year intervals ($p < 0.01$) than would be expected assuming that the frequency of intervals between false spring approximates and exponential in randomly distributed data.

These results are consistent with the analysis of the 331 year frost ring chronology, and indicate that the interannual occurrence of intense false spring events in the twentieth century meteorological record has been nonrandom. These results also suggest that the long frost ring chronology may provide a valid estimate of the secular variability of intense false spring episodes and the associated atmospheric anomalies over the past 331 years.

Given the apparent association between La Nina episodes and the warm winters of false spring, some of the nonrandomness in false spring occurrence due to the many one- and three-year intervals may reflect multiyear La Nina episodes. In fact, the inverse teleconnection between ENSO extremes and winter temperatures over Texas and Oklahoma (e.g., Ropelewski and Halpert 1986; Kiladis and Diaz 1989; and discussed above) suggest that some fraction of the decade-long changes in false spring frequency (e.g., Fig. 51) may be partially related to similar decadal changes in the frequency

and/or intensity of ENSO extremes. For example, the occurrence of seven fairly intense false spring events from 1920 to 1939, following only two relatively weak false spring events from 1900 to 1919 may not have been entirely coincidental (Fig. 51). Rasmussen and Wallace (1983) identify seven El Nino episodes between 1900 and 1919, but only three from 1920 to 1939. Examination of the SOI (Jones, personal communication) average for just the winter-spring (Dec.-May) season when positive SO indices or La Nina conditions appear most relevant to false spring (Fig. 48A) reveals nine years from 1900 to 1919 with negative indices, including seven with indices $\leq$ -0.50. Only five winter-spring SO indices fell below zero from 1920 to 1939, and only two were below -0.50 (i.e., 1924 and 1926). Also, no false spring events were recorded by oak trees from 1975 to 1982, and none were registered in the regional temperature data until perhaps 1989. No strong La Nina events were registered from 1976 until 1988 (Jones, personal communication; Kerr 1990), but the La Nina event of 1988 was followed by false spring-like conditions over portions of the Southern Plains in 1989. Unseasonably warm weather occurred in this region late in March, 1989 (WWCB 1989a), and low temperatures of 23°F and 22°F were recorded on April 11 at Springfield and Kansas City, Missouri (WWCB 1989b). These critical cold temperatures (< 23°F) apparently did not penetrate further south into the study area (WWCB 1989b), but it is not known whether this

event caused frost ring injury in oak trees of central Missouri. However, heavy freeze damage was reported for fruits and some vegetable crops in Arkansas, Texas, Georgia, and the Carolinas (WWCB 1989b).

The prevalence of positive winter-spring SO indices or La Nina conditions appears to favor warm winters over the Southern Plains, and may increase the risk of frost damage to prematurely advanced vegetation from late season cold waves. The prevalence of negative winter-spring SO indices or El Nino conditions tends to promote cool winters over the Southern Plains which may help maintain plant dormancy and lower the risk of false spring.

Examination of the long El Nino records compiled from historical sources by Quinn et al. (1978) and Hamilton and Garcia (1986) reveal several interesting oppositions with the chronology of frost rings in the Southern Plains. For example, many intense false spring episodes indicated by widespread frost damage occurred in between, or during the spring of El Nino years. The four years with the most widespread frost damage between 1800 and 1865 were 1806, 1826, 1828, and 1857 (Fig. 51), and all four occur between or at the beginning of El Nino events identified by Quinn et al. (1978), and may signify La Nina conditions during the preceding winter. Hamilton and Garcia (1986) identify 15 probable years from 1541 to 1828 when major El Nino events appear to have started. None of the 11 probable events from 1650 to 1828

were followed in the next spring by frost ring/false spring in the Southern Plains, but seven were preceded by frost ring events earlier in spring of the same year (three events) or in the spring of the previous year (four events). Given the tendency of the ENSO phenomenon to switch between extremes on a roughly biennial basis, this apparent phasing between frost ring occurrence in oak and major El Nino events does not contradict any of the major El Nino events reconstructed by Hamilton and Garcia (1986), and may in fact indicate that several were preceded by prominent La Nina events. Specifically, the frost ring data in conjunction with the Hamilton and Garcia (1986) El Nino chronology suggest that 1700 to early 1701; 1718-1719; 1726-1727; 1768-1769; 1789-1790; 1813 to early 1814; and 1827 to early 1828 may have been prominent La Nina episodes.

In general, given the level of association between the frost ring chronology and La Nina events during the past 120 years (e.g., Appendix 1), perhaps roughly 44 percent of the 70 frost ring years between 1650 and 1980 (Fig. 51, Appendix 1) may imply La Nina conditions in the tropical Pacific. This approximate level of association is not adequate to permit confident identification of past La Nina episodes, but may be useful supplementary evidence when used in conjunction with other evidence for La Nina conditions.

Considering a longer timescale, no frost rings were recorded from 1845 to 1856, but Quinn et al. (1978) cite

evidence indicating that six El Nino events may have occurred during this particular 12-year period. The period from 1746 to 1777 is also notable because only two relatively weak false spring events were registered in the frost ring chronology. The Quinn et al. (1978) El Nino chronology is quite incomplete during at this time, but the Canadian black spruce chronology contains eight light rings during this period, including six from the late summer of 1745 to 1759 (Filion et al. 1986, Appendix 1). Light rings are believed to represent cool conditions during late summer and may frequently reflect El Nino conditions (see above), as well as explosive volcanic eruptions (Filion et al. 1986). Other periods of opposition between the oak frost and spruce light ring records are evident in Appendix 1, particularly the period from 1740 to 1745 when four oak frosts but no spruce light rings were recorded, and the period from 1859 to 1863 when four light rings and no oak frost rings were recorded.

In spite of these intriguing examples, the occurrence or absence of false spring in the Southern Plains certainly cannot be invariably linked to La Nina or El Nino extremes, respectively. Many examples of the lack of association, and even the occurrence of strong El Nino conditions before and during false spring episodes could be cited. For example, the first and third largest positive winter-spring SOI averages between 1866 to 1980 were not followed by frost damage (i.e., 1904 and 1917, although 1917 did fulfill the

meteorological definition of false spring), while the lowest negative winter-spring SOI average from 1866 to 1980, was followed by frost damage (i.e., 1926, Appendix 1).

At first glance, the period from 1810 to 1821 also appears to indicate that atmospheric conditions unrelated to La Nina are capable of inducing false spring and widespread frost damage over the Southern Plains region. Oak frost damage was recorded during 8 of the 12 years from 1810 to 1821, the highest frequency of frost injury for any comparable 12-year period from 1650 to 1980 (Fig. 43, Appendix 1). During this same period, the largest volcanic dust veil during recorded history appears to have formed (e.g., Lamb 1870; Newhall and Self 1982; LaMarche and Hirschboeck 1984; Strothers 1984), and three or four moderate to strong El Nino events may also have developed (Quinn et al. 1978; Lough and Fritts 1985). However, these potentially powerful forcing mechanisms do not necessarily rule out the occurrence of strong La Nina conditions during the same 12-year interval, and the tree-ring evidence from Quebec and the Southern Plains may in fact provide circumstantial evidence for an amplified ENSO and associated extratropical circulation during the 1810's. This possibility is suggested by the remarkable agreement between the oak frost ring and spruce light ring chronologies from 1814 to 1819 (Appendix 1). Four frost rings and four light rings occurred during this evidently unusual six year period, and all four light rings occurred in the

late-summer of years when false spring conditions and earlier caused frost damage in the Southern Plains (i.e., 1814, 1816, 1817, and 1819; Appendix 1). Three of these years may also have been the starting years of El Nino events (i.e., 1814, 1817, and 1819, Quinn et al. 1978). These observations raise the possibility that the biennial tendency of the ENSO phenomenon may have been amplified, changing from La Nina conditions before and during oak frost ring formation to El Nino conditions later in the summer and fall of spruce light ring formation, perhaps resembling the monthly SO indices for the six modern years when oak frost rings were followed by spruce light rings (Fig. 50).

The large to cataclysmic eruptions of Mayon (1814) and Tambora (1815) in the tropical western Pacific, and the large tropical eruptions of Soufriere (1812) and Colima (1818; Simkin et al. 1981) make it difficult to resist speculation on the role of stratospheric aerosols in the possible amplification of the ENSO phenomenon during the 1810's (e.g., Handler 1984).

The evidence presented above is clearly not adequate to document an enhanced ENSO, much less the possible influence of volcanic forcing on ENSO activity. But the apparent ENSO signals in North American tree-ring data, and the remarkable concurrence of frost and light ring years from 1814 to 1819 are intriguing. If the ENSO was actually amplified during the 1810's, whether by volcanic forcing or for other reasons,

it could help to explain many of the regional ambiguities in the worldwide temperature response to the Tambora eruption (e.g., Angell and Korshover 1985).

VII. SUMMARY AND CONCLUSIONS

This study has developed a detailed chronology of frost injured tree rings using deciduous oaks of the southcentral United States. Frost injury is frequent and widespread in this region, particularly in a zone extending from southwest Missouri into central Texas. The frost ring chronology is based on some 1650 tree-ring specimens from 42 collection sites, and includes 70 exactly dated frost years from A.D. 1650 to 1980. All 70 frost years were identified on the basis of a significant proportion of frost injured specimens recorded at two or more collection sites. This is the most detailed and well replicated frost ring chronology yet reported, and should have considerable value for tree-ring dating and paleoclimatology in the central United States.

Frost rings in deciduous oaks of the Southern Plains region occur exclusively in the springwood portion of the annual ring, and are recognized by collapsed vessels, disrupted rays, abnormal parenchyma cells, and a discolored lesion at the beginning of the annual ring. Several lines of evidence leave no doubt that these unique damaged rings are the exclusive result of subfreezing temperatures during the active differentiation of xylem cells early in the spring growing season. The anatomical features of frost rings have previously been shown through empirical and experimental studies to be the specific result of subfreezing temperatures. Severe subfreezing cold waves during the late winter or early

spring were actually recorded for the Southern Plains region in the available instrumental temperature data for every frost ring year since the late-nineteenth century, and for every earlier frost ring event for which documentary weather data were obtained.

Frost injured rings in deciduous oaks of the Southern Plains reflect anomalous atmospheric conditions that occur on both climatological and meteorological timescales during the winter and spring. These unusual conditions have been referred to variously as "backward spring" or "false spring", and include unseasonably mild winter temperatures which are abruptly terminated early in the growing season by an often record-breaking cold wave. These backward winter and spring temperatures can take a heavy toll on crops and native vegetation, and may introduce an episodic influence on wildlife population dynamics because subfreezing temperatures during the flowering and leafing stage can drastically reduce or eliminate mast production in deciduous oaks (e.g., Fowells 1965).

Three threshold temperature criteria were used to specifically define the unusual false spring weather and climate conditions reflected by frost rings in oaks of the Southern Plains. These minimum thresholds are based on the mildest warm and cold temperature departures recorded in regional temperature data for all twentieth century frost ring years. The specific false spring weather anomaly recorded by

frost rings in oaks is defined as the occurrence of a minimum daily temperature $\leq$ 23°F (-5°C) on or after March 21st in Oklahoma and Missouri (on or after March 1st in Texas), if preceded by a warm spell with a mean daily minimum temperature $\geq$ 40°F (4.4°C) and no single daily minimum temperature below 27 F (-2.8°C) for a 10-day period beginning 13 days prior to the hard freeze event. All frost ring years since 1899 meet or exceed these minimum temperature thresholds, and only four additional years not registered by frost injury to oak trees fulfill these criteria in the three regional temperature averages. Using this specific definition of false spring and just the 13 frost ring years registered at sites near the three regional temperature averages, the frost ring chronology has recorded at least 75% of all intense false spring events which actually occurred during the twentieth century, and presumably over the past 331 years as well. However, it is quite likely that the frost ring chronology constitutes a complete record of the suite of atmospheric and prior growth variables actually responsible for frost injury. Unfortunately, this suite of variables has yet to be fully defined.

The meteorological definition of false spring could be refined, and in so doing the number of events not registered by frost injury to trees could presumably be reduced. Ideally, a precise definition of false spring would be based on continuous meteorological data recorded instrumentally at

a network of tree-ring sites located throughout the Southern Plains region. Such long-term instrumentation requires considerable financial and logistical support, not to mention the natural occurrence of false spring anomalies at the instrument localities. But it could have several added benefits including better definition of the tree growth response to weather and climate variability essential for paleoclimatic reconstruction. More detailed analyses of the presently available meteorological data recorded near the collection sites might also help to more precisely define the specific weather conditions implied by frost rings.

Old-growth trees are often less susceptible to late freeze injury due in part to reduced vigor and a slower initiation of spring growth. The tree-ring samples included in this study predominantly represent mature and old-growth trees, which were deliberately selected in order to maximize chronology length. To counteract possible age bias in the summary frost ring chronology for the Southern Plains, additional representative sampling of all age classes was conducted at four of the most frost-sensitive forest sites located from central Texas into southwestern Missouri. Analyses suggest that the summary chronology of frost rings for the entire Southern Plains region from 1650 to 1980 is not significantly biased by the decreased frost susceptibility of old trees. This no doubt reflects the representative samples from the four frost sensitive sites and particularly

the solid replication of some 1650 tree-ring specimens from 42 collection sites. Nevertheless, the frost ring chronologies available for some individual collection sites dominated by old-growth specimens may indeed under-represent the true number of false spring events which actually occurred at some of these sites during the past century. If additional representative sampling of all age classes was conducted at these particular collection sites, then the proportion of available sites with evidence for frost injury in a given year could be used to approximate the intensity of past false spring events. False spring episodes of different intensities might also be more clearly related to large-scale atmospheric mechanisms.

The frequency of frost injury in the available oak collections suggests that the region along the eastern margin of the southern Great Plains extending from central Texas through central Oklahoma into southwestern Missouri is subject to the highest incidence of false spring events in the study area. Differences in photoperiod, winter hardening, and the advection and/or modification of warm and cold air masses may explain much of the decline in frost ring frequency in trees growing near the northern and southern margins of the study area. Many tree-ring chronologies from deciduous oaks are available elsewhere in the midwest and eastern United States (e.g., Duvick and Blasing 1981; Cook and Jacoby 1983), and could be consulted to better define the geographic

distribution of the false spring signal in the eastern deciduous forest. The chronology and spatial pattern of seventeenth century false spring events could also be improved with additional collections from oak timbers preserved in early historic buildings.

The meteorology of false spring invariably involves a warm and cold phase, each typically characterized by contrasting circulation and surface air conditions. Several specific meteorological conditions have been repeatedly identified during each phase of twentieth century false spring episodes. The warm phase often includes zonal flow across the Northern Plains, confluence aloft near the Great Lakes, a surface anticyclone near the Southeast, and an upper-level trough near Southern California which together favor warm air advection into the southcentral United States. The cold phase is usually characterized by a deep upper-level trough over the central United States, associated with a strong, migratory surface disturbance and cold front which advect unseasonably cold polar or arctic air into the Southern Plains. This cold air advection is usually accompanied by a powerful ridge of surface high pressure extending from the arctic to southern Texas.

The severe freeze event is certainly the most prominent meteorological signal of false spring, but the principal climatological signal is ironically the warm winter temperatures which help promote early season tree growth. The

co-occurrence of a meteorological and climatological signal in tree-ring data is unusual, and the oak frost-ring chronology provides a reasonably detailed record of these combined causes of false spring episodes over the Southern Plains for the past 331 years.

Because the temperature anomalies of false spring tend to be widespread and extreme, they often appear to reflect large-scale abnormalities in atmospheric circulation over North America, and certain unusual configurations of atmospheric boundary conditions related to the ENSO and perhaps to worldwide volcanic activity. The best evidence for circulatory control over the temperature anomalies of false spring may actually be depicted on the synoptic maps of the 17 events from 1899 to 1974, and summarized in the composite maps for the warm and cold phases of false spring in Fig. 45. The distribution of surface temperature, winds, and the tracks of surface pressure centers frequently document major circulation changes between the warm and cold phase. These changes often appear to be consistent with a reverse PNA circulation pattern during the warm phase, which in some notable cases appears to migrate eastward during the cold phase bringing severely cold air into the southcentral United States in the deep trough of this migrating circulation pattern. However, these maps depict the instantaneous conditions of the atmosphere for selected days at the height of the warm and cold phase, so they tend to exaggerate the

circulation changes associated with false spring.

Attempts to further specify the circulation patterns responsible for false spring over the Southern Plains have been constrained by the lack of upper air data prior to 1947. Only five frost events that occurred between 1947 and 1980 are contemporaneous with upper air data. The use of circulation indices based on height data from selected pressure centers has greatly simplified the processing of the enormous Northern Hemisphere data set of twice daily 700 mb height observations, but it has also placed arbitrary constraints on the analysis of false spring circulation patterns. Other modes of circulation not associated with the Pacific/North American (PNA) pattern such as the North Atlantic Oscillation (NAO) could well be responsible for some false spring events, but these possibilities have not been investigated.

In spite of these shortcomings, some large-scale associations between the PNA pattern and false spring have been tentatively identified. The reverse PNA pattern appears to be associated with above average winter temperatures over the Southern Plains and eastern United States (Wallace and Gutzler 1981). Strong reverse PNA conditions persisted for several days to weeks prior to the hard freeze during three post-1947 false spring episodes, although these daily departures are statistically significant for only three days during 1955. Combined PNA indices from the five most recent

episodes were below average during the 10-day warm spell just prior to the hard freeze ($p = 0.077$), and may have changed from a reverse PNA to positive PNA mode between the warm and cold phases of false spring. However, there are many inconsistencies between the PNA indices of these five available events. In fact, given the development of a cut-off low near Southern California, winter warming over the Southern Plains appears to be possible under the opposite extremes of the PNA pattern. Nevertheless, the anomalous upper-level trough over California and anomalous ridge over the Southeast typical of the reverse PNA pattern definitely favor large-scale warm air advection into the southcentral United States.

A more complete description of the possible large-scale circulation control over false spring will be difficult to obtain without a longer record of circulation. A long PNA index based on sea level pressure data (e.g., Wallace and Gutzler 1981), or estimated from the surface temperature field (e.g., Klein 1983), could provide coverage for most of the twentieth century, greatly increasing the sample of false spring events available for comparison with the circulation indices.

The occurrence of false spring also appears to be related to other large-scale atmospheric and volcanic forcing mechanisms. The statistical link with La Nina events is perhaps the most credible of these various possible

associations because La Nina is known to be associated with warm winters over the Southern Plains region (e.g., Horel and Wallace 1981; Ropelewski and Halpert 1986; Kiladis and Diaz 1989; this study), which is the primary climatological signal of false spring. Strong La Nina conditions prevailed during the several months prior to and concurrent with 11 of the 22 false spring episodes between 1877 and 1980, a substantially higher rate of co-occurrence than would be expected given two independent phenomena. Considering just a winter-spring SOI average from 1866 to 1980 (Dec.-May), positive SOI indices were observed during 19 of the 26 false spring years. Strongly negative winter-spring SO indices (< -0.5), indicative of El Nino conditions, were observed during only 2 of the 26 false spring years between 1866 and 1980. As a result the composite monthly average SO indices computed for all 26 false spring events remains persistently positive for seven months during the winter-spring, and the January SOI average is significantly above the average of all remaining non-false spring months ($p = 0.02$). These results illustrate the prevalence of La Nina conditions in the tropical Pacific prior to, and during false spring episodes over the southern Great Plains. Given this apparent extratropical connection, the frost ring chronology of false spring events over the Southern Plains might be cautiously used in conjunction with other proxy evidence concerning the ENSO phenomenon (e.g., Quinn et al. 1978; Lough and Fritts 1985; Hamilton and Garcia

1986) to help identify possible La Nina episodes back to A.D. 1650.

The evidence for a La Nina influence on false spring seems adequate to warrant further examination of the apparent tropical teleconnections with false spring-like weather over the southcentral United States. Further investigation might relax the rigid criteria used to define false spring in this study because the near false spring event of 1989 followed La Nina conditions, but did not fulfill the meteorological definition of false spring used in the analysis.

The strength of the ENSO signal in extratropical climate appears to be dependent in part on the pre-existing configuration of midlatitude circulation (e.g., Rasmussen and Wallace 1983), and this may be true also for the La Nina connection with false spring. For example, La Nina conditions and the reverse PNA pattern both appear to be individually related to warm winters over the Southern Plains, and this warming appears to be most pronounced when these two circulation signals occur in phase (i.e., La Nina conditions beginning in the previous year, and a reverse PNA pattern established during the current winter). Conversely, the influence of each signal on winter temperatures over the Southern Plains may be weakened when they (infrequently) occur out of phase. This preconditioning effect may have occurred in December of both 1973 and 1975 when La Nina conditions were matched with a positive PNA pattern (Kiladis and Diaz 1989;

Yarnal and Diaz 1986), and December mean temperatures were near normal in Texas, Oklahoma, and Missouri (Karl et al. 1983a,b,c) and false spring conditions did not occur.

If La Nina conditions are linked to warm winters over the Southern Plains region, the question naturally arises as to how, or why an often record-setting cold wave penetrates the region in late winter or early spring to cause heavy frost damage. The principal La Nina teleconnection with Southern Plains temperature appears to be largely on the climatological time scale, and the meteorological features of the more transitory cold wave may occur independently of ENSO forcing. However, it is possible to identify synoptic mechanisms related to the long-term La Nina influence on warm winter temperatures over the southeastern United States, which might help to breed the intensely cold Canadian air masses subsequently responsible for the hard freeze which terminated false spring. A confluent zone of upper air winds was noted during the warm phase of the five most recent false spring episodes, and probably developed during many previous episodes (Fig. 47A). This confluence is associated with southwesterly flow from the upper air trough usually present over Southern California during the warm phase, which then merges with zonal westerly flow over the northcentral United States. Confluence of winds aloft in this region would tend to isolate polar air masses in Canada, where radiative processes could further intensify air mass cooling (e.g., Namias 1950). If a

mesoscale disturbance of sufficient strength subsequently develops along the polar front, the severely cold Canadian air may be advected southward, and may then produce the often record-setting hard freeze of false spring episodes. The potential for development of such a disturbance would often be high during the late winter-early spring transition season when the prevailing winter circulation regime often weakens.

Consequently, the La Nina-related circulation patterns which favor warm winters in the South, particularly confluence over the northcentral United States, may also help to intensify the brief but destructive late-winter cold wave which makes false spring such a remarkable meteorological event. If this hypothesis is accurate there should be evidence for below normal winter temperatures in Canada during La Nina conditions. van Loon and Madden (1981) report a positive correlation between winter temperature (DJF) over Canada and the Southern Oscillation (as measured by sea level pressure at Cocos Island). They also document the negative correlation between the SO and winter temperature over the southeastern United States and the Gulf of Mexico. These surface air temperature teleconnections seem to be time stable (van Loon and Madden 1981), and indicate that winters tend to be cool in Canada and warm in the Southern Plains during La Nina events. Yarnal and Diaz (1986) also report below normal winter temperatures on the Pacific coast of Canada and Alaska during La Nina years, and the annual temperatures illustrated

by Rasmussen and Wallace (1983) for southwestern Canada usually fall below average during the starting years of La Nina events. Therefore, the apparent La Nina influence on warm winters over the Southern Plains may also increase the potential for the severe late-season outbreak of subfreezing air which abruptly terminates all false spring episodes.

The association between the frost-ring record of false spring and the chronology of explosive volcanic eruptions from 1650 to 1980 is statistically significant, but must be viewed with some skepticism. Certainly the volcanic eruption chronology is under-reported before about 1880 (Newhall and Self 1982), and probably severely so before 1800. However, most of the chronological agreements between the Newhall and Self (1982) record of explosive eruptions and false spring occurrence during a subsequent 14-month period are found during the nineteenth century. There is no statistically significant association between these two chronologies during the twentieth century when the record of explosive volcanism is most accurate. Also, the expected, through poorly documented, cooling effect of volcanic eruptions is difficult to relate to the principal climatological signal of false spring, which is warmer than normal winter temperatures over the Southern Plains. Explosive volcanism might be related to the more transitory hard freeze of false spring, but the possible physical mechanisms responsible for such a relationship are not clear.

Statistical evidence has been reported which appears to link the occurrence of frost rings in bristlecone pine (LaMarche and Hirschboeck 1984) and light rings in black spruce (Filion et al. 1986) to large explosive volcanic eruptions worldwide. However, questions concerning the true strength of this volcanic signal are raised by the inevitable doubts concerning the accuracy of the pre-twentieth century volcanic chronology, and by the obscurity of a large and persistent temperature response to selected eruptions, particularly over the extended three-year intervals employed in the previous studies linking the bristlecone and spruce ring abnormalities to eruptions (cf. Bradley 1988). Most of these doubts were raised by LaMarche and Hirschboeck (1984) when they first reported the apparent volcanic signal in bristlecone pine frost rings.

Preliminary evidence has been presented in Chapter 6 which indicates that El Nino conditions may also influence the formation of frost and light rings in bristlecone pine and black spruce, respectively. This evidence definitely suffers from many of the same problems involved in the volcanic eruption chronology, especially doubts regarding the accuracy of the El Nino chronology before 1866. Nonetheless, bristlecone pine frost rings and spruce light rings both exhibit statistically significant El Nino signals during the modern period (1866 to present). This apparent El Nino signal has the added virtue of being consistent with the

extratropical teleconnection of the El Nino phenomenon identified in modern meteorological data, particularly in the case of black spruce grown in northern Quebec.

Light rings are believed to reflect cold conditions during August or September (Filion et al. 1986), and the starting years of El Nino events have been related to below normal summer and fall temperatures in northern Quebec (Kiladis and Diaz 1989). A significant number of light ring years occurred during the starting year of El Nino events when the temperature teleconnection also exists.

Bristlecone pine frost rings also reflect cold conditions in August or September (for latewood injuries), but the regional El Nino teleconnection during this season appears to be above average precipitation (Kiladis and Diaz 1989; Schonher and Nicholson 1989). Nevertheless, heavy precipitation at arid, high elevation bristlecone pine forests might at times be accompanied by subfreezing temperatures, or may favor frost injury by helping to extend the growing season into fall when the risk of subfreezing temperatures normally increases.

Both explosive volcanic eruptions and El Nino conditions may be capable of inducing the North American climate anomalies actually responsible for frost rings in bristlecone pine and light rings in black spruce. However, because the ENSO phenomenon is the dominate global climate signal known, and is teleconnected with seasonal climate anomalies in the

Great Basin and in northern Quebec (e.g., Rasmussen and Wallace 1983, Kiladis and Diaz 1989), El Nino conditions may presently provide the most plausible large-scale forcing mechanism to explain the late summer-early fall climate anomalies responsible for light rings in black spruce and possibly frost rings in bristlecone pine. The apparent volcanic signal certainly remains plausible and is supported by considerable evidence (LaMarche and Hirschboeck 1984, Filion et al. 1986), but it suffers from the obscurity of a strong and persistent three-year temperature signal associated with selected modern eruptions (e.g., Angell and Korshover 1985, Mass and Portman 1989), and from the lack of well documented physical mechanisms to relate worldwide volcanic eruptions to extended three-year temperature anomalies over North America (e.g., Mass and Portman 1989).

Comparisons between the frost ring record in oaks of the Southern Plains and the light ring record in Canadian black spruce reveal several interesting chronological relationships that <u>might</u> reflect in part contrasting ENSO signals in each data set. Light rings rarely develop in the late summer before oak frost injury the following spring. This pattern is statistically significant, and may reflect the frequent development of La Nina conditions during the year before oak frost injury, and El Nino conditions before light ring formation (e.g., Fig. 50). Also, oak frost rings and spruce light rings do not occur sequentially in the same year more

often than would be expected by chance, but they did occur together during the exact same year four times from 1814 to 1819 (i.e., 1914, 1916, 1817, 1819, Appendix 1). To the degree that the oak and spruce ring anomalies reflect opposite ENSO signals, this remarkable sequence of co-occurrences might reflect amplified ENSO activity during the six years from 1814 to 1819. La Nina conditions could have been prevalent before and during oak frost injury in the spring, only to reverse phase in late spring to El Nino conditions prior to, during, and after light ring formation in August or September. Quinn et al. (1978) present independent evidence indicating that three moderate to strong El Nino events may actually have occurred during three of these four years (1814, 1817, 1819), and Lough and Fritts (1985) reconstruct one of the most extreme El Nino events in over 300 years from 1815 to 1816.

The period from 1814 to 1819 was also characterized by four large volcanic eruptions in the tropics, including the eruption of Tambora in 1815, which was perhaps the largest volcanic eruption in the post-glacial period (Stothers 1984). The tree ring data discussed above and previously reported meteorological data for 1816 (e.g., Ludlum 1968; Landsberg and Albert 1974; Stothers 1984) highlight unusual climate conditions over North America and western Europe during the mid to late 1810's, which might reflect both ENSO and volcanic forcing. If the ENSO phenomenon was actually amplified from 1814 to 1819, it could help explain many ambiguities in the

worldwide surface air temperature response to the Tambora eruption. In fact, given the cataclysmic 1815 eruption of Tambora in the western Pacific center-of-action associated with the Southern Oscillation, and a possibly enhanced ENSO during the late 1810's, it is difficult to resist speculations concerning the potential for interactions between dense stratospheric aerosols over the equatorial Pacific and ENSO activity (cf. Handler 1984; Mass and Portman 1989).

The large-scale climatic or meteorological implications of intraannual ring width abnormalities such as frost rings have not been extensively investigated. This analysis has demonstrated that antecedent climatic conditions and short-term meteorological events are responsible for frost rings in deciduous oaks of the Southern Plains. These false spring conditions include above normal winter temperatures and the subsequent outbreak of subfreezing polar or arctic air. The frost ring record of these contrasting atmospheric signals provides a unique perspective on past weather and climate conditions which cannot normally be derived from annual ring width or density chronologies. The recurrence of specific meteorological conditions during all twentieth century false spring events registered by frost rings reasonably allow the inference of these same synoptic features during preinstrumental frost ring years, and thereby establishes the feasibility of "dendrometeorology", the reconstruction of short-term meteorological conditions from tree-ring data. The

warm winter signal implied by frost rings in oaks is also statistically independent of paleoclimatic reconstructions based on ring width or density chronologies, and therefore might be useful for independent verification of regional winter temperature reconstructions for the past 331 years.

The apparent influence of opposite ENSO signals in tree-ring abnormalities formed in Canada, the Great Basin, and the Southern Plains suggest an interesting avenue for further research. Proper exploitation of these opportunities will require the additional development of detailed and well replicated frost or light ring chronologies in North America and worldwide.

REFERENCES

Anderson, J.R., and Gyakum, J.R. 1989. A diagnostic study of Pacific basin circulation regimes as determined from extratropical cyclone tracks. Monthly Weather Review 117:2672-86.

Andrews, J.F. 1962. The weather and circulation of February 1962. Monthly Weather Review May 1962.

Angell, J.K., and Korshover, J. 1985. Surface temperature changes flowing six major volcanic episodes between 1780 and 1980. Journal of Climate and Applied Meteorology 24:937-51.

Arkansas Gazette. 1826. March 7 and 28, 1826.

_____. 1828a. February 6, 1828.

_____. 1828b. April 9, 1828.

_____. 1870a. February 17, 1870.

_____. 1870b. April 17, 1870.

_____. 1876. March 24, 1876.

_____. 1894. March 26-29, 1894.

_____. 1920. April 6, 1920.

_____. 1921. March 28, 1921.

_____. 1936. April 4, 1936.

Bailey, I.W. 1925. Frost rings as indicators of the chronology of specific biological events. Botanical Review 80:93-101.

Barnston, A.G., and Livezey, R.E. 1987. Classification, seasonality and persistence of low-frequency atmospheric circulation patterns. Monthly Weather Review 115:1083-1126.

Beebe, R.G. 1956. Tornado composite charts. Monthly Weather Review 84:127-42.

Bennett, W.C. 1931a. The weather elements. Monthly Weather Review Jan. 1931.

_____. 1931b. The weather elements. Monthly Weather Review Feb. 1931.

_____. 1931c. The weather elements. Monthly Weather Review, Mar. 1931.

_____. 1932. The weather elements. Monthly Weather Review, Feb. 1932.

Blackmon, M.L., Y.H. Lee, and Wallace, J.M. 1984. Horizontal structure of 500 mb height fluctuations with long, intermediate and short time scales. Journal of the Atmospheric Sciences 41:961-79.

Blasing, T.J., Stahle, D.W., and Duvick, D.N. 1988. Dendroclimatic reconstruction of annual precipitation in the southcentral United States from 1750 to 1980. Water Resources Research 224:163-71.

Bomar, G.W. 1983. Texas Weather. Austin:University of Texas Press.

Boyce, J.S. 1938. Forest pathology. New York: McGraw-Hill Book Company.

Boyce, R. 1929. Frost rings and the Spruce Budworm biogenese. Botanical Review 10:33-45.

Bradley, R.S. 1988. The explosive volcanic eruption signal in Northern Hemisphere continental temperature records. Climatic Change 12:221-43.

Bradley, R.S., Diaz, H.F., Kiladis, G.N., and Eischeid, J.K. 1987. ENSO signal in continental temperature and precipitation records. Nature 327:497-501.

Braun, E.L. 1950. Deciduous Forests of Eastern North America. Philadelphia:The Blakiston Co.

Brinkmann, W.A.R. 1979. Growing season length as an indicator of climatic variations? Climatic Change 2:127-38.

Bruner, W.E. 1931. The vegetation of Oklahoma. Ecological Monographs 1:99-188.

Bryson, R.A., and B.A. Goodman. 1980. Volcanic activity and climatic changes. Science 207:1041-44.

Christensen, K. 1987. Tree-rings and insects: the influence of cockchafers on the development of growth rings in oak trees. In Proceedings of the International Symposium on Ecological Aspects of Tree-Ring Analysis. Marymount College, Tarrytown, NY, August, 1986, pp. 142-54.

Cleaveland, M.K. In press. Volcanic effects on Colorado Plateau Douglas-fir tree rings. In Proceedings of the Meeting, The Year Without a Summer? Climate in 1816, ed. C.R. Harington. Ottawa: Canadian National Museum of Natural Sciences.

Cleaveland, M.K., and Stahle, D.W. 1989. Tree ring analysis of surplus and deficit runoff in the White River, Arkansas. Water Resources Research 25:1391-1401.

Clarke, F.H. 1892. Saturday, March 19, 1892. Weather-Crop Bulletin, Arkansas State Weather Service, and U.S. Dept. Agriculture, Weather Bureau.

Cline, I.M. 1892. Week ending March 21, 1892. Weekly Weather-Crop Bulletin, Texas Weather Service, and U.S. Dept. Agriculture, Weather Bureau.

Cline, I.M. 1899. Weekly Crop Bulletin, April 4, 1899, Texas Section, Climate and Crop Service, USDA Weather Bureau.

Cochran, W.G. 1954. Some methods for strengthening the common X^2 tests. Biometrika 10:417-51.

Conover, W.J. 1980. Practical Nonparametric Statistics. New York: John Wiley and Sons.

Cook, E.R. 1985. A time series analysis approach to tree-ring standardization. Ph.D. dissertation, University of Arizona, Tucson.

Cook, E.R. and Holmes, R.L. 1984. Program ARSTND and users manual. Laboratory of Tree-Ring Research, Tucson:University of Arizona.

Cook, E.R., and Jacoby, G.C. 1983. Potomac River streamflow since 1730 as reconstructed by tree rings. Journal of Climate and Applied Meteorology 22:1659-72.

Court, A. 1974. Climate of the conterminous United States. In Climates of North America, ed. R.A. Bryson and F.K. Hare, pp. 193-341. Amsterdam: Elsevier Scientific Publishing Company.

Davis, N.E. 1972. The variability of the onset of spring in Britain. Quarterly Journal of the Royal Meteorological Society 98:763-77.

Day, P.C. 1914. The weather of the Month. Monthly Weather Review, April 1914.

_____. 1920. The weather elements. Monthly Weather Review, April 1920.

_____. 1923. The weather elements. Monthly Weather Review, Jan. 1923.

_____. 1926. The weather elements. Monthly Weather Review, Feb. 1926.

Dean, J.S. 1969. Chronological Analysis of Tsegi Phase Sites in Northeastern Arizona. Papers of the Laboratory of Tree-Ring Research, No. 3, Tucson:University of Arizona Press.

Dean, W.E., Bradbury, J.P, Anderson, R.Y., and Barnosky, C.W. 1984. The variability of Holocene climate change: evidence from varved lake sediments. Science 226:1191-94.

Decker, W.L. 1951. Late spring and early fall killing freezes in Missouri. Missouri Agricultural Experiment Station Bulletin 649:3-15.

Dickson, R.R. 1974. Weather and circulation of February 1974. Monthly Weather Review 102:403-7.

Dickson, R.R., and Namias, J. 1976. North American influences on the circulation and climate of the North Atlantic sector. Monthly Weather Review 104:1255-65.

Douglas, A.V., and Englehart, P.J. 1981. On a statistical relationship between autumn rainfall in the central equatorial Pacific and subsequent winter precipitation in Florida. Monthly Weather Review 109:2377-82.

Douglass, A.E. 1935. Dating Pueblo Bonito and other ruins of the Southwest. National Geographic Society, Contributed Technical Papers, Pueblo Bonito Series 1, Washington, DC.

_____. 1941. Crossdating in dendrochronology. Journal of Forestry 39:825-31.

Druffel, E.M. 1982. Banded corals: changes in oceanic Carbon-14 during the Little Ice Age. Science 218:13-19.

Duvick, D.N., and Blasing, T.J. 1981. A dendroclimatic reconstruction of annual precipitation amounts in Iowa since 1680. Water Resources Research 17:1183-89.

Dyksterhuis, E.J. 1948. The vegetation of the Western Cross Timbers. Ecological Monographs 18:325-76.

Esbensen, S.K. 1984. A comparison of intermonthly and interannual teleconnections in the 700 mb geopotential height field during the Northern Hemisphere winter. Monthly Weather Review 112:2016-32.

Fahn, A. 1974. Plant Anatomy. Oxford:Pergamon Press.

Filion, L., Payette, S., Gauthier, L., and Boutin, Y. 1986. Light rings in subarctic conifers as a dendrochronological tool. Quaternary Research 26:272-79.

Fowells, H.A. 1965. Silvics of Forest Trees of the United States. Agricultural Handbook #271. USDA, Forest Service.

Frazier, H.M. 1957. The weather and circulation of March 1957. Monthly Weather Review. March 1957, 89-98.

Fritts, H.C. 1969. Bristlecone pine in the White Mountains of California: growth and ring-width characteristics. Papers of the Laboratory of Tree-Ring Research, No. 4. Tucson: University of Arizona Press.

Fritts, H.C. 1976. Tree-Rings and Climate. London:Academic Press.

Fritts, H.C., and Swetnam, T.W. 1989. Dendroecology: a tool for evaluating variations in past and present forest environments. Advances in Ecological Research 19:111-88.

Gilliland, R.L., and Schneider, S.H. 1984. Volcanic, CO_2 and solar forcing of Northern and Southern Hemisphere surface air temperatures. Nature 310:38-41.

Glerum, C., and Farrar, J.L. 1966. Frost ring formation in the stems of some coniferous species. Canadian Journal of Botany 44:879-86.

Glock, W.S. 1951. Cambial frost injuries and multiple growth layers at Lubbock, Texas. Ecology 32:28-36.

Graybill, D.A. 1987. A network of high elevation conifers in the western U.S. for detection of tree-ring growth response to increasing atmospheric carbon dioxide. In Proceedings of the International Symposium on Ecological Aspects of Tree-Ring Analysis. Marymount College, Tarrytown, NY, August, 1986, pp. 463-74.

Greely, A.W. 1890. Week ending March 15, 1890. Weather-Crop Bulletin, No. 4. Washington: War Department, Signal Officer.

Green, R.A. 1965. The weather and circulation of March 1965. Monthly Weather Review 93:392-98.

Griffiths, J.F., and Ainsworth, G. 1981. One Hundred Years of Texas Weather, 1880-1979. Monograph Series No. 1, Office of the State Climatologist, College Station:Texas A&M University.

Griffiths, J.F., and Strauss, R.F. 1985. The variety of Texas weather. Weatherwise 38:137-41.

Hamilton, K., and Garcia, R.R. 1986. El Nino/Southern Oscillation events and their associated midlatitude teleconnections 1531-1841. Bulletin of the American Meteorological Society 67:1354-61.

Handler, P. 1984. Possible association of stratospheric aerosols and El Nino type events. Geophysical Research Letters 11:1121-24.

Harmon, J.R. 1971. Tropospheric waves, jet streams, and United States weather patterns, Resource Paper No. 11. Washington, DC: Association of American Geographers.

Harper, H.J. 1960. Drought years in central Oklahoma from 1710 to 1959 calculated from annual rings of post oak trees. Proceedings Oklahoma Academy of Science 1960:23-29.

Harris, H.A. 1934. Frost ring formation in some winter-injured deciduous trees and shrubs. American Journal of Botany 21:485-98.

Henry, A.J. 1899. The weather of the month. Monthly Weather Review, April 1899.

Hickman, W.C. 1920. Weather and crops in Arkansas, 1819 to 1879. Monthly Weather Review, August, 1920:447-51.

Holmes, R.L. 1983. Computer-assisted quality control in tree-ring dating and measurement. Tree-Ring Bulletin 43:69-78.

Horel, J.D., and Wallace, J.M. 1981. Planetary-scale atmospheric phenomenon associated with the Southern Oscillation. Monthly Weather Review 109:813-29.

Horstmeyer, S.L. 1989. In search of Cincinnati's weather. Weatherwise 42:320-27.

Hughes, M.K., Schweingruber, F.H., Cartwright, D., and Kelly, P.M. 1984. July-August temperature at Edinburgh between 1721 and 1975 from tree-ring density and width data. Nature 308:341-44.

Jacoby, G.C., and D'Arrigo, R. 1989. Reconstructed Northern Hemisphere annual temperature since 1671 based on high latitude tree-ring data. Climatic Change 14:39-59.

Jacoby, G.C., Sheppard, P.R., and Sieh, K.E. 1988. Irregular recurrence of large earthquakes along the San Andreas fault: evidence from trees. Science 241:196-99.

Jenne, R.L, and McKee, T.B. 1985. Data. In Handbook of Applied Meteorology, ed. D.D. Houghton, pp. 1175-1281. New York: John Wiley & Sons.

Johnson, F.L., and Risser, P.G. 1973. Correlation analysis of rainfall and annual ring index of central Oklahoma blackjack and post oak. American Journal of Botany 60:475-78.

Jones, P.D. 1988. The influence of ENSO on global temperatures. Climate Monitor 17:80-89.

Jones, P.D. 1989. Personal communication, Climatic Research Unit, University of East Anglia, Norwich, England.

Jurney, D.H. 1987. Dendrochronology of historic structures. In Historic Buildings, Material Culture, and People of the Prairie Margin, ed. D.H. Jurney and R.W. Moir, pp. 55-72. Dallas: Archaeology Research Program, Southern Methodist University.

Karl, T.R., L.K. Metcalf, M.L. Nicodemus, and Quayle, R.G. 1983a. State wide average climatic history, Texas 1888-1982. National Climate Data Center, Asheville, N.C.

_____. 1983b. Statewide average climatic history, Oklahoma 1892-1982. National Climate Data Center, Asheville, N.C.

_____. 1983c. Statewide average climatic history, Missouri 1882-1982. National Climate Data Center, Asheville, N.C.

Kelly, P.M., and Sear, C.B. 1984. Climatic impact of explosive volcanic eruptions. Nature 311:740-43.

Kerr, R.A. 1990. Global warming continues in 1989. Science 247:521.

Kibler, C.L., and Martin, R.H. 1955. Damaging cold wave of March 23-31, 1955. Monthly Weather Review 82:78-82.

Kiladis, G.N., and Diaz, H.F. 1989. Global climatic anomalies associated with extremes in the Southern Oscillation. Journal of Climate 2:1069-90.

Kincer, J.B. 1923. The effect of weather on crops and farming operations. Monthly Weather Review, March 1923.

_____. 1926. The effect of weather crops on and farming operations. Monthly Weather Review, March 1926.

Klein, W.H. 1955. The weather and circulation of February 1955. Monthly Weather Review, February 1955:38-44.

_____. 1983. Objective specification of monthly mean surface temperature from mean 700 mb heights in winter. Monthly Weather Review 111:674-91.

Konrad, C.E., and Colucci, S.J. 1989. An examination of extreme cold air outbreaks over eastern North America. Monthly Weather Review 117:2687-2700.

Koss, W.J., Owenby, J.R., Steurer, P.M., and Ezell, D.S. 1988. Freeze/frost data. Climatography of the U.S. No. 20, Supplement No. 1. National Climatic Data Center, Asheville, NC.

Kramer, P.J., and Kozlowski, T.T. 1979. Physiology of Woody Plants. New York:Academic Press.

LaMarche, V.C., Jr. 1961. Rate of slope erosion in the White Mountain, California. Geological Society of America Bulletin 72:1579.

LaMarche, V.C., Jr. 1970. Frost damage rings in subalpine conifers and their application to tree-ring dating problems. In Tree-ring Analysis with Special Reference to Northwest American Forest Bulletin 7, ed. J.H.G. Smith and J. Worrall, pp. 99-100. Vancouver: University of British Columbia. .

LaMarche, V.C., and Harlan, T.P. 1973. Accuracy of tree-ring dating of bristlecone pine for calibration of radiocarbon time scale. Journal of Geophysical Research 78:8849-58.

LaMarche, V.C., and Hirschboeck, K.K. 1984. Frost rings in trees as records of major volcanic eruptions. Nature 307:121-26.

Lamb, H.H. 1970. Volcanic dust in the atmosphere; with a chronology and assessment of its meteorological significance. Philosophical Transactions of the Royal Society of London, Series A. 266:425-533.

Landsberg, H.E., and Albert, J.M. 1974. The summer of 1816 and volcanism. Weatherwise 27:63-66.

Lawrence, D.B. 1950. Estimating dates of recent glacier advances and succession rates by studying tree growth layers. American Geophysical Union Transactions 31:243-48.

Levitt, J. 1980. Responses of Plants to Environmental Stresses. Volume 1. New York:Academic Press.

Lockwood, J.G. 1987. Atmospheric Circulation, Global. In The Encyclopedia of Climatology, ed. J.E. Oliver and R.W. Fairbridge, pp. 131-40. New York: Van Nostrand Reinhold.

Lough, J.M., and Fritts, H.C. 1985. The Southern Oscillation and tree rings, 1600-1961. Journal of Climate and Applied Meteorology 24:952-66.

_____. 1987. An assessment of the possible effects of volcanic eruptions on North American climate using tree-ring data, 1602 to 1900 A.D. Climatic Change 10:219-39.

Ludlum, D.M. 1966. Early American Winters 1604-1820. Boston:American Meteorological Society.

_____. 1968. Early American Winters II, 1821-1870. Boston:American Meteorological Society.

_____. 1982. The American Weather Book. Boston:Houghton Mifflin.

_____. 1984. The Weather Factor. Boston:Houghton Mifflin.

Maddox, R.A., C.F. Chappell, and Hoxit, L.R. 1979. Synoptic and meso-scale aspects of flash flood events. Bulletin of the American Meteorological Society 60:115-23.

Mass, C.F., and Portman, D.A. 1989. Major volcanic eruptions and climate: a critical evaluation. Journal of Climate 2:566-93.

Meehl, G.A. 1987. The annual cycle and interannual variability in the tropical Pacific and Indian Ocean regions. Monthly Weather Review 115:27-50.

Mogil, H.M. 1985. The "Blue Norther", sudden, surprising cold. Weatherwise 38:149-50.

Monthly Weather Review (MWR). Various Dates. Weather of the Month.

Moran, J.M., and Morgan, M.D. 1977. Recent trends in the hemispheric temperature and growing season indices in Wisconsin. Agricultural Meteorology 18:1-8.

Namias, J. 1947. Characteristics of the general circulation over the Northern Hemisphere during the abnormal winter 1946-47. Monthly Weather Review 75:145-52.

_____. 1950. The index cycle and its role in the general circulation. Journal of Meteorology 7:130-39.

Nash, T.H., Fritts, H.C., and Stokes, M.A. 1975. A technique for examining non-climatic variation in widths of annual tree rings with special reference to air pollution. Tree-Ring Bulletin 35:15-24.

National Oceanic and Atmospheric Administration (NOAA). 1974a. Daily weather maps, weekly series, March 18-24, 1974. Washington: U.S. Dept. of Commerce, Environmental Data Service.

_____. 1974b. Storm data for the United States, March 1974. Washington: U.S. Dept. of Commerce, Environmental Data Service.

National Weather Service (NWS). 1962. Constant pressure charts, North America (daily 700 mb). Washington, D.C.:National Meteorological Center, NOAA.

_____. 1965. Constant pressure charts, North America (daily 700 mb). Washington, D.C.:National Meteorological Center, NOAA.

_____. 1974. Constant pressure charts, North America (daily 700 mb). Washington, D.C.:National Meteorological Center, NOAA.

Newhall, C.G., and Self, S. 1982. The Volcanic Explosivity Index (VEI): an estimate of the explosive magnitude for historical volcanism. Journal of Geophysical Research 87:1231-38.

Ott, L. 1984. An Introduction to Statistical Methods and Data Analysis. Boston: Duxbury Press.

Panshin, A.J., and de Zeeuw, C. 1970. Textbook of Wood Technology, Vol. 1. New York:McGraw-Hill.

Philander, S.G. 1990. El Nino, La Nina, and the Southern Oscillation. San Diego: Academic Press.

Pielke, R.A., Styles, T., and Biondini, R.M., 1979. Changes in growing season. Weatherwise 32:207-10.

Posey, J.W. 1962. The weather and circulation of March 1962. Monthly Weather Review June 1962, 252-58.

Quinn, W.H., Zopf, D.O, Short, K.S., and Kuo Yang, R.T.W. 1978. Historical trends and statistics of the Southern Oscillation, El Nino and Indonesian droughts. Fishery Bulletin 76:663-78.

Rampino, M.R., and Self, S. 1984. The atmospheric effects of El Chichon. Scientific American 250:48-57.

Rasmussen, E.M., and Wallace, J.M. 1983. Meteorological aspects of the El Nino/Southern Oscillation. Science 222:1195-1202.

Rhoads, A.S. 1923. The formation and pathological anatomy of frost rings in conifers injured by late frosts. U.S. Department of Agriculture Bulletin 1131:1-15.

Rogers, J.C. 1984. The association between the North Atlantic Oscillation and the Southern Oscillation in the Northern Hemisphere. Monthly Weather Review 112:1999-2015.

Ropelewski, C.F., and Halpert, M.S. 1986. North American precipitation and temperature patterns associated with the El Nino/Southern Oscillation (ENSO). Monthly Weather Review 114:2352-62.

Rosenberg, N.J., and Myers, R.E. 1962. The nature of growing season frosts in and along the Platte Valley of Nebraska. Monthly Weather Review 90:471-76.

Rumney, G.R. 1987. Climate of North America. In The Encyclopedia of Climatology, ed. J.E. Oliver and R.W. Fairbridge, pp. 612-24. New York: Van Nostrand Reinhold.

SAS Institute, Inc. 1985. SAS User's Guide: Statistics. Version 5 Edition. Cary, North Carolina: SAS

Institute, Inc.

Schonher, T., and Nicholson, S.E. 1989. The relationship between California rainfall and ENSO events. Journal of Climate 2:1258-69.

Schweingruber, F.H. 1988. Tree Rings. Dordrecht: D. Reidel.

Sigafoos, R.S. 1964. Botanical evidence of floods and flood-plain deposition. U.S. Geological Survey, Professional Paper 485-A.

Simkin, T., Siebert, L., McClelland, L., Bridge, D., Newall, C., and Latter, J.H. 1981. Volcanoes of the World. Stroudsberg, PA: Hutchinson Press.

Simkin, T., and Seibert, L. 1984. Explosive eruptions in space and time: durations, intervals, and a comparison of the world's active volcanic belts. In Explosive Volcanism: Inception, Evolution, and Hazards, National Research Council. Washington: National Academy Press.

Shroder, J.F. 1980. Dendrogeomorphology: review and new techniques in tree-ring dating. Progress in Physical Geography 4:161-88.

Skaggs, R.H., and Baker, D.G. 1985. Fluctuations in the length of the growing season in Minnesota. Climatic Change 7:403-14.

Smiley, T.L, editor. 1955. Geochronology, with special reference to the southwestern United States. Tucson: University of Arizona Bulletin 26(2a), Physical Science Bulletin 2.

Smith, J.W. 1920. Influence of weather on crops and outdoor operations. National Weather and Crop Bulletin, No. 14, Series 1920, April 6, 1920, USDA Weather Bureau.

_____. 1921a. Effect of weather on crops and farming operations. Monthly Weather Review, March 1921.

_____. 1921b. Influence of weather on crops and outdoor operations. National Weather and Crop Bulletin, No. 13, 1921, USDA Weather Bureau.

Soil Conservation Service (SCS). 1975. Soil Taxonomy. Washington: U.S. Dept. of Agriculture.

Stahle, D.W. 1978. Tree-ring dating of selected Arkansas log building. M.A. thesis, University of Arkansas,

Fayetteville.

_____. 1979. Tree-ring dating of historic buildings in Arkansas. Tree-Ring Bulletin 39:1-29.

Stahle, D.W., and Hehr, J.G. 1984. Dendroclimatic characteristics of post oak across and precipitation gradient in the southcentral United States. Annals of the Association of American Geographers 74:561-73.

Stahle, D.W., Hehr, J.G., Hawks, G.G., Cleaveland, M.K., and Baldwin, J.R. 1985a. Tree-Ring Chronologies for the Southcentral United States. Tree-Ring Laboratory, Office of the State Climatologist, University of Arkansas, Fayetteville.

Stahle, D.W., Hehr, J.G., Baldwin, J.R., and Cleaveland, M.K. 1985b. Frost rings in post oak from the southcentral United States. Program Abstracts, Association of American Geographers, Detroit, MI. April 21-24, 1985.

Stahle, D.W. and Cleaveland, M.K. 1988. Texas drought history reconstructed and analyzed from 1698 to 1980. Journal of Climate 1:59-74.

Stahle, D.W., Cleaveland, M.K., and Hehr, J.G. 1988. North Carolina climate changes reconstructed from tree rings: A.D. 372 to 1985. Science 240:1517-19.

Stark, L.P. 1957. The weather and circulation of January 1957. Monthly Weather Review January 1957, 19-27.

_____. 1965. The weather and circulation of February 1965. Monthly Weather Review 93:366-72.

Steel, R.G.D., and Torrie, J.H. 1980. Principles and Procedures of Statistics, 2nd Edition. New York:McGraw-Hill.

Stockton, C.W. 1975. Long-term streamflow records reconstructed from tree rings: Papers of the Laboratory of Tree-Ring Research, No. 5, Tucson:University of Arizona Press.

Stockton, C.W., and Meko, D.M. 1983. Drought recurrence in the Great Plains as reconstructed from long-term tree-ring records. Journal of Climate and Applied Meteorology 22:17-29.

Stokes, M.A., and Dietrich, J.H., editors. 1980. Proceedings of the Fire History Workshop. General

Technical Report RM-81, Rocky Mountain Forest and Range Experiment Station, Ft. Collins.

Stokes, M.A., and Smiley, T.L. 1968. An Introduction to Tree-Ring Dating. Chicago:University of Chicago Press.

Stothers, R.B. 1984. The great Tambora eruption in 1815 and its aftermath. Science 224:1191-98.

Suckling, P.W. 1986. Fluctuations of last spring-freeze dates in the southeastern United States. Physical Geography 7:239-45.

Swetnam, T.W. 1988. El Nino events and fire occurrence during the past three centuries in the Southwestern U.S. Workshop on Wildfire Severity and Global Climate Change, National Center for Atmospheric Research and the USDA Forest Service. Boulder, CO, Sept. 29, 1988.

Swetnam, T.W., Thompson, M.A., and Sutherland, E.K. 1985. Using dendrochronology to measure radial growth of defoliated trees. Agriculture Handbook 639. Washington: USDA, Forest Service.

Taubensee, R.E. 1974. Weather and Circulation of March 1974. Monthly Weather Review 102:466-71.

Thom, H.C.S., and Shaw, R.H. 1958. Climatological analysis of freeze data for Iowa. Monthly Weather Review 86:251-57.

Thompson, L.G., Mosely-Thompson, E., Bolzan, J.F., and Koci, B.R. 1985. A 1500-year record of tropical precipitation in ice cores from the Quelccaya Ice Cap, Peru. Science 229:971-73.

Thompson, M.A. 1981. Tree rings and air pollution: a case study of Pinus monophylla growing in east central Nevada. Environmental Pollution (Series A) 26:251-65.

U.S. Weather Bureau(A). 1899-1980. Climatological data for the United States by Sections, (Arkansas, Missouri, Oklahoma, and Texas). Washington: U.S. Department of Agriculture, subsequently U.S. Department of Commerce.

U.S. Weather Bureau(B). 1899-1980. Daily Weather Maps, Weekly Series. (United States).

U.S. Weather Bureau(C). 1899-1980. Daily Series, Synoptic Weather Maps, Northern Hemisphere Sea Level.

van Loon, H., and Madden, R.A. 1981. The Southern

Oscillation. Part I: Global associations with pressure and temperature in northern winter. Monthly Weather Review 109:1150-62.

Wallace, J.M., and Gutzler, D.S. 1981. Teleconnections in the geopotential height field during the Northern Hemisphere winter. Monthly Weather Review 109-784-812.

War Department. 1873. Office of the Chief Signal Officer, General summaries for the weeks ending April 7 and April 17, 1873. Weekly Weather Chronicle March and April, 1873.

War Department. 1880. Weekly Weather Chronicle, March 1-16, 1880. Office of the Chief Signal Officer.

Weekly Weather and Crop Bulletin (WWCB). 1931. No. 13, Series 1931, March 13, 1931.

_____. 1932. No. 11, series 1932, March 15, 1932.

_____. 1936. No. 14, series 1936, April 7, 1936.

_____. 1940. No. 16, series 1940, April 16, 1940.

_____. 1943a. No. 8, series 1943, February 23, 1943.

_____. 1943b. No. 9, series 1943, March 2, 1943.

_____. 1943c. No. 10, series, 1943, March 9, 1943.

_____. 1955. Vol. XLII, No. 13, March 28, 1955.

_____. 1957. Vol. XLIV, No. 15, April 15, 1957.

_____. 1962. Vol. XLIX, No. 10, March 5, 1962.

_____. 1965. Vol. 52, No. 13, March 22 and 29, 1965.

_____. 1974. Vol. 61, No. 13, March 26, 1974.

_____. 1989a. Vol. 76, No. 13, April 4, 1989.

_____. 1989b. Vol. 76, No. 15, April 18, 1989.

Winston, J.S. 1955. The weather and circulation of March 1955. Monthly Weather Review, March, 1955:72-77.

Woffinden, C.M. 1957. Weather and circulation of February 1957. Monthly Weather Review, February 1957, 53-61.

Yamaguchi, D.K. 1983. New tree-ring dates for recent eruptions of Mount St. Helens. Quaternary Research 20:246-50.

Yanosky, T.M. 1983. Evidence of floods on the Potomac River from anatomical abnormalities in the wood of flood-plain trees. U.S. Geological Survey Professional Paper 1296.

_____. 1984. Documentation of high summer flows on the Potomac River from the wood anatomy of ash trees. Water Resources Bulletin 20:241-50.

Yarnal, B., and Diaz, H.F. 1986. Relationships between extremes of the Southern Oscillation and the winter climate of the Anglo-American Pacific coast. Journal of Climatology 6:197-219.

APPENDIX 1

Oak, Pine, and Spruce Chronologies,

The VEI, El Nino and La Nina Events

APPENDIX 1

The summary frost ring chronology derived from deciduous oaks of the southcentral United States is listed from 1650 to 1980 along with the bristlecone pine frost ring chronology (just 1650 to 1969; LaMarche and Hirschboeck 1984) and the black spruce light ring chronology (just 1650 to 1980; Filion et al. 1986). This appendix also includes those years from 1650 to 1980 with a Volcanic Explosivity Index (VEI) $\geq$ 4 (Newhall and Self 1982), and El Nino and La Nina years form 1866 to 1980. Years of frost or light ring occurrence are indicated by an "X" (note that the bristlecone pine frost ring of 1902 occurred in the earlywood). Years with VEI $\geq$ 4 are indicated by the month of occurrence (1-12) by an "X" if the month is unknown, or by the range of months for years with multiple large eruptions. The first year of El Nino and La Nina event identified by Kiladis and Diaz (1989) are indicated by an "X" from 1877 to 1980. Events before 1877 (or 1882 in the case of La Nina events) and the subsequent years of multi-year events are based on the SO index (Jones, personal communication) and are indicated by a "C".

APPENDIX 1

Year	Oak	Bristle-Cone Pine	Black Spruce	VEI	El Nino	La Nina
1650						
1						
2						
3						
4						
5						
6						
7						
8						
9	X					
1660	X	X		10-11		
1						
2						
3				8		
4	X					
5						
6						
7						
8						
9						
1670						
1				X		
2						
3				5		
4						
5						
6						
7	X					
8	X					
9						
1680		X		X		
1						
2						
2						
4						
5						
6	X			2		
7						
8			X			
1689	X					

Year	Oak	Bristle-Cone Pine	Black Spruce	VEI	El Nino	La Nino
1690						
1						
2						
3				2		
4	X		X			
5						
6						
7						
8			X			
9						
1700						
1	X					
2						
3						
4						
5						
6						
7				12		
8						
9						
1710						
1	X					
2			X			
3						
4						
5						
6	X		X			
7						
8						
9	X					
1720						
1				5		
2						
3						
4						
5						
6	X					
7	X				8	
8						
1729						

Year	Oak	Bristle-Cone Pine	Black Spruce	VEI	El Nino	La Nina
1730	X					
1						
2		X	X			
3						
4						
5	X					
6						
7						
8						
9				8		
1740	X					
1	X			8		
2						
3						
4	X			11		
5	X		X			
6						
7						
8						
9			X			
1750						
1	X					
2			X			
3						
4						
5			X	10		
6						
7			X			
8						
9			X	9		
1760						
1		X				
2				12		
3						
4			X	X		
5				X		
6				4		
7						
8				4		
1769	X					

Year	Oak	Bristle-Cone Pine	Black Spruce	VEI	El Nino	La Nina
1770						
1			X			
2				8		
3						
4						
5						
6						
7						
8	X			X		
9	X					
1780						
1						
2						
3				5-7		
4			X			
5						
6	X		X			
7						
8						
9						
1790						
1	X					
2						
3				X-3		
4						
5				X		
6	X					
7						
8						
9						
1800			X			
1						
2			X	X		
3						
4						
5		X				
6	X					
7						
8						
1809						

Year	Oak	Bristle-Cone Pine	Black Spruce	VEI	El Nino	La Nina
1810	X					
1	X					
2				4		
3						
4	X		X	2		
5				4		
6	X		X			
7	X	X	X			
8				X-2		
9	X		X			
1820	X					
1	X					
2			X	3		
3						
4						
5				X		
6	X					
7						
8	X	X				
9						
1830						
1		X				
2	X					
3	X					
4						
5				1		
6			X			
7		X				
8						
9	X					
1840						
1						
2			X			
3	X					
4	X		X			
5				9		
6			X			
7						
8						
1849				12		

Year	Oak	Bristle-Cone Pine	Black Spruce	VEI	El Nino	La Nina
1850						
1						
2						
3			X	12		
4				2		
5						
6				9		
7	X					
8						
9			X			
1860			X			
2						
2			X			
3			X			
4						
5						
6		X				
7	X					
8			X		C	
9				10		
1870	X					
1		X				
2				X		C
3	X			1		
4						
5				3		
6	X					
7				X-6	X	
8			X			C
9						C
1880	X				X	
1				7		
2						
3				8-10		
4		C	C		X	
5						
6	X			1-6		X
7						
8				7	X	
1889				10		X

Year	Oak	Bristle-Cone Pine	Black Spruce	VEI	El Nino	La Nina
1890	X					
1					X	
2	X					X
3						
4	X		X			
5						
6					X	
7						
8						X
9	X			11	X	
1900						
1						
2		X		5-10	X	
3				5		X
4			X		X	
5						
6						X
7				3		
8						X
9				3		
1910			X			
1				1	X	
2		X	X	6	C	
3	X			1	X	
4	X			1		
5						
6						X
7				4		C
8			X	4-10	X	
9				8	C	
1920	X					X
1	X			12		
2						
3	X		X		X	
4						X
5					X	
6	X				C	
7						
8						X
1929				6		

Year	Oak	Bristle-Cone Pine	Black Spruce	VEI	El Nino	La Nina
1930					X	
1	X			3		X
2	X			1-4	X	
3						
4			X			
5						
6	X		X			
7				5		
8						X
9					X	
1940	X				C	
1		X	X		C	
2						X
3	X					
4						
5				1		
6			X	11		
7			X	3		
8						
9						X
1950				12		C
1				1	X	
2				2		
3				7	X	
4						X
5	X		X	7		C
6			X	3		C
7	X		X		X	
8						
9						
1960						
1						
2	X					
3			X	3	X	
4				11		X
5	X	X	X	9	X	
6				4-8		
7			X			
8				6		
1969			X		X	

Year	Oak	Bristle-Cone Pine	Black Spruce	VEI	El Nino	La Nina
1970						X
1						C
2			X		X	
3				7		X
4	X			10		
5				6		X
6				1	X	
7					C	
8			X			
9				2		
1980				5		